University of Nottingham

SCHOOL OF BIOSCIENCES

Analysis of potential target genes to deliver plant abiotic stress tolerance

Jasmine Jane Littler, MSc, BSc (Hons)

Supervisors: Prof Zoe Wilson, Prof Erik Murchie

Acknowledgements

I would first like to thank my supervisors Zoe and Erik, for a huge amount of help, support and guidance through many different aspects of the PhD, both in and out of the lab. I would also like to thank Jordan Robson, for not only being a mentor and training me, but also for giving me confidence along the way. Thank you to Racheal Webster for both support along the journey and friendship. Also thank you to Alice Haslam and Rachel Jackson, who helped me navigate the last few years of my PhD.

To Mum and Dad, thank you for all that you have done over the last 27 years, making sure I always achieved the best I could, even if I didn't realise it at the time. Scaz and Naz, I hope I'm now the coolest big sister, even if I'm getting more embarrassing as you get older. To Grandma, thank you for always supporting me, inspiring me, and fuelling me with all my favourite foods. To William, I hope this inspires you to be the smartest Littler out of us all. And to Matt, thank you for always being there- even from across the world, I can’t wait to see what post-PhD life has in store for us. I couldn't have done it without you all.

A special mention to UoN waterpolo past and present, who truly made university a life changing experience, both in and out of the pool. With an extra special thanks to Joyce and Tilly.

Abstract

With ongoing climate change, the need for crops to grow with yield stability in a range of stressful environments is increasingly challenging. Improvement needs to be made to the abiotic stress tolerance of crop plants in order to meet the food demands of an increasing population. Heat has particularly negative effects on reduced photosynthetic efficiency, enzyme activity, and changes in metabolic processes, while drought and waterlogging stress cause stomatal closure, reduced photosynthesis, disrupted nutrient uptake, and cellular damage, ultimately hindering growth and development.

One method of increasing plants tolerance to abiotic stress is through targeted mutagenesis. In this study, several genes were selected from a previously published Genome Wide Association Study (GWAS) (Robson et al., 2023) as candidate genes linked to photosynthetic heat stress tolerance in Rice. In *A. thaliana*, T-DNA insertion mutations in putative orthologue genes to those selected in rice were grown under normal conditions and high temperature stress (22°C and 32°C). Chlorophyll fluorescence was used to characterise mutant lines for photosynthetic heat stress tolerance, fertility, and root architecture. T-DNA insertion lines carrying mutations in *ATP BINDING CASSETTE F 5(ABCF5), ZINC NUTRIENT ESSENTIAL1 (ZNE1),* and the relatively uncharacterised gene, *T8P21,* all showed positive photosynthetic traits after five days of heat stress, while mutants in *CALLOSE SYNTHASE 1 (CALS1)*, *SYNAPTOTAGMIN 2 (SYTB)* and *ALBINO OR PALE GREEN 3 (APG3)* showed increased sensitivity to heat stress.

Alongside the identification of genes associated with photosynthetic heat stress tolerance, Targeting Induced Local Lesions in Genomes (TILLING) mutations in *Hordeum vulgare* in pathways associated with abiotic stress tolerance in the field were explored. TILLING lines in two components of the Arg/N-degron pathway, which is a conserved pathway associated with abiotic stress tolerance were assessed. TILLING mutations targeting genes in this pathway: *PROTEOLYSIS 6 (PRT6) and Gln-specific N-terminal amidase (NTAQ),* were tested in the field. Alongside these TILLING mutants, *ABSCISIC ACID INSENSITIVE 5(ABI5)* mutants were also tested in the field in *Hordeum vulgare*.

Overall, this study has conducted an analysis to identify candidate genes for targeted mutagenesis to overcome abiotic stress in crops at different points in crop development, including both identifying target genes, and testing on the field.

Contents

List of Tables

List of Figures

Sebastian. Error bars indicate standard error of the mean. * denote statistical significance between WT and mutant (P<0.05).

Figure 2.12: Comparisons of Wild Type (WT) and TILLING mutants in the gene Prt6 in the background cultivars Voyager and Sebastian. a) Growth stage after 715 degree days b) Growth stages after 934 degree days c) Growth stages after 1187 degree days d) Growth stage after 1358 degree days. Error bars indicate standard error of the mean. Significant difference between mutant line and WT of the same cultivar indicated by; (#)P<0.1 (*)P<0.05 (**)P<0.01 (***) P<0.001.

Figure 2.13: Comparisons of Wild Type (WT) and TILLING mutants in the gene Prt6 in the background cultivars of Sebastian and Voyager. a) Above ground biomass b) Height c) Estimated weight at anthesis d) Biomass partitioning as a percentage of total overall biomass. e) Internode lengths as a percentage of total stem length between Node (IN) 1 and 3. Error bars indicate standard error of the mean. Significant difference between mutant line and WT of the same cultivar indicated by; (#)P<0.1 (*)P<0.05 (**)P<0.01 (***)P<0.001.

Figure 2.14: Comparisons of Wild Type (WT) and TILLING mutants in the gene Ntaq. a) total grain weight per plant per individual plant b) Harvest index c) Fruiting efficiency d) 1000 grain weight. Error bars indicate standard error of the mean. Significant difference between mutant line and WT indicated by; (#) P<0.1 (*)P<0.05 (**)P<0.01 (***)P<0.001.

Figure 2.15: Comparisons of growth stage development in Wild Type (WT) and TILLING mutants in the gene Ntaq in the background cultivar Sebastian a) Development of Growth stages over degree days b) Degree days until the first node is detectable (GS31). Error bars indicate standard error of the mean. Significant difference between mutant line and WT indicated by; (#)P<0.1 (*)P<0.05 (**)P<0.01 (***)P<0.001.

Figure 2.16: Comparisons of development in Wild Type (WT) and TILLING mutants in the gene Ntaq in the background cultivar Sebastian a)Growth stages after 715 degree days b) Growth stages after 1358 degree days. Error bars indicate standard error of the mean Error bars indicate standard error of the mean. Significant difference between mutant line and WT indicated by; (#)P<0.1 (*)P<0.05 (**)P<0.01 (***)P<0.001.

Figure 2.17: Comparisons between Wild Type (WT) and TILLING mutants in the gene Ntaq in the background cultivar Sebastian a) Total above ground biomass b) Height c) Estimated weight at anthesis d) Above ground Biomass partitioning. Error bars indicate standard error of the mean. Significant difference between mutant line and WT indicated by; (#) P<0.1 (*)P<0.05 (**)P<0.01.

Figure 2.18: Comparisons of spikes in Wild Type (WT) and TILLING mutants in the gene Ntaq in the background cultivar Sebastian a) Spike length b) Grain per spike. Error bars indicate standard error of the mean. Significant difference between mutant line and WT indicated by; (#) P<0.1 (*)P<0.05 (**)P<0.01 (***)P<0.001.

Figure 2.19: Comparisons of Wild Type (WT) and TILLING mutants in the gene Abi5. a) total grain weight per plant b) Harvest index (HI) c) Fruiting efficiency (FE) d) 1000 grain weight (TGW). Error bars indicate standard error of the mean. Significant difference between mutant line and WT indicated by; (*)P<0.05.

Figure 2.20: Comparisons of growth stage development in Wild Type (WT) and TILLING mutants in the gene Abi5 in the background cultivar Sebastian a) Development of Growth stages over degree days b) Degree days until first detectable node (GS31) c) Degree days until anthesis (GS61) d) Growth stages after 715 degree days e) Growth stages after 1358 degree days. Error bars indicate standard error of the mean. Significant difference between mutant line and WT indicated by; (#)P<0.1 (*)P<0.05 (**)P<0.01 (***)P<0.001.

Figure 2.21: Comparisons between Wild Type (WT) and TILLING mutants in the gene Abi5 in the background cultivar Sebastian a) Total above ground biomass b) Estimated weight at anthesis c) Height d) Above ground Biomass partitioning. Error bars indicate standard error of the mean. Significant difference between mutant line and WT indicated by; (*)P<0.05 (**)P<0.01.

Figure 2.22: Comparisons between Wild Type (WT) and TILLING mutants in the gene Abi5 in the background cultivar Sebastian a) Spike infertility b) Spike length. Error bars indicate standard error of the mean. Significant difference between mutant line and WT indicated by; (#)P<0.1, (*)P<0.05, (**)P<0.01, (***)P<0.001.

Figure 3.1: From Yamaguchi et al., (2006): Phylogenetic Tree of Glucan Synthases. Multiple alignment of deduced callose synthase (GSL, Glucan synthase-like) amino acid sequences were done by ClustalW 1.83. Phylogenetic trees were constructed using the NJ (Neighbour-Joining) algorithm and drawn with the NJplot program.

Figure 3.2: Schematic diagram of the gene SYTB in A. thaliana. Dark grey boxes show exons, orange boxes show the untranslated regions (UTRs), and the green arrow shows the location of the T-DNA insertion. Primers are highlighted in purple, with genotyping primers being used for testing homozygosity (as per table 3.2), and qRT-PCR primers used for analysis of gene expression (as per table 3.3).

Figure 3.3: Schematic diagram of the gene SIS8 in A. thaliana. Dark grey boxes show exons, orange boxes show untranslated regions (UTRs) and the green arrow shows the location of the T-DNA insertion. Primers are highlighted in purple, with genotyping primers being used for testing homozygosity (as per table 3.2), and qRT-PCR primers used for analysis of gene expression (as per table 3.3).

Figure 3.4: Schematic diagram of the gene WRKY55 in A. thaliana. Dark grey boxes show exons, orange boxes show untranslated regions (UTRs) and the green arrow shows the location of the T-DNA insertion. Primers are highlighted in purple, with genotyping primers being used for testing homozygosity (as per table 3.2), and qRT-PCR primers used for analysis of gene expression (as per table 3.3).

Figure 3.5: Schematic diagram of the gene CALS1 in A. thaliana. Dark grey boxes show exons, orange boxes show untranslated regions (UTRs) and the green arrow shows the location of the T-DNA insertion. Primers are highlighted in purple, with genotyping primers being used for testing homozygosity (as per table 3.2), and qRT-PCR primers used for analysis of gene expression (as per table 3.3).

Figure 3.6: Schematic diagram of the gene BCH1 in A. thaliana. Dark grey boxes show exons, orange boxes show untranslated regions (UTRs) and he green arrow shows the location of the T-DNA insertion. Primers are highlighted in purple, with genotyping primers being used for testing homozygosity (as per table 3.2), and qRT-PCR primers used for analysis of gene expression (as per table 3.3).

Figure 3.7: Schematic diagram of the gene BCH2 in A. thaliana. Dark grey boxes show exons, orange boxes show untranslated regions (UTRs) and the green arrow shows the location of the T-DNA insertion. Primers are highlighted in purple, with genotyping primers being used for testing homozygosity (as per table 3.2), and qRT-PCR primers used for analysis of gene expression (as per table 3.3).

Figure 3.8: Schematic diagram of the gene GAPB in A. thaliana. Dark grey boxes show exons, orange boxes show untranslated regions (UTRs) and the green arrow shows the location of the T-DNA insertion. Primers are highlighted in purple, with genotyping primers being used for testing homozygosity (as per table 3.2), and qRT-PCR primers used for analysis of gene expression (as per table 3.3).

Figure 3.9: Schematic diagram of the gene ABCF5 in A. thaliana. Dark grey boxes show exons, orange boxes show untranslated regions (UTRs) and the green arrow shows the location of the T-DNA insertion. Primers are highlighted in purple, with genotyping primers being used for testing homozygosity (as per table 3.2), and qRT-PCR primers used for analysis of gene expression (as per table 3.3).

Figure 3.10: Schematic diagram of the gene APG3 in A. thaliana. Dark grey boxes show exons, orange boxes show untranslated regions (UTRs) and the green arrow shows the location of the T-DNA insertion. Primers are highlighted in purple, with genotyping primers being used for testing homozygosity (as per table 3.2), and qRT-PCR primers used for analysis of gene expression (as per table 3.3).

Figure 3.11: Schematic diagram of the gene HO2 in A. thaliana. Dark grey boxes show exons, orange boxes show untranslated regions (UTRs) and the green arrow shows the location of the T-DNA insertion. Primers are highlighted in purple, with genotyping primers being used for testing homozygosity (as per table 3.2), and qRT-PCR primers used for analysis of gene expression (as per table 3.3).

Figure 3.12: Schematic diagram of the gene DIS1 in A. thaliana. Dark grey boxes show exons, orange boxes show untranslated regions (UTRs) and the green arrow shows the location of the T-DNA insertion. Primers are highlighted in purple, with genotyping primers being used for testing homozygosity (as per table 3.2), and qRT-PCR primers used for analysis of gene expression (as per table 3.3).

Figure 3.13: Schematic diagram of the gene DG1 in A. thaliana. Dark grey boxes show exons, orange boxes show untranslated regions (UTRs) and the green arrow shows the location of the T-DNA insertion. Primers are highlighted in purple, with genotyping primers being used for testing homozygosity (as per table 3.2), and qRT-PCR primers used for analysis of gene expression (as per table 3.3).

Figure 3.14: Schematic diagram of the gene ZNE1 in A. thaliana. Dark grey boxes show exons, orange boxes show untranslated regions (UTRs) and the green arrow shows the location of the T-DNA insertion. Primers are highlighted in purple, with genotyping primers being used for testing homozygosity (as per table 3.2), and qRT-PCR primers used for analysis of gene expression (as per table 3.3).

Figure 3.15: Schematic diagram of the gene MUSE3 in A. thaliana. Dark grey boxes show exons, orange boxes show untranslated regions (UTRs) and the green arrow shows the location of the T-DNA insertion. Primers are highlighted in purple, with genotyping primers being used for testing homozygosity (as per table 3.2), and qRT-PCR primers used for analysis of gene expression (as per table 3.3).

Figure 3.16: Schematic diagram of the gene T8P21 in A. thaliana. Dark grey boxes show exons, orange boxes show untranslated regions (UTRs) and the green arrow shows the location of the T-DNA insertion. Primers are highlighted in purple, with genotyping primers being used for testing homozygosity (as per table 3.2), and qRT-PCR primers used for analysis of gene expression (as per table 3.3).

Figure 3.17: Relative expression of chosen T-DNA insertion mutants in A. thaliana in each gene of interest (relative to housekeeping gene) . Tissue taken from leaf samples at bolting. Error bars indicate SD.

Figure 3.18: The relative expression of each gene in both Oryza sativa and A. thaliana leaf tissue from data retrieved from TAIR electronic Fluorescent Pictograph (eFP) browser http://bar.utoronto.ca/efp/cgi-bin/efpWeb.cgi, in the form of fold change values at different time intervals. For BCH, two orthologues were found in A. thaliana, and bch1 was used for this visualisation. Error bars indicate SD.

Figure 3.19. Relative expression of Genes of interest in A. thaliana in shoot tissue after 24 hours of various environmental stresses from data retrieved from TAIR electronic

Figure 4.5: Secondary rate of response to heat (M_2) of T-DNA insertion mutants and WT (Col-0) of same treatment groups. T-DNA insertion mutants of A. thaliana genotypes and Col-0 (WT) a) in control conditions b) after prior exposure at 32°C for five days c) subsequent three days recovery. * denotes significant difference (P<0.05) to the WT of the same treatment. Error bars indicate SEM.

Figure 4.6: F_v/F_m of T-DNA insertion mutants and WT (Col-0) of same treatment groups at stable light level L15. T-DNA insertion mutants of A. thaliana genotypes and Col-0 (WT) a) in control conditions b) after prior exposure at 32°C for five days c) subsequent three days recovery. * denotes significant difference (P<0.05) to the WT of the same treatment. Error bars indicate SEM.

Figure 4.7: The response of chlorophyll fluorescence parameters (see Table 2 for full descriptions) to stepwise changes in photosynthetic photon flux density (--- PPFD) in A. thaliana Col-0 ecotype. After a dark adaptation period of 45mins, PPFD was increased to 500 µmol m^{-2} s^{-1} for 15 min. Subsequently, PPFD was decreased to 100 µmol m m^{-2} s^{-1} 1 for 15 min and then increased to 500 µmol m^{-2} s^{-1} for 15min. From measurements of maximal (Fm) and minimal (Fo) fluorescence the following parameters can be calculated: photochemical quenching (a—qP)PSII quantum yield of PSII (b— ΦPSII), fraction of open PSII reaction centres (c—qL), and maximum non-photochemical quenching (d—NPQ). Measurements were taken every minute and error bars indicate standard error.

Figure 4.8: Correlation between F_v/F_m and other chlorophyll fluorescence parameters at steady state at L15 and L30. a/b) qP-photochemical quenching. c/d) qL-photochemical quenching. e/f) ΦPSII - fraction of open PSII reaction centres. g/h) NPQ

Figure 4.9: ΦPSII of T-DNA insertion mutants and WT (Col-0) of same treatment groups at stable light level L15. T-DNA insertion mutants of A. thaliana genotypes and Col-0 (WT) a) in control conditions b) after prior exposure at 32°C for three days c) after prior exposure at 32°C for five days and d) subsequent three days recovery. * denotes significant difference (P<0.05) to the WT of the same treatment. Error bars indicate SEM.

Figure 4.10: F_q'/F_m' (ϕPSII) of T-DNA insertion mutants and WT (Col-0) of same treatment groups at stable light level L30. T-DNA insertion mutants of A. thaliana genotypes and Col-0 (WT) a) in control conditions b) after prior exposure at 32°C for three days c) after prior exposure at 32°C for five days and d) subsequent three days recovery. * denotes significant difference (P<0.05) to the WT of the same treatment. Error bars indicate SEM..

Figure 4.11: qL of T-DNA insertion mutants and WT (Col-0) of same treatment groups at stable light level L15. T-DNA insertion mutants of A. thaliana genotypes and Col-0 (WT) a) in control conditions b) after prior exposure at 32°C for three days c) after prior exposure at 32°C for five days and d) subsequent three days recovery. * denotes significant difference (P<0.05) to the WT of the same treatment. Error bars indicate SEM.

Figure 4.12: qL of T-DNA insertion mutants and WT (Col-0) of same treatment groups at stable light level L30. T-DNA insertion mutants of A. thaliana genotypes and Col-0 (WT) a) in control conditions b) after prior exposure at 32°C for three days c) after prior exposure at 32°C for five days and d) subsequent three days recovery. * denotes significant difference (P<0.05) to the WT of the same treatment. Error bars indicate SEM.

Figure 4.13: qP of T-DNA insertion mutants and WT (Col-0) of same treatment groups at stable light level L15. T-DNA insertion mutants of A. thaliana genotypes and Col-0 (WT) a) in control conditions b) after prior exposure at 32°C for three days c) after prior exposure at 32°C for five days and d) subsequent three days recovery. * denotes significant difference (P<0.05) to the WT of the same treatment. Error bars indicate SEM.

Figure 4.14: qP of T-DNA insertion mutants and WT (Col-0) of same treatment groups at stable light level L30. T-DNA insertion mutants of A. thaliana genotypes and Col-0 (WT) a) in control conditions b) after prior exposure at 32°C for three days c) after prior exposure at 32°C for five days and d) subsequent three days recovery. * denotes significant difference (P<0.05) to the WT of the same treatment. Error bars indicate SEM.

List of Abbreviations

10-fTHF	10-formyltetrahydrofolate
ABA	Abscisic Acid
ABCF	General Control Non-Repressible
ABF	ABRE binding factor
ABI5	ABA Insensitive5
ABRE	ABA Response Element
Ac	Acetyl
AI	Autoinhibitory
AITR	ABA-Induced Transcription Repressor
ANCOVA	Analysis of Covariance
ANOVA	Analysis of Variance
AP	Root abundant
APG	Albino or Pale Green
AREB	ABA-Responsive Element Binding
Arg	Arginine
ARP	Actin-Related Protein
Asn	Asparagine
ATE	Arginyl-tRNA-Protein Transferase
ATP	Adenosine Triphosphate
AVPI	H^+- Inorganic Pyrophosphatase
BAAP	Bengal and Assam Aus Panel
BBSRC	Biotechnology and Biological Sciences Research Council
BC	Backcross
BCH1/2	Beta-Carotene Hydroxylase
BERF	Barley Ethylene Response Factor
BKN3	Barley Knotted1-like Homeobox
BLAST	Basic Local Alignment Search Tool
BO1/2	Beta-ohase
BRZ	Brassinazole Resistant
BV	Biliverdin
bZIP	Basic Leucine Zipper
CALS1	Callose Synthase 1
CCD	Carotenoid Cleavage Dioxygenase
CDC48A	Cell division cycle 48A
cDNA	Complementary Deoxyribonucleic Acid
Col-0	Columbia-0 (*Arabidopsis* Strain)
COVID	Coronavirus Disease
CPR1	Constitutive expressor of PR Genes
CRISPR	Clustered Regularly Interspaced Short Palindromic Repeats
CAS9	CRISPR-associated protein9
D1/2	Domain1/2

DERF1	Drought-Responsive Ethylene Response Factor
DG1	Delayed Greening1
DGAT1	Diacylglycerol Acyltransferase1
DIG8	Drought Inhibited Growth of Lateral Roots
DIS1	Distorted Trichomes1
DNA	Deoxyribonucleic Acid
dNTP	Deoxynucleotide Triphosphate
DREB	Dehydration Responsive Element Binding Protein
Ds	Disassociation
DSM	Drought Sensitive Mutant
DST	Drought and Salt Tolerance
eFP	Electronic Fluorescent Pictograph
EMS	Ethyl Methanesulfonate
ERAI	Enhanced Response to Abscisic Acid
ERF	Ethylene Response Factor
f	Formyl
FAD7	Fatty Acid Desaturase
FAR1	Far-Red Impaired Response1
FE	Fruiting Efficiency
FHY3	Far-Red Elongated Hypocotyls3
fMet	Formylmethionine
GA	Gibberellic Acid
GABI-KAT	German Arabidopsis Functional Genomics Network - Knockout Arabidopsis T-DNA
GAPB	Beta Subunit of Glyceraldehyde 3-Phosphate Dehydrogenase
GAPDH	Glyceraldehyde 3-Phosphate Dehydrogenase
GED1	Greening After Extended Darkness
Gln	Glutamine
Gly	Glycine
GMO	Genetically Modified Organism
GN	Grain Number
GSH1	Gluthione
GSL	Glucan Synthase-Like
GWAS	Genome-Wide Association Study
HEMA	Glutamine tRNA Reductase
His	Histidine
His	Histidine
HO	Haemoglobin Oxygenase
HorTILLUS	*Hordeum* TILLING University of Silesia
HRE	Hypoxia Response ERF
HSA1	Heat Stress Sensitive Albino
HSF	Heat Shock Factor
HST	Heat Stress Tolerant
iCASE	Industrial Collaborative Awards for PhD Students

ICS1	Isochorismate Synthase1
IN	Internode
IRT	Iron Regulated Transporter
J_{max}	Photosynthetic Electron Transport
JR3	Jasmonate-Responsive
LCH	Light-Harvesting Complex
LCYB1	β-ring Cyclase1
LEA3	Late Embryogenesis Abundant3
LED	Light Emitting Diode
Leu	Leucine
LHC	Light-Harvesting Complex
MAPK	Mitogen-Activated Protein Kinase
MAPKK	Mitogen-Activated Protein Kinase Kinase
MAPKKK	Mitogen-Activated Protein Kinase Kinase Kinase
MES	2-(N-morpholino)ethanesulfonic Acid
MF	Microfilament
MORF2	Mitochondrial RNA Modification Factor2
mPTP	Mitochondrial Permeability Transition Pore
mRNA	Messenger RNA
MS	Murashige and Skoog Medium
MSHI	Mutant S Homolog1
MUSE3	SNC1 Enhancing3
MYB5	My Elob Lastosis5
NADH	Nicotinamide Adenine Dinucleotide (NAD) + hydrogen (H)
NADPH	Nicotinamide Adenine Dinucleotide Phosphate
NCBI	National Centre for Biotechnology Information
NCED	9-cis-epoxycarotenoid Dioxygenase
NLR	Nucleotide-Binding, Leucine-rich Repeat
NPQ	Non-Photochemical Quenching
NPR1	Nonexpresser of PR Genes
Nt	N-Terminal
NTAN	N-Terminal Asparagine Amidase
NTAQ	N-Terminal Glutamine Amidase
OsT	Oligosaccharyltransferase
OST2	Oligosaccharyltransferase Subunit2
PBS3	*avr*PphB Susceptible3
PCO	Plant Cysteine Oxidase
PCR	Polymerase Chain Reaction
PDF1	Plant Defensin
PGIP1/2	Polygalacturonase Inhibiting Protein1
PID	Proportional-Integral-Derivative
PIN3/7	Pin-Formed3/7
PMS3	Photo-Period Sensitive Male Sterile3

PP2C	Phosphatase2C
PPFD	Photosynthetic Photon Flux Density
PPR	Pentatricopeptide Repeat
PR	Pathogenesis-related
Pro	Proline
PRT6/1	Proteolysis6/1
PSI	Photosystem I
PSII	Photosystem II
PstDC3000	*Pseudomonas syringae* pv. tomato strain DC3000
PSY1	Phytoene Synthase 1
PUB	Plant U-Box
PYL	PYR-like Proteins
PYR	Pyrabactin Resistance Proteins
qRT-PCR	Quantitative Real-time PCR
QTL	Quantitative Trait Loci
RAB21/6B	ABA-responsive21/6B
RAF	ERF Transcription Factor
RAP	Related to AP
RBOH	Respiratory Burst Oxidase Homologs
RCAR	Regulatory Components of ABA Receptor
RING	Really Interesting New Gene
RNA	Ribonucleic Acid
RNAi	RNA Interference
ROS	Reactive Oxygen Species
RPS2	Resistance to *Pseudomonas syringae2*
SA	Salicylic Acid
SAG	Senescence-associated Gene
SAIL	Syngenta Arabidopsis Insertion Library
SALK	Salk Institute for Biological Studies
SAPK2	Sucrose Non-Fermenting-1-Related Protein Kinase2
SD	Standard Deviation
SE	Standard Error
SEM	Standard Error of the Mean
SFC	SKP1-CULLIN1-F-box
SIG6	Signal Protein6
SIGnAL	Salk Institute Genomic Analysis Laboratory
SIS8	Sugar Insesnistive8
SKP1	S-phase kinase-association protein1
SLAC	Slow Anion Channel
SLs	Strigolactones
SNC1	Suppressor of npr1-1, Constitutive1
SNF1	Sucrose Nonfermenting
SNP	Single Nucleotide Polymorphism

SnRK2	SNF1-Related Protein Kinase2
SPP	Stromal Processing Peptidase
SRL1/2	Semi Rolled Leaf1/2
SSIV	SuperScript™ IV
SYT/SYTB	Synaptotagmin
T34	Biofungicide *Trichoderma asperellum* T34
TAG	Triacylglycerol
TAIR	The *Arabidopsis* Information Resource
TALENS	Transcription Activator-Like Effector Nucleases
T-DNA	Transfer DNA
TF	Transcription Factor
TGW	Thousand Grain Weight
TILLING	Targeting Induced Local Lesions in Genomes
TRE	Trehalose
tRNA	Transfer RNA
tRNA	Transfer RNA
UBP21	Ubiquitin-Specific Protease21
UBR	Ubiquitin Protein Ligase E3 Component N-Recognin
UK	United Kingdom
USA	United States of America
UTR	Untranslated Region
UV	Ultraviolet
WISC	Wisconsin Mutation Database
WRKY55	WRKY DNA-Binding Protein55
WT	Wild Type
ZFN	Zinc Finger Nucleases
ZIP	Basic Leucine Zipper
ZIP23	Basic Leucine Zipper
Z-ISO1	ζ-carotene isomerase1
ZNE1	Zinc nutrient essential
ZRT	Zinc regulated transporter
ϕPSII	Quantum Yield of Photosystem II

1 Introduction

1.1 Global food security and abiotic stress

Enhancing crop production, yield and stability under adverse conditions, is essential to meet the growing demand to feed a population that is projected to reach 9.7 billion by 2050 (Anderson et al., 2020; Dhankher & Foyer, 2018). The instability of future climate threatens global crop production and food security worldwide. Climate change refers to "long-term shifts in temperatures and weather patterns" according to the UN (United Nations, 2024). The impact climate change has on food security not only has implications for developing countries but is also a significant threat to developed countries (Lake 2012; Godfray et al., 2010; Schnitter & Berry, 2019).

The AR6 Synthesis Report: Climate Change (2023) stated that despite progress towards climate mitigation, global warming is likely to exceed 1.5°C above pre-industrial levels in the 21st century, with a predicted rise of 3.2°C by 2100 if current global climate policies remain. The Paris Agreement, a legally binding international treaty on climate change adopted at the UN Climate Change Conference (COP21) in 2015 set goals to hold "the increase in the global average temperature to well below 2°C above pre-industrial levels" and pursue efforts "to limit the temperature increase to 1.5°C above pre-industrial levels.". Global warming is predicted to have a huge impact on many sectors, with agriculture being one of the most vulnerable sectors to climate change. It's predicted that by 2080, world agricultural production could drop by 10-14.5%, with a drop of 16.9%-25.3% in developing countries (Cline, 2007). By 2050, it is predicted that crop yields will not be able to nourish the world's population (Ray et al., 2019).

The effect climate change could have on agricultural systems in developing countries may be additive to malnutrition and food insecurities in communities where there are already issues surrounding food security (Schnitter & Berry, 2019). In developing countries, adverse conditions directly affect farmers, which disrupts food accessibility for local communities (Rani & Reddy, 2023; Murniati, 2020), and in more developed countries, climate change has the potential to increase food prices, diminish nutritional

quality of diets and exacerbate nutritional inequalities (Masipa, 2017; Lake et al., 2012; Brizmohun, 2019).

Stress refers to a state where a plant is in non-ideal conditions, which negatively impacts a plants growth, development or metabolism. Significant impacts of stress in crop species are a major threat to yields and productivity due to the impacts on growth and development. Stress can then be categorised into biotic and abiotic stress. Biotic factors are organisms which share the plants environment such as pathogens, insects, pests and weeds, causing stress through competition, wounding, etc, whereas abiotic stress is caused by temperature, light, water, nutrient deficiency, toxicity, among other non-living factors. Stresses can be long or short term, and in a variety of intensities, with different plant species and individuals having differing tolerances to stress (Tardieu et al., 2018).

More than 50% of crop losses in agriculture occur due to abiotic stress (Minas et al., 2017), and abiotic stress causes around 50% of the worlds crop yield variability (Vogel et al., 2019). With global warming, multifactorial stress (two or more stress factors impacting a plant) is also predicted to increase in frequency, complexity and intensity (Mazdiyasani and AghaKouchak, 2015; Legmann and Rillig 2014; Sala et al., 2000). Even with low level stress, the increase in number of stress factors simultaneously impacting a plant causes a severe decline in plant growth and survival (Zandalinas et al., 2021).

Commonly in plant sciences, stress tolerance and resilience refer to a plants ability to adapt to environmental conditions which negatively impacts a plants growth, development or metabolism. Tolerance more refers to the processes in which plants adapt to survive and maintain productivity under stress whereas resilience is used more in terms of plants ability to recover after undergoing stress, and returning to normal growth and development after exposure, however these two terms are sometimes used interchangeably. Mechanisms for plant stress tolerance and resilience include changing gene expression, adjusting metabolisms, structural modifications, repair mechanisms and antioxidant systems (Tardieu and Tuberosa, 2010). The way in which plants respond to stress and its tolerance is highly dependent on the species, developmental stage, and previous stress exposure.

A major concern for food security is yield lost to excess heat. The Intergovernmental Panel on Climate Change (IPCC) only predicts an increase of 1.5 °C or more in the next two decades, but this small increase in mean temperature can contribute to catastrophic heat wave events plus more intense, more frequent and longer lasting temperature extremes worldwide (Karl and Trenberth 2003; Rohini et al., 2019; Masson-Delmotte et al., 2021).

In mild elevations in heat, changes in enzyme kinetics can be detected by the plant, which can trigger signalling cascades and adaptations. Low-level temperature increases influence gene expression, leading to the modulation of growth regulators such as auxins, gibberellins, and cytokinin's resulting in elongated hypocotyl and petioles, narrow leaves and early flowering (Casal and Balasubramanian, 2019). In order to prepare for further increases in temperature, heat-responsive transcription factors, including members of the *HEAT STRESS TRANSCRIPTION FACTOR* family are upregulated, which prime the plant for potential future temperature spikes. Mildly elevated temperatures can also alter photosynthetic and respiration rates, which can in turn increase growth, with plants showing high phenotypic plasticity in photosynthetic characteristics (Hikosaka et al., 2005).

When temperature rises to much higher levels than a plants optimal range, heat stress occurs, causing physiological and metabolic disruptions. Heat is sensed in the plant though thermosensors and thermosensitive elements- elements within the plant that change in structure/activity when experiencing heat stress, such as changes in fluidity of membranes or changes in protein shape (Lamers et al., 2020; Dai Vu et al., 2019). Thermosensors may be directly affected by heat by changes in proteins including the peroxidation or remodelling of phospholipids, and the unfolding, misfolding or aggregation of proteins. Thermosensors can also be indirectly affected through other parts of the cell such as altered metabolic fluxes, accumulation of reactive oxygen species (ROS), release of Adenosine Triphosphate (ATP) from cells, or reduced energy levels. When exposed to heat stress, plants alter the expression of stress-responsive genes, heat shock proteins, and antioxidant enzymes, involving complex molecular responses. (Khan et al., 2020).

Mild heat stress can slow growth and development of a plant, whereas prolonged or extreme heat stress can cause cellular damage, reduced reproductive success, and plant

death. Heat shock can occur when a plant experiences sudden and extreme heat, which can cause immediate cellular damage (Ahn et al., 2004). Heat stress can also disrupt plant hormones, crucial for signalling, which also can result in physiological changes that affect plant growth, development, and stress tolerance (Li et al., 2021). ROS such as O_2, $^{\cdot-}H_2O_2$, and OH are typical products of metabolic processes, however under high temperature, can accumulate and cause damage through metabolic arrest. When ROS accumulate, they can cause redox imbalance, lipid peroxidation, plus the degradation of chlorophyll, nucleic acids, and proteins (Saeed et al., 2023).

With climate change, temperatures are likely to increase, which can have particularly negative effects on photosynthetic efficiency, enzyme activity, and changes in metabolic processes, reducing both yield and crop quality (Moore et al., 2001; Karki et al., 2021; Lavkush et al., 2022). If heat stress occurs during important development stages such as flowering, it can disrupt pollen development, pollination, fertilisation, and seed development, which in turn can lead to reduced yield in crops such as cereals, where uninterrupted seed development is crucial for high yield. The effect of heat stress and other stresses commonly found in areas where heat stress occur, are additive. Other stresses like drought can exacerbate the negative impact of heat, as well as terminal heat stress leading to irreversible damage (Khan et al., 2020; Cohen et al., 2020). In order to mitigate the effects of heat stress on crop productivity and therefore food security, heat stress responsive genes need to be identified as well as genes conferring tolerance to heat, in order for genetic resources to be developed for enhancing heat stress tolerance (Jagadish et al., 2020).

Alongside heat stress, drought is also a significant threat to global food security by negatively impacting crop productivity and yield. Not only does climate change increase the frequency in which instances of drought are likely to occur, but also increases the intensity of the drought stress, which has implications for crop growth through reduced photosynthesis, impaired nutrient uptake, and hindered growth and development (Leng & Hall, 2019; Alabdallah et al., 2021). Water demand for agriculture is predicted to double by 2050, alongside a predicted drop in fresh water availability by 50% (Gleick, 2000).

Drought stress occurs when water availability in the soil is insufficient to meet plant demands, leading to dehydration, reduced cellular turgor, and metabolic disruption.

Plants have evolved to cope with drought through; drought avoidance- the process of quickly reducing water loss by stomatal closure and inhibited growth, drought escape- the process of accelerating a plants life cycle before stress occurs, and drought tolerance -maintaining growth by osmotic adjustment, reactive oxygen species (ROS) scavenging, and activation of stress-related genes (Skirycz et al., 2010; Kooyers, 2015).

Plants have several mechanisms to maintain water balance, such as increasing water uptake though the roots, reducing water loss by transpiration, and adjusting osmotic processes in cells (Rodrigues et al., 2019). Plants sense drought primarily through changes in water potential, which leads to osmotic stress, triggering the plant hormone abscisic acid (ABA) among other specific signalling responses including brassinosteroids, and ethylene phytohormone pathways (Aslam et al., 2022; Tardieu et al., 2018). Stress response pathways can also involve antioxidant and metabolite production and mobilization to maintain cellular homeostasis (Bailey-Serres et al., 2019; Aslam et al., 2022). ABA can trigger the immediate closure of stomata, which is an immediate reaction to reduce water loss through transpiration, by binding to its guard cell localised receptor (Postiglione and Muday, 2020). This induces a signalling cascade including synthesis of ROS, which are also induced by oxidative stress, and can cause cellular damage to the plant (Sun et al., 2020; Postiglione and Muday, 2020). Part of this signalling cascade includes the signalling responses of brassinosteroids, , and ethylene phytohormone pathways (Aslam et al., 2022; Tardieu et al., 2018), where hormone crosstalk can promote mechanisms avoid further stress (Kuromori et al., 2018), for example the use of modifying root architecture. During prolonged instances of water stress, plants can adapt root architecture to suit their environment, growing longer, deeper roots with reduced branching angles, allowing more water capture in soils that retain deep moisture content, or alternatively in soils that experience low precipitation, roots adapt to stay shallow (Dinneny, 2019). Auxin signalling allows for hydro patterning, by favouring lateral root emergence to areas of soil with higher water contents (Robbins and Dinneny, 2018). Vascular tissues in the plant -the xylem and the phloem, can signal water availability signals as well as moving photoassimilates between the shoots and the roots (Scharwies and Finneny, 2019).

While small increases in respiration can be seen in mild drought stress, the closure of stomata reduces CO_2 availability and transpiration, which in turn reduces

photosynthesis and therefore growth and yield (Rodrigues et al., 2019). The effects of drought can have different effects depending on what stage of development the plant is in. In early stage of development, germination can be particularly sensitive to drought, reported in many major crop species including but not limited to maize, sorghum and wheat (Queiroz et al., 2019; Patanè et al., 2013; Qayyum et al., 2011). Drought occurring at the vegetative stage in development can show leaf wilting, decline in plant height and interruption in establishment of buds and flowers (Bhatt and Rao, 2005). Limited water can cause decrease in nutrient uptake, especially nitrogen and potassium (Bista et al., 2020) with the reduction in nutrients having an effect on stem and shoot length (Gheidary et al., 2017; Razmjoo et al., 2008). Plant yield can also be reduced due to plant biomass decreasing from changes in root to shoot ratios (Akhtar and Nazir, 2013). Leaf number is also impacted by drought, which is vital for photosynthesis and therefore growth (Bhargavi et al., 2017). These factors that affect yield of vital crops worldwide has resulted in the need to develop drought-tolerant crop varieties through genetic modification and traditional breeding approaches that enhance crop resilience to water scarcity (Liu et al., 2022).

With some similarities to the effects of drought on plants, over 12% of agricultural land worldwide as being considerably affected by waterlogging stress (Setter and Waters, 2003). Waterlogging impacts the soils properties, displacing gasses with the influx of water into soil pores, and accumulating toxic compounds as anaerobic respiration takes place. Waterlogging stress effects the plant by reducing oxygen availability in the root due to slow diffusion rates in waterlogged conditions, which triggers a cascade of responses in plants, and impacts their growth and survival (Qi et al., 2019). While the oxygen sensors involved in waterlogging are so far unknown, anaerobic polypeptides with altered expression in early hypoxic stress have been identified (Asan et al., 2007; Agarwal and Grover, 2006).

Root hydraulic conductivity declines in waterlogged conditions, reducing the amount of photoassimilates available for the plant (Tan et al., 2018; Malik et al., 2002). Hypoxic or anoxic conditions of the soil result in a change in nutrient concentration soils become rich in Mn^{2+} and Fe^{2+}, devoid of NO_3^- and SO_4^{2-}, with higher concentrations building up the longer the waterlogging conditions last (Ponnamperuma, 1984). Soil waterlogged for only hours or days can still have a large negative effect on dryland crop yield (Leyshon and Sheard, 1974). The impact

waterlogging has on growth and development largely depends on factors such as species, growth stage, soil type, duration of the stress, and depth of waterlogging (Tian et al., 2021; Herzog et al., 2016). The main affects waterlogging has on crops is reduced growth in several major structures. Waterlogging stress leads to a reduction in leaf size, elongation rates, and increasing rates of senescence (Malik et al., 2001; Trought and Drew 1980) as well as effecting root structures: halting seminal root growth and promoting adventitious roots (although restricting overall length) (Trought and Drew 1980; McDonald et al., 2001). In these root structures, an increase of ethylene activates programmed cell death in root cortical cells and the aerenchyma in adventitious roots, which also releases CO_2 and toxic volatile substances from submerged tissues (Pan et al., 2021). This increase of anaerobic respiration in the roots leads to lower ATP production, which can inhibit growth (Gibbs and Greenway, 2003; Huang and Johnson, 1995) Waterlogging causes a decrease in nutrients in shoots and reduce concentrations of non-structural carbohydrate concentrations, which in turn reduce root and shoot biomass accumulation (Trought and Drew 1980; Malik et al., 2001). These effects can have a detrimental effect on yield final yield (Zheng et al., 2004; Dickin et al., 2008; Malik et al., 2002), therefore adapting crops to cope with waterlogging is a crucial target for breeding future crops.

To improve crop tolerance of abiotic stresses, several practices can be used individually or in conjunction with each other. Farming practices have evolved over time with practices like conservation tillage, cover cropping, and precision irrigation can help maintain soil moisture, prevent erosion, and reduce temperature fluctuations (Rangappa., et al., 2024 ;Sher et al., 2021; Quintarelli et al., 2022; Adeyemi et al., 2017). Farmers can also use these methods alongside optimized planting schedules and agroforestry practices to enhance plant adaptation to environmental stressors (Soni et al., 2017; Kirda, 2002). Implementing precision agriculture, including sensor-based monitoring and data-driven fertilization, ensures crops receive optimal nutrients and water, minimizing stress impacts (Zhou et al., 2021; Shin et al., 2022; Khanal et al., 2017). Crop protection such as bio stimulants, protective coatings, and stress-mitigating agrochemicals are more commonly being used in modern agriculture, including to mitigate risk of pest and disease damage, which can increase susceptibility to abiotic stress (Ma et al., 2022; Zheng et al., 2012; Prokisch et al., 2024; Suzuki et al., 2014). Farmers can also incorporate the use of landraces into their rotations, which

are heterogeneous, local adaptations of domesticated species, which have developed naturally to withstand harsh environmental conditions such as drought, salinity, and extreme temperatures (Sangam et al., 2016).

While improving farming practices, farmers can provide added crop resilience to a changing climate, but due to the increasing threat of abiotic stress on plants, there is a also a need for new genetic resources to enhance abiotic stress tolerance to implement in crop breeding and development (Wang et al., 2016; Numan et al., 2021; Capell et al., 2004). One method for combatting the issues faced by climate change and its impact on crops is genome editing, in which genes related to abiotic stress are targeted (Kaur et al., 2022). By developing stress-tolerant crop varieties, sustainable food production can be improved by enhancing the resilience of agricultural systems to changing environmental conditions and abiotic stresses.

1.2 Targeted mutagenesis of crops for abiotic stress tolerance

Genetic manipulation as become a tool to improve crops, which reduces time constraints of traditional plant breeding, and facilitates access to novel genes and traits that may not be available through crossing. Genetically modifying a crop also allows for novel expression of specific genes, such as tissue and growth stage specific expression or silenced expression. The process of genetically manipulating crops for improving tolerance to abiotic stress has many steps, which vary in time and cost, and it is worth noting that these steps may not be linear, and some steps may be omitted in certain circumstances, be collaborative with other lab groups, or be based off findings in peers publications. The first step is to identify a gene to target and to obtain plants (usually first in a model species such as *A. thaliana*) with mutations in that gene of interest. These mutants can be then tested in growth room or glasshouse conditions to confirm phenotypes, before generating and testing orthologue mutations in crop species or species of interest. After this experimentation, if the mutants show promising performance in the growth room and glasshouse conditions, the experimentation can be moved to field trials, where usually, crop species are tested in regular outdoor conditions to assess yield and growth parameters, before being tested in outdoor conditions with abiotic stress. At this point, if lines show promise in the field, bulking and commercial production may occur.

The process of identifying genetic candidates generally falls into two categories: forward and reverse genetics. Forward genetics is identifying genetics or a mutation linked to an observable trait (phenotype), whereas reverse genetics links a known genetic change to an unknown phenotype (Griffiths et al., 2004). Development of technologies such as sequencing technology, quantitative trait loci (QTL) sequencing, gene cloning, bulk segregant analysis and gene mapping have allowed these processes to advance the identification of genes linked to valuable crop traits (Choudhary et al., 2023). After genes are identified, some methods require procuring mutant lines through screening in order to produce clean mutant lines. Some of these methods are detailed further in this study.

Once genes of interest are identified, performance needs to be evaluated, which in most cases start with assessing performance in model species (to cut time and costs) in small scale glasshouse or growth room trials. In terms of abiotic stress tolerance, this would usually be exposure to different treatments of stress and measurement of several parameters to look at growth, development and plant survival. In this closed environment, exposing plants to treatment is easier to apply and control than in field environments. It is usually at this stage that if research is being done in model non-crop species, mutant lines in orthologue genes are developed in crops, and similar tests are done to see if phenotypes are conserved among species.

Lines showing promise in terms of performance in these closed environments can then be tested in the field. The translation to growing plants in the field is crucial, due to the need for crops to cope with a range of environments that can be hard to replicate, such as large fluctuations in temperature, light and soil conditions (Poorter et al., 2016). A meta-analysis of plants grown in the field opposed to in growth room and glasshouse conditions has shown phenotypic and morphological differences in plants (Poorter et al., 2016). In terms of developing crops for abiotic stress tolerance, lines may be tested first in non-stressed conditions, in order to assess their yield compared to current commercial lines, before testing in areas of known stress or specialist equipment to replicate natural stress, Lines in crops that show promise in terms of yield and performance under stress may then go forward to commercially be produced

In order to be commercially viable, genetically modified lines need to be competitive with current commercial lines by gathering data from various field trials over multiple

years, as well as undergoing strict testing to assess risks to the environment and human health (Raybould, 2012). After safety approval and cultivar registration, seeds are bulked and deployed, ready to be grown by farmers (Kedisso et al., 2022).

The one of the main focusses of this study is the use of targeted mutations in genes of interest, looking in particular at the gene identification, and testing in the growth room and field. In this study, genetic material targeted mutagenesis is the specific change in genetic material, using of a variety of techniques including, Transfer-DNA (T-DNA), Targeting Induced Local Lesions in Genomes (TILLING), Ribonucleic Acid (RNA) interference (RNAi), Clustered Regularly Interspaced Short Palindromic Repeats (CRISPR)/CRISPR-Associated Protein (Cas)-derived DNA binding domains, Transcription Activator-Like Effector Nucleases (TALENs), Zinc Finger Nucleases (ZFNs), and fast neutron mutagenesis, among others (Shahwar et al., 2023). These methods allow precise and specific modifications in the genome of plants. Targeted mutagenesis allows research into gene functions, improvement of crop traits, and enhances understanding of plant genetics. Targeted mutagenesis allows mutations in genes that were previously challenging to access, as well as to simultaneously mutate multiple loci and create large deletions (Lloyd et al., 2005).

TILLING is an approach using reverse genetics, which uses chemical mutagenesis alongside high-throughput screening in order to identify specific point mutations in target genes (McCallum et al., 2000a, McCallum et al., 2000b). TILLING lines are generated using mutagens such as ethyl methanesulfonate (EMS), which result in several point mutations in the genome across a number of individuals (Griffiths et al., 2004) The lines are then screened to find individuals which contain mutations in genes of interest. One of the disadvantages of TILLING lines is that commonly, newly developed TILLING lines also contain unwanted mutations, alongside the mutation of interest (Enders et al., 2015). Therefore, backcrossing TILLING lines is common practice in order to remove these unwanted mutations, which can take considerable amounts of time. TILLING has been successfully used in plant research to create mutants for functional genomics studies and crop improvement (Suzuki et al., 2007; Chen et al., 2014; Muth et al., 2008; Uauy et al., 2009; Sabetta et al., 2011; Slade et al., 2012; Chawade et al., 2010; Kumar et al., 2013). One of the key advantages of TILLING is its ability to enable development of mutant collections for gene function analysis, creating genetic diversity, and identifying novel alleles for crop improvement

(Chawade et al., 2010; Slade et al., 2012). The nature of TILLING mutations being developed through chemical mutagenesis, means in the UK, field trials can easily be carried out with current legislature, as they are not classified as genetically modified organisms (GMOs).

A T-DNA insertion mutation is the integration of foreign DNA from *Agrobacterium tumefaciens* into the plant genome. A T-DNA fragment is inserted into the genome at a specific point, which is flanked by border sequences (O'Malley et al., 2015). The inserted DNA can have a range of effects on the genome, as they can induce base substitutions, insert short sequences, and cause small deletions in the plant genome at the specific site targeted, which can disrupt or activate the targeted gene (Zhao et al., 2009). T-DNA insertions are stable and can be used to generate knock-out alleles for reverse genetics and targeted gene function studies. The ease at which T-DNA insertions can be obtained makes them commonly used in plant science, with efficient methods for T-DNA transformation available, (Pucker et al., 2021; Clough and Bent, 1998) and large collections of *Arabidopsis thaliana* (*A. thaliana)* T-DNA insertion lines available including Salk Institute for Biological Studies (SALK), German Arabidopsis Functional Genomics Network - Knockout Arabidopsis T-DNA (GABI-KAT), Syngenta Arabidopsis Insertion Library (SAIL), and Wisconsin Mutation Database (WISC) lines (in Col-0, however collections in other backgrounds exist) , which cover most loci (Sessions et al., 2002; Alsonso et al., 2003; Rosso et al., 2003.; Woody et al., 2007). Tools to assist selection of mutants have also been developed (largely online and available/accessible to all), and possible mutants can often be shipped within days, proving a convenient and cost effective method of research, without the need to remove unwanted mutations as seen in TILLING lines (O'Malley et al., 2015). T-DNA mutants also have the benefit of being easily detectable, with many T-DNA insertion mutants obtained from databases such as SALK/SAIL containing universal primers for detection through Polymerase Chain Reaction (PCR)-based approaches and sequence analysis (Pan et al., 2005). It's noted that this method of generating mutant lines can have problems: some percentage of lines from some seed banks do not contain the annotated T-DNA insertion at the identified locus (12.6 % of Salk and 14.5 % of SAIL lines), and a large class of these insertion lines have a high false positive rate when testing for presence of the insertion, cross contamination of lines, induced DNA rearrangements, and added time taken to check the genotype of

lines after receiving them from banks (Clark and Krysan 2010; O'Malley et al., 2015). Alongside this, a small number of genes have no corresponding viable lines in these banks, or all inserts in specific genes result in a lethal phenotype (O'Malley et al., 2015).

There have been many success stories in terms of engineering plants for abiotic stress tolerance through mutagenesis. Some strategies involve mechanisms to overcome one type of stress, while other strategies target mechanisms for overcoming more than one type of stress.

With drought being an ongoing problem for crop production, which will increase due to changing climate, several candidates in many species have been modified for enhanced drought stress tolerance. Due to the significance of ABA in response to several abiotic stresses, *ABA-induced transcription repressors (AITRs*) have been highlighted as targets. Mutations in the *AITR* family in *A. thaliana* showed increased tolerance to both drought and salinity stress without a reduction in plant fitness (Chen et al., 2021). Other work in *A. thaliana* for increased drought stress tolerance has been seen in CRISPR-CAS9 mutations in the structural gene *OLIGOSACCHARYLTRANSFERASE SUBUNIT 2*(*OST2)*, vacuolar H^+*-INORGANIC PYROPHOSPHATASE* (*AVP1*) regulating gene, *TREHALOSE 1* (*TRE1*), and activation through CRISPR-CAS9a in *ABSCISIC ACID-RESPONSIVE ELEMENT BINDING* (*AREB1*) gene. Targets for increased drought stress tolerance have also been seen in cereal crops including Rice, where mutagenesis through CRISPR-CAS9 has targeted regulatory genes *DROUGHT-RESPONSIVE ELEMENT BINDING 1 (DERF1), PHOTO-PERIOD SENSITIVE MALE STERILE 3 (PMS3), MUT S HOMOLOG 1 (MSH1), MY ELOB LASTOSIS 5 (MYB5),* and *STROMAL PROSESSING PEPTIDASE* (*SPP),* among others such as rice *ENHANCED RESPONSE TO ABSCISIC ACID1* (*OsERA1), SEMI ROLLED LEAF1 (SRL1), SRL2* and rice *DROUGHT AND SALT TOLERANT (OsDST),* plus genes acting downstream of SUCROSE NON-FERMENTING 1 RELATED PROTEIN KINASE 2 (SAPK2): rice *LATE EMBRYOGENESIS ABUNDANT 3 (OsLEA3),* rice *BASIC LEUCINE ZIPPER 23 (OsbZIP23), SLOW ANION CHANNEL 1 (OsSLAC1),* and *OsSLAC7* (Zhang et al., 2014; Ogata et al., 2020; Liao et al., 2019; Yadav et al., 2023; Lou et al., 2017). Increased drought tolerance in other crops such as wheat has also been accomplished by targeted mutagenesis, in wheat *DEHYDRATION RESPONSIVE*

ELEMENT BINDING PROTEIN (TaDREB2) and ETHYLENE RESPONSE FACTOR 3 (TaERF3) (Abdallah et al., 2022; Kim et al., 2018) and targets in other crop species such as maize (Guo et al., 2014; Shi et al., 2015; Shi et al., 2017) tomato (Illouz-Eliaz et al., 2020; Lui et al., 2020; Wang et al., 2017; Li et al., 2019), chickpea (Badhan et al., 2021; Razzaq et al., 2020), cotton (He et al., 2020), rapeseed (Wu et al., 2020).

Another crucial step to increasing food security is increasing crop resilience to heat stress. Several approaches have been used to increase resilience to heat stress in plants through targeted mutagenesis. In *A. thaliana*, genes such as the transcription factor DEHYDRATION RESPONSIVE ELEMENT BINDING PROTEIN2A (*DREB2A)* (Sakuma et la 2006), *A. thaliana HEAT SHOCK FACTOR (AtHSF1)* (causing constitutive heat shock protein synthesis) (Lee et al., 1995), and *FATTY ACID DESATURASE 7* (*FAD7*) (Murakami et al., 2000) have all successfully been targeted to induce enhanced heat stress tolerance. In Rice, the transcription factor HEAT STRESS TOLLERANT 1 (HST1) can be targeted through mutagenesis for increased heat tolerance, as well as the rice UBIQUITIN SPECIFIC PROTEASE21 (OsUBP21) (Ding et al., 2019). A targeted mutagenesis approach can also be seen in other species include the targeting lettuce *9-CIS-EPOXYCAROTENOID DIOXYGENASE 4* (*LsNCED4)* in lettuce, which allowed germination at higher temperatures (Bertier et al., 2018). Alongside targeting specific genes for knockout or downregulation for stress tolerance, some targeted genes result in increased sensitivity which allows greater understanding of the mechanisms behind stress resistance. This was the case with targeting genes such as *HEAT STRESS SENSITIVE ALBINO 1 (HSA1)* in tomato (Qui et al., 2018) and *BRASSINAZOLE RESISTANT 1* (*BRZ1)* in tomato, which regulates ROS formation (Yin et al., 2018), with these knockouts producing heat sensitive plants, allowing further understanding of the importance of these genes in heat stress. This understanding can then be used to target genes for overexpression or other regulatory mechanisms to manipulate these genes for increased stress tolerance.

1.3 Photosynthesis as a target for crop improvement

Photosynthesis is a vital process for the survival and reproduction of plants, algae, and photosynthetic bacteria, involves the conversion of solar energy into chemical energy Haxo & Blinks (1950). In photosynthesis, Photosystem II (PSII) and its associated

pigment protein complexes play crucial roles, each contributing distinct functions vital for efficient light harvesting and protection against photodamage. PSII serves as the primary protein complex responsible for initiating the light-dependent reactions of photosynthesis. Along with the antenna light harvesting complexes it absorbs photons and transfers the captured energy to a special pair of reaction centre chlorophyll molecules, triggering electron transport and ATP synthesis (Nelson & Junge, 2015). PSII includes light harvesting complex IIs (LHCIIs) which contain pigments, among which are chlorophyll *a*, chlorophyll *b* and carotenoids. Chlorophyll *a* and *b* are the most prominent pigments and involved in the absorption primarily of red and blue light, whereas carotenoids are accessory pigments involved in the absorption of yellow orange and red light. Carotenoids can harvest energy from light before passing energy to chlorophylls through a low energy state transfer: singlet-singlet excitation transfer, in order to extend the range of light in which plants can absorb (Hashimoto et al., 2016). They also have a putative role in quenching chlorophyll in photoprotective mechanisms (below).

Chlorophyll molecules are bound to the chlorophyll binding proteins within the LHC of PSII and Photosystem I (PSI). On the absorption of light, chlorophyll goes from ground state to a singlet excited state. To return to the ground state, the chlorophyll molecule needs to dissipate energy. There are four main ways in which it can dissipate energy. One method to dissipate excitation energy is through photosynthetic reactions to provide energy and reducing power for CO_2 assimilation, driving plant growth and development. The chlorophyll molecule can also dissipate this energy through non-photochemical quenching (NPQ) where the energy is dissipated by heat. The plant can also dissipate a small amount (1 – 2 %) of energy though light, termed chlorophyll fluorescence. The chlorophyll can also convert to a triplet chlorophyll, which can then excite oxygen for it to return to its ground state, which produces toxic ROS. Through absorbing excessive energy from chlorophyll, carotenoids can also deactivate triplet chlorophyll and release the energy through polyene vibration therefore preventing photodamage to LHCs in PSII (Frank and Cogdell 1996; Jahns and Holzwarth 2012).

Under abiotic stress conditions the efficiency of photosynthesis is significantly impacted, leading to limitations in the performance of the photosynthetic machinery (Muhammad et al., 2021) by disrupting PSI, PSII, electron transport, carbon fixation, ATP generation, and stomatal conductance, with varying degrees of sensitivity among

different components (Nouri et al., 2015). One of the more sensitive aspects of photosynthesis to abiotic stress is the activity of PSII. Abiotic stress factors such as heat, salinity, drought, and high light intensity can damage PSII, which leads to photoinhibition and also disrupts redox signalling pathways (Gururani et al., 2015). When the repair of PSII is inhibited, the damage caused by stress can be increased (Nath et al., 2013). Studies have shown that abiotic stressors like salinity can inhibit PSII activity by affecting both the acceptor and donor sides of PSII, which reduces photosynthetic capacity and can lead to the destruction of chlorophyll (Athar et al., 2015). During abiotic stress, ROS accumulate such as hydrogen peroxide (H_2O_2), and singlet oxygen ($^1O2$), which can cause a decline in photosynthetic efficiency (Wu et al., 2017).

Improving photosynthesis in crop plants is a goal for enhancing plant productivity and therefore ensuring food security. Genetic targets are being explored to optimise photosynthesis, plant productivity and therefore potentially increase yield. One approach involves targeting plant components to accelerate recovery from photoprotection. This would increase productivity by enabling crop plants to readjust their systems more efficiently when transitioning from excess sunlight to shadier conditions (Kromdijk et al., 2016). Optimising canopy structure can also maximise canopy photosynthetic CO_2 uptake, especially under elevated CO_2 conditions (Song et al., 2013). Architectural properties of the canopy could provide targets for enhancement, including leaf length, width, and orientation, to enhance light interception and photosynthetic efficiency (Murchie and Burgess, 2022). Several enzymatic components of photosynthesis have been targeted, like sedoheptulose-1,7-bisphosphatase (Subphase) to increase photosynthesis and grain yield in wheat (Driever et al., 2017).

1.4 Thesis objectives

This thesis aims to identify candidate genes for targeted mutagenesis in future crop improvement approaches, as well as in field characterisation of previously developed genetic resources with a view for improving abiotic stress tolerance of crops.

The first objective of this study aims to assess TILLING mutants in key genes within in the Arg/N-degron pathways in field conditions, to bridge the gap between previous studies in growth room/glasshouse conditions and growth in the field.

The second objective of the study is to identify candidate genes underlying loci linked with photosynthetic heat stress in Rice from a GWAS previously carried out by Robson et al., (2023). From these genes, T-DNA insertion mutations in model species *A. thaliana* can be obtained to provide genetic resources for testing photosynthetic heat tolerance which will then be tested for photosynthetic heat tolerance. This should assess which mutants show tolerance or sensitivity mainly using chlorophyll fluorescence imaging and pigment content analysis, as well as to identify genes important in heat stress tolerance.

The final objective of this study is to use other indicators of heat stress such as fertility and root architecture to test the phenotypes of the T-DNA insertion mutations. This can then be used to identify candidate genes with most promise for future genetic improvement of crops.

2 Field performance of mutants conferring abiotic stress in N-degron pathways and ABA signalling

2.1 Introduction

With an expanding population, there is higher demand for food, but with ongoing climate change and extreme weather conditions, it is becoming increasingly difficult to meet demand. In order to improve food security, strategies need to be developed to close the yield gap in crops, by increasing yields and minimising crop losses. One such strategy to reduce crop losses is by improving crop survival under abiotic stress by manipulation of crops on a molecular level. This study also explores the potential molecular targets within the PLANT CYSTEINE OXIDASE (PCO) branch of the Arg/N-degron pathway and the ABA signalling pathway. These pathways have been shown previously in the model species *A. thaliana* to be involved in the regulation of plant development and response to environmental stress (Gibbs et al., 2014a; Gibbs et al., 2014b; Licausi *et al*., 2011; Ng et al., 2014). There is evidence that these roles are also present in Barley (*Hordeum vulgare)* (Mendiondo et al., 2016; Vicente et al., 2017; Seiler et al., 2011; Hong et al., 1992) an important cereal grown globally both economically and in terms of food security. This economically important crop can be used as a model species for other crop species, plus has published methods for gene editing and available TILLING resources are available through collaboration (Mendiondo et al., 2016), therefore is an ideal species to study these pathways.

By further understanding the role of PRT6 and N-TERMINAL GLUTAMINE AMIDASE (NTAQ) in the N-degron pathways and ABA INSENSITIVE 5 (ABI5) within the ABA signalling pathway in barley, the manipulation of these pathways can be explored as a possible target for future plant breeding to enhance abiotic stress tolerance in Barley.

2.1.1 The N-degron pathways

The N-degron pathways are highly conserved among prokaryotes and eukaryotes. The N-degron pathways regulate the half-life of proteins through targeted degradation. Targets of the pathways are proteins recognised by the nature of their amino- (N-)

terminus (Nt) residue. If an Nt residue is “destabilising”, it is exposed on the protein (accessible for enzymatic components) and has an accessible downstream lysine(s), this is termed an N-degron. Destabilising Nt residues can undergo post translational modifications within the N-degron pathway, resulting in the N-degron being recognised by an ubiquitin E3 ligase (N-recognin) and therefore is signalled for degradation.

Eukaryotes (excluding plants) contain the following branches of the N degron pathways: arginylation (Arg)/N degron pathway, Acetylation (Ac)/N-degron pathway (Hwang et al., 2010), formyl-(f)Met/N-degron pathway, Pro/N-degron pathway (Varshavsky 2019) and Gly/N-degron pathway (Timms et al., 2019). In plants, the Ac/N degron pathway has been reported (Gibbs, 2015) however there is wider research on the Arg/N-degron pathway. The main focus of this study will be in the Arg/N-degron pathway.

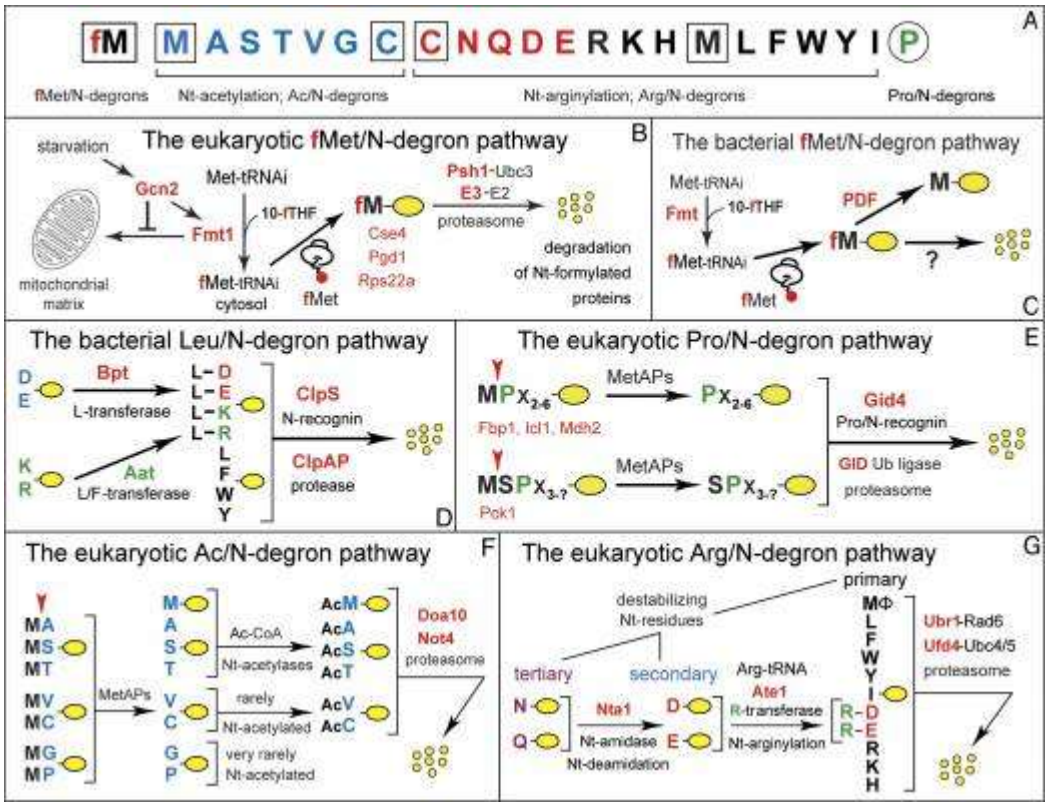

Figure 2.1: From Varshavsky (2019); N-degron pathways. Nt-residues are indicated by single-letter abbreviations. A yellow oval denotes the rest of a protein substrate. (A) Twenty amino acids of the genetic code are arranged to delineate specific N-degrons. Nt-Met is cited three times because it can be recognized by the Ac/N-degron pathway (as Nt-acetylated Ac-Met), by the Arg/N-degron pathway (as unacetylated Nt-Met), and by the fMet/N-degron pathway (as Nt-formylated fMet). Nt-Cys is cited twice, because it can be recognized by the Ac/N-degron pathway (as Nt-acetylated Cys) and by the

Arg/N-degron pathway (as an oxidized, arginylatable Nt-Cys sulfinate or sulfonate, formed in multicellular eukaryotes but apparently not in unstressed S. cerevisiae). (B) The eukaryotic (S. cerevisiae) fMet/N-degron pathway (Kim et al., 2018); 10-fTHF, 10-formyltetrahydrofolate. (C) The bacterial (E. coli) fMet/N-degron pathway (Piatkov et al., 2015). (D) The bacterial (V. vulnificus) Leu/N-end rule pathway (Graciet et al., 2006). (E) The eukaryotic (S. cerevisiae) Pro/N-degron pathway (Chen et al., 2017, Dougan et al., 2018, Dong et al., 2018). (F) The eukaryotic (S. cerevisiae) Ac/N-degron pathway (Shemorry et al., 2013). (G) The eukaryotic (S. cerevisiae) Arg/N-degron pathway (Varchavsky et al., 2011, Tasaki et al., 2012)

2.1.2 The Arg/N-Degron pathway

The Arg/N-degron pathway (recognising unmodified basic or hydrophobic residues) can then be subdivided (depending on the E3 ligase recognising the residue) into the PROTEOLYSIS 6 (PRT6)/N-degron pathway and the PRT1/N-degron pathway (Garzón et al., 2007; Potuschak et al., 1998). PRT1 recognises residues: Phe, Tyr, Trp, Leu and Ile, while PRT6 recognises: Arg, Lys and His. E3 Ubiquitin protein ligases support ubiquitin conjugating enzyme E2 transfer ubiquitin to recognised substrates by forming a Gly-Lys isopeptide bond. Protein substrates with a ubiquitin chain are then recognised by the 26S proteasome and degraded to short peptides.

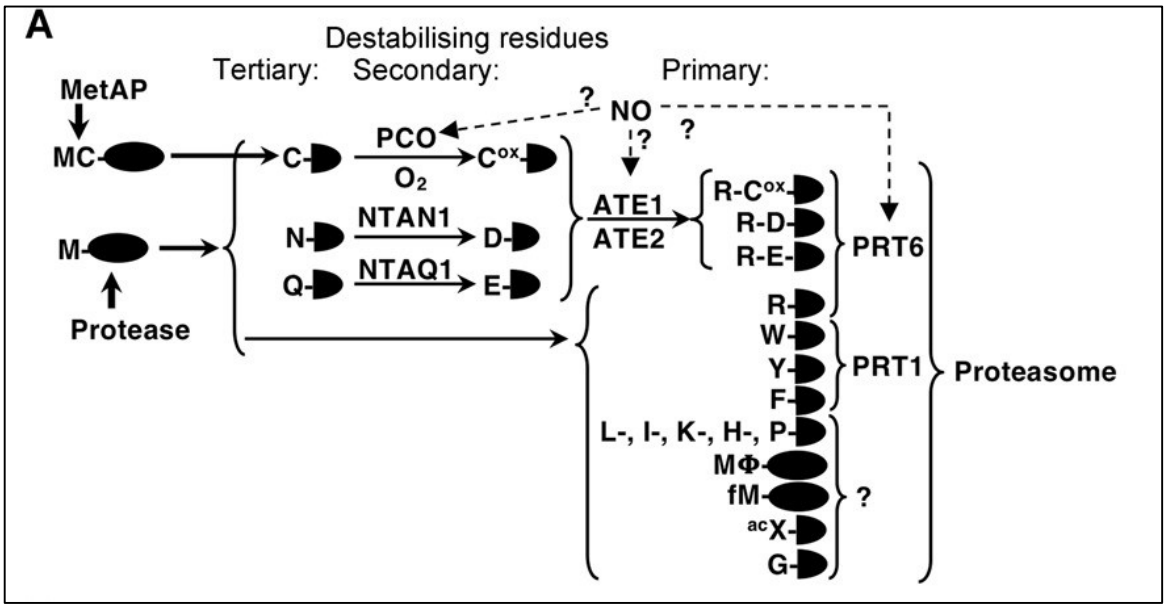

*Figure 2.2: From Holdsworth et al., 2020: Schematic representation of plant Arg/N-degron pathways. Cleavage of proteins by exo- or endo-peptidases leads to the production of novel Ct-proteoforms that may have destabilizing residues. The identity of primary, secondary and tertiary destabilizing residues is shown. The single amino-acid code is used. fMet, formyl-Met; ^{ac}X, Nt-acetylated residue; **Φ** denotes hydrophobic residues; C^{OX}, Cys-sulfinic acid; PCO, plant cysteine oxidase; NTAQ1, AT; NTAN1, Nt-Asn amidase; MetAP, Methionine amino-peptidase. The functional position of nitric oxide (NO) in the PCO branch of the PRT6 N-degron pathways is not currently known.*

In the PRT6 N-degron pathway, residues on the protein (destabilising residues) are recognised by PRT6. The residues can be divided into tertiary, secondary and primary destabilising residues. Tertiary destabilising residues Gln and Asn are converted to secondary destabilising residues Glu and Asp by amidohydrolases NTAQ and N-TERMINAL ASPARAGINE AMIDASE (NTAN), respectively. The tertiary destabilising residue Nt-Cys is oxidised to form secondary destabilising residue Cys-sulphinic acid by PLANT CYSTEINE OXIDASE (PCO)s (Weits et al., 2014). The secondary destabilising residues can then be converted to primary destabilising residues by arginylation by ARGINYL- TRANSFER-RNA (tRNA) TRANSFERASE (ATE) (Graciet et al., 2009), before being recognised by PRT6. In the PRT/N-degron pathway, apart from initial protease action in cleaving Met to reveal a N-terminal residue recognised by PRT1, there are no known further modifications of the residue. The residues Ala, Gly, Ser, Thr, Val, Met and Pro are all residues that are not recognised by PRT6 or PRT1 and are known as 'stabilising' residues.

2.1.1 Substrates of the Arg/N-Degron pathway

In plants, there are few confirmed substrates of the N-degron pathways, and substrates found are all in the PRT6/N-degron pathway. Substrates for the pathway require a destabilising residue in the form MCGAIL. In *A. thaliana*, the Group VII ERF HYPOXIA RESPONSE ERF (HRE)1, HRE2, RELATED TO AP (RAP)1.12, RAP 2.2 and RAP2.3) have all been shown to be substrates of the PRT6 N degron pathway (Gibbs et al., 2011, Licausi et al., 2011; Gibbs et al., 2018; Vicente et al., 2017, Gibbs et al., 2014; Wang et al., 2018) and in Poplar (*poplus*) the substrate Pop_ERFB2-1 has also been identified in vivo studies in protoplast (Dalle Carbonare et al., 2019).

Group VII ERFs, BARLEY ETHYLENE RESPONSE FACTOR1 (HvBERF1) and HvRAF have been found to be substrates of the N-degron pathways in Barley (Mendiondo et al., 2016 and Mendiondo et al., unpublished). The Group VII ERF BERF1 has most similarity to *A. thaliana* RAP2.12 and mediates *BARLEY KNOTTED1-LIKE HOMEOBOX 3* (*Bkn3*) gene by ethylene (Osnato et al., 2010), which is a substrate of the PRT6 N-degron pathways in vitro (Mendiondo et al., 2016). Also found in Barley, the group VII ERF *Hordeum vulgare ROOT ABUNDANT*

AP2/ERF TRANSCRIPTION FACTOR (*HvRAF*), which when overexpressed in *A. thaliana* leads to the upregulation of stress response genes such as *PLANT DEFENSIN 1.2 (PDF1.2), JASMONATE RESPONSIVE 3 (JR3), PATHOGENESIS-RELATED 1 (PR1), PR5*, and *GLUTHIONE 1* (*GSH1)* (Jung et al., 2007). Overexpression was also seen to increase tolerance to pathogens, and tolerance of root growth and germination under high salinity (Jung et al., 2007).

2.1.1 The Arg/N-Degron pathway and stress responses

The study by Gibbs et al., (2011) showed in *A. thaliana* that mutants *ate1ate2* and *prt6* showed genes relating to anaerobic metabolism including *ADH1*, *SUS4* and *PDC1* were constitutively expressed, similarly to Wild Type (WT) seedlings under induced hypoxia. In the same study, 7-day old seedlings were grown in argon chambers under hypoxic conditions for 9hrs and 12hrs before three days recovery. *Prt6* and *ate1ate2* mutants showed enhanced survival compared to WT (**Figure 2.3**) (Gibbs et al., 2011). Repeated studies with the same prt6 T-DNA insertion line also showed higher submergence tolerance than WT when submerged for longer periods.

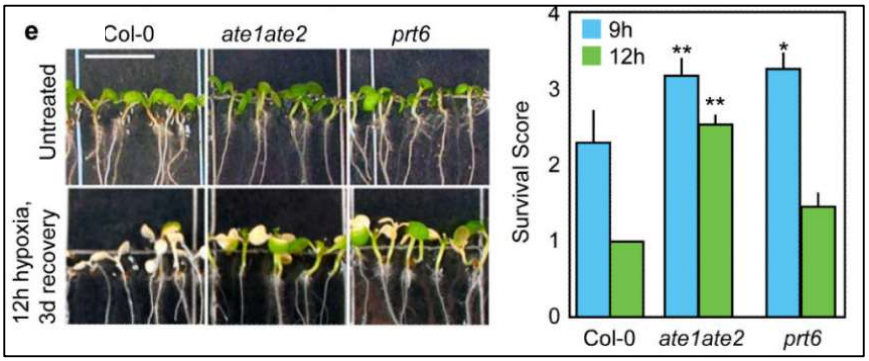

*Figure 2.3: From Gibbs et al., (2011). Seedlings after 12 h of hypoxia and three days recovery. Scale bar 0.6 cm. f. N-degron pathways mutants are less sensitive to hypoxia stress. Data are mean of replicate experiments ± SD; * = P < 0.05, ** = P < 0.01.*

A similar study released in the same year by Licausi et al., (2011) showed contradicting results when 5-week-old *ate1 ate2* and *prt6* T-DNA insertion line mutants grown in soil were submerged for 84hrs had lower chances of survival compared to WT. Differences in results could be due to the differences in relative humidity of the plants,

differing oxygen content in the plants or the different growing conditions or age of plants in the studies.

Several other studies have shown that mutants of the enzymatic components of the Arg/N-degron pathway support Gibbs' findings of increased submergence tolerance (Riber et al., 2015, Weits et al., 2014). Riber et al., (2015) showed *prt6* mutants *greening after extended darkness* (*ged1*) mutant allele, which is a knockout mutant, not only showed survival under periods under darkness but also under submergence in both dark and light conditions. Weits et al., (2014) showed that in overexpression of the Arg/N-degron component *PCOs* (*PCO1* and *PCO2*) a decrease in survival rate after submergence of *A. thaliana*. This suggests an inability to activate a hypoxia response without the presence of O_2 as a co-substrate, as shown when the PCO-overexpressors were exposed to anoxia. It was also shown that in aerobic conditions a double *pco1pco2* mutant increased expression of hypoxia marker genes (Weits et al., 2014). PCO1 and PCO2 can also be induced by Group VII ERF transcription factor RAP2.12, creating a feedback loop to regulate the response. The Group VII ERFs accumulation under submergence can pre-adapt plants to further hypoxia survival, priming the plant for future submergence, shown to be enhanced in *prt6* mutants (Hartman et al., 2019). The link between the stabilisation of Group VII ERFs and the upregulation of hypoxia response genes explains the phenotypes seen in these studies, as explored in the *ATE* double mutant *ate1ate2* - shown to upregulate hypoxia response genes (De Marchi et al., 2016; Mustroph et al., 2009).

2.1.2 Arg/N-degron pathway mutants used for further study in field

In Mendiondo et al (2016), to investigate the role of PRT6 in barley waterlogging, two missense mutations in *PRT6* developed through Targeting Induced Local Lesions In Genomes (TILLING) were identified. Both mutants had a decrease in expression of Prt6 RNA and showed to be less effected by waterlogging than the WT (**Figure 2.4**) (Mendiondo et al., 2016). The mutants also showed a higher chlorophyll content after hypoxia, as well as increased hypoxia-related genes with and without waterlogging stress (Mendiondo et al 2016). These mutants have therefore shown to be of similar phenotypes to that seen in RNAi lines in *PRT6* and have shown to be important targets

for plant breeding. In previously published works, these mutants have been shown to enhanced waterlogging tolerance in glasshouse and growth room conditions, however, have not been tested in field conditions.

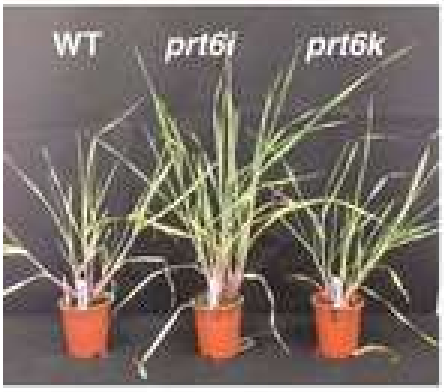

Figure 2.4: From Mendiondo et al (2016). Phenotypes of two barley TILLING lines containing mutations in PRT6. Photograph of 20-day-old plants following 20 days of waterlogging, showing enhanced growth of TILLING lines compared to WT (Sebastian).

2.1.3 ABI5- a transcription factor promoted by ABA

Abscisic acid (ABA) first discovered in the 1960s as a hormonal factor affecting the abscission of fruit, has several key roles in plants such as: maintaining seed dormancy (Finkelstein et al., 2008), inhibiting root growth (Luo et al., 2014), inducing stomatal closure (Hsu et al., 2021; Desikan et al 2004) inhibition of leaf senescence through Ca^{2+} and Calmodulin signalling (Song et al., 2016; Dai et al., 2018) and the promotion of ripening in fruits (Leng et al., 2014). ABA has an important role in cellular processes within the plant such as seed dormancy, germination, vegetative growth and root architecture (Xiong and Zhu 2003; Finkelstein et al., 2008 and Harris 2015). ABA has also been shown to play a key role in environmental stresses by regulating physiological responses such as stomatal closure and altering gene expression (Cutler et al., 2010; Kim et al., 2010; Yamaguchi-Shinozaki and Shinozaki 2006; Shinozaki and Yamaguchi-Shinozaki 2007; Seki et al., 2003).

ABA receptors and phosphatases PYRABACTIN RESISTANCE PROTEINS(PYR), PYR-LIKE PROTEINS (PYL), REGULATORY COMPONENTS OF ABA RECEPTOR (RCAR), PHOSPHATASE 2C (PP2Cs) form a complex which prevents

the phosphorylation of SUCROSE NONFERMENTING 1 (SNF1)-RELATED PROTEIN KINASE 2 (SnRK2s) which allows SnRK2 to activate the basic leucine zipper transcription factors (bZIP) ABA INSENSITIVE 5 (ABI5) through phosphorylation (Banerjee and Roychoudhury 2017; Dejonghe et al., 2018; Yoshida 2019).

Among the transcription factors promoted by ABA, the bZIP ABA INSENSITIVE 5 (ABI5), AREB and ABA response element (ABRE) binding factors (ABFs) have shown to interact with ABREs within promoters in order to induce transcription (Hobo et al., 1999; Choi et al., 2000; Finkelstein and Lynch, 2000; Uno et al., 2000; Casaretto and Ho, 2003). In particular, this chapter will focus on ABI5.

In stressful conditions, SnRK2s phosphorylate ABI5 at its trans-activation domain which in turn regulates genes promoting stress responses. One such response is the inhibition of polygalacturonases POLYGALACTURONASE INHIBITING PROTEIN 1 (PGIP1) and PGIP2 which inhibit germination through retardation of seed coat rupture (Kanai et al., 2010), therefore ABA is a key regulator of germination. This regulatory role in germination can play a key role in delay in germination in unfavourable growing conditions. During salinity, and osmotic stress, ABI5 works synergistically with ABI4 to regulate the expression of *DIACYLGLYCEROL ACYLTRANSFERASE 1* (*DGAT1*) which in turn regulates the biosynthesis of Triacylglycerol (TAG), a key component of seeds and crucial for embryonic development (Kong et al., 2013).

The expression of *ABI5* extends beyond early development throughout the life of the plant (Brocard et al., 2002). *Abi5* mutants reduce the inhibitory effect of NO_3 on lateral root development (Signora et al., 2001). In Barley, an *Abi5* mutant showed increased drought resistance with better membrane protection, higher flavonoid content, and faster stomatal closure as well as the upregulation of genes associated with cell protection mechanisms (Collin et al., 2020).

Overall, ABI5 has a key role in ABA signalling and the stress response of plants including cereals. This makes it a candidate for targeted mutagenesis for crop breeding. Mendiondio (unpublished) has developed five TILLING mutations within HvABI5, which have not been tested in field conditions. In this chapter, these lines are tested in field conditions.

2.1.4 Study focus

In results outlined in this chapter focusses on a small number of the genes associated with the Arg/N-degron pathway (*PRT6, PRT1, NTAQ*) and in the ABA signalling pathway (*ABI5*). This chapter aims to assess two TILLING mutants (*prt6i* and *prt6.k*) shown in Mendiondo et al., (2016) to have enhanced tolerance to waterlogging, as well as unpublished mutants in *Prt6* from the same TILLING screen (*prt6.e, prt6.h, ubr.f* and *ubr.c*). Alongside mutants of *PRT6*, Mendiondio (unpublished) also developed TILLING lines in the gene *NTAQ*, another key component of the Arg/N degron pathway: *Ntaq.f* and *Ntaq.i,* and five mutant alleles in *Abi5* (Mendiondo unpublished). Barley is used in this study due to its use as a model species for cereals due to simple diploid genome.

The TILLING lines in *Prt6*, *Ntaq* and *Abi5* were tested in field to explore their performance during the plant development. This study assesses if field conditions result in phenotypic effects previously not seen in glasshouse conditions and assess if the mutant lines have any phenotypic trade-offs associated with the mutations.

2.2 Methods

2.2.1 Alignments and domain exploration of genes

In order to see the conservation of the genes *PRT6*, *ABI5* and *NATQ* and confirm that they are orthologues of genes found across multiple species, a BLAST search and an alignment was carried out between the model species *A. thaliana* and Barley (*Hordeum vulgare*) as well as alignment with other species in order to see conserved domains within the genes (**Appendix I**).

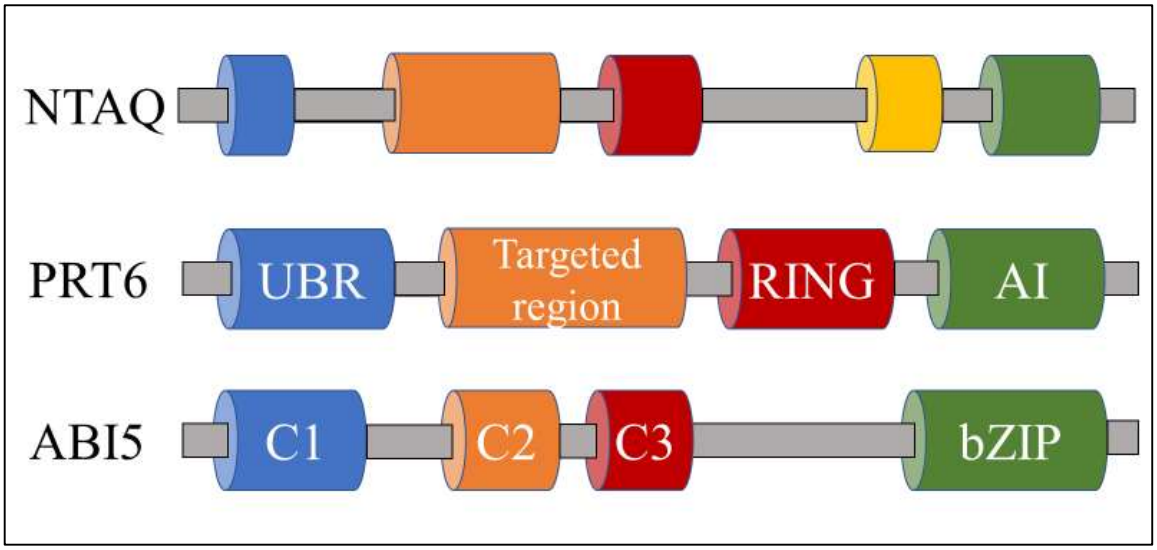

Figure 2.5: Domains of target genes. NTAQ (unnamed domains), Plant E3 ligase PRT6: UBR Box domain (UBR), Autoinhibition domain (AI), and zinc finger domains: Really Interesting New Gene (RING) domain and ABI5: C1, C2 and C3 domains and Basic L Zipper (bZIP) domain.

As can be seen in **Figure 2.5**, the domains in PRT6 are the Ubiquitin Protein Ligase E3 Component N-Recognin (UBR) box domain, the Really Interesting New Gene (RING) domain and the Autoinhibitory (AI) domain, therefore alignments were done individually by domain as can be seen in **Figure 2.5**. The UBR box in *A. thaliana* and Barley show 87.5% matching amino acid sequences. As expected, the UBR box domain is not as highly conserved between plants and animals as shown by the conservation between A. *thaliana*/Barley and Human (alignment between A. *thaliana* and Human 47.22% and Barley and Human alignment at 44.44%). Alignments are more conserved especially in the first region of the domain. The RING domain shows less similarities between species. Between *A. thaliana* and Barley, there is a 65.57% similarity in the AI domain, whereas between Barley and Human there is 47.54% similarity and a value of 42.62% similarity between A. *thaliana* and Human. This alignment is a strong indicator that the *PRT6* gene plays an important role in the function of the protein due to the conservation of domains between species, and therefore makes a good target for gene editing and TILLING.

Table 2.1:TILLING mutants

Gene	Mutation ID	Base pair change (WT to Mutant)	Exon	Amino acid change	Domain
Prt6	*Ubr.c*	G1482A	2	G241Q	UBR box
Prt6	*Prt6.e*	C7388T	10	L1541L	Targeted TILLING fragment
Prt6	*Prt6.h*	G7300A	10	Q1511Q	Targeted TILLING fragment
Prt6	*Prt6.i*	C7514T	10	P1583S	Targeted TILLING fragment
Prt6	*Prt6.k*	G7394A	10	A1543T	Targeted TILLING fragment
Abi5	*Abi5.d*	G1751A	-	R274K	Close to bZIP domain
Abi5	*Abi5.e*	G1588A	-	D220N	Non conserved
Abi5	*Abi5.o*	T1135G	-	F69V	C1 domain
Abi5	*Abi5.r*	G1747A	-	V273M	Close to bZIP domain
Abi5	*Abi5.w*	C1445T	-	P159L	Close to C3 domain
Ntaq	*Ntaq.f*	G1918A	2	A105T	Splice junction (Exon2)
Ntaq	*Ntaq.i*	G1582A	-	A105T	-

Table 2.1; TILLING mutants in Barley, the exon they are targeting and corresponding base changes and amino acid changes from WT to mutant. Prt6.i and prt6.k as described in Mendiondo et al., (2016)

TILLING lines containing mutant alleles of *Prt6*, *Abi5* and *Ntaq*, were developed from the *Hordeum vulgare*-TILLING-University of Silesia (HorTILLUS) population of

spring barley cultivar 'Sebastian' created in the Department of Genetics, University of Silesia, after double treatment of seeds with sodium azide (NaN_3) and N-nitroso- N-methylurea. The mutations were identified by Dr Guillermina Mendiondo at the University of Nottingham as described by Mendiondo et al., (2016) and unpublished mutants are included in this study. Several alleles were identified. In the gene *Prt6*, six alleles were selected, named *prt6.e*, *prt6.h*, *prt6.i*, *prt6.k*, *ubr.c* and *ubr.f*, which were used to develop TILLING lines. The mutants *prt6i* and *prt6.k* have been previously described by Mendiondo et al., (2016) however the other four mutants are yet unpublished. Alleles *prt6.e*, *prt6.h*, *prt6.i* and *prt6.k* were all selected from a TILLING fragment which sits between the AI domain and the RING domain, overlapping with the ring domain. five alleles were selected in the *Abi5* gene to be taken forward into the field trials, and two alleles found in *Ntaq*. These were selected by how conserved the area of the domain is and the resulting amino acid changes by the SNPs. **Table 2.1** and **Figure 2.1** show the positions of the TILLING mutations to be in conserved therefore important regions of the gene.

The TILLING mutants also contain unwanted mutations that are produced during the mutagenesis. These unwanted mutations can cause phenotypic effects on the plants by disrupting gene function in other areas of the genome. The *Prt6* alleles were chosen for a backcrossing programme to remove these unwanted mutations.

2.2.2 Backcrossing of *Prt6* TILLING mutants

In order to reduce these unwanted mutations, the *Prt6* mutants were backcrossed with the Wild Type cultivar Sebastian (background) through a collaboration (Nottingham research Fellowship Mendiondo) by the Barley research team at ABInBev in Fort Collins, CO USA prior the beginning of the PhD project. Barley lines that had been backcrossed by the ABInBev team were provided as a part of this Industrial Collaborative Awards for PhD Students (iCASE) Biotechnology and Biological Sciences Research Council (BBSRC) project. Progeny were then screened for the desired mutation in the *Prt6* gene, and mutants again bred with the background cultivar WT. Alongside this, the mutant alleles were backcrossed into another Barley cultivar -Voyager (ABInBev). This cultivar is not normally grown in the UK (highly

susceptible to Powdery Mildew) however is an integral cultivar in the breeding programmes of ABInBev in the USA.

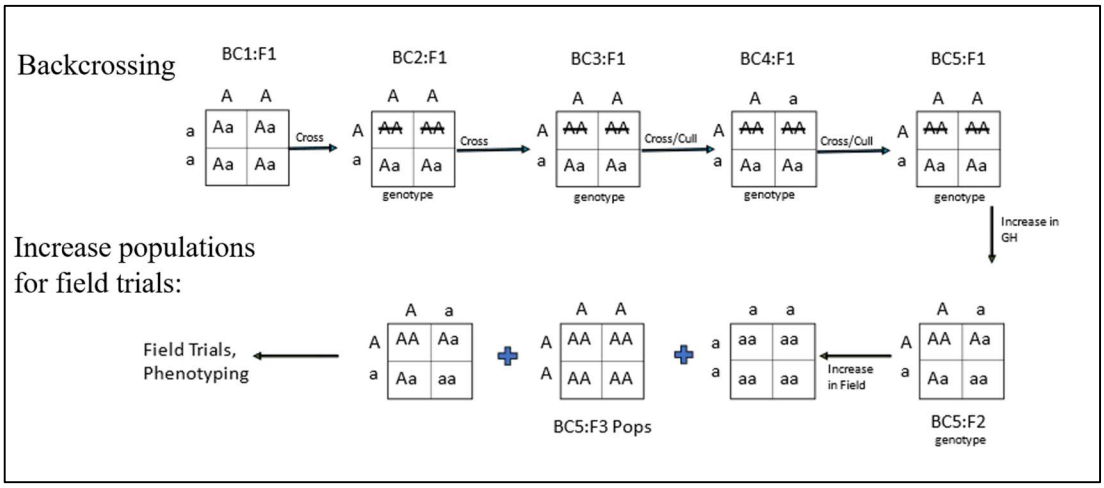

Figure 2.6: Backcrossing programme performed by the Barley research team at ABInBev, Fort Collins, CO. BC refers to Backcrossing, followed by a number referring to the cycle of backcrossing, i.e. BC1=first cycle of backcrossing. A and a referring to the WT and mutant alleles respectively. Figure curtesy of Audrey McDonald (AbInBev).

Backcross 3 (BC3) seeds were received from the team at ABInBev in four mutations, *Prt6.e/h/i/k*, with the rest of the mutants used in this study being from non backcrossed lines. These seeds were received as heterozygous seeds, therefore needed to be genotyped and bulked in order to have material for field trials.

Prt6.e/h/i/k were genotyped using primers targeting the amplification of a small region flanking the targeted domain. DNA was extracted and a PCR run using specific primers as show in **Table 2.6**. The DNA was then digested with the restriction enzymes and cutsmart buffer (**Table 2.2**). The products of the restriction digests were run on a 2.5% agar gel. Bands were compared to virtual digests and known controls to indicate which individuals contained the mutant alleles (**Appendix III**). Plants with WT alleles were discarded.

Table 2.2:Primers used for genotyping TILLING lines.

Gene	Forward primer	Reverse primer	Restriction enzyme
Prt6.e	GCACTTACACCTAGCTTTGTACAG	TATGAATCCACTCGATGAATTCAATTCG	DraI
Prt6.h	GCACTTACACCTAGCTTTGTACAG	ttttttttttttTTGACATTCTATCACGAGAAG	AluI
Prt6.i	aaAAAAAAAAATTTCAGCATCTGAAAGGCTA	ttttttttttttTTGACATTCTATCACGAGAAG	AluI
Prt6.k	GCACTTACACCTAGCTTTGTACAG	TATGAATCCACTCGATGAATTCAATTCG	HindIII

Table 2.2 Primers used to amplify a small section of the gene around the specific TILLING line in PRT6. Restriction enzymes are used to differentiate between WT and Mutant lines.

2.2.3 Field trials

In order to test the performance of the mutants in the field environment, *Prt6*, *Abi5* and *Ntaq* TILLING lines as previously described were sown in a light sandy loam soil at University of Nottingham's Sutton Bonington Campus in late May 2021 . The seeds were sown in two rows (360seeds/m^2) using a Haldrup precision seed drill using a randomised block design (**Appendix II** contains plot map). Fertiliser, herbicide, fungicide and insecticide were used throughout the growth as needed as shown in (**Appendix II**: Field trial year 2021 report generated by field trial technicians at Sutton Bonington Campus- John Alcock and Matthew Tovey). Ten plants in each plot were marked with a wire ring at the base and measurements taken on a weekly schedule on the ten plants, noting leaf on the main stem, tiller number, growth stage (Using Zadoks system) and height. *Hordeum vulagre* seeds were sown in two rows (360seeds/m^2) using a Haldrup precision seed drill.

At harvest, the same ten plants from each plot were separated by hand from the plot, air dried in a glasshouse, and individually measured for length (height), dry weight, stem weight, leaf weight, internode lengths, ear number, ear weight, seed weight, ear length, infertile ear number and seed number. Estimated weight at anthesis was calculated by subtracting grain weight from total postharvest biomass. Fruiting efficiency was estimated as the ratio between grain number and weight of chaff. Harvest index was calculated as a ratio of amount of grain produced relative to the total biomass.

2.2.4 Statistical analysis

For analysis of field trial data both pre and post harvest, using RStudio4.2.0, Analysis of variance (ANOVA) were conducted using a blocking factor and regression analysis was conducted to establish the correlation between traits.

2.3 Results

2.3.1 Field trial

Due to late sowing, disease was prolific throughout the second half of the growing season due to non-ideal conditions allowing fungal infections to thrive even through chemical treatment. Voyager as a non-recommended cultivar for the UK suffered from disease more than Sebastian, however both were heavily affected. There was a large amount of lodging in the latter stages of maturity due to high winds and layout of the narrow plots within the field. String supported by upright canes were used to support plots that had partially lodged to avoid losing the rest of the plot however lodging caused a loss of some post-harvest measurements. Appendix II provides further details on field conditions including chemical applications. Data presented in this chapter is from a single year of trials conducted in 2021, due to losses in previous years growth trials due to Coronavirus disease (COVID-19) pandemic.

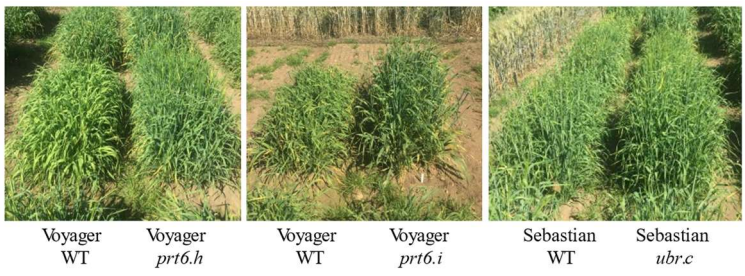

Figure 2.7: Photos of TILLING mutants in Prt6 next to Wild type of the same cultivar.

Photos were taken from above the field on three different occasions as seen in **Figure 2.7**. These photos show clear visible differences in senescence, density and height. The

visible differences in growth can also be seen in **Figure 2.8**. The wild type plants have slightly paler or yellow in colour and appear to have a shorter bushier growth.

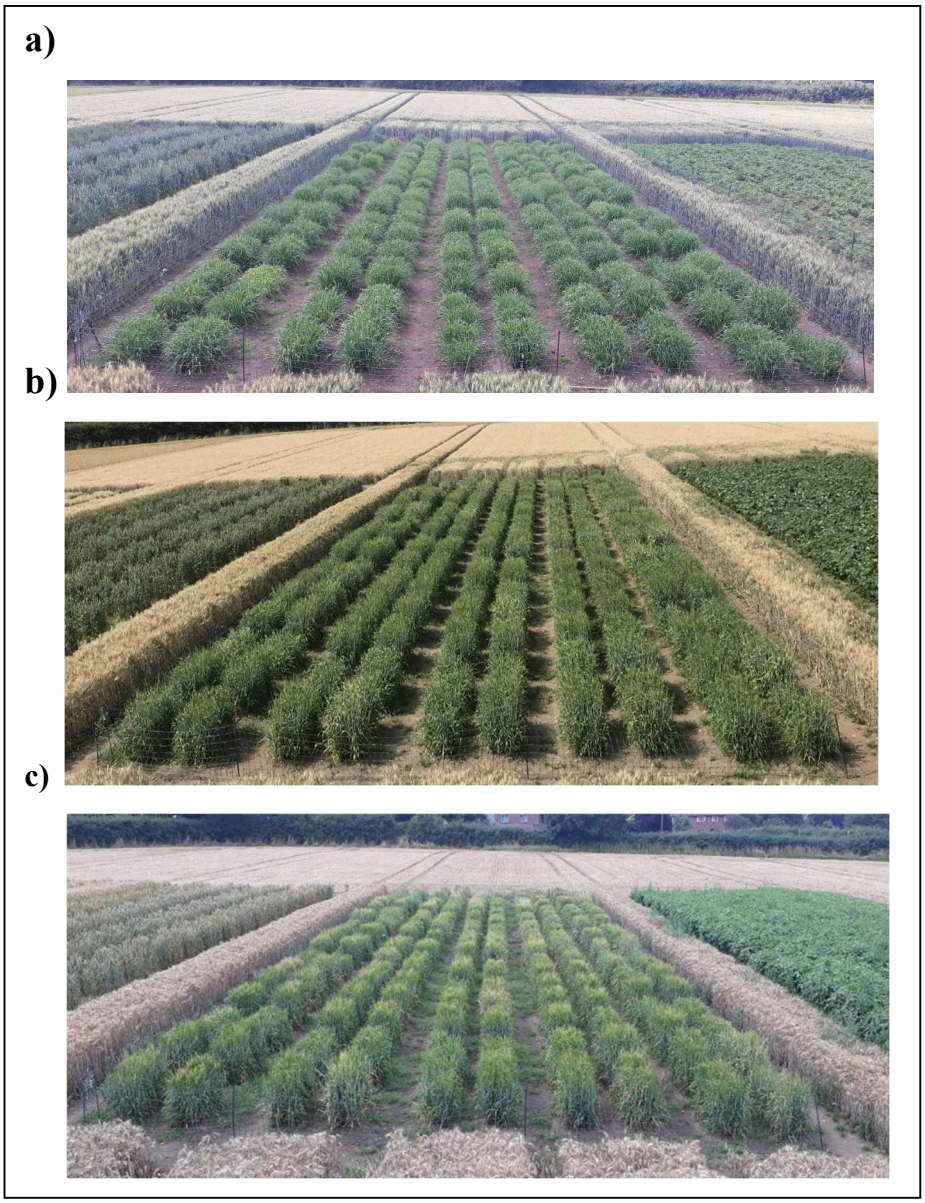

Figure 2.8; PRT6 N-degron pathway field trials at Sutton Bonington campus. Taken on: a) 09/07/21, b) 21/07/21, c)03/08/21. The photos show visible differences in growth, development and signs of senescence between alleles (provided by Mr John Alcock).

In order to understand and quantify these visible differences seen in **Figure 2.7** and **Figure 2.8**, the development of the plants and post-harvest measurements are assessed.

2.3.2 Performance of *Prt6* mutants in the field

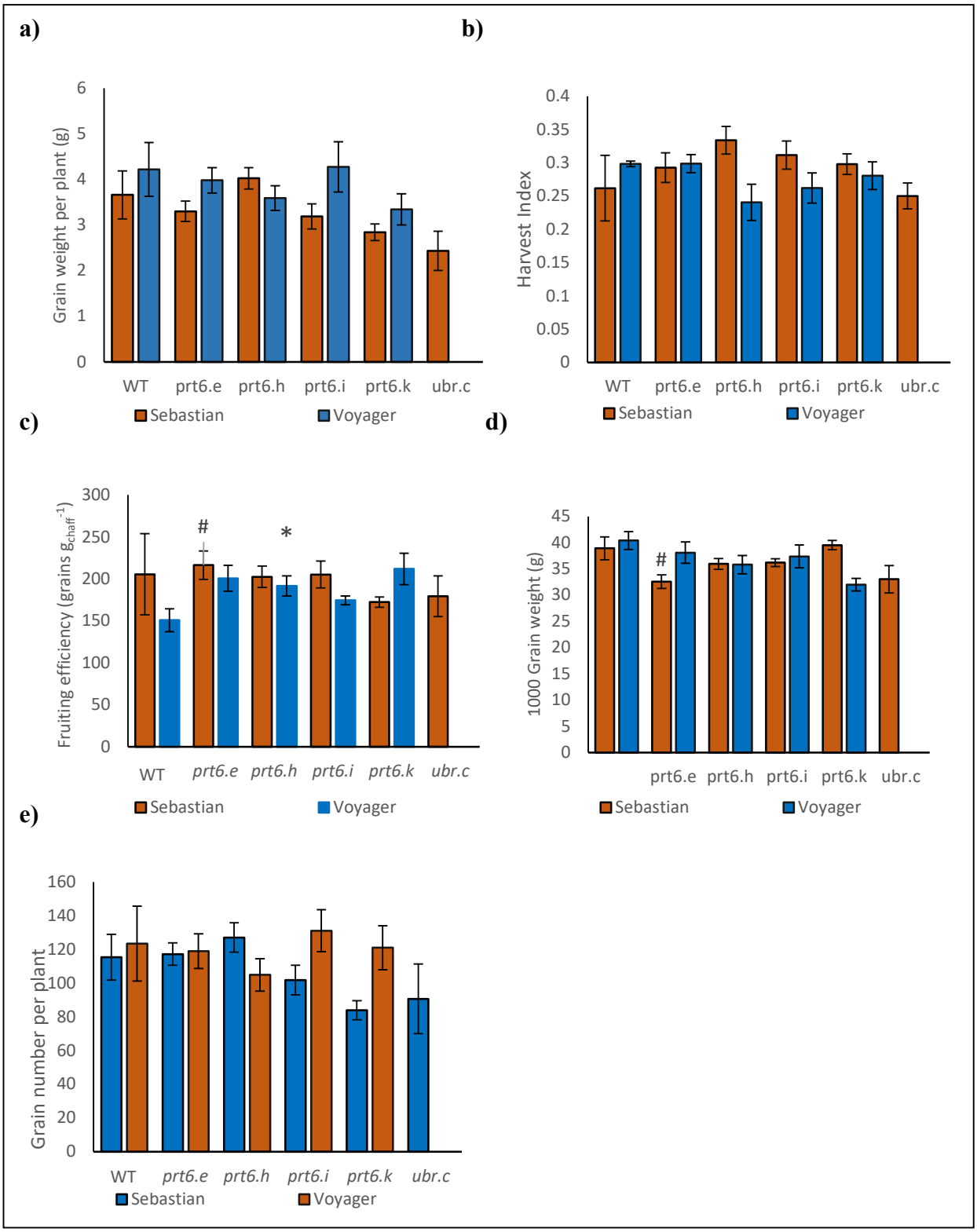

Figure 2.9: Comparisons of Wild Type (WT) and TILLING mutants in the gene Prt6 in the background cultivars of Sebastian and Voyager. a) Total grain weight per individual plant b) Harvest index per plant c) Fruiting efficiency d)1000 grain weight e) Grain number per plant. Error bars indicate standard error of the mean. Significant difference between mutant line and WT indicated by; (#) P<0.1 (*)P<0.05 (**)P<0.01 (***)P<0.001.

Five TILLING mutants were assessed in field during one growth season. Grain number (GN) across all mutations showed no significant difference to the WT. Size

and weight of grain can be determined by Thousand Grain Weight (TGW). The mutations in the Prt6 gene did not lead to differences in TGW except in *prt6.e* in the Sebastian background, where *prt6.e* (32.958g) showed a weak significant (P<0.1) decrease from the WT (38.923) (**Figure 2.9**). When calculating total grain weight per plant, there were no significant differences between WT and *Prt6* mutants (**Figure 2.9**). *Prt6.h* in the Voyager background had significantly (P<0.05) higher Fruiting Efficiency (FE) (191.74) than the WT (150.88) (P<0.05), whilst no significant differences were observed in the same mutation in the Sebastian cultivar (**Figure 2.9**). Similarly, in the Sebastian background the *prt6.e* mutation indicated there was a weak significant (P<0.1) increase between the mutant (216.43) and WT (205.65) FE (**Figure 2.9**). No significant differences in harvest index (HI) between WT and *Prt6* were seen (**Figure 2.9**).

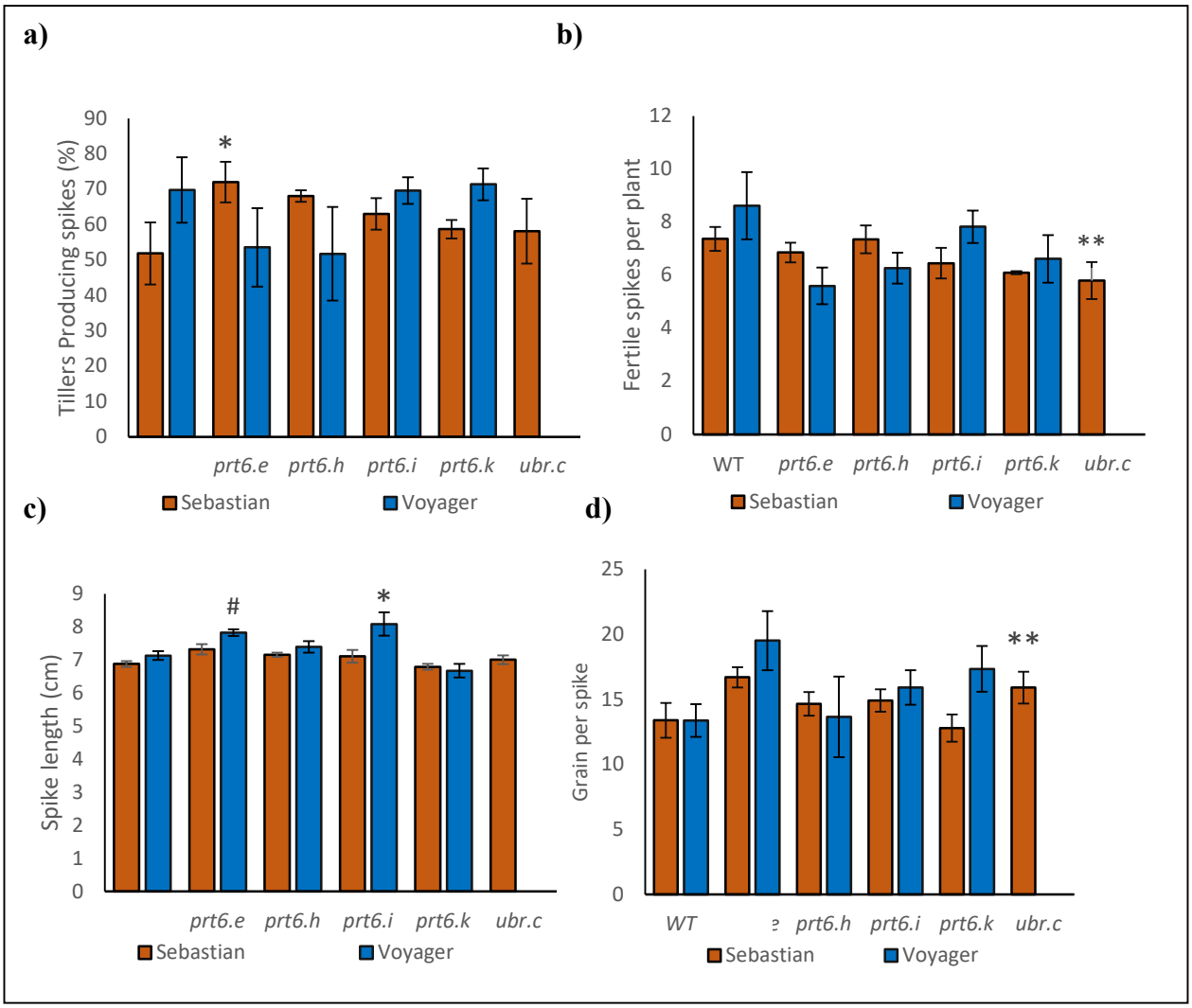

Figure 2.10: Comparisons of Wild Type (WT) and TILLING mutants in the gene Prt6 in the background cultivars of Sebastian and Voyager. a) Percentage of Tillers producing spikes b) Fertile spikes c) Spike length d) Grain per spike. Error bars indicate standard error of the mean. Significant difference between mutant line and WT indicated by; (#)P<0.1 (*)P<0.05 (**)P<0.01 (***)P<0.001.

In order to look into factors that may affect yield it is important to gain further understanding of spike growth. Fertile spikes were counted as number of spikes per plant containing seed, this adds to the overall grain number and therefore can affect yield. *Ubr.c* showed to have significantly (P<0.05) fewer fertile spikes per plant (5.8) than the WT (7.775) however had a significantly (P<0.05) higher percentage of tillers producing spikes (20% increase) (**Figure 2.10**). These two factors could counteract each other, resulting on neither having a large effect on yield. *Ubr.c* also produced significantly (P<0.05) more grain per spike with an increase of 2.52 grains per spike (**Figure 2.10**). Significance differences in spike length between mutant and WT was only seen in the Voyager background (**Figure 2.10**), where the WT average spike length of 7.13cm was significantly (P<0.05) increased in *prt6.i* to 8.09cm, and a weak significance (P<0.1) increase was seen in *prt6.e* to a length of 7.83cm (**Figure 2.10**).

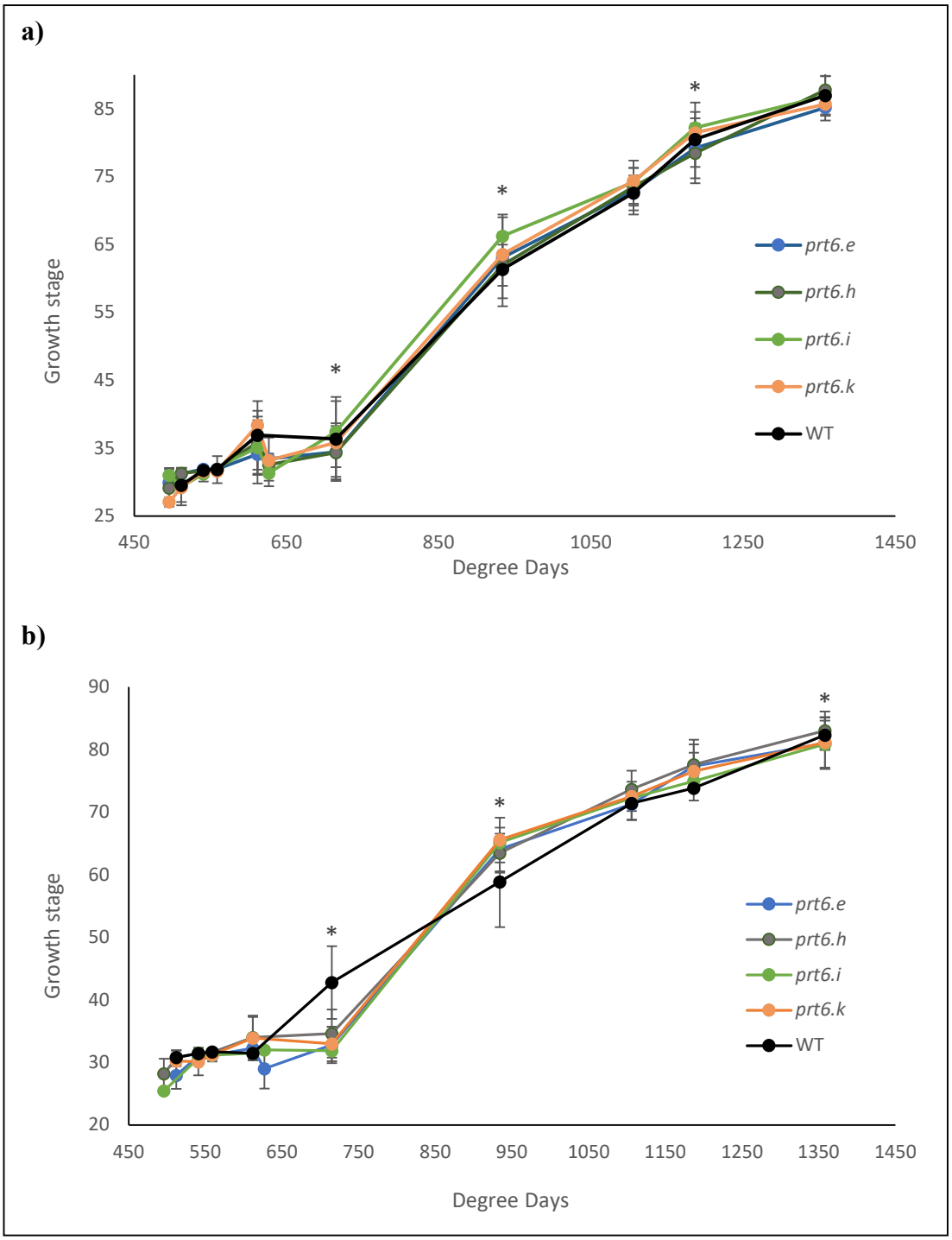

*Figure 2.11: Comparisons of growth stage development in Wild Type (WT) and TILLING mutants in the gene Prt6 in the background cultivars a) Voyager and b) Sebastian. Error bars indicate standard error of the mean. * denote statistical significance between WT and mutant (P<0.05).*

The development seen in the WT and *Prt6* mutants in the background voyager show a similar trend in overall development of growth stages (**Figure 2.11**). At 715 degree days, *prt6.h* showed a significantly (P<0.05) lower growth stage (34.36) to the WT (36.37), and *prt6.e* showed a weak significance (P<0.1) to the WT with a lower

average growth stage of 36.37 (**Figure 2.12a**). At 934 degree days, while the WT average growth stage was 61.35, *prt6.e*, *prt6.i, prt.k* was significantly (P<0.05) higher with 63.05, 66.23, and 63.54 respectively (**Figure 2.12.b**). At 1187 degree days the individual voyager mutants had different results, with *prt6.e* (79.18) and *prt6.h* (78.435), significantly (P<0.05) lower than the WT (80.49) and *prt6.i* (82.19) showing significantly (P<0.05) higher growth stages. *Prt6.k* showed a weak significant (P<0.1) difference to the WT with a higher average growth stage of 81.46 (**Figure 2.12c**). At 1358 degree days, non of the Voyager mutants showed a significant (P<0.05) difference (**Figure 2.12d**). Overall this shows that there may be a slight delay in growth in *prt6.e* and *prt6.h* earlier in the growth cycle, there is then an increase in speed of development in order to show no delay at 934 degree days. Another small delay in development was seen in *prt6.e* and *prt6.h* again at 1187 degree days, however all mutants showed no significant differences on the last reading before harvest.

In the Sebastian background, there are key differences in development of the mutants compared to the WT at 715 degree days and 934 degree days. At 715 degree days, *prt6.e* (32.78), *prt6.h* (34.61), *prt6.i* (31.86) and *prt6.k* (32.95) were all at a significantly (P<0.05) lower growth stage than the WT (42.75), showing a delay in development (**Figure 2.12a**). At 934 degree days the opposite was seen, where the mutants *prt6.e* (64.03), *prt6.h* (63.43), *prt6.i* (65.12) and *prt6.k* (65.54) were all at significantly (P<0.05) higher growth stages than the WT (58.85) showing an increased growth rate (**Figure 2.12b**). The mutants also showed higher growth stages to the WT (73.8) at 1187 degree days (*prt6.e* =77.32, *prt6.h*=77.58, *prt6.i*=74.90 and *prt6.k*=76.51) (**Figure 2.12c**). At the last measurement before harvest at 1358 degree days, while *prt6.i* and *prt6.k* showed no significant difference to the WT (82.3), *prt6.e* showed a significantly (P<0.05) lower growth stage of 81 and *prt6.h* showed a significantly (P<0.05) lower growth stage of 83.02 (**Figure 2.12d**). Overall, this shows a similar trend in voyager where mutants show a delayed start followed by a higher growth rate between the growth stages of approximately GS31 to GS61.

Due to the trend of an increase in growth rates during the middle of the growing season, the time taken to reach GS31 and GS61 were calculated however no significant differences were seen between the WT and any of the mutants.

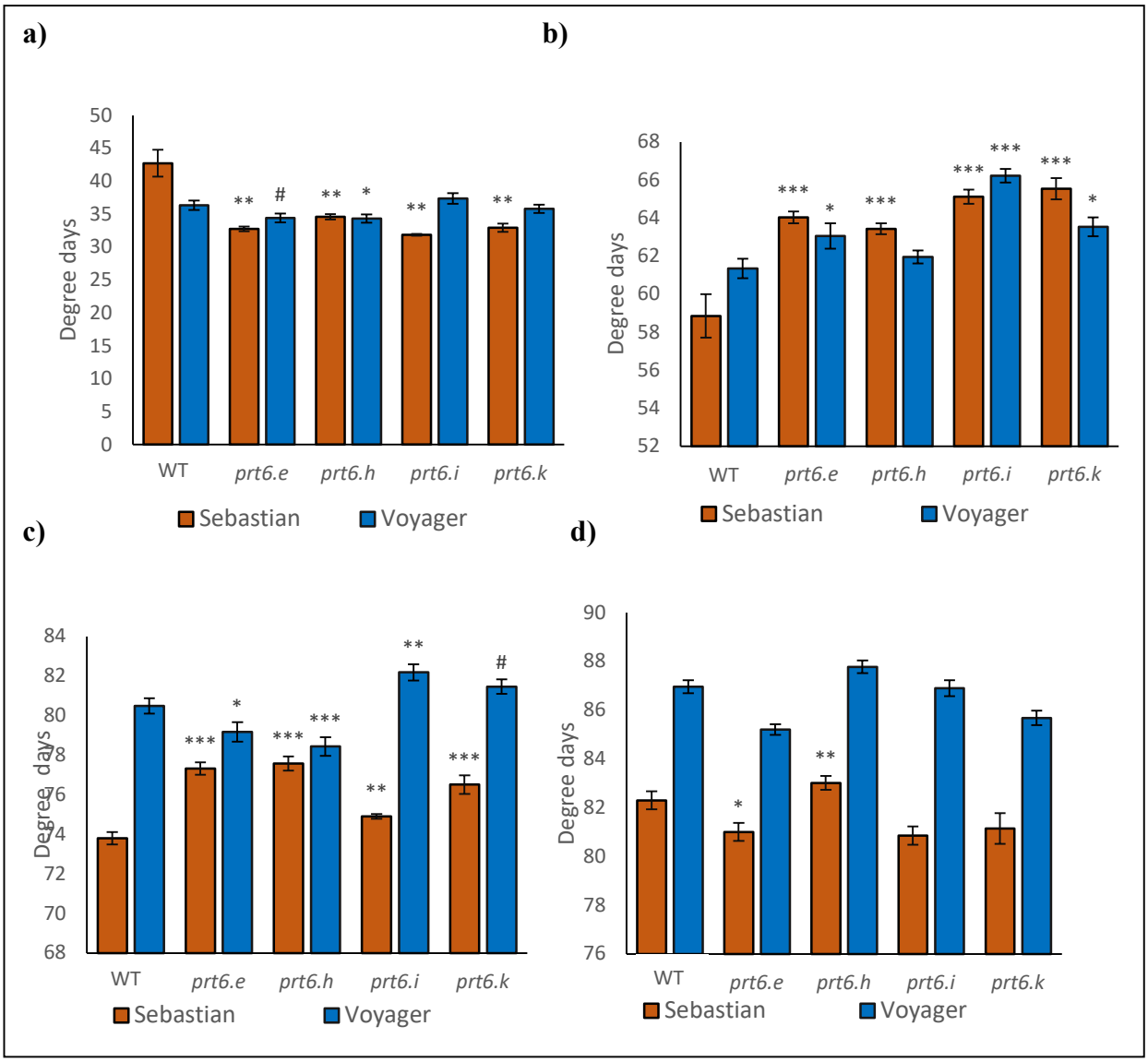

Figure 2.12: Comparisons of Wild Type (WT) and TILLING mutants in the gene Prt6 in the background cultivars Voyager and Sebastian. a) Growth stage after 715 degree days b) Growth stages after 934 degree days c) Growth stages after 1187 degree days d) Growth stage after 1358 degree days. Error bars indicate standard error of the mean. Significant difference between mutant line and WT of the same cultivar indicated by; (#)P<0.1 (*)P<0.05 (**)P<0.01 (***) P<0.001.

There was shown to be no significant differences between the WT and mutants in above ground biomass in the Voyager background, however a significant (P<0.05) decrease was seen in *Ubr.c* (8.45g) to the WT (9.94g) (**Figure 2.13a**). There was also a weak significant (P<0.1) decrease seen in *prt6.k* from 9.94g to 8.65g. Weight at anthesis gives a strong determination of the grain weight at harvest (Fischer 1985, Slafer et al., 2005). *Ubr.c* was the only mutant that showed a significant (P<0.05) difference in weight at anthesis with a biomass of 14.51g which was significantly (P<0.05) higher than the WT (7.20g) (**Figure 2.13c**) however this did not have a

significant effect on TGW, total grain weight per plant, FE or GN. *Ubr.c* was also the only mutant to show a significant ($P<0.05$) difference to the WT in biomass partitioning, where there was a higher percentage of biomass in the stem and less in the ear than the WT.

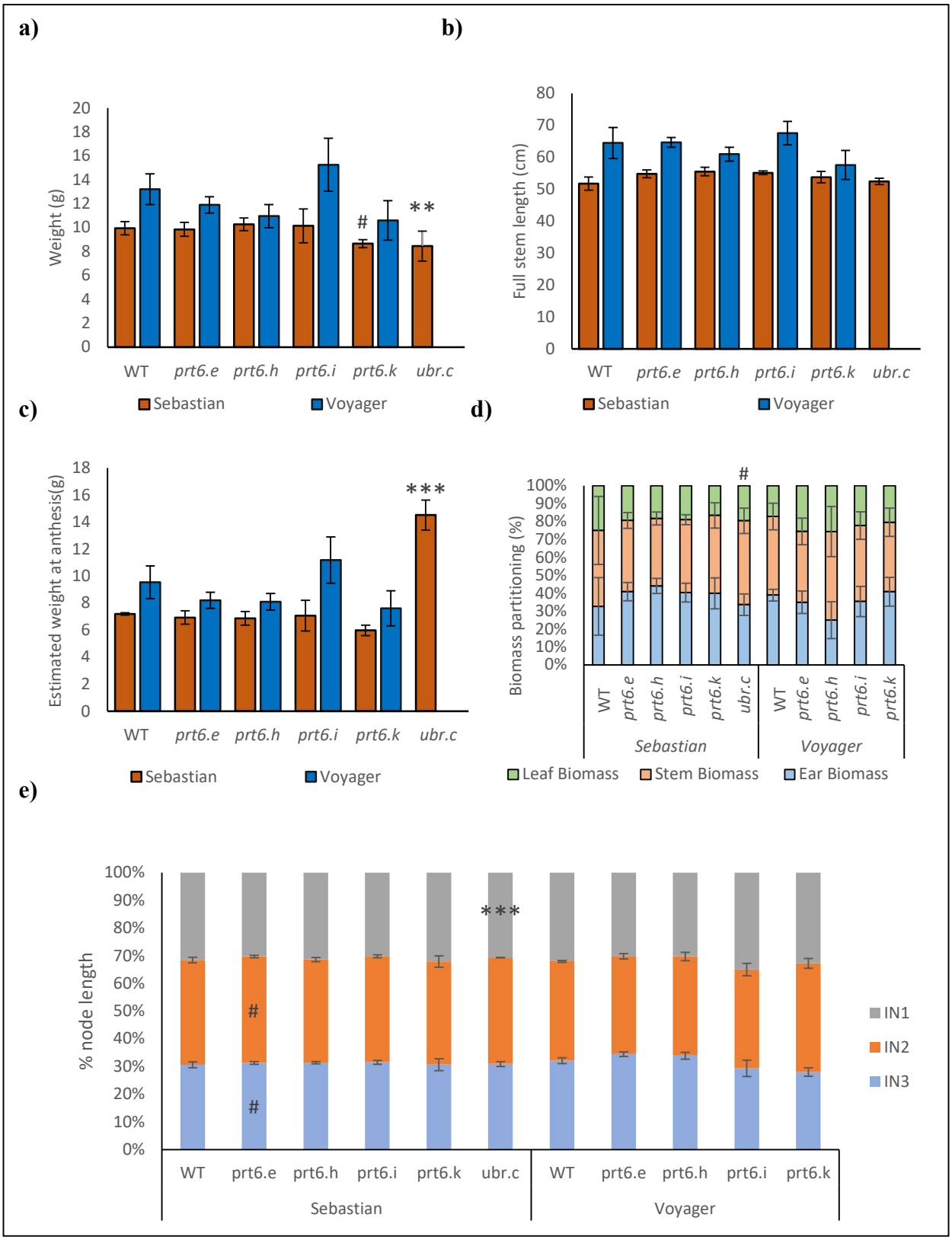

Figure 2.13: Comparisons of Wild Type (WT) and TILLING mutants in the gene Prt6 in the background cultivars of Sebastian and Voyager. a) Above ground biomass b) Height c) Estimated weight at anthesis d) Biomass partitioning as a percentage of total overall biomass. e) Internode lengths as a percentage of total stem length between Node (IN) 1 and 3. Error bars indicate standard error of the mean. Significant difference between mutant line and WT of the same cultivar indicated by; (#)P<0.1 (*)P<0.05 (**)P<0.01 (***)P<0.001.

In the Sebastian background, *Ubr.c* showed a significant ($P<0.05$) decrease in partitioning to Internode 1 (IN1) and an increase in IN2 and IN3, while *prt6.e* showed a weak significant decrease ($P<0.1$).

Summary of *Prt6* mutants

Table 2.3: Summary of *prt6* lines

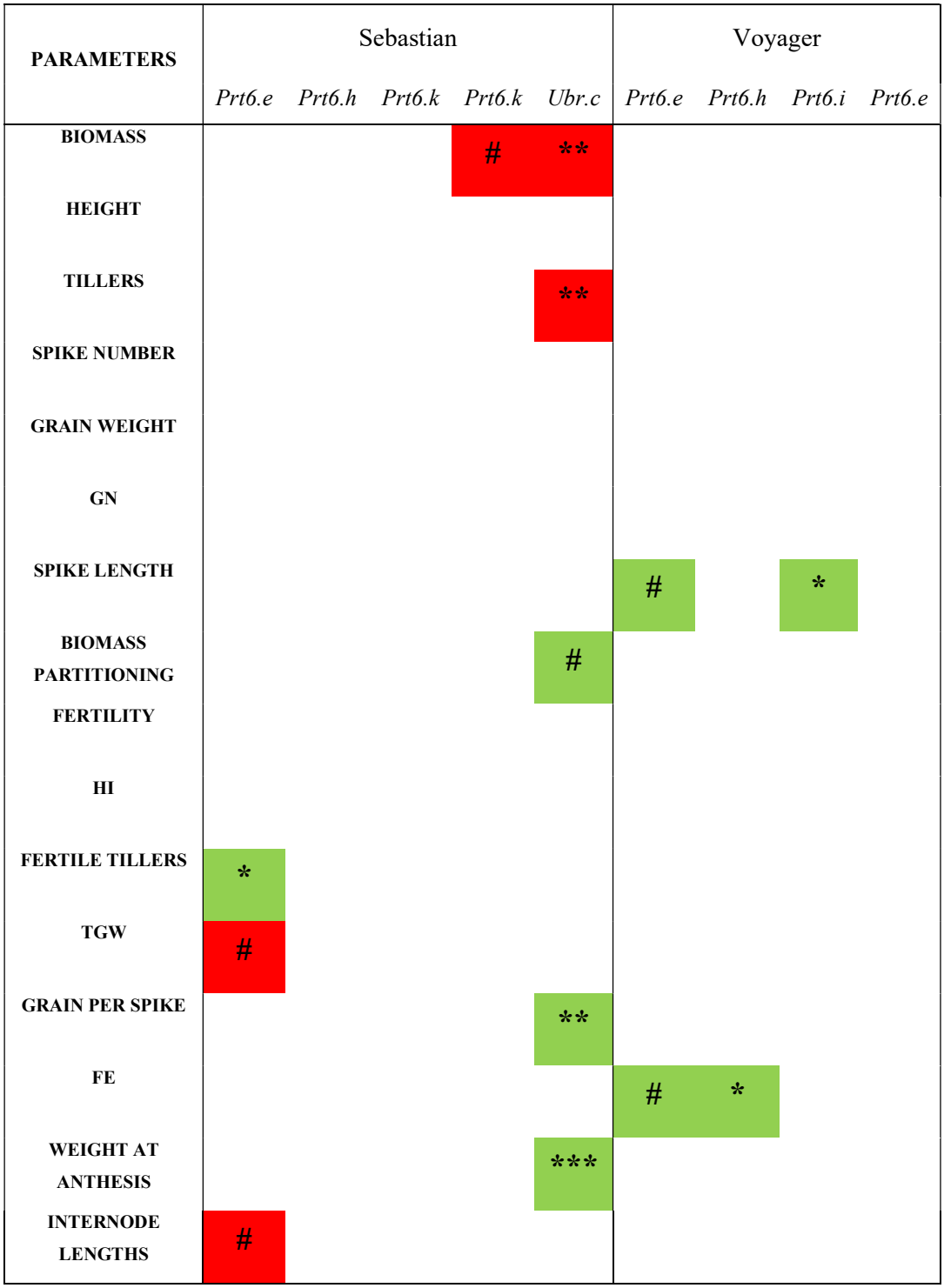

Table 2.3: Comparisons of TILLING mutants in the gene Prt6 in the background cultivars of Sebastian and Voyager. Green indicates the trait being positively different to the WT whereas red indicates the trait is negative in comparison to the WT. Significant difference between mutant line and WT indicated by; (#)P<0.1 (*)P<0.05 (**)P<0.01 (***)P<0.001.

Results show that in *Prt6* mutants- *prt6.e, prt6.h, prt6.i, prt6.k and ubr.c,* the only negative traits were found in biomass, spike number, TGW and internode length. These negative traits were only found in *ubr.c*, *prt6.e* and *prt6.k* in Sebastian background. No negative traits were found in the Voyager background. *Prt6.i* and *prt6.h* showed no negative traits, while *prt6.e* and *prt6.k* only showed positive changes in the Voyager cultivar. Several positive trait differences were found in the mutants such as spike length, biomass partitioning, number of tillers producing spikes, grain per spike, FE and weight at anthesis.

2.3.3 Performance of *Ntaq* mutants in field conditions

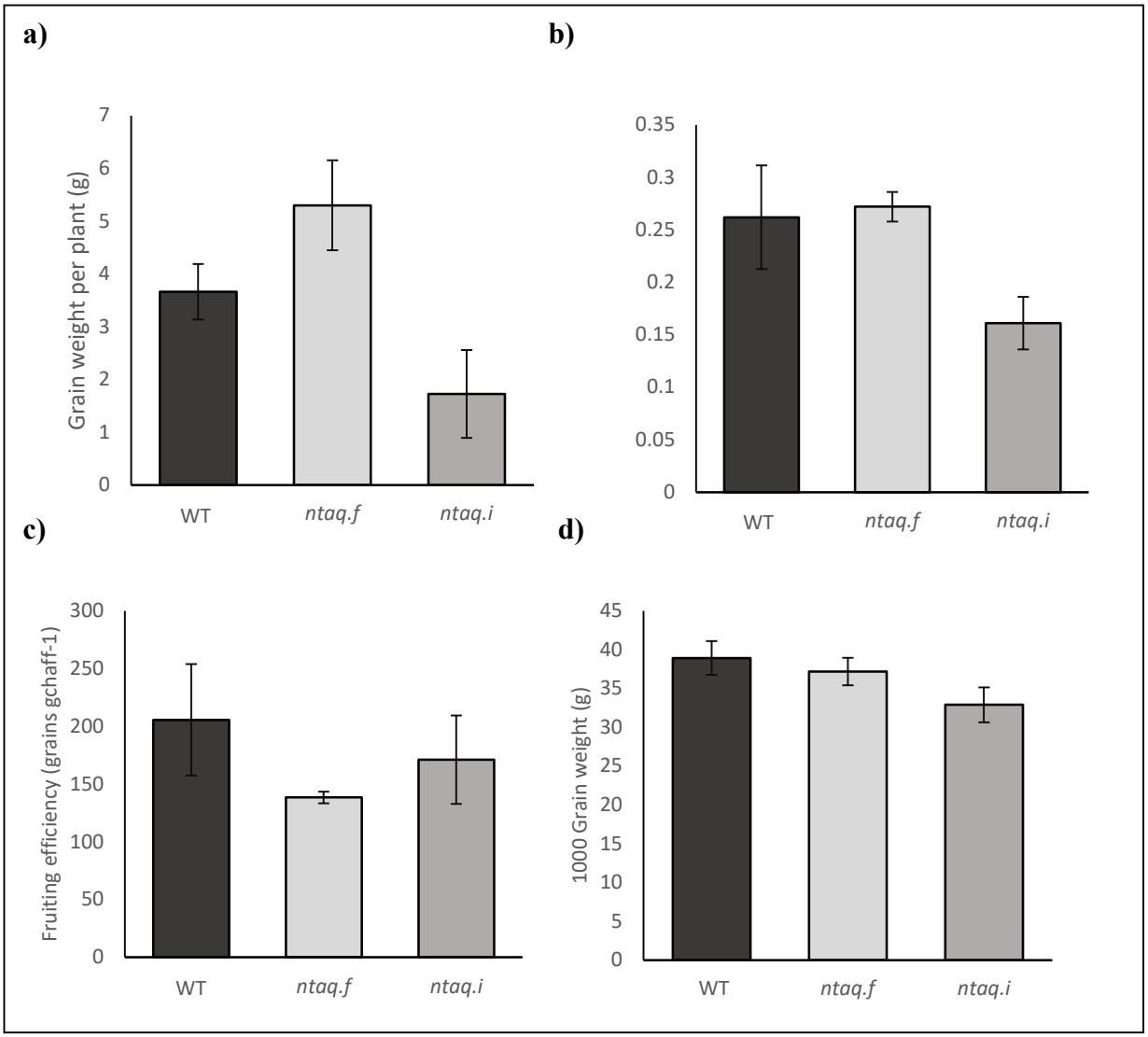

Figure 2.14: Comparisons of Wild Type (WT) and TILLING mutants in the gene Ntaq. a) total grain weight per plant per individual plant b) Harvest index c) Fruiting efficiency d) 1000 grain weight. Error bars indicate standard error of the mean. Significant difference between mutant line and WT indicated by; (#) P<0.1 (*)P<0.05 (**)P<0.01 (***)P<0.001.

Grain weight and HI are important measures of economic success as a crop, and there were no significant difference in WT and *Ntaq* mutants (**Figure 2.14a**, **Figure 2.14b**). There were also no significant differences observed in FE and 1000 grain weight (**Figure 2.14c, Figure 2.14d**).

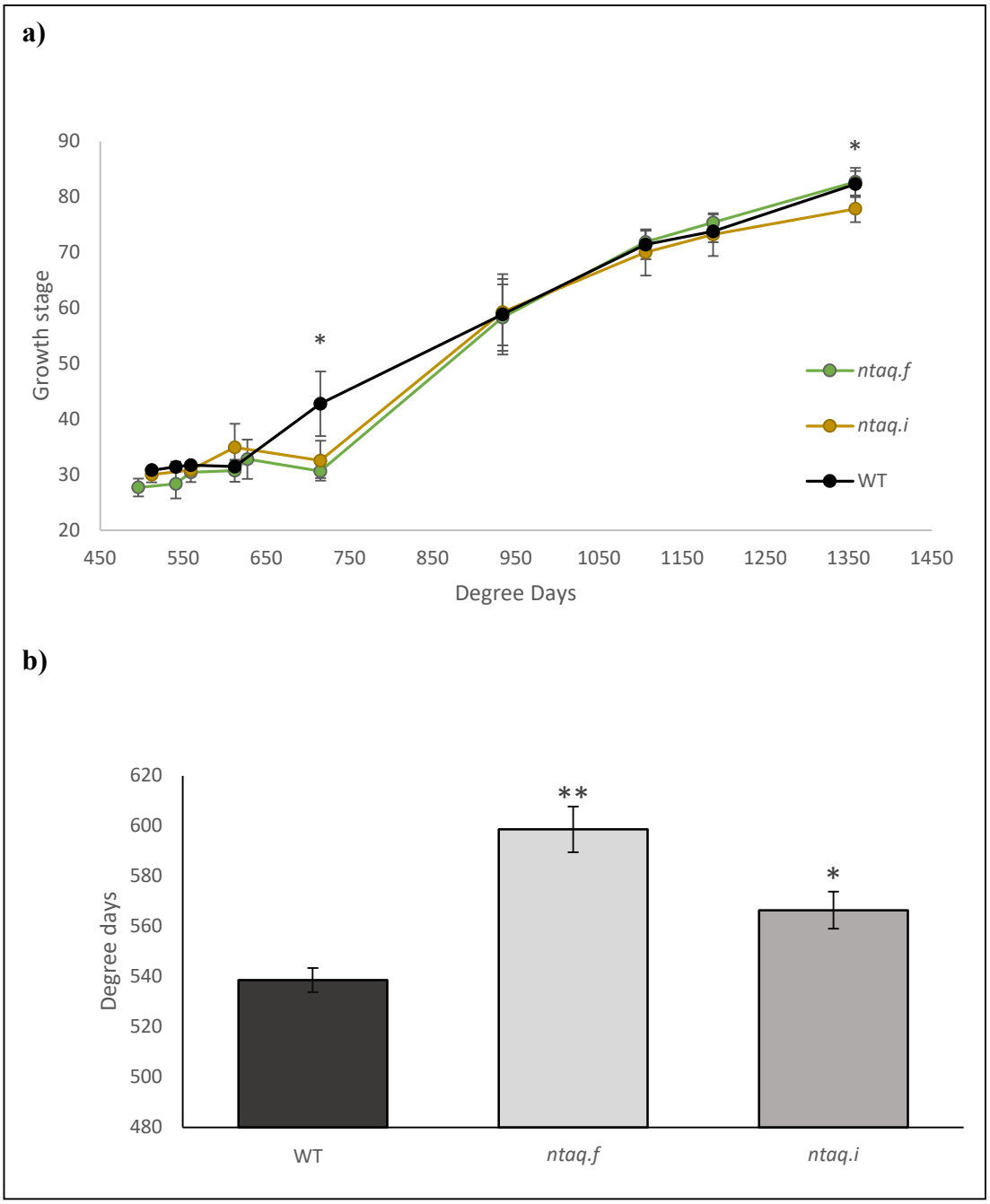

Figure 2.15: Comparisons of growth stage development in Wild Type (WT) and TILLING mutants in the gene Ntaq in the background cultivar Sebastian a) Development of Growth stages over degree days b) Degree days until the first node is detectable (GS31). Error bars indicate standard error of the mean. Significant difference between mutant line and WT indicated by; (#)P<0.1 (*)P<0.05 (**)P<0.01 (***)P<0.001.

Both *Ntaq* mutants showed that the time it takes to reach GS31 was longer than that of the WT (**Figure 2.15b**). The trend in development of *Ntaq* mutants showed that key differences could be seen at 715 degree days and 1358 degree days (**Figure 2.16**). At 715 degree days, both *ntaq.f* (30.63) and *ntaq.i* (32.72) showed a significantly ($P<0.05$) lower growth stage than the WT (42.75). After 934 degree days no significant differences were observed, indicating that there was an increase in growth rate. At 1358 degree days, there was a significantly ($P<0.05$) lower growth stage in *ntaq.i* (77.85) than the WT (82.3), but no significant difference was seen in *ntaq.f* (**Figure 2.16b**). The delay in development, may occur before 715 degree days, due to significant ($P<0.05$) differences in the time it takes to reach GS31.

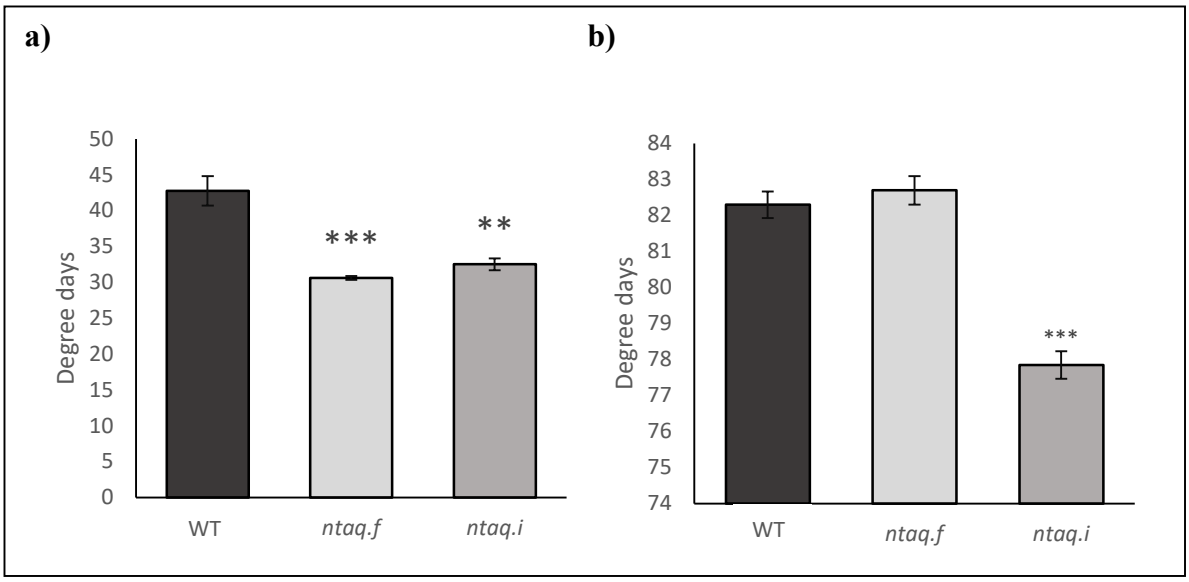

Figure 2.16: Comparisons of development in Wild Type (WT) and TILLING mutants in the gene Ntaq in the background cultivar Sebastian a)Growth stages after 715 degree days b) Growth stages after 1358 degree days. Error bars indicate standard error of the mean Error bars indicate standard error of the mean. Significant difference between mutant line and WT indicated by; (#)P<0.1 (*)P<0.05 (**)P<0.01 (***)P<0.001.

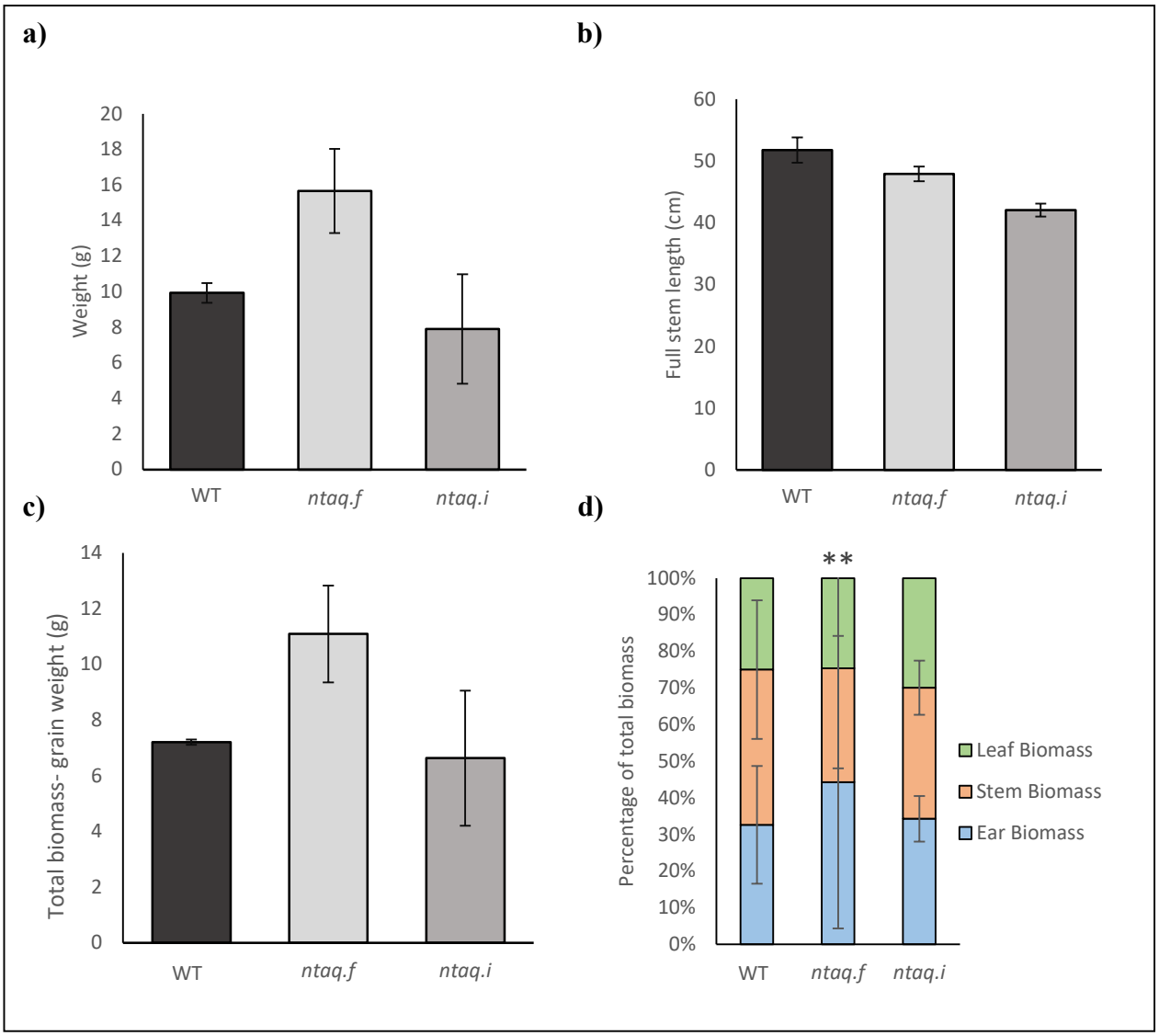

Figure 2.17: Comparisons between Wild Type (WT) and TILLING mutants in the gene Ntaq in the background cultivar Sebastian a) Total above ground biomass b) Height c) Estimated weight at anthesis d) Above ground Biomass partitioning. Error bars indicate standard error of the mean. Significant difference between mutant line and WT indicated by; (#) P<0.1 (*)P<0.05 (**)P<0.01.

Both mutations in *Ntaq* showed no significant difference in Biomass or height to that of the WT (**Figure 2.17**). There were also no significant differences in estimated weight at anthesis. Biomass partitioning showed that *ntaq.f* accumulated a significantly (P<0.05) larger proportion of biomass to the ears and less to the stem and leaf (**Figure 2.17**). *ntaq.f* accumulated 36.5% of its biomass to the ear and WT only accumulated 12.0% in the ear (**Figure 2.17**).

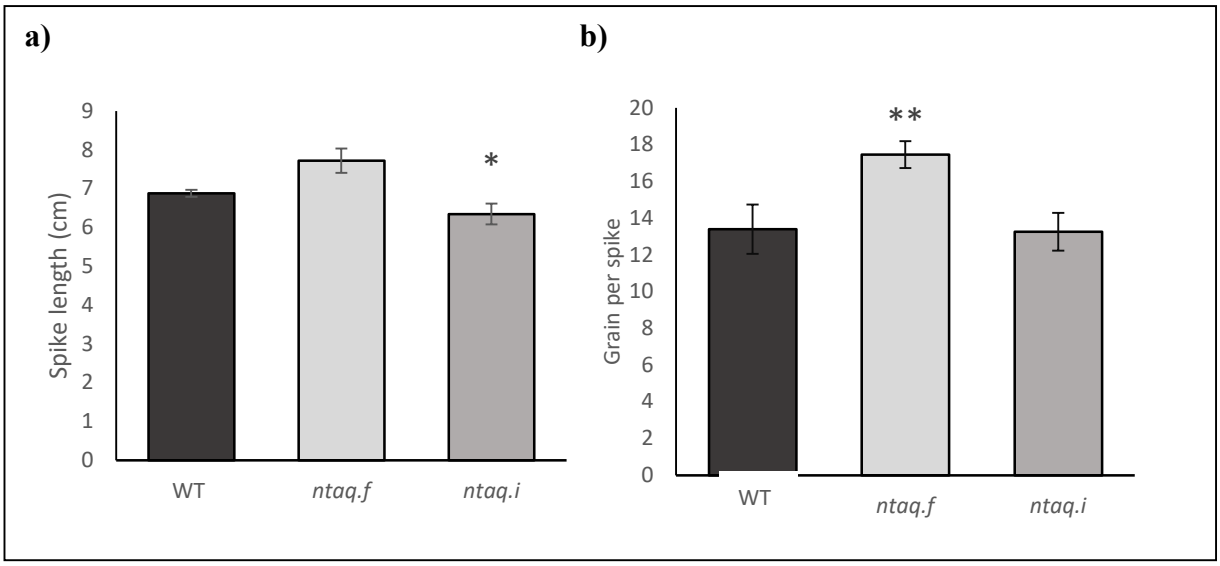

Figure 2.18: Comparisons of spikes in Wild Type (WT) and TILLING mutants in the gene Ntaq in the background cultivar Sebastian a) Spike length b) Grain per spike. Error bars indicate standard error of the mean. Significant difference between mutant line and WT indicated by; (#) P<0.1 (*)P<0.05 (**)P<0.01 (***)P<0.001.

Spike length showed a significant (P<0.05) difference between WT (6.88cm) and *ntaq.i* (6.35com) (**Figure 2.18**), however *ntaq.i* showed no significant difference in grain per spike. Whilst *ntaq.f* showed no significant difference in spike length, grain per spike was significantly (P<0.05) increased (17.47 grains per spike) from that of the WT (13.40 grains per spike) (**Figure 2.18**).

Summary of *Ntaq* results

Table 2.3: Summary of *ntaq* lines

PARAMETERS	*ntaq.i*	*ntaq.f*
BIOMASS		
HEIGHT		
TILLERS		
SPIKES		
TOTAL GRAIN WEIGHT PER PLANT		
GN		
SPIKE LENGTH	*	
BIOMASS PARTITIONING		**
FERTILITY		
HI		
TILLERS PRODUCING SPIKES		
TGW		
GRAIN PER SPIKE		**
FE		
WEIGHT AT ANTHESIS		
INTERNODE LENGTHS		

Table 2.4: Comparisons of TILLING mutants in the gene Ntaq in the background cultivars Sebastian Green indicates the trait being positively different to the WT whereas red indicates the trait is negative in comparison to the WT. Significant difference between mutant line and WT indicated by; (#)P<0.1 (*)P<0.05 (**)P<0.01 (***)P<0.001.

In summary, the very few differences were seen between *ntaq* mutants and WT. *ntaq.f* showed to have improved biomass partitioning and higher number of grains per spoke than the WT, however *ntaq.i* had a reduced spike length.

2.3.4 ABI5 mutants

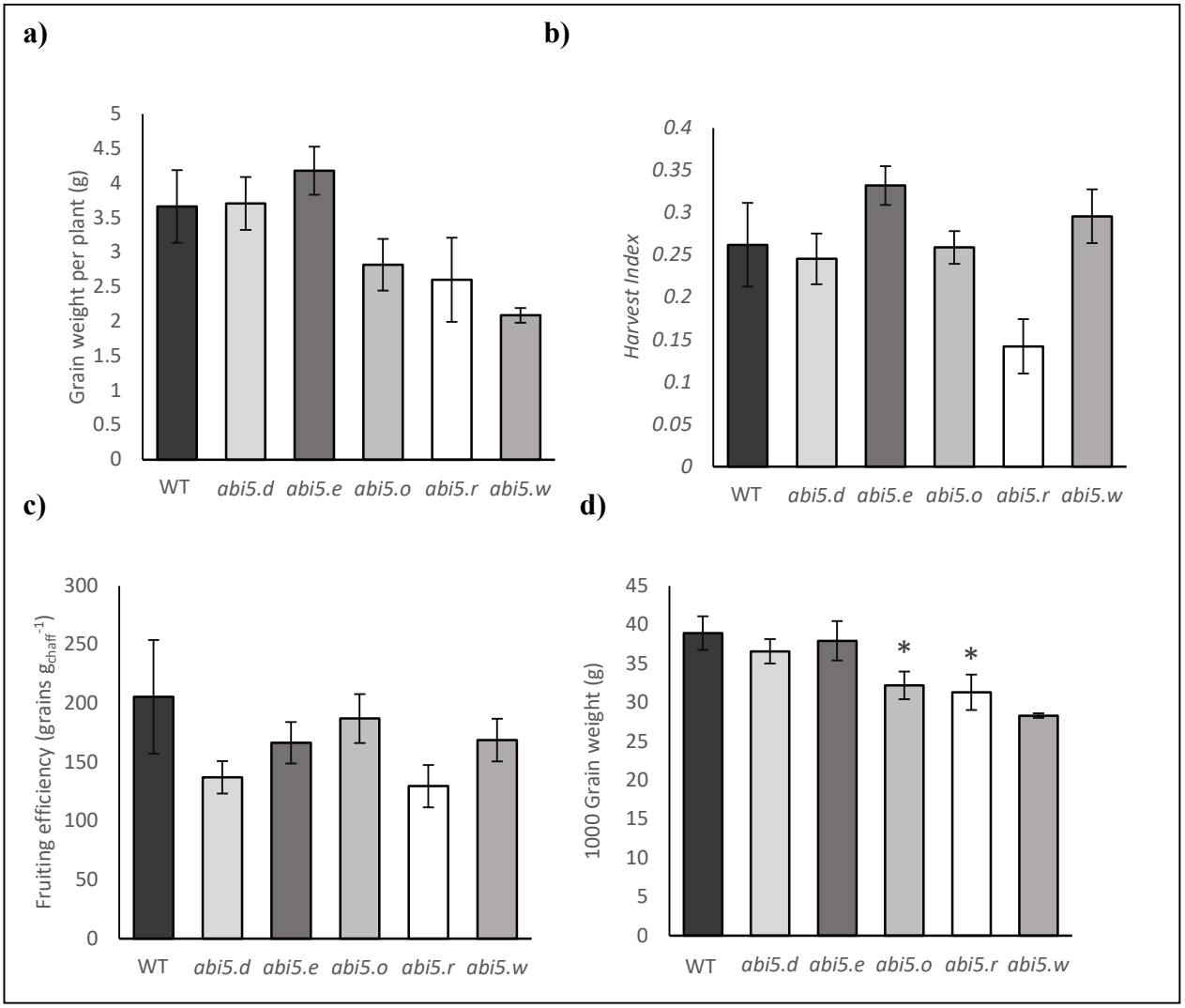

Figure 2.19: Comparisons of Wild Type (WT) and TILLING mutants in the gene Abi5. a) total grain weight per plant b) Harvest index (HI) c) Fruiting efficiency (FE) d) 1000 grain weight (TGW). Error bars indicate standard error of the mean. Significant difference between mutant line and WT indicated by; (*)P<0.05.

Abi5 mutants showed no significant differences to the WT in total grain weight per plant, HI, or FE (**Figure 2.19**). Whist WT showed a TGW of 38.92g, *abi5.o* and *abi5.r* showed a significant (P<0.05) decrease in TGW to 32.20g and 31.33g respectively (**Figure 2.19b**).

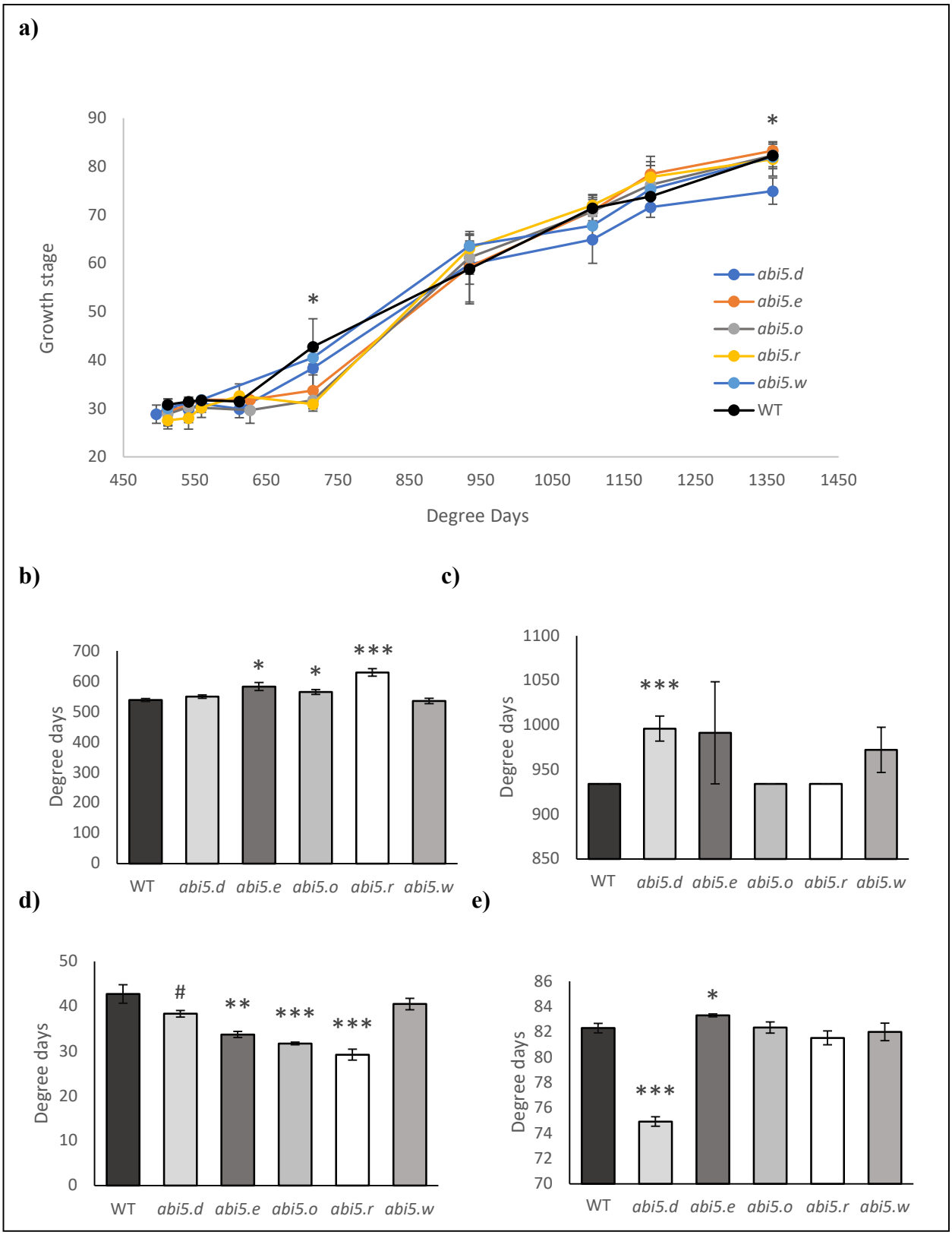

Figure 2.20: Comparisons of growth stage development in Wild Type (WT) and TILLING mutants in the gene Abi5 in the background cultivar Sebastian a) Development of Growth stages over degree days b) Degree days until first detectable node (GS31) c) Degree days until anthesis (GS61) d) Growth stages after 715 degree days e) Growth stages after 1358 degree days. Error bars indicate standard error of the mean. Significant difference between mutant line and WT indicated by; (#)P<0.1 (*)P<0.05 (**)P<0.01 (***)P<0.001.

The development of *Abi5* mutants showed differences to the WT across the growing season. A delay was seen before GS31 in the mutants *abi5.e* (582.84 degree days), *abi5.o* (565 degree days) and *abi5.r* (629.23 degree days) which all took significantly ($P<0.05$) longer to than the WT (538.62 degree days) (**Figure 2.20b**). The delay was also seen at 715 degree days in *abi5.e* (GS33.7), *abi5.o* (GS31.7) and *abi5.r* (GS29.2) where they all showed significantly ($P<0.05$) less development than the WT (GS42.75) (**Figure 2.20d**). By GS61 there were no signs in delays in development except in *abi5.d* (996.11 degree days) which took longer to reach GS61 than the WT (934 degree days) (**Figure 2.20c**). By 1358 degree days, all mutants showed no significant delay in growth stages to the WT (GS82.3) except *abi5.d* which had a significant ($P<0.05$) delay in development (GS74.92). At 1358 degree days *abi5.e* showed a significant ($P<0.05$) increase averaging a Growth stage of 83.3 (**Figure 2.20e**).

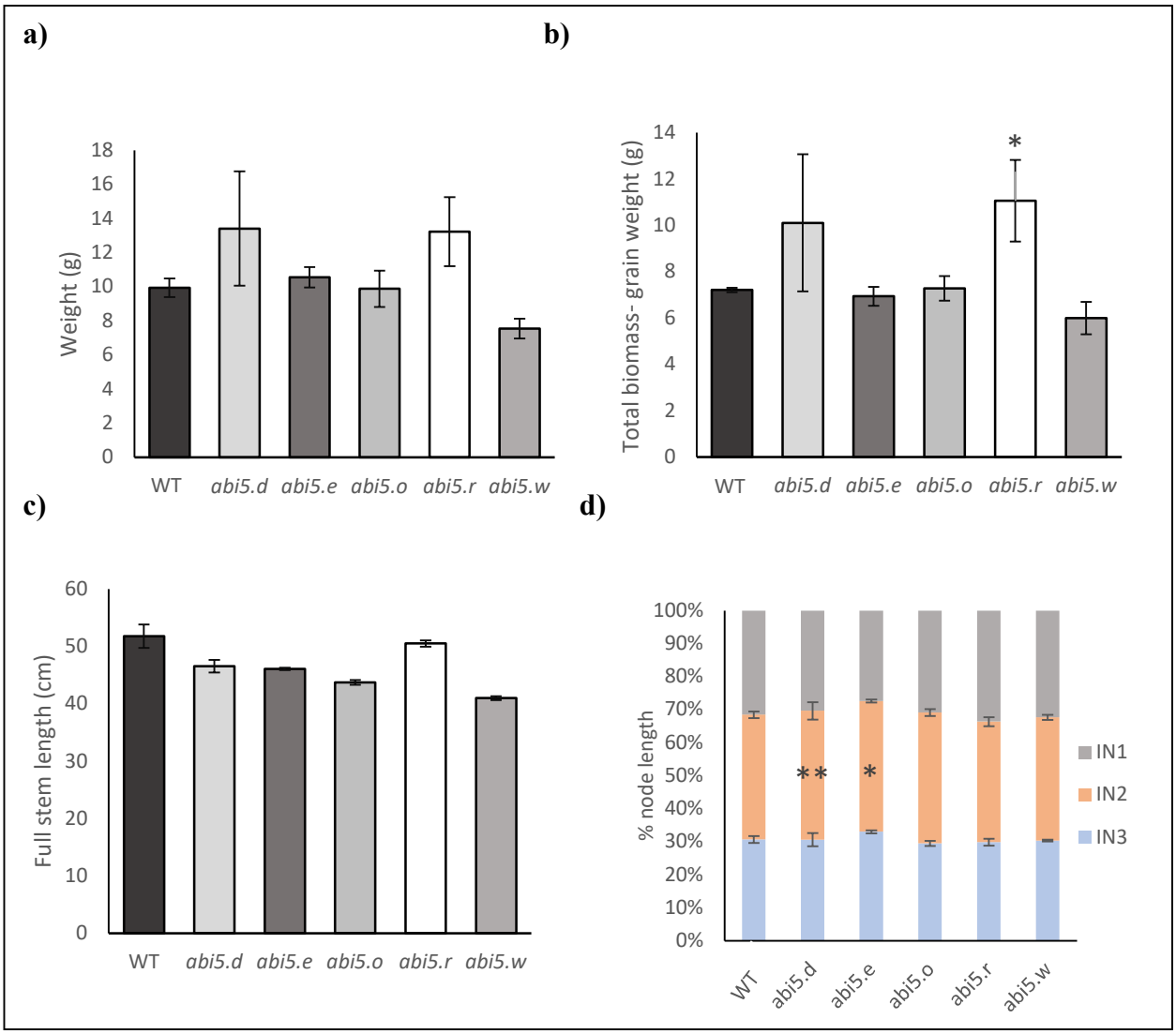

Figure 2.21: Comparisons between Wild Type (WT) and TILLING mutants in the gene Abi5 in the background cultivar Sebastian a) Total above ground biomass b) Estimated weight at anthesis c) Height d) Above ground Biomass partitioning. Error bars indicate standard error of the mean. Significant difference between mutant line and WT indicated by; (*)P<0.05 (**)P<0.01.

No significant difference between WT and *Abi5* mutants were seen in height and above ground biomass, which are two main factors in determining yield (**Figure 2.21**). There was a significant increase estimated weight at anthesis in *abi5.r* (11.06g) from the WT (7.20) (**Figure 2.21b**), which can be a determinant of grain weight. This is the inverse of what was seen in **Figure 2.19d** where there was a significantly (P<0.05) lower TGW than the WT.

Previous studies have shown that an increased length of IN1 and decreased partitioning to IN2 and IN3, enhanced spike dry matter partitioning, spike growth and grain number in wheat (Rivera-Amado et al., 2019). *Abi5.d* and *abi5.e* had

significantly (P<0.05) reduced biomass partitioning to the 1st internode (IN1) and therefore increased biomass to IN2 and IN3 (**Figure 2.21d**). The WT partitioned 31.55% to IN1, 37.82% to IN2 and 30.63% to IN3. *Abi5.d* partitioned 30.47% to IN1, 39.13% to IN2 and 30.69 to IN3, which increased the percentage of partitioning into IN2 and decreased partitioning into IN1 significantly (P<0.05) (**Figure 2.21d**). *Abi5.e* partitioned 27.40% into IN1, 39.60% into IN2 and 32.99% into IN3, which also shows an increase in the percentage of partitioning into IN2 and decreased partitioning into IN1 significantly (P<0.05) (**Figure 2.21d**). This result indicates that there may be a negative effect on enhanced spike dry matter partitioning, spike growth and grain number due to the findings by Rivera-Amado et al., (2019).

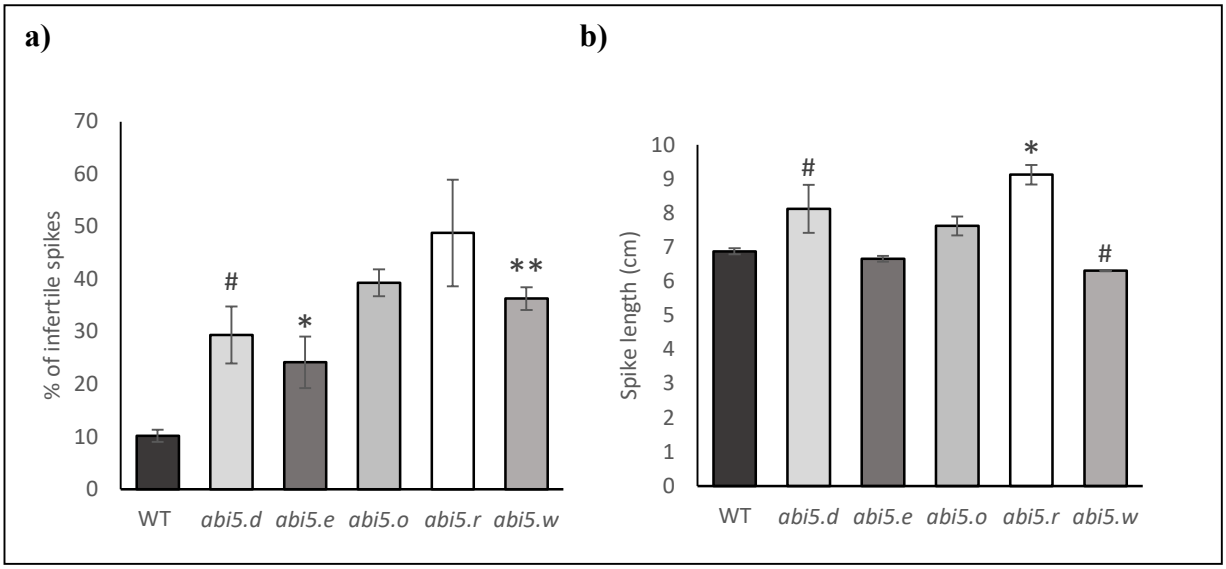

Figure 2.22: Comparisons between Wild Type (WT) and TILLING mutants in the gene Abi5 in the background cultivar Sebastian a) Spike infertility b) Spike length. Error bars indicate standard error of the mean. Significant difference between mutant line and WT indicated by; (#)P<0.1, (*)P<0.05, (**)P<0.01, (***)P<0.001.

A significant (P<0.05) increase in spike infertility was seen in the *Abi5* mutants *abi5.e* and *abi5.w*, and a weak significant increase (P<0.1) was seen in abi5.d (**Figure 2.22a**). The WT showed average infertility was 10.16% whereas *abi5.d*, *abi5.e* and *abi5.w* had an infertility rate of 29.41, 24.18 and 36.36% respectively (**Figure 2.22a**). *Abi5.d* showed an average of 8.13cm spikes, which was a weak significant increase (P<0.1) to the WT (6.88cm). *Abi5.r* showed a significant (P<0.05) increase to the WT with an

average length of 9.13cm. The opposite was seen in *abi5.r* where a weak significant (P<0.1) decrease was observed with 6.31cm (**Figure 2.22b**).

Summary of *Abi5* mutants

Table 2.3: Summary of *abi5* lines

PARAMETERS	ab5.d	abi5.e	abi5.o	abi5.r	abi5.w
BIOMASS					
HEIGHT					
TILLERS					
SPIKES					
TOTAL GRAIN WEIGHT PER PLANT					
GN					
SPIKE LENGTH	#			*	#
BIOMASS PARTITIONING					
FERTILITY	#	*			**
HI					
TILLERS PRODUCING SPIKES					
TGW			*	*	
GRAIN PER SPIKE					
FE					
WEIGHT AT ANTHESIS				*	
INTERNODE LENGTHS	**	*			

Table 2.5: Comparisons of TILLING mutants in the gene Abi5 in the background cultivars of Sebastian and Voyager. Green indicates the trait being positively different to the WT whereas red indicates the trait is negative in comparison to the WT. Significant difference between mutant line and WT indicated by; (#)P<0.1 (*)P<0.05 (**)P<0.01 (***)P<0.001.

2.4 Discussion

Testing in field allows us to analyse how the mutants compare to the WT, as any trade-offs in parameters such as grain weight would cause a lower drive for use in future breeding programmes. When growing new crop lines in the field, ideally there should

be a low number of trade-offs in the mutants compared to the wild type, so that it can provide security of yield alongside potential for enhanced survival under stress.

Overall, on the field there were clear visible differences in greenness, The difference in greenness may be due to senescence or may be due to differences in leaf pigments, this could be explored in the next trial by testing chlorophyll content. The differences were further explored these by analysing growth and development traits in individual plants both pre and post-harvest.

2.4.1 Differences in *Prt6* performance doesn't affect grain weight per plant

Yield is the important economic measure of the success of the crop. The grain weight per plant can give a very strong indication of yield, and non of the *Prt6* mutants showed any significant differences to the WT. A factor used to estimate yield is the survival rate of floret primordia, which can be seen through calculated Fruiting efficiency (FE), which is the grains set per unit dry weight at anthesis. None of the mutants showed any decrease in FE, and in the Voyager background *prt6.e* and *prt6.h* had an increase in FE. Harvest index shows the ratio of grain to total dry shoot matter, forming an indication of reproductive efficiency and can indicate the economic proportion of the crop, however none of the *Prt6* mutants showed differences in HI compared to the WT. Another trait that is strongly associated with yield is TGW, which largely is due to grain size. None of the mutants had a significantly lower TGW than the mutant, and in the voyager background, *prt6.e* had a higher TGW. The increase in TGW was not enough to make a difference in grain weight per plant.

Both height and above ground biomass can be useful tools in assessing the interception of solar irradiance by the photosynthetic area of a canopy which is therefore determining the amount of assimilates. Ramos et al., (1985) described the relationship between biomass and yield in Barley. Height and Biomass can indicate the amount of possible assimilates that the plant contains that can then be contributed to grain. *Ubr.c* had a higher weight at anthesis (biomass), however both *ubr.c* and *prt6.k* in the Sebastian background had a lower biomass than the WT at harvest. This could influence yield by providing less assimilates to the grain of the plant, however no

significant differences were observed for total grain weight per plant, therefore any differences in partitioning of biomass were not enough to have an effect on plant grain weight. Disease can have a large effect on height and biomass, therefore a following field trial without high impact of disease will give more input into the changes in height and if this will have a substantial effect on biomass.

The correlation between growth and development traits were calculated. The results showed overall show that there is little evidence that mutations in *Prt6* cause changes to the relationship between total grain weight per plant and the two contributing factors to overall yield: TGW and GN.

The stem elongation period overlaps in the growth cycle with spike growth, causing competition between the two for assimilates, however there are differences in competition in the different internodes. In a study by CIMMYT, spring wheat elite lines showed that decreased biomass partitioning to the 2nd and 3rd internode down from the spike (IN2 and IN3), enhanced spike dry matter partitioning, spike growth and grain number (Rivera-Amado et al., 2019). *Ubr.c* showed a significant decrease in partitioning to IN1 and an increase in IN2 and IN3, while *prt6.e* showed a weak significant ($P<0.1$) decrease in IN1 and an increase in IN2 and IN3. This result indicates that there may be a negative effect on enhanced spike dry matter partitioning, spike growth and grain number due to the findings by Rivera-Amado et al., (2019).

There was a delay in development seen in some *Prt6* mutants, which was followed by an increase in rate of development which resulted in the plants reaching the same growth stages as the WT in some of the later growth stages. This suggests a delay in initial growth, followed by rapid growth, which could influence tolerance to abiotic stress, in which initial growth stages are particularly susceptible.

Overall, results showed that the mutations in *PRT6* result in growth similar to that of the commercial cultivars, and in one of the cultivars, no negative traits were seen at all. *Prt6.h*, and prt6i showed no negative traits on the field therefore there were no negative trade-offs in growth and development with these specific mutations in *Prt6*, whereas *prt6.k* showed a lower biomass, however this is not an overly negative trait, as it had no effect on any other parameters tested. Out of all the mutants, *ubr.c* and *prt6.e* showed a couple of negative traits, with *prt6.e* having a lower TGW in the Sebastian cultivar, and shorter internode lengths, and *ubr.c* having a lower biomass

and spike number, however the lower spike number did not have an effect on Grain number.

The mutant with the positive trait differences in growth and development were found in *ubr.c*, which also had the most negative differences in traits. This may be due to *ubr.c* being the only mutant that did not undergo backcrossing, therefore may still carry unwanted mutations elsewhere in the genome, although shows strong differences due to the mutation being in a more highly conserved domain than the other mutants.

2.4.2 *Ntaq* mutant *ntaq*.f shows only enhanced performance in field

The spike of the plant is an indication of the potential for grain and therefore yield. Increased spike length can allow more grains per spike. While *ntaq.i* had a shorter spike length, it did not affect grain number indicating the difference in length is not enough to limit grain per spike. This was the only negative trait seen in, and given it had no effect on grain per spike, therefore the difference isn't a concern for breeding potential. *Ntaq.f* had no negative traits and showed to have enhanced biomass partitioning and more grains per spike. There was a large variation in *Ntaq* mutants in total grain weight per plant, HI and FE, which shows that there is a need to repeat this in another field trial in order to confirm there are no significant differences between mutant and WT.

The development of the *Ntaq* mutants showed a delay in development early in growth stages, After around 715 degree days, rate of crop development increases to show similar growth stages to that of the WT. Later on in the growth cycle, after the completion of anthesis, there is a delay in *ntaq.i*, in which milk development and dough development of the grain is delayed.

Overall, there were very few differences between mutants in *Ntaq* and the WT, which is very positive in terms of outlook of these mutants in breeding programmes. Whilst these mutants need to undergo further testing in growth room and glasshouse conditions to confirm waterlogging and hypoxia tolerance phenotypes. These results in field conditions provide confirmation of being able to compete with performance of the WT.

2.4.3 *Abi5* mutants show lower TGW and higher rates of infertility

TGW is a main contributing factor of yield, as it indicates the weight of grain and therefore has an impact on economic value of the crop, therefore a lower TGW seen in these mutants is a negative trait. Three of the mutants showed an increase in spike infertility. This causes a waste of resources in the plant to produce spikes but no grain, and can reduce yield, however there was not a significant difference in grain weight per plant as seen in **Figure 2.19a**.

Overall *Abi5* mutants showed a range of negative traits and few positive traits when compared with the WT. Negative traits included Spike length in the *abi5.w* mutant, however *abi5.d* and *abi5.e* showed spike length to be longer than the WT and therefore positively affected by the mutation. More concerning in terms of viability of targeting this mutant for breeding was the mutant having a negative effect on fertility, which shows an increased amount of assimilates that are wasted and not going into the formation of grain. The mutants that did not show a negative performance in terms of fertility, showed a negative performance in TGW, which is another key trait as TGW shows the size and weight of grains, and therefore links to the economic value of the crop. When analysing internode lengths, in *abi5.d* and *abi5.e* there was more length partitioned to IN2 and IN3 which can be used to indicate that there may be a negative effect on enhanced spike dry matter partitioning, spike growth and grain number (Rivera-Amado et al., 2019). Another field trial that has less disease throughout the growing season may show different results, as mutations within the *Abi5* gene may be more susceptible to disease affecting this trial.

2.5 Conclusions

This study aimed to assess the viability of *Prt6*, *Ntaq* and *Abi5* mutants as candidates for future crop breeding in Barley as a model species. Total grain weight per plant was unaffected in any of the mutants in *prt6* and *ntaq* however there was a mix of mutations having negative trade offs and positive effects on the crop. With damage by pests and disease being unavoidable in this trial due to weather conditions and late sowing, it is unknown if any of the negative or positive effects may be due to increased or decreased

susceptibility. Therefore, a further trial is needed with increase disease and pest control. This will give data in conditions hopefully without high disease infection rates which give lower reliability in results. This could be assessed by scoring plants for pathogen infection in order to attain if differences in growth and development could be due to pathogen infection. This will also allow us to see if different seasons produce any variation in results, or if the same trends are seen.

The mutants in *Prt6* and *Ntaq* which belong to the PCO branch of the Arg/N-degron pathway both showed a delay in development until around the time of anthesis. With further analysis of other components of the pathway, further understanding of if this delay is seen in the pathway as a whole, or just these specific mutations.

Abi5 mutants showed to be very mixed in having negative traits when comparing to the WT. In particular the mutations caused a negative effect on TGW and Fertility which are two main factors when looking at the success of the crop viability. Neither of these negative traits consequently had an effect on the total grain weight per plant, however, is concerning for future targeting of *ABI5*. These mutants may still carry unwanted mutations from the original TILLING lines, as the lines used on the field were not backcrossed, therefore shouldn't be ruled out for future breeding.

What is more pressing in moving forward in crop breeding using targeted mutagenesis of *NTAQ* and *ABI5* is further assessment of these mutants in abiotic stress conditions. Looking at the mutations in *PRT6*, further field trials are needed more than growth room and glasshouse experimentation, including field trials in hypoxia and drought stress.

3 Identifying photosynthetic heat stress tolerant mutants in *A. thaliana*

3.1 Introduction

3.1.1 The gaps in identification of photosynthetic heat tolerance

With predictions of future adverse weather effects due to climate change, heat stress of crop species is a major factor in future global food security. Heat stress affects productivity and yield of crops due to disrupting several biological processes, one of the most susceptible of which is photosynthesis due to the nature of its thermosensitive components (Berry and Bjorkman 1980).

It is crucial therefore that detection methods are developed for rapidly predicting photosynthetic heat tolerance in plants, to aid in breeding and gathering information on gene function associated with heat stress tolerance. Chlorophyll fluorescence has been used as a marker to gain information on the workings of key photosynthetic component PSII, which can be used to estimate photosynthetic outputs. Chlorophyll fluorescence is useful in rapidly screening lines in order to link them to phenological responses (Baker and Rosenqvist, 2004; Furbank et al., 2009). The outputs of chlorophyll fluorescence studies can also indicate plant stress. One such method was developed by Ferguson et al., (2020) demonstrating the use of rapid temperature responses of photosystem II efficiency to predict genotypic variation in rice heat tolerance. This method calculates the rate of initial decline in PSII when plants are exposed to heat, as well as the secondary, more rapid rate of decline which occurs after a breakpoint, termed T_{crit} (Ferguson et al, 2020).

3.1.2 Genome-wide association studies (GWAS) aid identification of genes associated with photosynthetic heat tolerance

Genome-wide association studies (GWAS) have proven to be a powerful tool in identifying genetic factors associated with complex traits in plants (Liu, 2023). In a recent study by (Robson et al., 2023), GWAS was conducted to dissect the genetic basis of photosynthetic heat tolerance in African (*Oryza glaberrima*) and Asian (*Oryza sativa)* rice. This research involved the characterisation of the genetic underpinnings of photosynthetic heat tolerance. By analysing chlorophyll fluorescence in a large number of rice accessions exposed to heat stress, GWAS was used to identify genetic loci associated with photosynthetic heat tolerance traits, providing insights into the genetic mechanisms underlying heat tolerance in rice.

The study utilized high-throughput phenotyping techniques, to assess photosynthetic performance under heat stress conditions and correlate these phenotypic data with genotypic information obtained through GWAS. The method by Ferguson et al., (2020) was used as a basis for phenotyping for photosynthetic heat tolerance to associate with genetic loci.

This approach allows for the detection of genetic markers linked to photosynthetic heat tolerance, which can be further investigated to understand the molecular pathways involved in conferring heat tolerance in rice.

3.1.3 Chapter aims

In this chapter, genes were selected from loci highlighted by Robson et al (2023) as loci possibly associated with photosynthetic heat tolerance in Rice. Literature searches were conducted to provide further insight into the role of these genes in photosynthetic heat tolerance and general heat stress, selected putative orthologues of those genes in the model species *A. thaliana* were selected in order for further study.

Expression of both *A. thaliana* and rice genes were assessed in order to see differences between the two species, as well as the expression patterns. T-DNA insertion mutants were selected in the *A. thaliana* genes of interest, and expression in these mutants was

confirmed in order to further assess any potential role for these genes in heat stress tolerance.

3.2 Methods

3.2.1 Selection of candidate genes for study

Results of a GWAS performed in the study by Robson et al., (2023) were obtained which highlighted candidate genes linked to photosynthetic heat tolerance traits. The GWAS processed significant SNPs into putative QTLs based on average genome-wide linkage disequilibrium (150 kb and 243 kb respectively in *Oryza glaberrima* and Bengal and Assam Aus Panel (BAAP) populations, in accordance with previously published data), resulting in a list of genes potentially underlying genetic loci associated with photosynthetic heat tolerance.

From this list, literature searches were carried out and genes that had links with abiotic stresses were highlighted, before making a final selection based upon the criteria of:

- genes that had links to heat stress tolerance but were uncharacterised for photosynthetic heat stress tolerance
- genes with links to other abiotic stresses such as drought, salinity and cold temperatures

Additionally, a relatively uncharacterised gene (*T8P21*) was chosen due to changes in expression under heat stress (Sharma et al., (2021), and the future potential of phenotyping a largely unstudied genotype.

3.2.2 Identification of *A. thaliana* orthologues and selection of T-DNA insertion lines

A. thaliana orthologues of selected genes were identified by orthologue searching on Ensembl Plants (plants.ensembl.org). Where there were multiple orthologues of the same gene, the gene with highest conservation percentage was chosen.

T-DNA insertion mutants were selected using the T-DNA express tool from the Salk Institute Genomic Analysis Laboratory (SIGnAL) tool (signal.salk.edu/cgi-bin/tdnaexpress) where *A. thaliana* gene IDs were used as queries. T-DNA insertion

mutants were then selected due to gene coverage for the gene of interest, preference was given to those lines with insertions near the beginning of a gene's sequence. SALK lines were then ordered from the Nottingham *Arabidopsis* Stock Centre (NASC). T-DNA insertion lines and NASC ID's can be found in **Table 4.1**.

Table 3.1: Chosen T-DNA insertion lines

***Oryza sativa* ID**	***A. thaliana* ID**	***Oryza sativa* name**	***A. thaliana* name**	**T-DNA insertion line**	**NASC ID**
Os05g0315100	At5G67570		*DG1*	SALK_018461C	N656226
Os05g0316100	At3G08650		*ZNE1*	SALK_085591	N682606
Os05g0316200	At2G38000		*T8P21*	SALK_025891C	N683908
Os03g0427900	At5G15400	*PUB1*	*MUSE3*	SAIL_713_A12	N861119
Os02g0448400	At1G20080	*SYN2*	*SYTB*	SALK_135307	N677964
Os11g0678000	At1G73660		*SIS8*	SALK_004541	N571182
Os05g0321900	At2G40740	*WRKY75*	*WRKY55*	SALK_070182	N570182
Os03g0437100	At1g05570	*DRZ1/CALS1*	*CALS1/GSL6*	SAIL_1_H10	N860340
Os03g0125100	At4G25700	*BCH1*	*BCH1/BO1*	SALK_061761	N561761
Os03g0125100	At5G52570	*BCH2/DSM2*	*BCH2/BO2*	SAIL_1242_B12	N862184
Os03g0129300	At1G42970	*GADPH*	*GAPB*	SAIL_267_F01	N872664
Os11g0603200	At5G64840	*ABCF6*	*ABCF5*	SALK_113472C	N664827
Os11g0657100	At3G62910		*APG3*	SALK_117765C	N668914
Os03g0395000	At2G26550	*HO2*	*HO2*	SALK_113008C	N660113
Os08g0128300	At1G13180		*DIS1*	SALK_010045C	N661446

Table 3.1: Chosen genes, gene ID's in both Rice and A. thaliana, other common gene names, and line and NASC ID for T-DNA insertion mutants used.

3.2.1 *A. thaliana* growing conditions

A. thaliana Columbia-0 (Col-0) ecotype along with the selected mutants were grown in Levington M3 compost with Biofungicide *Trichoderma asperellum* cepa T34 (T34) biological control in 10cm pots (two plants per pot). *A. thaliana* were grown until around day of bolting (+/- 1 day either side of bolting in order to limit number of plant groupings) in growth rooms at 22°C in 16hr days under fluorescent lighting with a 3:3:1 ratio of red:green:blue light with Photosynthetic Photon Flux Density (PPFD) of 205(± 8.6 SD) µmol/m^2/s, Hypoline™ (Bioline AgroSciences) was applied to soil surface of pots weekly for prevention of scarid fly larvae. Trays were rotated every week to minimise localised environmental effects.

3.2.2 Confirmation of T-DNA insertions in target genes

Crude DNA extraction

DNA was extracted for confirmation of homozygosity of T-DNA insertion lines through a method adapted from Berendzen et al., (2005).

Single leaves of 1.5-week-old *A. thaliana* mutants were taken and placed directly into 100µl Sucrose buffer, made up of 50mM Tris-Cl (pH 7.5), 300mM NaCl, and 300mM sucrose, then placed on ice. The samples were then crushed using a pipette tip, always remaining in the buffer. The sample was then heated to 99°C for 10 minutes, before being then briefly spun at 3000g for five seconds. Samples were then stored at -20℃.

PCR to confirm homozygosity of T-DNA insertion lines

T-DNA insertion lines were genotyped for homozygosity using PCR visualisation.

Table 3.2:Primers used for genotyping T-DNA insertion lines

Gene	LP	RP
DG1	CGCTTAATGGTATCCCTCTCC	AATTCTTCCACATCAACGTCG
ZNE1	GATAGCAGCAGTTGAAGTGGG	CTGTGCCCTTCTTCTTTGTTG
T8P21	AGCAGGTTTAGCCGCTACTTC	TGCAACACACAAGCTTACCAG
MUSE3	GAACTCGTCTGGTATTTCCCC	GAGCTTGCCATGACTTTGAAC
SYTB	GCTGCATCGCAAGAAAATAAG	CAAGCAAGCCACCAGTAGAAG
SIS8	TCCAGCAATGGTATTGAAAGC	TAATACTCACAGTCCCGTGCC
WRKY55	TTGCGATAGAGAGACAATGGC	TTTGGATGAACTGGTCGTTTC
CALS1	TTAGACATTCAGGGGTTCGTG	TGGAGAACCAATGTTTTCGTC
BCH1	GACAACCATGCCACAAGTCTC	GTGGACCTCTCCGATTTCTTC
BCH2	CCTATTCGGTGGAAGAAGAGG	TGAATCGGAATAAGCATGGAC
GAPB	GAATGGTGCAGCTCTAAGCAC	CCTACCAATCCTTCCAAAACC
ABCF5	AGAGCAAGCCAGAATATTGGC	GGAAGAGTTCCAAAAACGGAG
APG3	TTTAATTTTCGGGGTTTCGAG	TTACGGCCATACAAACGAGTC
HO2	ACACATTAACTGGGGATGCTG	CTTCTTCCTTCTCGGTGTCAG
DIS1	AATTGCTGGCAAAGATGTCAC	AGCTCTTCGTGTGTCAATTGG

Table 3.2: Table detailing primers used for genotyping mutant lines in A. thaliana.

PCR was performed using 0.5 µl of supernatant from the crude DNA extraction added to 25 µl REDTaq ReadyMix (Sigma Aldrich), 1µl Forward Primer (**Table 3.2**), 1µl Reverse Primer (**Table 3.2**), and 22.5µl water. This was then cycled using the following conditions, before being stored at -20°C.

Temperature	Time	Cycles	
95°C	1 min	1x	*Initial Denaturation*
95°C	15 seconds		*Denaturation*
60°C	15 seconds	40x	*Annealing*
72°C	30 seconds		*Extension*

PCR products were then visualised via gel electrophoresis using 2% agar gel (See **Appendix V**)

3.2.3 Confirmation of gene expression in T-DNA insertion mutants

Primer identification

For each gene of interest, the NM accession number was gathered from National Centre for Biotechnology Information (NCBI), linking the messenger RNA (mRNA) of the gene to the Nucleotide database. The NM accession number was then used for Primer-BLAST analysis at NCBI (www.ncbi.nlm.nih.gov/tools/primer-blast/), to find primers specific to the gene of interest, using the standard search criteria, with a PCR product size of between 80-200bp in *A. thaliana*. Primer pairs were chosen with lowest off site target sites, as well as ideally targeting the start of the gene i.e. Exon 1, as well as a high blocking f value.

RNA extraction

Whole leaf samples were taken from two week old *A. thaliana* mutants and Col-0 (WT) and placed straight into 1.5ml Eppendorf tubes which were then immediately placed in liquid nitrogen. If samples were not used immediately, they were placed in 70°C until use. Before RNA extraction, samples were briefly taken out of liquid nitrogen and weighed. RNA extraction was done using the QIAGEN RNeasy Kit, where grinding was done using pestle and mortar with the addition of liquid nitrogen to keep the sample frozen while grinding. Extracted RNA was then stored at -70°C until use.

Complementary Deoxyribonucleic Acid (cDNA) synthesis

RNA was tested for quality and concentration using a nanodrop (Thermo Scientific). Concentration was used to calculate requirements for 1.5µg cDNA. 1.5µg RNA was added to 1µl 50 µM Oligo $d(T)_{20}$ primer, and Deoxynucleotide Triphosphate (dNTP) mix, before the reaction was made up to 13µl with sterile distilled water. This was mixed and briefly centrifuged before being heated to 65°C for five minutes, then placed on ice for 1 minute. A mix of 4µl 5X SuperScript^{TM} IV (SSIV) Buffer (Vortexed and brie fly centrifuged), 1µl 100mM DTT, 1µl RNaseOUT Recombinant RNase Inhibitor and 1ul SSIV Reverse Transcriptase was mixed in a 1.5ml Eppendorf and briefly centrifuged. The two mixes were then combined and incubated at 50°C for five minutes. The reaction was then inactivated by heating at 80°C for 10 minutes. The cDNA was stored at -20°C until required.

Quantitative reverse transcriptase PCR (qRT-PCR)

4.5ul SYBR Green™ was added to 5ug cDNA, and serial dilutions of primer pairs as detailed in **Table 3.3**, this was then made up to a total volume of 7ul with water in each well of a 480 well plate and kept on ice. An amplification cycle of 95°C for 10 minutes before 45 cycles of 95°C for 30 seconds, 58°C for 30 seconds, then 72°C for 1 minute using a qTower (Analytik Jena). Optimisation of primer concentration was carried out using WT RNA, before testing both mutant and WT samples for each primer pair at optimal concentration. To calculate Relative Gene Expression (E), Ct values were adjusted according to previously calculated primer efficiencies (x) and then normalised to the housekeeping gene PP2A3 (H) using the equation $E = 100x^{H-Ct}$.

Table 3.3: Primers used expression analysis

Gene	Forward Primer	Reverse Primer
DG1	ATGGATGCTTCGGTGGTGAG	GTACTTGAGCAGCCTCCGTT
ZNE1	ACTGTGCTGGAGAAAACTTGC	AACCTCCCACTGAGCATTCG
T8P21	AAGCCTCTGCTTTCAGGATCAG	GGGGTCTTGATAACGGGAGG
MUSE3	TTGGGCAGCAGTGTTTCTCT	ACTGTAGAACACGCTCACGG
SYTB	AGACTATGACGATGATGCTGGG	CCGATCGTTGTTCCAAATCCA
SIS8	AGATCCCGGCACGCTTATTC	TTGTCTCCAGGACTAGCGGA
WRKY55	ACCAACATCGAAGCAAACTGT	TTTTCCGGTAAGCTGGACTCG
CALS1	CGTGGCAGTTTATCATTGGCT	GCATCTTTGTTTGGCCGCTT
BCH1	TGTGGCACGCTTCTCTATGG	CCTAACCCGGCGCCAAA
BCH2	GCCGTTGGGATGGAGTTTTG	ACGCTCCTTCTCTTGGTTTGT
GAPB	GCTCTCGCCGTCTCAAGAAT	TTGGAGGAGCATTGAGCAGG
ABCF5	GAGCCCAAGTCTCCACCATC	AGTCTTGCTGAGAGGGTTGC
APG3	TCGATGACGACGAGTCCAAC	CGGCCACGAGACTAGACAAA
HO2	CGGGAGTTTTGCTGGTTTTTAG	CCAGCTCCTTTCCTTCCAGA
DIS1	ATTCACACCCTCTGGTGAGC	TCGATGACAATAGCGGGTCG

Table 3.3. T-DNA insertion mutations showing Forward and Reverse primers for quantitative RT-PCR.

3.2.4 Expression profiling of T-DNA insertion mutants

Microarray data for each gene during abiotic stress were retrieved from The Arabidopsis Information Resource (TAIR) Electronic Fluorescent Pictograph (eFP) browser http://bar.utoronto.ca/efp/cgi-bin/efpWeb.cgi, in the form of fold change values at different time intervals.

3.3 Results

3.3.1 Selecting candidate genes

From the GWAS performed by Robson et al., (2023), a number of genes were identified for further characterisation of their potential role in resilience to heat stress (Chapter 4 and 5). Fourteen genes of interest were identified as good candidates for further study due to the following findings using literature searches and expression profiles:

DELAYED GREENING 1 (DG1)

DELAYED GREENING 1 (DG1) plays a crucial role in chloroplast development and gene expression in plants. *DG1* is named after the distinct phenotype seen in mutants, with early seedlings showing chlorotic plant structures including leaf and stem, before recovering to the normal green colouring in further development (Gong et al., 2014). This phenotype can be explained through studies showing DG1 is involved in regulating early chloroplast development in *A. thaliana* (Chi et al., 2010). The *DG1* gene is a nuclear-encoded factor associated with the chloroplast transcription machinery, essential for plant growth and development (Gong et al., 2014). Studies have shown that DG1 regulates chloroplast gene expression in *A. thaliana* cotyledons by interacting with chloroplast sigma factor SIGNAL PROTEIN 6 (SIG6) (Chi et al., 2010). DG1 is a P-type pentatricopeptide repeat (PPR) protein that is targeted to the chloroplast, it directly binds with RNA, is required for editing specific chloroplast transcripts, therefore mutants show defects in chloroplast gene expression, leading to abnormalities in chloroplast development and function (Sun et al., 2020). DG1 is also reported to interact with Mitochondrial RNA Modification Factor 2 (MORF) proteins, especially MORF2 (Sun et al., 2020). MORF proteins are involved in RNA editing in plastids and mitochondria, with mutants of some MORF proteins causing chloroplast RNA editing defects (Takenaka et al., 2012).

In *A. thaliana DG1* missense mutations, thermosensitivity has been reported, with ambient elevated temperature causing newly developed leaves to turn pale green, with small, abnormally shaped plastids, and less developed thylakoid membranes and starch granules than that of the WT (Yan et al., 2020). Yan et al., (2020) also reported a reduction of maximum photochemical efficiency of photosystem II (F_v/F_m) after raised temperatures to 26 °C from 22°C in missense mutations, while in knockout mutations, (F_v/F_m) ratios were substantially lower in plants under three weeks compared to the WT in control conditions (Chi et al., 2008). Yan et al (2020) hypothesized that increased temperatures reduce DG1 function by weakening the interaction between DG1 and MORF2.

BETA CAROTENE HYDROXYLASE 1 and 2 (BCH1/2)

Key components of the carotenoid biosynthesis pathway, BETA-CAROTENE HYDOXYLASE 1 (BCH1) (also known as BETA-OHASE (BO1)) and BCH2 (also known as BO2 or DROUGHT SENSITIVE MUTANT (DSM2)) are non-heme di-iron enzymes responsible for β-ring hydroxylation of β-carotene, producing zeaxanthin (Bouvier et al., 1998; Sun et al., 1996; Tian and DellaPenna, 2001; Tian, 2003; Kim and DellaPenna, 2006). Zeaxanthin can then be epoxidized, leading to antheraxanthin, violaxanthin, and neoxanthin (Niyogi et al., 1998).

Links between *BCH1* overexpression and improved drought stress tolerance has been seen in carrot (*Daucus carota* L.) *DcBCH1*. Abiotic stress tolerance has also been seen in Indian mulberry, *Morus indica* cv. K2, *BCH1* overexpression lines, which resulted in enhanced tolerance to high light, heat and Ultraviolet (UV) irradiation (Saeed et al., 2015). The silencing of *BCH1* also results in increased carotenoid content and b-carotene levels (Diretto et al., 2007).

In the GWAS conducted by Robson et al., (2023), *Os03g0125100* (*BCH1* or *DSM2)* was highlighted as a genetic locus associated with heat stress tolerance. In Rice, it was shown that overexpression of *OsBCH1* increased xanthophylls and ABA synthesis, conferring drought and oxidative stress resistance. A large study to characterise *OsDSM2* and the links to abiotic stress tolerance was carried out by Du et al., (2010). The study showed in drought conditions, T-DNA insertion mutants in *OsDSM2* are shown to have a reduction in the ABA precursor zeaxanthin and reduced ABA, as well as faster water loss throughout leaves, and reduced fertility, photosynthesis rate, chlorophyll content, biomass and grain yield. The stomatal aperture and malondialdehyde level were increased in the mutant, which was also found to have increased sensitivity to oxidative stress. The study by Du et al., (2010) also characterised photosynthetic properties of the *OsDSM2* T-DNA insertion mutants, where it was shown that there was a significant reduction in both F_v/F_m and NPQ.

In *A. thaliana*, two beta-carotene hydroxylases are found- *AtBO1* (*At4G25700*) and *AtBO2* (*At5G52570*). Photosynthetic characterisation in a study by Kim et al., (2009) showed a reduction in F_v/F_m in both *AtBO1* and *AtBO2* mutants, suggesting reduced photosynthetic potential. This study also indicated that double mutants in *AtBO1* and *AtBO2* reduce NPQ induction and adaptation to high light stress and suggested that

there is a level of redundancy in the two BCH enzymes. Tian et al., (2003) demonstrated that mutation of *AtBO1* had a more severe effect on violaxanthin and antheraxanthin reduction than *AtBO2* did, which did not have a significant difference to the WT, apart from a small decrease in neoxanthin (Tian et al., 2003). T-DNA insertion mutations in *AtBO1* was also seen to have a higher Lutein content than that of WT (Tian et al., 2003). The double *AtBo1:At*Bo2 mutant shows an additive carotenoid phenotype, with 80% reduction in xanthophylls. NPQ has also seen to have a slower induction speed and magnitude in *AtBo1* and *AtBo2* than WT, with *AtBo1* having a slower induction and lower magnitude than *AtBo2* (Tian et al., 2003), similar to patterns seen in rice (Du et al., 2010).

Beta subunit of GLYCERALDEHYDE-3-PHOSPHATE DEHYDROGENASE (GAPB)

Localised to the chloroplast, GLYCERALDEHYDE-3-PHOSPHATE DEHYDROGENASE (GAPDH) is a protein that catalyses phosphorylation and oxidation of glyceraldehyde-3-phosphate, converting it to 1,3-bisphosphoglycerate producing nicotinamide adenine dinucleotide (NAD) + hydrogen (H) (NADH) using NAD+ as an electron acceptor (Meyer-Gauen et al., 1994; Backhausen et al., 1998). This categorises GAPDH as a key housekeeping gene, and a key component of glycolysis, driving ATP generation. The overexpression of GAPDH (in rice) results in the increased photosynthetic assimilation in elevated CO_2 environments (Suzuki et al., 2021). GAPDH can be split into two distinct subunits- GAPA and GAPB, the main difference being the C-terminal extension on GAPB (Baalmann et al., 1996). The chloroplast localised beta subunit of glyceraldehyde 3-phosphate dehydrogenase (GAPB) has been linked to high salinity stress tolerance in a close relative of *A. thaliana*- *Thellungiella halophila* (Chang et al., 2015).

In the GWAS by Robson et al., (2023), *Os03g0129300* was highlighted as a genetic locus associated with heat stress tolerance. *Os03g0129300* encodes for the Beta subunit of glyceraldehyde-3-phosphate dehydrogenase (OsGAPB). In low light conditions, overexpression of *OsGAPB* in rice has been shown to increase CO_2 assimilation rate, chlorophyll content and fresh weight, suggesting this gene is a good candidate for manipulating rice tolerance to low light stress, due to low light

significantly inhibiting GABDH accumulation (Liu et al., 2020). Other GAPB orthologues in various species have been seen, such as *ThGAPB* in the highly saline tolerant *Thellungiella halophila*, and the overexpression of *ThGAPB* in *A. thaliana* showed enhanced salt tolerance.

Zhang et al., (2016) demonstrated that the orthologue of *OsGAPB* in *A. thaliana* - *AtGAPB*, had increased expression in abiotic stress conditions. In salt solution, *AtGAPB* was upregulated in both root and shoot, whereas in heat *stress* AtGAPB was only upregulated in shoots, and in cold treatments *AtGAPB* was intensely transcribed (Zhang et al., 2016). During drought treatment, *AtGAPB* in shoots was upregulated at first before being later down regulated, and in roots *AtGAPB* was intermittently up and downregulated (Zeng et al., 2016). T-DNA insertion mutations in *GAPB* have been shown to have a significantly lower rosette dry weight and leaf number (Alqurashi, 2019). Simkin et al., (2023) demonstrated that T-DNA insertion lines having no significant differences in ΦPSII, a decrease in photosynthetic carbon fixation rates, and a lower rate of photosynthetic electron transport (J_{max}). In the same study, growth parameters such as leaf number and final biomass were also seen to be reduced in *AtGapb* mutants (Simkin et al., 2023). Overall, the crucial role of *GAPB* as part of the Calvin cycle and the changes in regulation with abiotic stress make this a gene of interest for further crop breeding.

ALBINO OR PALE GREEN 3 (APG3)

The translation elongation and termination in plant mitochondria are thought to be similar to the molecular mechanisms in bacteria. Bacterial type release factors (RF) have been found in *A. thaliana* (Raczynska et al., 2006). ALBINO OR PALE GREEN 3 (APG3) encodes a ribosome release factor 1, with the N-terminal region of APG3 is a transit peptide involved in chloroplast targeting and various mutants in this gene result in a chlorotic or albino phenotype (Motohashi et al., 2007). In the GWAS by Robson et al., (2023), *Os11g0657100* was highlighted as a genetic locus associated with heat stress tolerance, which is an orthologue of APG3 in *A. thaliana* (*At3G62910*).

Dissociation (Ds) transposable elements insertion lines in *APG3* showed seedling-lethal phenotypes and could only be grown past germination stage on agar with sucrose

supplement, suggesting that the albino *apg3-1* cannot grow photoautotrophically (Motohashi et al., 2007). In these Ds transposable elements insertion mutants, chlorophyll-a, chlorophyll-b, and β-carotene were at 19%, 26%, and 10% of pigment content found in wild-type plants, respectively. The mutants also had abnormal spherical plastids with low starch accumulation (Motohashi et al., 2007). Additionally, *apg3* mutants have also shown to have reduced chloroplast proteins including Rubisco (R. Motohashi et al., unpublished data). Zhang et al (2023) demonstrated that a mutant in *APG3* obtained through EMS mutation *drought inhibited growth of lateral roots* (*dig8*) had higher ROS levels, increased callose deposition, and decreased plasmodesmata permeability.

DISTORTED TRICHOMES 1 (DIS1)

The Actin-Related Protein 2/3 (ARP2/3) complex regulates the actin cytoskeleton function and organisation by pushing forward the edge of motile cells and endocytosis through producing branched filaments (Staiger and Blanchoin, 2006; Pollard, 2007). A subunit of this complex, ARP3 is also known as DISTORTED TRICHOMES 1 (DIS1), named after mutants of the gene displaying changes in the trichome, is linked to trichome, hypocotyl, and leaf epidermal cells, as well as having roles in gravitropism and phototropism (Hülskamp et al., 1994; Reboulet *et al.*, 2010). An orthologue of DIS1, *Os08g0128300* was highlighted as a genetic locus associated with heat stress tolerance in a GWAS performed by Robson et al., (2023). DIS1 regulates endocytosis and PIN3 and PIN7 recycling to the plasma membrane in the columella cells (Zou et al., 2016). Plant stomatal movement is also regulated by DIS1 through actin reassembly (Jiang et al., 2012). Linked to regulation in gravitropic response AtDIS1 mutants showed altered gravitropic curvature, with roots having impaired curvature by 43% and reduced growth by 15% in the dark after 24 hours (Reboulet et al., 2010).

AtDIS1 mutants also have increased water loss through transpiration, which is suggested to be due to the changes in stomatal regulation, as well as links to salt stress tolerance and resistance to pathogens (Jiang et al., 2012; Zhao et al., 2013; Sun et al., 2019; Qi et al., 2017). Sun et al., (2019) described a tomato subunit of ARP2/3 to be upregulated during incompatible host pathogen interaction using powdery mildew

pathogen *O. neolycopersici*, while Qi et al., (2017) described the required role of the ARP2/3 complex in resistance to *Puccinia striiformis* f. sp. *tritici* in wheat. The ARP2/3 complex is also linked to mitochondrial-dependent Ca^{2+} signalling in response to salt stress, and modulates microfilament (MF) dynamics and mitochondrial permeability transition pore (mPTP) opening, in order to regulate $[Ca^{2+}]_{cyt}$ signalling through the pore to maintain growth during salt stress (Zhao et al., 2013).

SYNAPTOTAGMIN 2 (SYTB)

Synaptotagmins are membrane trafficking proteins that can be found in both plants and animals. In *A. thaliana*, *SYNAPTOTAGMIN 1 (SYT1)* is involved in regulating endocytosis Fand intercellular transport as well as membrane repair (Schapire et al., 2008). Mutations in SYTB have been found to have abiotic stress tolerance including heat resistance (Schapire et al., 2008; Yamazaki et al., 2008, Perez Sancho et al., 2015). The silencing of SYT-5 has also shown to significantly improve the drought tolerance in rice (Shanmugam et al., 2021).

In the GWAS by Robson et al., (2023), Os02g0448400 was highlighted as a genetic locus associated with heat stress tolerance, which is the orthologue of *A. thaliana* Synaptotagmin 2 (AtSYTB) (At1G20080). Os02g0448400 has been seen to be a candidate for cold stress tolerance, due to the SYTB in plants is involved in secretion via unconventional protein transport from cytosol to the extracellular matrix (Zhang et al., 2011). The SYTB genes contain a transmembrane domain and two C2 domains which bind to phospholipids in plant membranes, which is regulate by Ca^{2+} ions (Wang et al., 2016). Localised to the Golgi apparatus, SYTB is expressed mainly in pollen grains, as well as a high level of expression in inflorescence and stamens (Zhang et al., 2011; Wang et al., 2015). Mutations in *AtSYTB* result in reduced rate of pollen tube growth, pollen tube length and decreased total pollen germination (Wang et al., 2015). Zhang et al., (2021) also suggested that is possibly involved in cold stress in rice through haplotype analysis.

ZINC NUTRIENT ESSENTIAL1 (ZNE1)

ZINC NUTRIENT ESSENTIAL1 (ZNE1) is a golgi-localised Zn^{2+} transporter that maintains Zn^{2+} homeostasis in leaves (Wang et al., 2021), separate to the zinc-regulated transporter (ZRT)/iron-regulated transporter (IRT)-like (ZIP) family of proteins. In *A. thaliana*, ZNE1 has been shown to have a role in regulating Zinc (Zn) content in seeds (Waters and Grusak, 2008) and AtZNE1 is a vital component in plant adaptation to excess Zn or Fe (Wang et al., 2021). AtZNE1 (At3g08650) is an orthologue of Os05g0316100, which was highlighted as a genetic locus associated with heat stress tolerance in a GWAS by Robson et al., (2023)

SUGAR INSENSITIVE 8 (SIS8)

Mitogen-Activated Protein Kinase (MAPK) pathways regulate cell cycles, growth and death in response to plant stress, and are composed of MAPK's, Mitogen-Activated Protein Kinase Kinases (MAPKK's) and Mitogen-Activated Protein Kinase Kinase Kinases (MAPKKK's) that work from sequential phosphorylation (Rodriguez et al., 2010). In the GWAS by Robson et al., (2023), *Os11g0678000* was highlighted as a genetic locus associated with heat stress tolerance, which is an orthologue of *Sugar insensitive 1 (SIS8*), a putative Raf-like MAPKKK (in the subgroup B3) (Ichimura et al., 2002). Isolated based on salt stress tolerance, AtSIS8 was first reported by Gao and Xiang (2008). Under normal growth conditions, growth and development of *sis8* is similar to that of WT, however during salt stress, the germination rate was barely affected by salt stress, and survival rate of seedlings during salt stress is also increased (Gao and Xiang 2008). Gao and Xiang (2008) also confirmed that the phenotype is independent of GA and ABA signalling, and overall findings suggested SIS8 was a negative regulator of salt stress, and off switch for stress response. As well as confirming the salt stress tolerance of SIS8, Huang et al., (2014) showed that SIS8 knockout mutants were also tolerant to high levels of sugar, whereas in WT *A. thaliana*, high concentrations of sucrose or glucose prevent development. *SIS8* overexpression results in hypersensitivity to sugar, with lower rates of cotyledon expansion and true leaf formation (Huang et al., 2014). Sharma et al., (2021) also showed that *Os11g0678000* expression in rice showed more than a two fold decrease in response to 37/42 °C heat in IR64/Annapurna seedlings according to RNA-seq.

MUTANT SNC1 ENHANCING 3 (MUSE3)

Plant U-box (PUB) proteins are involved with development, self-incompatibility and hormone responses, with 77 PUB genes in rice (Azevedo et al., 2001) and 64 *A. thaliana PUB* genes (Zeng et al 2008). Named after their U-box domain, *PUB* genes are involved in the protein degradation within cells, and the domain acts as a ubiquitin ligase (Sharma and Taganna, 2020; Yang et al., 2021). The involvement of *PUB* genes in salt tolerance have been reported several species including Wheat, Strawberry, Hot pepper, Rice and *A. thaliana* (Jiang et al., 2023; Cho et al., 2006; Cui et al., 2023; Kim et al., 2023, Byun et al 2017; Quin et al., 2020; Bergler et al., 2011; Hwang et al., 2015). *PUBs* have also been shown to be involved as negative regulation of ABA-mediated drought stress (Cho et al., 2006; Seo et al., 2012; Lui et al., 2011), with some PUB mutants in *A. thaliana* showing hypersensitivity to water stress (Adler et al., 2017). Different *PUB* genes have also been seen to be differentially induced following heat stress in both roots and shoots, with some being upregulated and some being down regulated (Adler et al., 2017)

In the GWAS by Robson et al., (2023), *OsPUB1* (*Os03g0427900*) was highlighted as a genetic locus associated with heat stress tolerance. The *A. thaliana* orthologue of *OsPUB1* is *SNC1-ENHANCING 3 (MUSE3*) (*AT5G15400*). The mutant *muse3* is an E4 ligase factor working downstream of E3 ligase subunit Constitutive expressor of PR Genes 1 (CPR1), a subunit of SKP1-CULLIN1-F-box (SCF), which facilitates ubiquitination and degradation of SURPRESSSOR OF NONEXPRESSOR OF PR GENES1 (NPR1) CONSTITUATIVE1 (SNC1) and RESISTANCE TO *PSEUDOMONAS SYRINGAE2* 2 (RPS2) along with other Resistance proteins (Huang et al 2014). This prevents Resistance protein overaccumulation and autoimmunity, therefore MUSE3 may be a key regulator of Resistance protein turnover to enable appropriate defensive output (Huang et al., 2014: Cheng et al., 2011; Gou et al., 2012). *Muse3* mutants exhibit enhanced disease resistance, due to the disruption of negative regulation of SNC1-mediated immunity by MUSE3 (Huang et al 2014). After MUSE3 recognises a ubiquitinated protein and adds additional ubiquitin molecules, *A. thaliana* CELL DIVISON CYCLE 48 A (AtCDC48A) interacts with MUSE3, providing energy

to shuttle poly-ubiquitinated nucleotide-binding, leucine-rich repeat (NLR) substrates to the proteasome for degradation (Copeland et al., 2016).

CALLOSE SYNTHASE 1 (CALS1)

Callose is a key component of plant cell walls, and although found at low levels, is crucial to plant development and defence. Callose also is involved in the regulation of bud dormancy in perennial plants (Singh et al., 2018; Tylewicz et al., 2018; Singh et al., 2019) and plays an important role in pollen development through isolating microspores with a callose layer to form tetrads (Enns et al., 2005). Callose regulates pore size in the phloem to regulate transport through accumulating on the sieve plates (Barratt et al., 2011; Xie et al., 2011), and controls plasmodesmata pore size through deposition of callose (Radford et al., 1998).

Synthesis of callose is through a multi-subunit protein complex which is localised on the cell membrane, with the most important subunit being the enzyme *CALLOSE SYNTHASE (CALS)*, also known as *GLUCAN SYNTHASE-LIKE (GSL)*. GSLs are involved in the first line of defence for plants against pathogens, such as accumulating callose on the cell wall, in order to thicken the cell wall upon invasion of pathogens (Miedes et al., 2014). Callose synthase genes have also been shown to be upregulated when exposed to drought stress, with an increased deposition of callose around the xylem and in and around the protoxylem vessels after drought treatments (Liao et al., 2023). CALS have also been linked to heat stress, where heat treatment induced callose deposition at phloem-pole pericycle interfaces in *A. thaliana*, inhibiting phloem unloading and restricting meristem size (Lui et al., 2022). During heat stress in rice, *OsGSL's* have been seen to be up and down regulated depending on cultivar, therefore the effect of GSLs may be species specific during heat stress (Luan et al., 2023).

In the GWAS by Robson et al., (2023), *OsGSL10* (*Os03g0128100*/*Os03g0128200*), was highlighted as a genetic locus associated with heat stress tolerance. In *A. thaliana*, 12 *CALS* genes have been identified (Verma and Hong, 2001). *Callose synthase 1* (*CALS1*), also known as *GSL6* in *A. thaliana* (*At1g05570*) is an orthologue of *OsGSL10* with close homology, although many of the GSL genes are very similar (**Figure 3.1**). In *A. thaliana*, AtGSL10 and AtGSL6 can be associated to the same

group of GSL's, as they both have functions associated with the synthesis of callose during pollen development and cell division. GSL6 in *A. thaliana* has been shown to be induced by SA, and provides a mechanism to stop the spread of virus' through reducing intercellular trafficking by inducting the synthesis of callose by plasmodesmata (Wang et al., 2013; Cui and Lee, 2016).

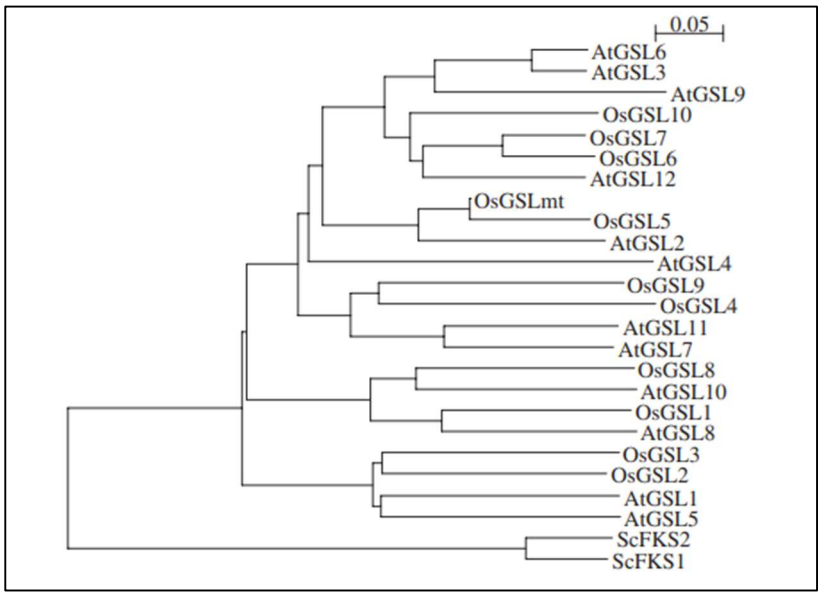

Figure 3.1: From Yamaguchi et al., (2006): Phylogenetic Tree of Glucan Synthases. Multiple alignment of deduced callose synthase (GSL, Glucan synthase-like) amino acid sequences were done by ClustalW 1.83. Phylogenetic trees were constructed using the NJ (Neighbour-Joining) algorithm and drawn with the NJplot program.

HEME OXYGENASE 2 (HO2)

Heme oxygenases (HOs) are plastid enzymes that catalyse the oxidative cleavage of haem to biliverdin (BV), iron and carbon monoxide, and can be split into the subfamilies of HO1-like (including HO2, HY1, HO3 and HO4) and HO2-like (HO2). While HO1 is known to be a plastid enzyme that syntheses chromophores in phytochromes, HO2 is not a functional HO enzyme, and contains an arginine residue in place of a conserved heme-binding histidine (His) residue found in HO1 (Davis et al., 2001; Li et al., 2014). HO2 binds to Proto IX, a precursor of heme and chlorophyll biosynthetic pathways (Gisk et al., 2010).

In the GWAS by Robson et al., (2023), OsHO2 (Os03g0395000) was highlighted as a genetic locus associated with heat stress tolerance. In rice, OsHO2 was previously

seen to be localised in the stroma of the chloroplast and was expressed more in early development than in maturity indicating its functional importance in early development (Li et al., 2014). In this same study, it was seen that a *HO2* mutant ylc2 had a reduction in chlorophyll accumulation of 77% and suggested a role in tetrapyrrole metabolism. It was also noted that the chlorophyll reduction was not due to heme-induced *GLUTAMYL tRNA REDUCTASE* (HEMA) inhibition (Li et al., 2014). This reduction in chlorophyll links with HO2 binding to Proto IX, a chlorophyll precursor (Li et al., 2014).

HO2 has also been identified in *A. thaliana*, *AtHO2* (*AT2G26550*). Mutations in *HO2* show photomorphogenic defects similar to *AtHO1* (Davis et al.,2001). Whilst stronger chlorotic phenotypes are seen in Rice, *ho2* mutants in *A*. *thaliana* have a less than 10% reduction in chlorophyll content (Emborg et al., 2006). Further to differences in chlorophyll*, A. thaliana ho2* mutants also exhibit reduced growth rate, accelerated flowering time, and reduced de-etiolation (Davis et al., 2001)

WRKY DNA-BINDING PROTEIN 55 (WRKY55)

The WRKY superfamily are a group of transcription factors which play a crucial role in regulating various processes including responses to both biotic and abiotic stresses, seed germination, senescence, and dormancy (Rushton et al., 2012). These transcription factors are characterized by the presence of DNA binding region: a 60 amino acid long peptide region, termed the WRKY domain. WRKY proteins bind to the cis-element 5′-TTGAC-C/T-3′, termed the W-box (Rushton et al., 1996; Chen and Chen 2000; Cormack et al., 2002). There are 72 WRKY members in *A. thaliana* (Rushton et al., 2010), 98 in *Oryza sativa* L. ssp. *japonica* and 102 in *Oryza sativa* L. ssp. *indica* (Ross et al., 2007). This large family of transcription factors (TFs) have been linked to seed development, trichome development, leaf senescence, and stress response (Hinderhofer and Zentgraf 2001; Johnson et al., 2002; Luo et al., 2005;Ülker and Somssich 2004; Li et al., 2006; Journot-Catalino et al., 2006; Xu et al., 2006; Zheng et al., 2006; Wang et al., 2006; Shen et al., 2007). In Rice, overexpression of *OsWRKY11* caused increased tolerance to heat and drought stress (Wu et al., 2009), and both overexpression in *OsWRKY45* in Rice and *GmWRKY54* in soybean led to increased drought and salt stress tolerance (Qiu and Yu., 2009; Zhou et al., 2008)

In the GWAS by Robson et al., (2023), *OsWRKY75* (*Os05g0321900*) was highlighted as a genetic locus associated with heat stress tolerance. Studies on WRKY75 have shown its involvement in various biological processes in plants. The study by Zafar et al., (2022) saw that *OsWRKY75* was significantly upregulated after exposure to White-Backed Planthopper infestation, similar to many other *WRKY* genes in Rice. Yuan et al., (2019) stated *OsWRKY75* had the highest number of *R. solani*-responsive cis-elements in its promoter region out of the WRKY Transcription factors, again linking its role to biotic stress resistance.

The orthologue of *WRKY75* in *A. thaliana* is *WRKY55* (*At2G40740*). The most prominent study done on AtWRKY55 was that of Wang et al., (2020). The study confirmed AtWRKY55's role as a transcriptional activator, and showed it was only present in the nucleus, which links with its role as a transcription factor (Wang et al., 2020). Overexpression mutants of *AtWRKY55* had increased bacterial pathogen resistance to (*Pseudomonas syringae* pv. tomato strain DC3000) (*Pst*DC3000) whilst T-DNA insertion mutations had increased susceptibility. A previous study by Dong et al., (2003) had highlighted *AtWRKY55* to be one of only few *WRKY* genes to have reduced pathogen induced expression and classed it one of the 49 defence-related *AtWRKY* genes. In *AtWRKY55* T-DNA insertion mutants, a delay in leaf senescence was seen, whereas overexpression of *AtWRKY55* caused acceleration of leaf senescence, supporting the hypothesis that AtWRKY55 plays a central role in controlling leaf senescence (Wang et al., 2020). It is also seen that AtWRKY55 upregulates genes the expression of *RESPIRATORY BURST OXIDASE HOMOLOGS D (RbohD), ISOCHORISMATE SYNTHASE 1 (ICS1), avrPphB SUSCEPTIBLE 3 (PBS3)* and *SENESCENCE- ASSOCIATED GENE 13 (SAG13)* (Wang et al., 2020; Breeze et al., 2011; Buchanan-Wollaston et al., 2005; Guo et al., 2004; Woo et al., 2016). It was also found in this study by Wang et al., (2020) that AtWRKY55 positively regulates transcription of ROS and salicylic acid (SA) biosynthesis genes, which controls the leaf senescence. ROS and SA are signalling molecules that also play important roles in stress response (Baxter et al., 2014; Rivas-San Vicente and Plasencia, 2011), therefore linking WRKY55 to plant stress responses through these signalling pathways.

GENERAL CONTROL NON REPRESSABLE 5 (ABCF5)

ATP binding cassettes (ABCs) play a role in regulating stress responses in plants, such as drought and salt stress (Jangam et al., 2016) as well as being induced by abiotic stresses, indicating their role in stress adaptation (Rensink et al., 2005; Liu et al., 2011). The ABCF subfamily of ABC's has been highlighted for its involvement in stress responses across different organisms (Jeong et al., 2014; Kou, 2024). ABC proteins play an active role in regulating ion channels, receptors and proteins involved in mRNA translation and ribosome biogenesis as well as transporting a wide range of substrates across biological membranes (Rea, 2007). There are eight subfamilies of the ABC proteins in rice, one of which is the ABCF subfamily, which is characterised by the presence of two nucleotide binding domains with no transmembrane domains (Verrier et al., 2008, Kos and Ford, 2009; Shoji, 2014).

ABCFs have been linked with tolerance and sensitivity to several abiotic stresses including drought, oxidative stress, salinity, selenium (Faus et al., 2021; Wu et al., 2023). The Rice gene *OsABCF6* was highlighted as genetic locus associated with heat stress tolerance in the GWAS performed by Robson et al., (2023).

In *A. thaliana* there are five members of ABCF family, with the most similar genetically to *OsABCF6* as *AtABCF5* (*At5G64840*). *ABCF5* T-DNA insertion mutants in *A. thaliana* show increased sensitivity to salt stress as well as increased tolerance to paraquat (a superoxide producer that can mimic the conditions of oxidative stress) and acetic acid (mimicking environmental drought) indicating increased resistance to drought and oxidative stress (Faus et al., 2021).

T8P21

In the GWAS by Robson et al., (2023), *Os05g0316200* was highlighted as a genetic locus associated with heat stress tolerance, which showed more than a two fold change response to 37/42°C heat in IR64 Annapurna seedlings according to RNA-seq by Sharma et al., (2021). This gene is relatively uncharacterised, however Hudson et al., (2003) previously described a significant fold change in expression of *T8P21* in mutations of *FAR-RED-IMPAIRED RESPONSE1* (*FAR1)* and *FAR-RED ELONGATED HYPOCOTYLS3* (*FHY3)*, which display reduced inhibition of

hypocotyl elongation, specific to far-red light, suggesting *T8P21* could show similar mutant phenotypes. *T8P21* also showed a fold change in expression after virus inoculation after five days (Whitham et al., 2003).

3.3.2 T-DNA insertion mutants of orthologue genes in *A. thaliana*

In order to study the effects of these genes during stress tolerance, with a focus on heat stress, and to assess whether mutations in these genes could aid developing crop genetics for stress tolerance, orthologues of the Rice genes chosen from the GWAS results by Robson et al., (2023) were found in *A. thaliana*.

T-DNA insertion mutants in each gene of interest were selected (**Table 3.2**), and primers were designed to both genotype the T-DNA insertion lines for homozygosity and to determine the expression of genes in the T-DNA insertion mutants via qRT-PCR. **Figures 3.2-3.16** show the structure of the chosen genes of interest in *A. thaliana* and the corresponding T-DNA insertion location and location of the primers used.

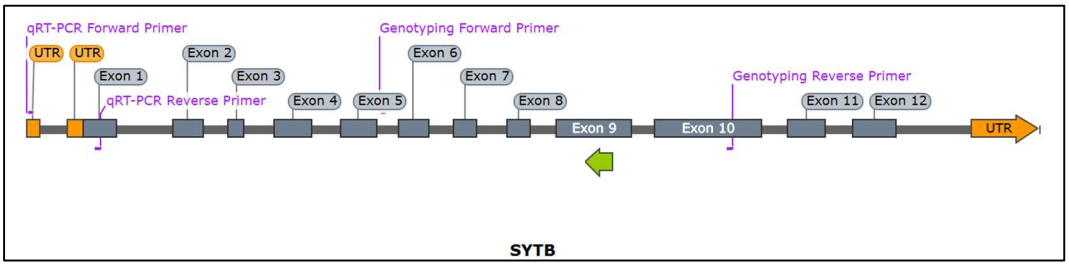

Figure 3.2: Schematic diagram of the gene SYTB in A. thaliana. Dark grey boxes show exons, orange boxes show the untranslated regions (UTRs), and the green arrow shows the location of the T-DNA insertion. Primers are highlighted in purple, with genotyping primers being used for testing homozygosity (as per table 3.2), and qRT-PCR primers used for analysis of gene expression (as per table 3.3).

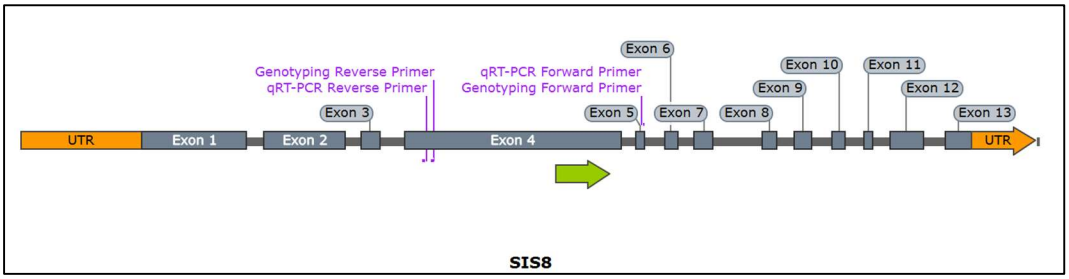

Figure 3.3: Schematic diagram of the gene SIS8 in A. thaliana. Dark grey boxes show exons, orange boxes show untranslated regions (UTRs) and the green arrow shows the location of the T-DNA insertion. Primers are highlighted in purple, with genotyping primers being used for testing homozygosity (as per table 3.2), and qRT-PCR primers used for analysis of gene expression (as per table 3.3).

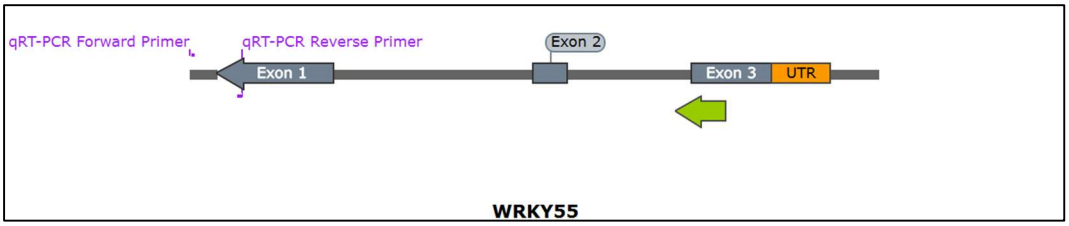

Figure 3.4: Schematic diagram of the gene WRKY55 in A. thaliana. Dark grey boxes show exons, orange boxes show untranslated regions (UTRs) and the green arrow shows the location of the T-DNA insertion. Primers are highlighted in purple, with genotyping primers being used for testing homozygosity (as per table 3.2), and qRT-PCR primers used for analysis of gene expression (as per table 3.3).

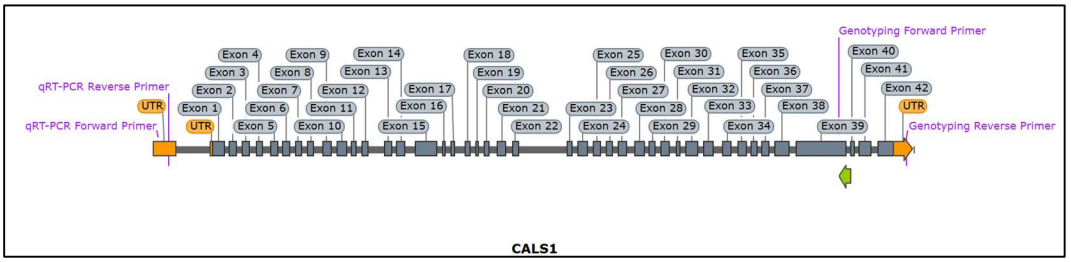

Figure 3.5: Schematic diagram of the gene CALS1 in A. thaliana. Dark grey boxes show exons, orange boxes show untranslated regions (UTRs) and the green arrow shows the location of the T-DNA insertion. Primers are highlighted in purple, with genotyping primers being used for testing homozygosity (as per table 3.2), and qRT-PCR primers used for analysis of gene expression (as per table 3.3).

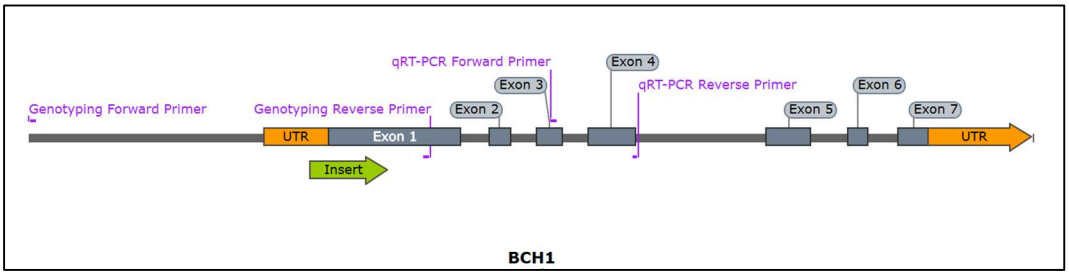

Figure 3.6: Schematic diagram of the gene BCH1 in A. thaliana. Dark grey boxes show exons, orange boxes show untranslated regions (UTRs) and he green arrow shows the location of the T-DNA insertion.

Primers are highlighted in purple, with genotyping primers being used for testing homozygosity (as per table 3.2), and qRT-PCR primers used for analysis of gene expression (as per table 3.3).

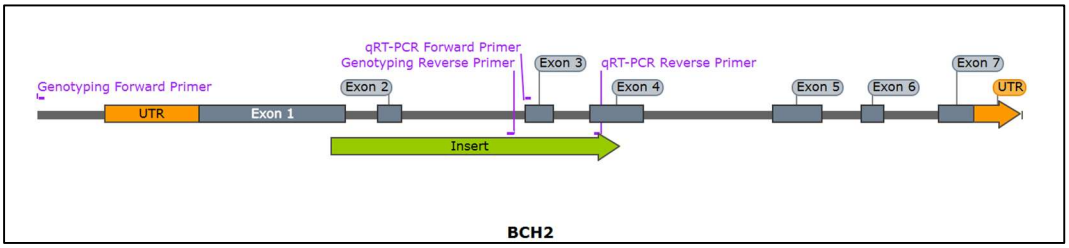

Figure 3.7: Schematic diagram of the gene BCH2 in A. thaliana. Dark grey boxes show exons, orange boxes show untranslated regions (UTRs) and the green arrow shows the location of the T-DNA insertion. Primers are highlighted in purple, with genotyping primers being used for testing homozygosity (as per table 3.2), and qRT-PCR primers used for analysis of gene expression (as per table 3.3).

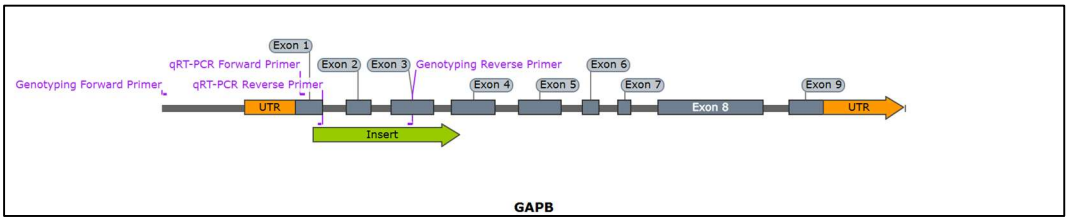

Figure 3.8: Schematic diagram of the gene GAPB in A. thaliana. Dark grey boxes show exons, orange boxes show untranslated regions (UTRs) and the green arrow shows the location of the T-DNA insertion. Primers are highlighted in purple, with genotyping primers being used for testing homozygosity (as per table 3.2), and qRT-PCR primers used for analysis of gene expression (as per table 3.3).

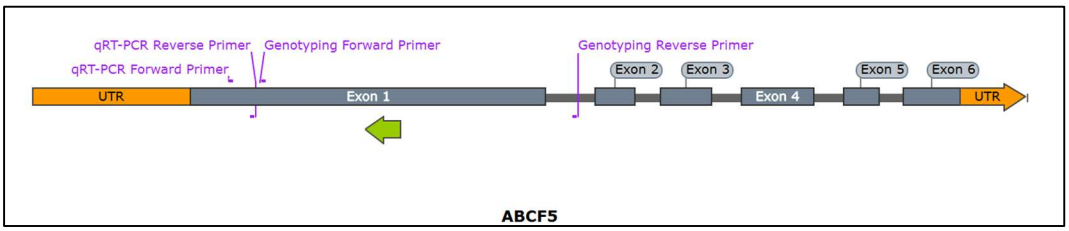

Figure 3.9: Schematic diagram of the gene ABCF5 in A. thaliana. Dark grey boxes show exons, orange boxes show untranslated regions (UTRs) and the green arrow shows the location of the T-DNA insertion. Primers are highlighted in purple, with genotyping primers being used for testing homozygosity (as per table 3.2), and qRT-PCR primers used for analysis of gene expression (as per table 3.3).

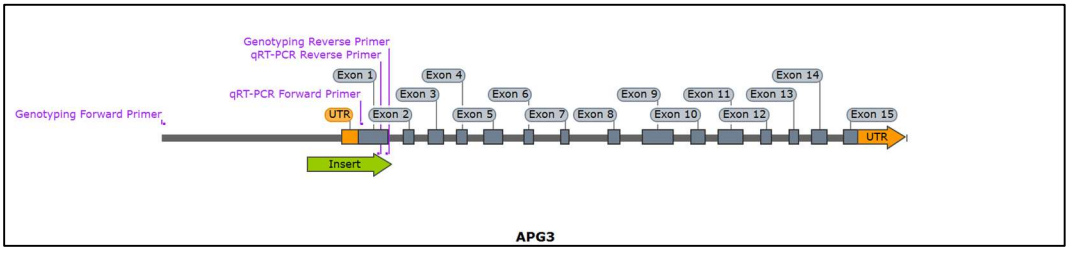

Figure 3.10: Schematic diagram of the gene APG3 in A. thaliana. Dark grey boxes show exons, orange boxes show untranslated regions (UTRs) and the green arrow shows the location of the T-DNA insertion. Primers are highlighted in purple, with genotyping primers being used for testing

homozygosity (as per table 3.2), and qRT-PCR primers used for analysis of gene expression (as per table 3.3).

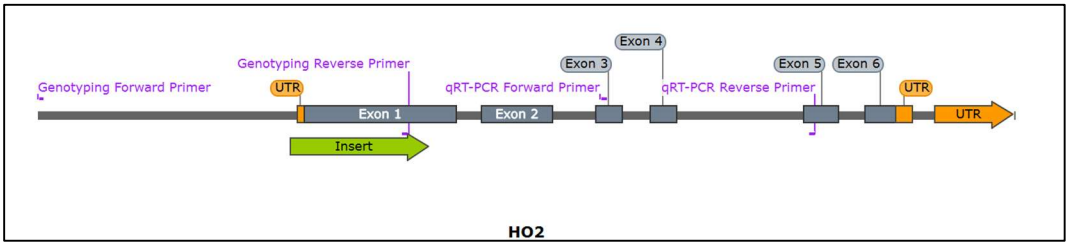

Figure 3.11: Schematic diagram of the gene HO2 in A. thaliana. Dark grey boxes show exons, orange boxes show untranslated regions (UTRs) and the green arrow shows the location of the T-DNA insertion. Primers are highlighted in purple, with genotyping primers being used for testing homozygosity (as per table 3.2), and qRT-PCR primers used for analysis of gene expression (as per table 3.3).

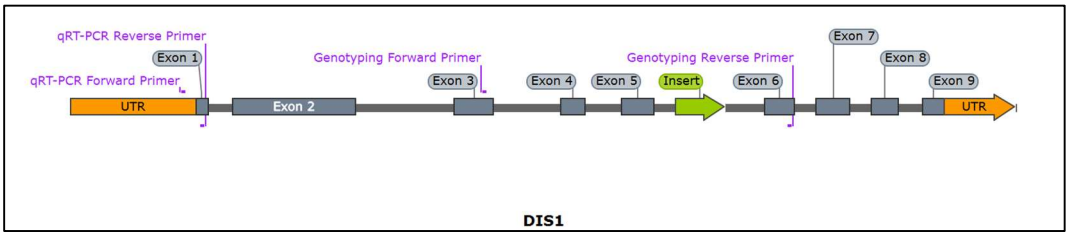

Figure 3.12: Schematic diagram of the gene DIS1 in A. thaliana. Dark grey boxes show exons, orange boxes show untranslated regions (UTRs) and the green arrow shows the location of the T-DNA insertion. Primers are highlighted in purple, with genotyping primers being used for testing homozygosity (as per table 3.2), and qRT-PCR primers used for analysis of gene expression (as per table 3.3).

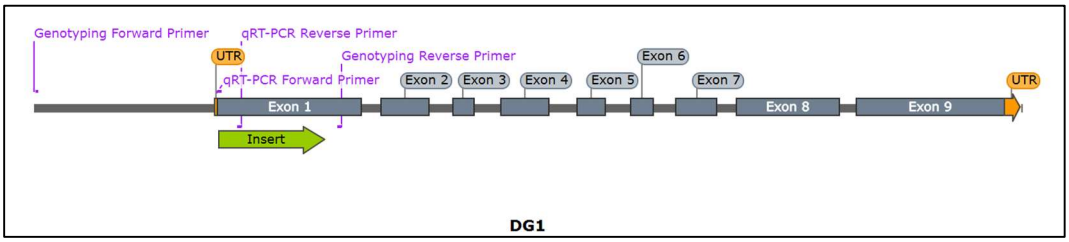

Figure 3.13: Schematic diagram of the gene DG1 in A. thaliana. Dark grey boxes show exons, orange boxes show untranslated regions (UTRs) and the green arrow shows the location of the T-DNA insertion. Primers are highlighted in purple, with genotyping primers being used for testing homozygosity (as per table 3.2), and qRT-PCR primers used for analysis of gene expression (as per table 3.3).

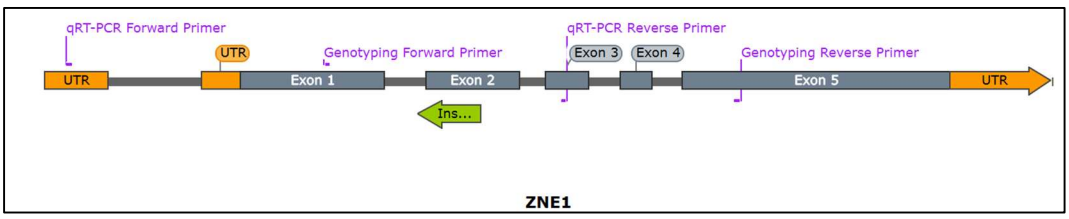

Figure 3.14: Schematic diagram of the gene ZNE1 in A. thaliana. Dark grey boxes show exons, orange boxes show untranslated regions (UTRs) and the green arrow shows the location of the T-DNA insertion. Primers are highlighted in purple, with genotyping primers being used for testing

homozygosity (as per table 3.2), and qRT-PCR primers used for analysis of gene expression (as per table 3.3).

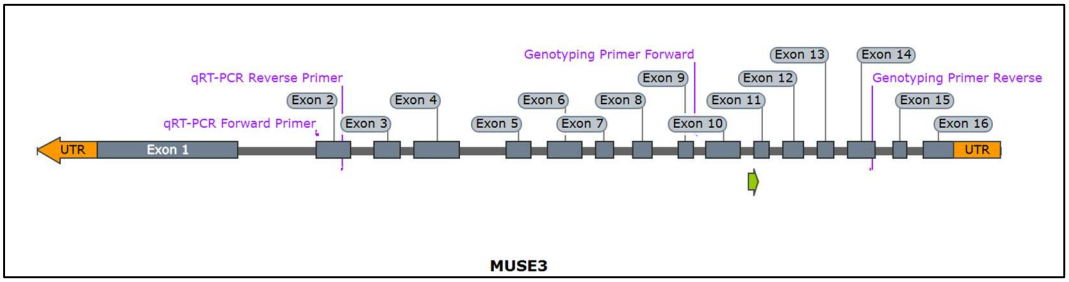

Figure 3.15: Schematic diagram of the gene MUSE3 in A. thaliana. Dark grey boxes show exons, orange boxes show untranslated regions (UTRs) and the green arrow shows the location of the T-DNA insertion. Primers are highlighted in purple, with genotyping primers being used for testing homozygosity (as per table 3.2), and qRT-PCR primers used for analysis of gene expression (as per table 3.3).

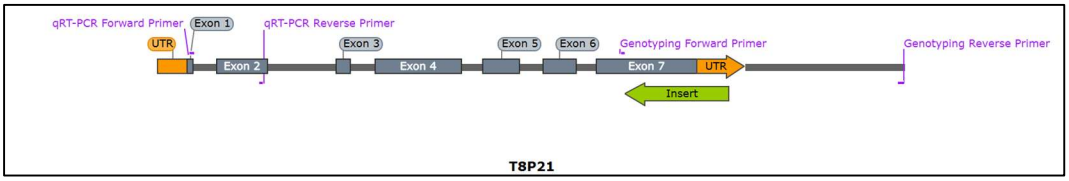

Figure 3.16: Schematic diagram of the gene T8P21 in A. thaliana. Dark grey boxes show exons, orange boxes show untranslated regions (UTRs) and the green arrow shows the location of the T-DNA insertion. Primers are highlighted in purple, with genotyping primers being used for testing homozygosity (as per table 3.2), and qRT-PCR primers used for analysis of gene expression (as per table 3.3).

Each T-DNA insertion line was grown and leaf samples taken to test lines for homozygosity of the mutations (See **Appendix V**). This resulted in genetic resources in *A. thaliana* to further test the roles of these genes in stress tolerance (Chapter 4 and 5).

3.3.1 Confirmation of gene expression in T-DNA insertion mutants

Quantitative reverse transcriptase PCRs (qRT-PCRs) were performed on the T-DNA insertion mutants in the selected genes. Relative expression was compared with the WT in each gene. The analysis of mutants revealed that *abcf5, apg3, bch1, bch2, dg1, gapb, muse3, sytb,* and *wrky55* exhibited no detectable expression of their target genes, consistent with knockout mutations. In contrast, *ho2, sis8, bch1,* and *zne1* exhibited

reduced expression of the target genes, indicating partial loss-of-function mutations. In *dis1* mutants, *DIS1* expression was reduced by 74%, mutation in *sis8* reduced *SIS8* expression by 32%, the *zne1* mutation reduced expression by 48% and *Ho2* had a reduced expression of 64% from expression seen in the WT (**Figure 3.17**).

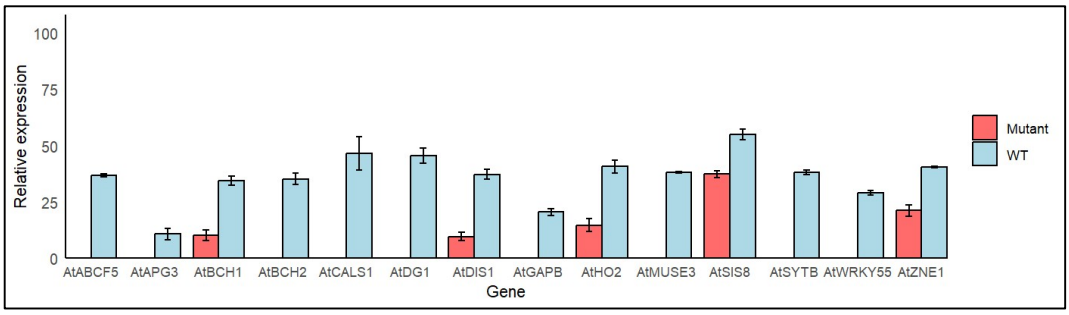

Figure 3.17: Relative expression of chosen T-DNA insertion mutants in A. thaliana in each gene of interest (relative to housekeeping gene) . Tissue taken from leaf samples at bolting. Error bars indicate SD.

3.3.2 Transcriptomic analysis of genes of interest

The expression of chosen genes of interest in WT lines of both Rice and *A. thaliana* were assessed in order to see the differential expression in the two species, and expression under abiotic stress, with a focus on heat stress. Analysis of data retrieved from TAIR electronic Fluorescent Pictograph (eFP) browser http://bar.utoronto.ca/efp/cgi-bin/efpWeb.cgi, in the form of fold change values at different time intervals showed large variation between expression of genes.

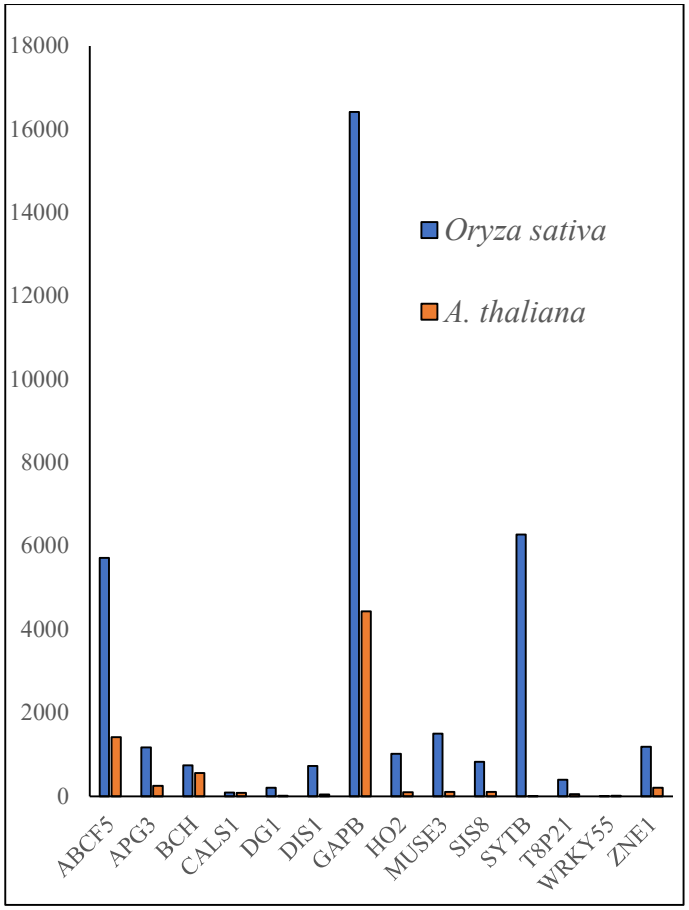

Figure 3.18: The relative expression of each gene in both Oryza sativa and A. thaliana leaf tissue from data retrieved from TAIR electronic Fluorescent Pictograph (eFP) browser http://bar.utoronto.ca/efp/cgi-bin/efpWeb.cgi, in the form of fold change values at different time intervals. For BCH, two orthologues were found in A. thaliana, and bch1 was used for this visualisation. Error bars indicate SD.

When looking at baseline expression in shoot tissue from Rice, *ABCF5*, *GAPB* and *SYTB* showed much higher expression than other genes studied, which was similar in *A. thaliana* in *ABCF5* and *GABP* but not *SYTB* (**Figure 3.18**). *CALS1*, *DG1*, *T8P21* and *WRKY55* had relatively lower expressions in both Rice and *A. thaliana* (**Figure 3.18**).

Figure 3.19 shows a visualisation of data gathered from TAIR electronic Fluorescent Pictograph (eFP) browser. In order to see if the genes of interest change in expression under different environmental stresses, relative expression levels under drought, genotoxic, osmotic, oxidative, cold, heat, salt, UV-B and wounding stress.

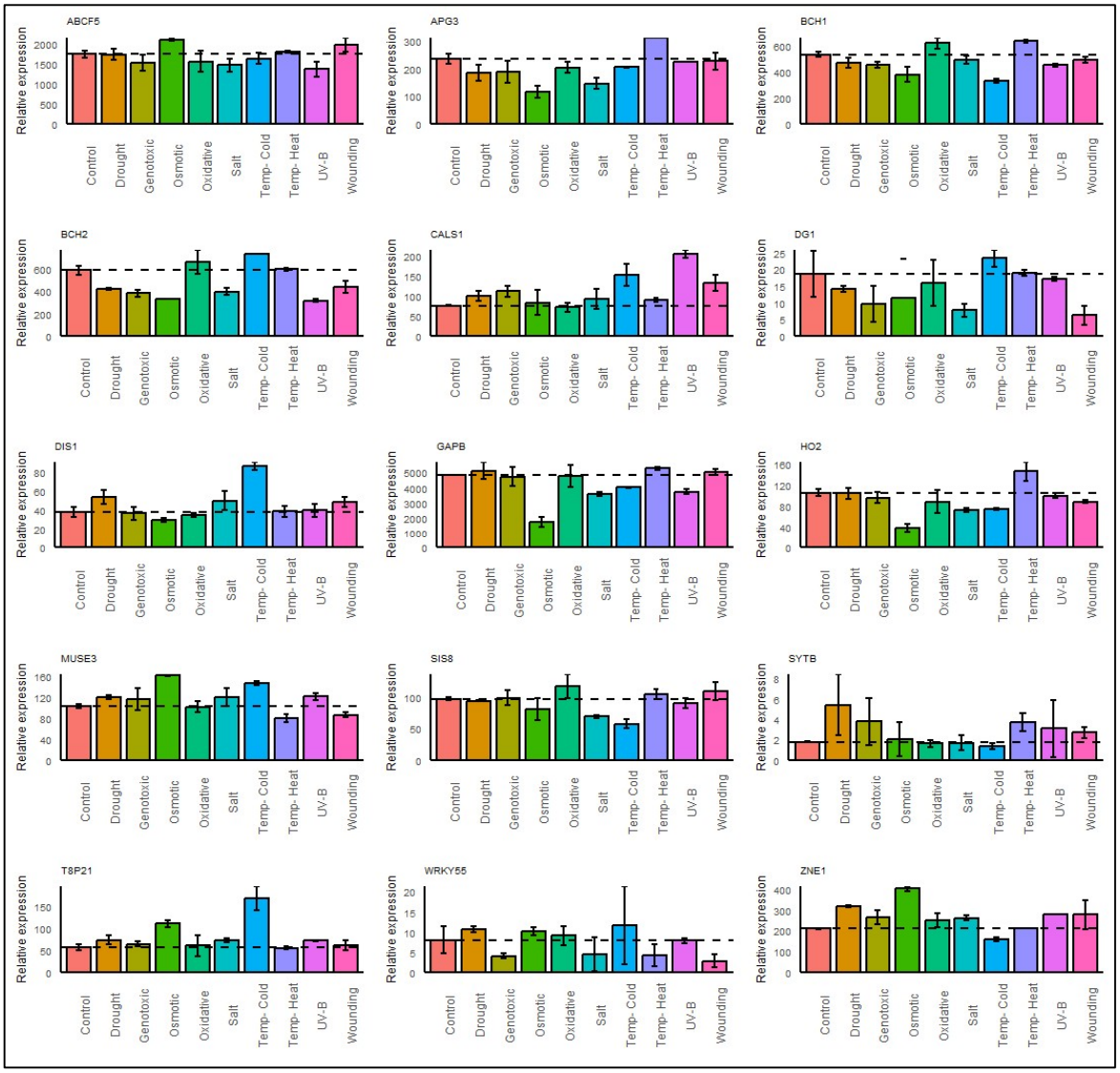

Figure 3.19. Relative expression of Genes of interest in A. thaliana in shoot tissue after 24 hours of various environmental stresses from data retrieved from TAIR electronic Fluorescent Pictograph (eFP) browser http://bar.utoronto.ca/efp/cgi-bin/efpWeb.cgi, in the form of fold change values. Dotted line indicates average expression in control conditions. Error bars indicate SD.

In *A. thaliana*, *ABCF5* is up regulated in both osmotic and wounding stress, whilst down regulated in Genotoxic and UV-B stresses. *APG3* is upregulated in heat stress while being down regulated during osmotic, oxidative, salinity and cold stress. *BCH1* showed to be up regulated in oxidative and heat stress, while being down regulated under other stress conditions observed, whilst *BCH2* had down regulation of all the stresses studied apart from oxidative and cold stress which showed *BCH2* to be upregulated, and in heat stress expression was similar to that of in control conditions. In drought, genotoxic, cold, heat, UV-B and wounding stress, *CALS1* was shown to have higher expression than in control conditions. *DG1* was down regulated in

drought, genotoxic, salinity, UV-B and wounding stress, whilst in cold stress was upregulated. *DIS1* was upregulated in drought, salt, cold and wounding stress, whilst being downregulated in osmotic and oxidative stress. *GAPB* only showed to be upregulated in heat stress, and was downregulated in osmotic, UV-B, salt and cold stress. *HO2* was only upregulated during heat and wounding, yet downregulated in osmotic, salt, cold and wounding stress. The only stress causing downregulation of *MUSE3* was heat stress whereas during drought, oxidative, cold and UV stress, *MUSE3* was upregulated. *SIS8* was seen to be only upregulated in oxidative stress, whereas this gene was downregulated in salt and cold stress. Drought, heat and wounding stress led to upregulation of *SYTB*, which was only downregulated by cold stress. *T8P21* was upregulated in drought, osmotic, salt, cold and UV-B stress, with *T8P21* showing similar expression to that of control conditions during the other stresses. *WRKY55* was upregulated by drought and osmotic stress whilst genotoxic, heat and wounding stress caused downregulation. *ZNE1* showed upregulation in drought, genotoxic, osmotic, salt and UV-B stress, and downregulated under cold stress.

With a focus on heat stress, the first 12.5 hours gene expression during exposure to heat stress in *A. thaliana* was visualized in **Figure 3.20**. This allowed visualisation of how plants were responding to stress by upregulation or downregulation of genes of interest.

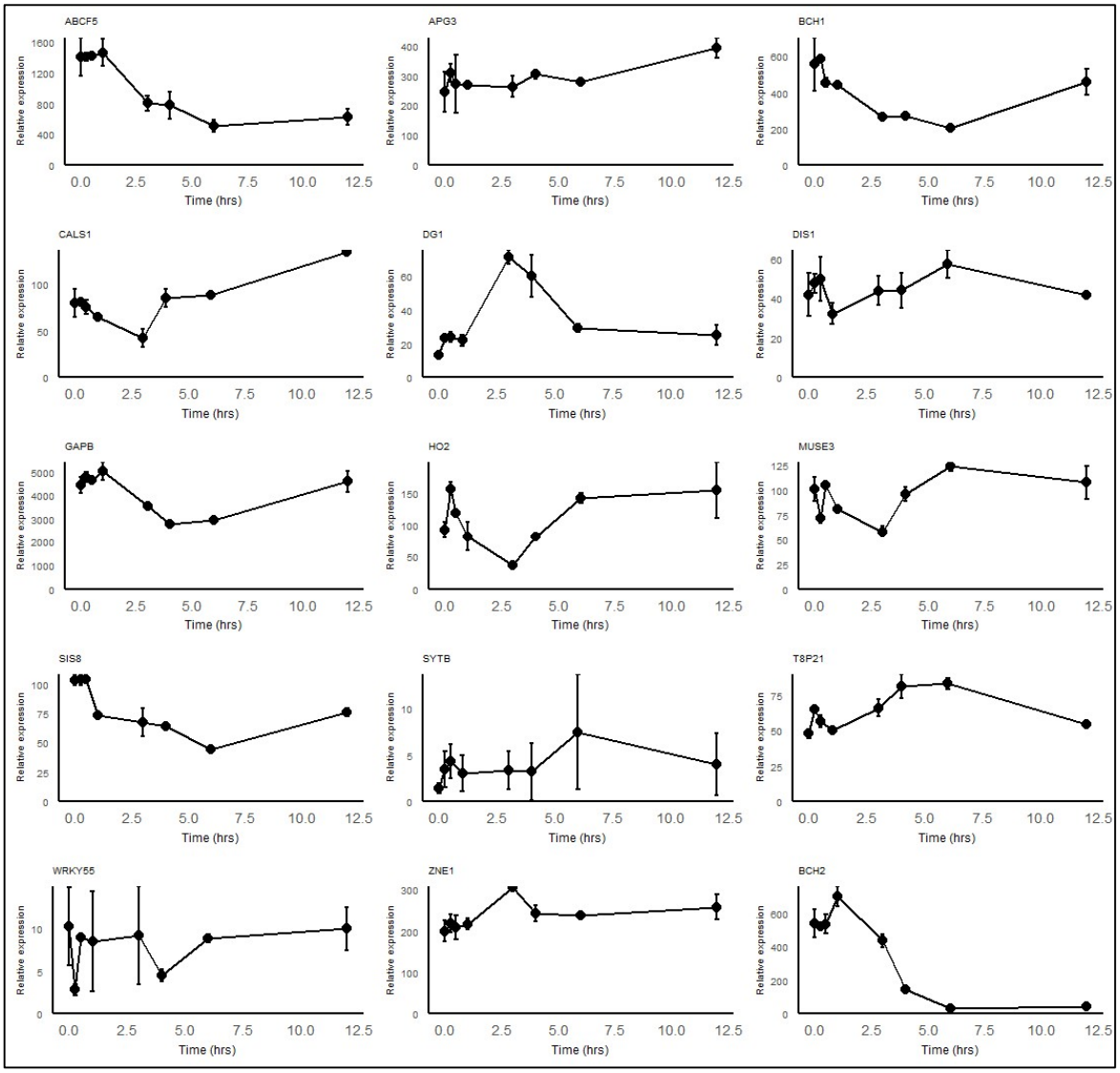

Figure 3.20. Relative expression of Genes of interest in A. thaliana shoot tissue in the first 12.5 hours of ongoing heat stress (data retrieved from TAIR electronic Fluorescent Pictograph (eFP) browser http://bar.utoronto.ca/efp/cgi-bin/efpWeb.cgi) in the form of fold change values at different time intervals. Error bars indicate SD.

SIS8 expression was seen to decrease in the first six hours of heat stress, then gradually increase to expression levels slightly below control conditions after 12.5 hours. *BCH1*, *GAPB* and *MUSE3* all showed similar expression patterns in the first few hours after exposure to heat stress, by gradually decreasing in expression before again rising to expression levels similar to control conditions after 12.5 hours. *CALS1* expression also gradually decreases when initially exposed to heat stress, although rises to higher expression levels than in control conditions. After being exposed to heat stress, *T8P21* and *ZNE1* had a small increase in expression levels in the first few hours of exposure, before returning to similar levels to that of expression in control conditions. In heat

stress, *DG1* at first has an increase in expression levels, before returning to levels seen in the first hour in heat stress. The expression of *HO2* in heat stress showed an opposite pattern to that of *DG1*, where a drop in *HO2* expression was seen before returning to expression levels seen in the first hour. In the first few hours of exposure to heat stress, *BCH2* has a small rise before being downregulated to a much lower level which remains relatively stable. *APG3* was expressed at similar levels to that seen in control conditions, then starts to increase expression after around six hours of heat stress. *WRKY55*, *DIS1* and *SYTB* expression levels appeared relatively stable in the first 12.5 hours of heat stress, not largely differing from expression levels seen in control conditions.

3.4 Discussion

Genes of interest were obtained from a GWAS performed by Jordan et al., (2023), by using literature searches to link genes with various abiotic stresses. These genes were then used to find orthologues in *A. thaliana*, in which T-DNA insertions were obtained and confirmed. The genes of interest were also analysed for expression levels in control conditions and during stress.

3.4.1 Obtaining T-DNA insertion mutation lines- a resource to identify candidate genes for stress tolerance.

Fifteen genes of interest were chosen due to various connections with abiotic stress and also gaps in literature which may be filled by study of mutations within the genes. With further study into these mutants focusing on photosynthetic stress tolerance, *DG1* was chosen as a candidate gene due to the thermosensitivity seen in missense mutations (Yan et al., 2020). The unique chlorotic phenotype seen in *Dg1* mutations is linked with defects in chlorophyll development during initial growth (Chi et al., 2010). With chlorophyll being a key component of photosynthesis, and the previous findings of knockout mutations having lower maximum photochemical efficiency of photosystem II (F_v/F_m) (Chi et al., 2008), further phenotyping of *Dg1* mutants in heat stress may give further detail of the effect on PSII and thermosensitivity.

A literature search for previous studies on *T8P21* showed this gene has undergone very little characterisation. The only literature on this gene showed that there are changes in expression of *T8P21* during heat stress and virus inoculation leaving a large knowledge gap, and if further study links this gene with stress tolerance, it could prove a novel new target for breeding strategies.

MUSE3 was chosen due to the links between *PUB* genes and ubiquitination- a key regulatory process, and links with abiotic stress tolerance as well as negative regulation of ABA-mediated drought stress (Cho et al., 2006; Seo et al., 2012; Lui et al., 2011). *PUB* genes are not only linked with regulating salt stress tolerance but also have been seen to be upregulated in heat stress. Further characterisation of *MUSE3* could identify if it is a *PUB* gene involved in stress responses.

The synaptotagmin SYTB has previously been found to have links to abiotic stress by reports of *SYTB* mutations having abiotic stress hypersensitivity (Schapire et al., 2008; Yamazaki et al., 2008, Perez Sancho et al., 2015; Yan et al 2017). The involvement of SYTB in various abiotic stresses means that this may be a key regulator of stress response, and further characterisation could assess whether this regulation is involved with photosynthetic stress tolerance.

SIS8 is a gene linked to salt and sugar tolerance (Huang et al., 2013; Gao and Xiang 2008). Due to the links to salt stress and the report by Sharma et al., (2021) of the downregulation of *SIS8* in response to heat, *Sis8* may be a candidate for heat stress tolerance regulation, therefore was chosen for further phenotyping.

WRKY55 was chosen as a candidate gene for further characterisation and phenotyping to assess links with stress tolerance. WRKY55 positively regulates transcription of the signalling molecules ROS and SA biosynthesis genes, which controls the leaf senescence and also play important roles in stress response (Wang et al., 2020; Baxter et al., 2014; Rivas-San Vicente and Plasencia, 2011). The links between these signalling molecules and stress tolerance lead to this gene being chosen for further phenotyping for heat stress tolerance.

ZNE1 was found to encode for a zinc transporter (Wang et al 2021), and although there are no reports of ZNE1 having a direct effect on abiotic stress tolerance, Zinc plays a vital role in stability of proteins and membranes within the plant and acts as a Superoxide dismutase (SOD) cofactor to facilitate ROS assembly and scavenging

(Khan et al., 2021). Zinc also functions as a component of carbonic anhydrase which is crucial in C4 photosynthesis (Faizan et al., 2021) as well as chlorophyll biosynthesis (Singh et al., 2018). The involvement of zinc in these processes make *ZNE1* as a zinc transporter a good candidate for further characterisation in terms of photosynthesis, and if differences in photosynthetic parameters are seen, it could also affect photosynthetic heat tolerance.

CALS1 was chosen as a gene of interest for further study due to the strong links between callose synthases and stress tolerance. Not only have *CALS* been linked to heat stress through species specific changes in expression, changes in phloem unloading and meristem size (Luan et al., 2023; Lui et al., 2022), but there is also a strong link to drought stress through control of calcium deposits on the xylem and protoxylem (Liao et al., 2023). Phenotyping under heat stress could provide more information on the role of *CALS1* in *A. thaliana* heat stress.

BCH1 and *BCH2* were chosen as candidate genes due to the strong links between *BCH* and various abiotic stresses including oxidative stress, high light, drought, heat and UV irradiation (Saeed et al., 2015; Du et al 2010). There are also reports of phenotypes of mutant *BCH* lines associated with pigment content and regulation. Even though there have been previous studies characterising *BCH* in heat stress and chlorophyll fluorescence imaging parameters such as F_v/F_m and NPQ, the strong links with different stresses, signalling pathways, and pigments, make both *BCH1* and *BCH2* ideal candidates for further phenotyping with a focus on photosynthetic heat tolerance.

ABCF5 was chosen as a gene for further study due to the role ABCs have in regulating stress responses in plants, such as drought and salt stress (Jangam et al., 2016) as well as being induced by abiotic stresses, indicating their role in stress adaptation (Rensink et al., 2005; Liu et al., 2011). *ABCF5* mutants in particular have been linked to drought and oxidative stress, and due to the broad variety of substrates of ABCF5, there may be overlap with mechanisms behind this stress tolerance with heat stress tolerance. Therefore, characterising *ABCF5* in *A. thaliana* under heat stress among may lead to further stress tolerance phenotypes in mutants.

GAPB was chosen as a gene of interest due to its important role in the key step of photosynthesis in the production of NADH. Due to the GWAS initially screening for loci associated with photosynthetic heat tolerance, further phenotyping in depth could

reveal if there are links between *GAPB* and mechanisms behind maintaining photosynthetic processes during heat stress. Other characterisation of *GAPB* mutants for key phenotypes such as fertility could assess how plant development is affected by mutagenesis in *GAPB*.

HO2 was chosen to be part of further study into photosynthetic heat tolerance due to its localisation to the chloroplast stroma (Li et al., 2014). Previous studies have highlighted reduced chloroplast accumulation in *HO2* mutants. The changes in chlorophyll content may have an effect on photosynthetic processes, including PSII, and therefore this mutant could have reduced photosynthetic function, which could also impact photosynthetic heat tolerance.

APG3 was chosen due to similar reasons to *HO2*, as *APG3* has strong links to pigment content. Not only was chlorophyll-a, chlorophyll-b, and β-carotene reduced in *APG3* mutants, but they also had higher ROS levels, increased callose deposition, and decreased plasmodesmata permeability (Zhang et al., 2023; Motohashi et al., 2007). Characterizing the photosynthetic processes through chlorophyll fluorescence could show if the mutant and the changes in pigments have an effect on parameters like photoinhibition and PSII efficiency. If there are changes in photosynthesis due to changes in pigment content, this could also have an impact on the photosynthetic heat tolerance of the plant.

DIS1 was chosen as previous studies have linked the gene to salt stress tolerance and resistance to pathogens (Jiang et al., 2012; Zhao et al., 2013, Sun et al., 2019, Qi et al., 2017). Due to DIS1 modulating MF dynamics and mPTP opening, in order to regulate $[Ca^{2+}]$cyt signalling, and Ca^{2+} not only being involved with stress perception signalling and also multifunctionally ensuring subsequent signal transduction, *DIS1* may be a good candidate for impacting heat tolerance.

3.4.2 Expression levels of genes of interest in T-DNA insertion mutations.

The genes *ABCF5*, *GAPB* and *SYTB* showed much higher expression than other genes studied in control conditions. This indicates that with a high baseline expression, they might play essential roles in maintaining normal cellular functions. Their high

expression under control conditions could be necessary for the plant's regular growth and development or fundamental processes such as metabolism, protein synthesis, or cellular homeostasis. *SIS8* had a relatively high expression in rice but not in *A. thaliana*, which could indicate the gene may have a more critical or specialized role in rice than in *A. thaliana*, or could be due to differences in regulatory control, environmental adaptation, or functional redundancy. *CALS1*, *DG1*, *T8P21* and *WRKY55* had relatively lower expressions in both Rice and *A. thaliana*, yet their differential expression after various stresses shows that they may be more involved in stress response rather than constitutive functions.

3.4.3 Expression levels of genes of interest during abiotic stress

Using readily available transcriptomic data from Efp browser, the genes of interest that were selected from the GWAS by Robson et al., (2023) and selected through literature searches, were assessed for differences in relative expression in a variety of abiotic stress conditions. One of the main characteristics being selected for with these genes was reports of abiotic stress links. The expression levels under abiotic stress showed that all candidate genes had at least some differences in relative expression in comparison to expression in control conditions. Both upregulation and downregulation of these genes were seen, which is to be expected due to the variety of roles of genes as well as the variety of abiotic stresses assessed. Some small links between abiotic stresses are seen such as similarities in response to drought, oxidative stress and salt stress. The differences in expression under different abiotic stress conditions as seen provide further evidence that these genes could have roles in abiotic stress conditions, cementing the choice of further characterisation of these genes under heat stress conditions (Chapter 4 and 5).

APG3, BCH1, CALS1, GAPB, HO2, SYTB all showed increased expression when exposed to high temperatures, whilst *MUSE3* and *WRKY55* had a decrease in relative expression after 24 hours. Looking at the first 12.5 hours of heat stress exposure, the mutants varied in speed of response.

One of the most dramatic changes in the first few hours of heat stress was in *BCH2*, which drastically reduced within six hours. Several of the genes showed an initial

reduction in expression before rising again such as *GAPB, CALS1, BCH1, MUSE3, HO2* and *SIS8*, which shows that it may not be one of the first responses to heat stress.

3.5 Conclusions

The work in this chapter was done with the goal of gaining resources to test mutant lines for changes in photosynthetic heat tolerance.

From a GWAS aimed at identifying genetic loci associated with photosynthetic heat stress tolerance, 14 underlying genes were selected for further characterisation for photosynthetic heat tolerance (see Chapters 4 and 5). The selection process used previous literature to search for genes that have abiotic stress links, photosynthetic links, or uncharacterised genes that have large mechanistic knowledge gaps like *T8P21*.

Looking at orthologues of the genes selected for further study, 15 orthologues in *A. thaliana* and T-DNA insertion mutants corresponding to those orthologues were obtained. Note that two genes were selected as *A. thaliana* orthologues of the Rice gene *BCH* due to the strong genetic linkage to both *BCH1* and *BCH2* as well as high interest in gene function. These T-DNA insertion mutants were genotyped for heterozygosity (**Appendix V**) before qRT-PCRs assessed the expression of the genes in mutant lines. Knockout expression was seen in most lines with the exception of *ho2, sis8, bch1* and *zne1* which showed to still have some expression level, which may have to be taken into account when assessing performance in further experimentation. These mutants provide possible candidates for testing photosynthetic heat tolerance to aid in gene identification for crop breeding for heat stress tolerance.

One of the first steps to confirming if these candidate genes may be linked to abiotic stress tolerance was looking at the relative expression of these genes under various conditions. Firstly, the baseline of these genes differed greatly, with some genes such as *GAPB* showing extremely high expression levels in control conditions, therefore could play important roles biologically, as also shown in literature.

Relative expression levels changed in the chosen genes when plants were exposed to abiotic stresses. This suggests that these genes may have roles in the regulation of

stress tolerance, and therefore characterisation of these mutants may allow confirmation of their involvement in stress responses.

4 Identifying photosynthetic heat stress tolerant mutants in *A. thaliana.*

4.1 Introduction

4.1.1 Effects of abiotic stress on photosynthesis

Photosynthesis a key component of yield and is a dynamic process with many components. Photosynthesis has high sensitivity to increasing temperatures and so heat stability is important target for breeding. The most heat sensitive component of photosynthesis is photosystem II (PSII) (Yamamoto, 2016; Yoshioka-Nishimura, 2018), which will be the focus of this chapter.

In chapter 3, genes of interest were selected from a Genome wide association study (GWAS) (Robson et al., 2023) performed on rice (*Oryza glaberrima* and *Oryza sativa*), to characterize photosynthetic heat stress tolerance. T-DNA insertion mutants in *A. thaliana* orthologue genes were selected, creating a set of mutants to explore photosynthetic heat tolerance in *A. thaliana*. Here, those mutants are tested for a range of photosynthetic traits under heat stress. The T-DNA-insertion mutations in genes of interest are tested for heat stress tolerance, photosynthetic stability, and suitability for future breeding.

PSII

As the initial site of light dependent photosynthetic reactions, PSII is crucial to the plant's productivity. Embedded in thylakoid membranes, PSII comprises of a large multisubunit chlorophyll-protein subcomplex (Shen et al., 2008). At the core, its reaction centre has a Domain 1 (D1)/D2 heterodimer and polypeptides, susceptible to damage from ROS generated during photosynthesis, necessitating their constant repair or replacement to maintain PSII function (Ferreira et al., 2004; Aro et al., 2005). Within the reaction centre, are associated cofactors responsible for electron transfer and water-splitting reactions. Surrounding the core of PSII are LHCs which contain pigments for light harvesting (Dekker et al., 2005; Nelson and Yocum, 2006). These

LHCs capture light energy and funnel it to the reaction centre, where photochemical reactions, initiating electron transport and ultimately leading to the generation of ATP and Nicotinamide adenine dinucleotide phosphate (NADPH) for carbon fixation (Green and Parson 2003).

PSII has been considered the most heat-sensitive component of photosynthesis (Berry and Björkman, 1980; Havaux, 1996), and further studies revealed that heat stress inhibits PSII repair (Sharkey, 2005; Allakhverdiev et al., 2008). Within PSII, the oxygen evolving complex, is inactivated in high heat stress (Nash et al., 1985), yet in moderate heat stress is not directly inactivated, and increases photoinhibition of PSII (Berry and Bjorkman 1980). In isolated *Symbiodinium* (corals), heat stress accelerated photodamage, however in tobacco moderate heat stress was found to not influence the extent of photodamage but inhibited the repair of photodamage.

Chlorophyll

An LHCII monomer binds a total of 18 pigments, including eight Chlorophyll *a* pigments and six Chlorophyll *b* pigments (Liu et al., 2004). These chlorophyll pigments absorb light energy across a broad spectrum of wavelengths, particularly in the blue and red regions, maximizing photon capture. Chlorophyll *a* acts as the primary electron donor in PSII, initiating the electron transport chain. Chlorophyll *b*, though structurally similar to chlorophyll *a*, extends the range of light absorption and transfers energy to chlorophyll *a*, enhancing the efficiency of light harvesting. P680 refers to the primary electron donor chlorophyll *a* molecule within the reaction center of PSII, named for its peak absorption wavelength of 680nm. P680 plays a central role in the light-dependent reactions of photosynthesis by capturing photons and initiating the process of photosynthetic electron transport. When excited by light, P680 donates an electron to the electron transport chain, starting a series of redox reactions.

As early as 1929 a relationship between chlorophyll content and rate of photosynthesis had been established (Emerson 1929). Even though the LHCs and their chlorophyll evolved to maximise photon interception (Green 2019), in dense canopies, it has been proposed that reducing chlorophyll improved light distribution to lower layers of the canopy (Gu et al., 2017; Song et al., 2017). A reduction in chlorophyll does not always mean a reduction in photosynthetic capacity at high light intensities where light

absorption is not limiting, as demonstrated by low-chlorophyll rice with high photosynthetic rates (Gu et al., 2017). At high light intensities, the content of Rubisco would often be more limiting than the chlorophyll content. Buttery and Buzzel (1977) suggested that a linear relationship between chlorophyll and photosynthesis is only linear below threshold light levels (which is species specific). Chlorophyll content has been reported to be positively correlated with grain yield and harvest index of wheat (Miri 2009). In Rice, a low chlorophyll *b* mutant showed a more stable F_v/F_m ratio in high light and a significant decrease in the susceptibility to photoinhibition (Dai et al., 2003).

Chloroplasts are one of the most heat sensitive organelles (Krause and Santarius, 1975). Heat stress has previously been reported to be linked with a reduction in chlorophyll in *A. thaliana* (Kipp and Boyle 2013; Lv et al., 2011), winter wheat (Ristic et al., 2007) and Barley (Bahrami et al., 2019). In the Barley landrace Tadmor, low chlorophyll content was linked to heat stress tolerance through decreasing leaf absorbance, which reduces the heating effect of solar radiation while stomata are closed during (Havaux and Tardy 1999).

Carotenoids

Carotenoids have a central role in photosynthesis, by increasing the range of available light wavelengths for absorption. Within the chloroplast, some of the most common carotenoids found are β-carotene, lutein, violaxanthin, neoxanthin and zeaxanthin. These pigments also have a structural role in formation of thylakoid membranes and regulate thylakoid membrane fluidity (Havaux and Gruszecki 1993; Havaux 1998; Bykowski et al., 2021). Carotenoid content is important economically in fruits and vegetables for human health as antioxidants and precursors to vitamin A. They protect against oxidative stress, reducing the risk of chronic diseases like cardiovascular disorders and cancer (Krinsky, 1993) and additionally, carotenoids promote eye health, reducing the risk of age-related macular degeneration (Wu et al., 2015).

Carotenoids have a radical scavenging role for example β-carotene and zeaxanthin can reduce superoxide molecules. (Telfer 2005; Umena et al., 2011). Carotenoids also play an important role in the photoprotective process NPQ, which is used to dissipate heat from PSII rapidly to prevent photooxidative intermediates (see below). The conversion

of xanthophyll carotenoids violaxanthin to zeaxanthin through the xanthophyll cycle results in a conformational change in the thylakoid membrane and induction of NPQ (Niyogi and Truong 2013; Murchie and Ruban 2020).

As antioxidants, carotenoids play a vital role in plant stress response and resistance. Whilst in algae *C. reinhardtii*, six hours exposure to 37°C heat resulted in an increase in β-Carotene, a decrease in carotenoid content after heat stress was seen in Barley (Bahrami et al., 2019) and sweet osmanthus (Wang et al., 2022). Wang et al., (2022) hypothesised that the repression of carotenoid genes such as *PHYTOENE SYTHASE 1*(*PSY1*), *ζ-CAROTENE ISOMERASE 1*(*Z-ISO1*) and *β-RING CYCLASE 1*(*LCYB1*), plus up-regulation of carotenoid degradation genes *NCED3*, and carotenoid cleavage dioxygenases: (*CCD*) *CCD1-1*, *CCD1-2*, and *CCD4-1* cause a decrease in carotenoids during heat stress.

Abscisic acid (ABA) is derived from carotenoids, and is involved in the regulation of stomata movement, germination, root development, leaf senescence, and response to stress. Alongside ABA, other phytohormones: strigolactones (SLs) are also derived from carotenoids and regulate plant growth and development.

Chlorophyll fluorescence

The processes of chlorophyll dissipating energy through, fluorescence, heat, or photochemistry, all work in competition with each other, therefore chlorophyll fluorescence can be used to calculate quantum efficiency of photochemistry and heat dissipation. Chlorophyll fluorescence is the measure of re-emitted light from PSII, as PSI light emission under 700nm does not have a significant contribution to overall chlorophyll fluorescence (Pfundel 1998; Baker 2008). The effect of the chosen T-DNA insertions on photochemistry and response to heat stress can be understood through gathering chlorophyll fluorescence parameters

Photosynthesis can be measured in a variety of ways, however measures such as gas exchange, spectroscopy and microscopy are labour intensive. Measuring chlorophyll fluorescence allows measurement of rapid responses *in vivo* and can be non-invasive therefore is a high throughput method of measuring photosynthesis.

Chlorophyll fluorescence can serve as an indicator of plant stress by proxy, as stress can reduce the ability of the plant to metabolise. Chlorophyll fluorescence has been used previously to indicate stress tolerance of water availability, nutrients, pollutants, temperature, and salinity (Guidi and Landi 2016). Assessing chlorophyll fluorescence allows the assessment of photosynthetic damage by stress (Jedmowski et al., 2015).

The PSII parameters: quantum efficiency of PSII (ϕPSII), Non-Photochemical Quenching (NPQ), open PSII centres (qL), level of photochemical quenching (qP) and maximum efficiency of PSII photochemistry (F_v/F_m) will be focussed on to assess performance of photosynthetic apparatus.

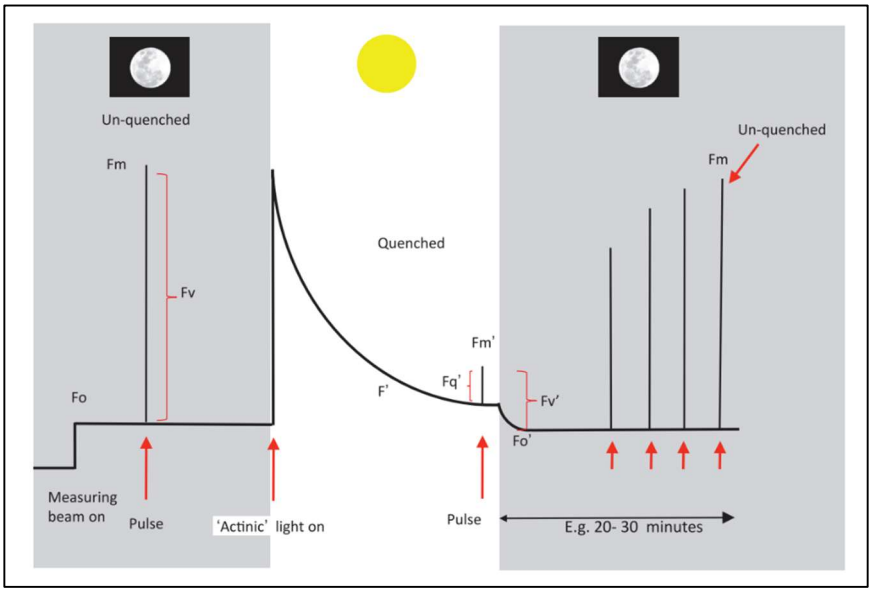

Figure 4.1: From Murchie and Lawson, 2013: A stylized fluorescence trace of a typical experiment using dark-adapted leaf material to measure photochemical and non-photochemical parameters. This would be typical of an induction at high irradiance of ≥500 µmol m^{-2} s^{-1}. A true 'Kautsky' effect would be measured at moderate illumination, for example <200 µmol m^{-2} s^{-1}, where transients corresponding to induction of photosynthesis are revealed. Note that the 'decay' of F_o' in the dark after switching off the actinic light would be accelerated by adding far-red (FR) light to stimulate PSI activity.

Table 4.1: Chlorophyll fluorescence parameters

Parameter	Formula	Definition
'denotes light adapted measures		
F		Steady state fluorescence emission
F_m		Maximum chlorophyll fluorescence
F_o		Minimum chlorophyll fluorescence
F_v	F_m-F_o	Variable chlorophyll fluorescence
F_v/F_m		Maximum efficiency of PSII photochemistry
NPQ	(F_m - F_m')/F_m'	Non-photochemical quenching
ϕPSII or F_q'/F_m'	(F_m'–F′)/F_m'	Quantum efficiency of PSII electron transport
qP	(F_m '-F')/(F_m '- F_o ')	Photochemical quenching
qL	((F_m '-F')/F_v')/(F_o '/F')	Estimate of fraction of open PSII centres

Table 4.1: A summary of parameters and equations commonly used when referring to chlorophyll fluorescence. Adapted from Murchie and Lawson (2013) and McCausland et al., (2019).

ϕPSII or F_q'/F_m' -Quantum efficiency of PSII electron transport

ΦPSII measures how effectively PSII converts absorbed photons into chemical energy, determining the proportion of light energy utilized for photochemistry (Genty et al., 1989; Murchie and Lawson 2013). ϕPSII signifies the ratio of electrons transferred through PSII to the number of photons absorbed, reflecting PSII's ability to initiate photochemical reactions and drive electron transport. ϕPSII is used to assess both PSII functionality and overall photosynthetic ability.

At low light levels, photosynthesis has a high ϕPSII, due to a higher abundance of downstream assimilatory reactions and consequent substrates. A higher ϕPSII indicates enhanced photosynthetic activity and efficient utilisation of absorbed light energy by PSII, therefore promoting increased photosynthetic assimilation and plant productivity.

Heat reduces the electron transport efficiency in both PSII and PSI (Mathur et al., 2014). In heat stress conditions, a decrease in ϕPSII has been reported in multiple species. Studies in wheat have reported a decrease ϕPSII after short term stress (Mathur et al., 2011, Chovancek et al., 2019). In Citrus tree Cleopatra mandarin (*Citrus reshni*), after being exposed to any combination of two and three stress factors of high-light stress, heat stress and water stress, a reduction in ϕPSII was seen, however no significant differences in ϕPSII were observed in similar species Carrizo citrange (*Citrus sinensis* × *Poncirus trifoliata*) unless exposed to all three abiotic stressors (Balfagon et al., 2022). A similar observation was made in chrysanthemum, where ϕPSII decreased when plants were exposed to both high light intensity and heat stress (Janka et al., 2015). The relevance of studies involving both heat and light intensity stress is relevant due to the prevalence of these abiotic stressors being seen simultaneously.

Open PSII centres (qL)

qL indicates the proportion of open PSII reaction centres (Kramer et al., 2004). Open PSII centres are reaction centres where the primary electron donor, P680, is in its oxidized state and ready to accept electrons from water molecules during the light-dependent reactions of photosynthesis. Quantification of qL is the fraction of open PSII reaction centres relative to the total number of PSII reaction centres. At higher light intensities, qL reduces as reaction centres close. qL has a curvilinear relationship with ΦPSII (Hogewoning et al., 2012).

qP- the level of photochemical quenching

qP (F_q'/F_v'), is the level of photochemical quenching, and relates maximum efficiency to operating efficiency. It is also non linearly related to proportion of open PSII reaction centres (qL). qP can be used as an indicator of the onset of photoinactivation, which is otherwise assessed through dark-adapted F_v/F_m, O_2 evolution or D1 degradation (Anderson et al., 1995; Ruban and Murchie, 2012; Ruban and Belagio, 2014). A very low qP, of less than 0.4 means a leaf may be prone to photoinhibition.

Maximum quantum efficiency of PSII photochemistry (F_v/F_m)

F_v/F_m takes the ratio of variable fluorescence (difference in maximum and minimum fluorescence) to maximum fluorescence, which represents the maximum potential quantum yield of PSII chemistry (Butler, 1978; Genty et al., 1989). In unstressed leaves, F_v/F_m is relatively stable at around 0.83 after dark-adaptation of a period of about 20 minutes. During plant stress, photoinhibition or quenching, F_v/F_m decreases, therefore F_v/F_m can be an indicator of plant stress or photoinhibition (Demmig and Bjorkman, 1987, Long et al., 1994, Demmig-Adams and Adams, 2006). A lower F_v/F_m may not always be a sign of decreased photosynthetic performance, as it correlates to the maximum quantum yield of photosynthetic gas exchange (CO_2 or O_2), and in high light conditions may not necessarily mean the reduction of photosynthetic performance (Demmig-Adams and Adams, 2006; Murchie and Niyogi, 2011).

Nonetheless lower F_v/F_m potentially has an adverse effect on the carbon gain in the plant. A reduction in F_v/F_m is usually due to the increase in non-photochemical quenching decreasing F_m, coupled with inactivation of PSII reaction centres, increasing F_o (Melis, 1999, Baker, 2008).

It is logical therefore that a decrease in F_v/F_m has successfully been used as an abiotic stress indicator in plants including heat stress (Willits and Peet, 2001; Molina-Bravo et al., 2011; Sharma et al., 2012). The use of F_v/F_m to provide quick high throughput screens for heat stress tolerance has been seen across several species including wheat (Sharma et al., 2012), tomato (Zhou et al., 2015), and rice (Ferguson et al., 2020), as well as in certain species of bryophytes (Jangerbrand and Kudo 2016). A study by Shama et al., (2015) showed wheat cultivars selected for heat tolerance from F_v/F_m had higher photosynthetic performance and accumulated dry matter, plus reduced senescence when exposed to heat stress. In cereals, a decrease in F_v/F_m has been seen in heat shocked plants as well as exposure to prolonged heat stress (Galova et al., 2000, Stefanov et al., 1996, Bahrami et al., 2019). Decreases in F_v/F_m have also been seen when exposed to long term heat stress in field and glasshouse conditions (Chovancek et al., 2019, Sharma et al., 2015, Gautam et al., 2014). Although there is a focus on higher F_v/F_m during stress conditions as a desirable trait, it's been noted that a higher F_v/F_m in control conditions does not necessarily mean a higher F_v/F_m in stress conditions (Sharma et al., 2015)

NPQ

NPQ is the dissipation of chlorophyll excitation energy through heat, which decreases risk of ROS forming (Björkman and Demmig-Adams, 1995). There are several subcomponents of NPQ, including qE, qH, qI, qM, qT, and qZ. The major contributor of NPQ is energy dependent quenching, termed qE where upon accumulation of protons in the thylakoid lumen, a ΔpH is created, causing acidification (Horton et al., 1996, Horton et al., 2008) This triggers NPQ through modifying the pigment composition of LHCII via the xanthophyll cycle, and activates PSBS and/or light harvesting complex stress-related proteins (Ruban et al., 2012, Peers et al., 2009, Niyogi et al., 2013, Tokutsu and Minagawa 2013). qE is rapidly induced and relaxed and responds to short term stress over seconds to minutes. qT is a process where phosphorylated antenna proteins move away from PSII under low light conditions by binding zeaxanthin to monomeric antenna proteins. This can take several minutes to induce and relax NPQ (Krause and Weis 1991, Ruban 2009, Dall'Osto et al., 2005). Another form of NPQ, photoinhibitory quenching (qI), results in decrease of ϕPSII due to D1 inactivation over 5-10 minutes.

A higher NPQ allows for plants to be better equipped at coping with excess light conditions and preventing photodamage and ROS formation. This photoprotective mechanism is crucial in environments with fluctuating light intensity and exposure to stressful conditions, where an efficient NPQ system allows plants to maintain photosynthetic performance. A low NPQ means that in low light conditions, less energy is dissipated by NPQ, therefore more energy can be used for photosynthesis. A large range between L15 and L30 NPQ is therefore optimal, so the plant can avoid damage in high light conditions, while utilising as much energy as possible for photosynthesis in low light conditions. This principle was used to show that accelerating the removal of NPQ in low light led to increased biomass and yield in tobacco and soybean (Kromdijk et al., 2016; De Souza et al., 2022).

An increase in NPQ capacity after heat stress has been observed in several species including wheat (Muatani et al., 2017; Qi et al., 2017), pearl millet (Shanker et al., 2022), pea (Georgieva & Yordanov, 1994), maize (Sinsawat et al., 2004) and *A. thaliana* (Zhang et al., 2010). This trend has also been seen after a heat wave in the tree species *Quercus ilex* in natural outdoor conditions (Drake et al., 2018). In Maize,

plants grown at 25°C saw an increase in NPQ when exposed to 30-40°C heat, whereas plants grown at 41°C only saw an increase in NPQ at temperatures above 45°C , indicating that prior heat can affect the response of NPQ (Sinsawat et al., 2004). In the model species *A. thaliana*, NPQ has increased with heat stress in several studies (Zhang and Sharkey 2009). Zhang et al., (2010) reported an initial decrease in NPQ after exposure to heat, before a steady increase in NPQ which remained higher after exposure.

4.1.1 Chapter aims.

This chapter aims to phenotype T-DNA insertion lines previously highlighted in Chapter 3 using high throughput phenotypic assays of tolerance to abiotic stress response with a focus on heat stress. By using A. *thaliana* with shorter growth cycles and genetically well characterised mutants it was possible to rapidly assess their photosynthetic properties. This chapter aims to gather a picture of how these insertion lines perform and identify candidate genes for further studies into their role in abiotic stress tolerance and future roles in crop breeding.

4.2 Methods

4.2.1 Plant growth conditions.

T-DNA insertion lines were obtained from SALK and SAIL collections from the Nottingham *A. thaliana* Stock Centre as seen in **Table 4.2.**

Table 4.2: List of T-DNA insertion mutants tested

Gene Name	Gene ID	SALK/SAIL ID	NASC ID
DG1	At5G67570	SALK_018461C	N656226
ZNE1	At3G08650	SALK_085591	N682606
T8P21	At2G38000	SALK_025891C	N683908
MUSE3	At5G15400	SAIL_713_A12	N861119
SYTB	At1G20080	SALK_135307	N677964
SIS8	At1G73660	SALK_004541	N571182
WRKY55	At2G40740	SALK_070182	N570182
CALS1	At1g05570	SAIL_1_H10	N860340
BCH1	At4G25700	SALK_061761	N561761
BCH2	At5G52570	SAIL_1242_B12	N862184
GAPB	At1G42970	SAIL_267_F01	N872664
ABCF5	At5G64840	SALK_113472C	N664827
APG3	At3G62910	SALK_117765C	N668914
HO2	At2G26550	SALK_113008C	N660113
DIS1	At1G13180	SALK_010045C	N661446

Table 4.2: Table depicting the T-DNA insertion mutants used in this chapter. The column 'Gene' denotes the name used throughout when referencing throughout. SALK/SAIL ID refers to the naming system used by the SALK Institute Genomic Analysis Laboratory for the specific T-DNA insertion used, and NASC ID refers to the Identification of the seed line used by Nottingham A. thaliana *Stock Centre (NASC).*

A. thaliana Columbia-0 (Col-0) ecotype along with the selected mutants were grown in Levington M3 compost with Biofungicide *Trichoderma asperellum* cepa T34 (T34) biological control in 10cm pots (two plants per pot). *A. thaliana* were grown until around day of bolting (+/- 1 day either side of bolting in order to limit number of plant groupings) in growth rooms at 22°C in 16hr days under fluorescent lighting with a 3:3:1 ratio of red:green:blue light with a Photosynthetic Photon Flux Density (PPFD) of 205(± 8.6 SD) µmol/m^2 /s. Hypoline^{TM} (Bioline AgroSciences) was applied to soil surface of pots weekly for prevention of scarid fly larvae. Trays were rotated every week to minimise localised environmental effects.

At point of bolting, eight plants (four pots) of each genotype were left in control conditions and eight plants were moved to a growth room of 32°C, at 16hr daylength and same light intensity from that of control conditions. Heat treatment of these plants lasted five days before being returned to the original growth conditions for the rest of their life cycle.

Considering day of bolting (+/-1 day) as Day 0, measurements were taken on Day three, Day five and Day eight, therefore for heat treatment, measurements were taken before heat was applied, then three days in heat, five days in heat, and after three days post-heat stress during subsequent recovery.

4.2.1 Chlorophyl assay

Whole mature leaf samples (around 1.5cm^2) were taken from plants, choosing the youngest mature leaf from each individual plant. Samples were taken before heat treatment at point of bolting at (Day 0) (3-4 weeks old), after three days heat treatment (Day 3), five days heat treatment (Day 5) and three days recovery (Day 8) in 1.5ml Eppendorf tubes and placed in liquid nitrogen before being stored at -70°C. The samples were individually weighed. A small metal ball was added with 1ml chilled 80% acetone. The sample was then lysed using the Qiagen Tissue Lyser II at 30 Hz for 2.5 min before being placed on ice for three minutes, and then lysed for a further 2.5 mins at 30Hz. The samples were then placed on ice for three minutes before being centrifuged at 3000rpm for five minutes at 4°C.

200ul of supernatant was transferred to a STERELIN 96 well plate. Absorbance at 470nm, 663nm, 646nm and 750nm were measured using a FLUOstar Omega Microplate Reader. Results were adjusted for pathlength following the methods of Warren (2008). Pathlength was calculated by taking microplate readings of absorbance of 200ul water (due to its known constants) at 977 nm and 900 nm (to blank the plate) and dividing by the known absorbance of water at 1cm (0.18) (**Appendix IV**: Equation [1].

Chlorophyll content was then calculated using formulas calculated using extinction co-efficient figures in Porra *et al.,* (1989) and Lichtenthaler and Wellburn (1983) (**Appendix IV**: Equation [2].

In order to show the chlorophyll content could be calculated through this path correction method using a microplate reader, 64 samples were measured for absorbance alongside measurement of the same samples in the microplate reader. For this, the same method was used until after the centrifugation step, 500ul of supernatant was added to 500ul 80% acetone and added to a SARSTEDT cuvette. Using the

Amersham Biosciences Ultrospec 2100 pro spectrophotometer, absorbance readings were taken at 470nm, 646nm, 663nm and 750nm. Chlorophyll content was then calculated using the equations above.

4.2.2 Chlorophyll fluorescence Imaging

A customised FluorCam imaging fluorometer (FluorCam, Photon System Instruments, Brno, Czech Republic) fitted with a red and white Light Emitting Diode (LED) panel was used for chlorophyll fluorescence imaging. The FluorCam was stationed in a dark room that was kept between 20°C and 22°C. Imaging was carried out as seen in McAusland et al., (2019) to measure photosynthetic parameters.

Induction and Relaxation of fluorescence parameters in response to light intensity

All plant material was dark adapted for 45 mins inside the FluorCam before imaging before F_v/F_m was measured after a saturating pulse of 4500 µmol m^{-2} s^{-1} for 0.8 s by white LEDs with actinic light. The protocol then consisted of three steps of 15 mins, the first being 500 µmol $m^{-2}s^{-1}$ followed by 100 µmol $m^{-2}s^{-1}$ and finally 500 µmol $m^{-2}s^{-1}$ Photosynthetic Photon Flux Density (PPFD). Measurements were taken every minute throughout the protocol. Determining NPQ induction and relaxation rates

Following methods shown in McAusland et al., (2019), NPQ was determined by model fitting for all samples (individual plants on individual days) by finding best fit through selecting from: parameter Weibull Type 1 (three parameters), Weibull type 1 (four parameter), Weibull Type 2 (four parameter), Log-logistic (two parameter), Log-logistic (three parameter), Log-logistic (four parameter) and Log-logistic (five parameter). Best fit for each sample was logged (see **Table 4.3**) and overall best fit model was chosen as Weibull Type 1 (four parameters) for induction curves and Weibull Type 2 (four parameters) for relaxation Using this model, Induction time (t) taken to reach 50% of the L30 NPQ value (I_{50}) and 50% of the L15 NPQ values (R_{50}).

Table 4.3: Model fitting for NPQ induction and relaxation rates

Row Labels	No. of best fit samples Induction	No. of best fit samples Relaxation
Cubic	2	2
Linear	1	0
Weibull Type 1 (3 parameter)	0	0
Weibull Type 1 (4 parameter)	**1689**	6
Weibull Type 2 (4 parameter)	48	**1544**
Log logistic (2 parameter)	0	0
Log logistic (3 parameter)	0	0
Log logistic (4 parameter)	120	353
Total	1860	1905

Table 4.3: A table summary of Models used to fit induction and relaxation data. No. of best fit samples shows the total number of samples which showed each model to be best fit of the data in induction and relaxation data. Underlined values indicate the values chosen to run whole dataset.

Temperature response of Quantum efficiency of PSII

For each plant, one single leaf was selected from the rosette- the oldest leaf not showing signs of senescence was chosen. Up to 80 leaf samples were placed immediately on damp filter paper on a 3mm thick aluminium sheet and arranged according to a reference map of sample numbers. Up to two sheets of filter paper and samples were measured at one time. A sheet of non-reflective glass was placed on top of samples so as not to disturb their position (as described by Ferguson et al., 2020). The aluminium sheet was placed in the FluorCam (described above) on two 400W silicone heater mats (model LM240, Thermosense, Bourne End, UK), which were controlled by proportional-integral-derivative (PID) controller (model CH102, Thermosense). A K-type bead thermocouple was placed between the glass and filter paper alongside the leaf samples to provide temperature feedback to the PID controller. The previous study by Robson et al., (2023) showed reliable temperature feedback when placed in this position.

Leaf samples were first dark adapted for 45 mins inside the FluorCam. For each temperature (21°C to 51°C) a light pulse determined F_o. A second saturating pulse measured maximum chlorophyll fluorescence (F_m), which allowed the calculation of F_v (F_m-F_o), and maximum quantum efficiency of PSII (F_v/F_m). After each measurement, the set temperature on the PID controller was increased by 1°C intervals. 120 seconds after setting the increase in temperature, the measurements were repeated, to allow the sample to heat to the new desired temperature. All measurements

were performed late afternoon, as to keep natural variation caused by time of day to a minimum.

Determining Tcrit, M_1, and M_2

FluorCam 7 software was used to extract raw data containing F_o, F_v and F_m values per leaf sample at each temperature point from 21°C to 51°C. As per described in Ferguson et al., (2020) the R package 'segmented' was used to determine the breakpoint where the relationship between F_v/F_m and temperature changes from a slow to rapid decline. The slope of the linear model of measurements before T_{crit} is denoted as m_1, and the slope of the linear model after T_{crit} is denoted m_2 (**Figure 4.2**).

4.2.3 Statistical analysis

Statistical analysis and visualisation of graphs were performed using R-studio (2023.12.1 Build 402) with R-4.3.1. Packages used included: ggpubr, sssci, ggplot2, plyr, multcompView, doBy, dyplyr, gghighlight, forcats, tidyverse, purr, sm, plotrix, Hmisc, corrplot, PerformanceAnalytics, fmsb, segmented, reshape2, DataCombine, stringer, broom, drc, and dplyr. Correlation matrices were also performed using R. ANOVA was used throughout using R with Tukey HSD test used to assess significant differences between sample means.

4.3 Results

4.3.1 Response of PSII under heat stress

By benchmarking photosynthetic heat tolerances of 15 T-DNA insertion lines as T_{crit}, m_1 and m_2 through segmented modelling, the response of maximum quantum efficiency of PSII to rapidly increasing temperatures is characterised .

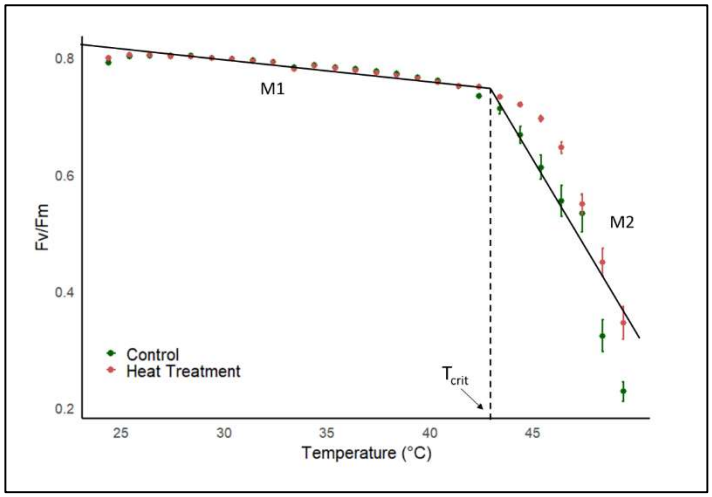

Figure 4.2: Graph showing an example of changes in Quantum efficiency of Photosystem II (PSII) (F_v/F_m) when exposed to increasing heat temperatures in WT (Col-0). The dotted line indicates the mean T_{crit} of samples whereas m_1 and m_2 denote the value of the slope before and after T_{crit}. Heat treated plants denoted by the red dots show plants that were exposed to 32°C heat for five days prior. Error bars denote SEM.

m_1 and m_2 were used as quantitative measures of primary and secondary rate of decline in efficiency of PSII alongside critical value (T_{crit}) which is temperature in which the response of F_v/F_m transitions from a slow to a rapid decline as seen in **Figure 4.2**. These values were then used to compare T-DNA mutants in genes of interest to WT (Col-0), as well as comparing the response to heat after a prior period of five day 32°C heat exposure and subsequent three days of recovery. Note that higher values of T_{crit} indicates higher tolerance of PSII to increased temperatures. Lower values of M_1 indicate higher tolerance of PSII to increased temperatures. Therefore, a shift to a lower T_{crit} would indicate sensitivity while no change or an increase could indicate tolerance. Higher values in comparison with the wild type control will indicate greater tolerance.

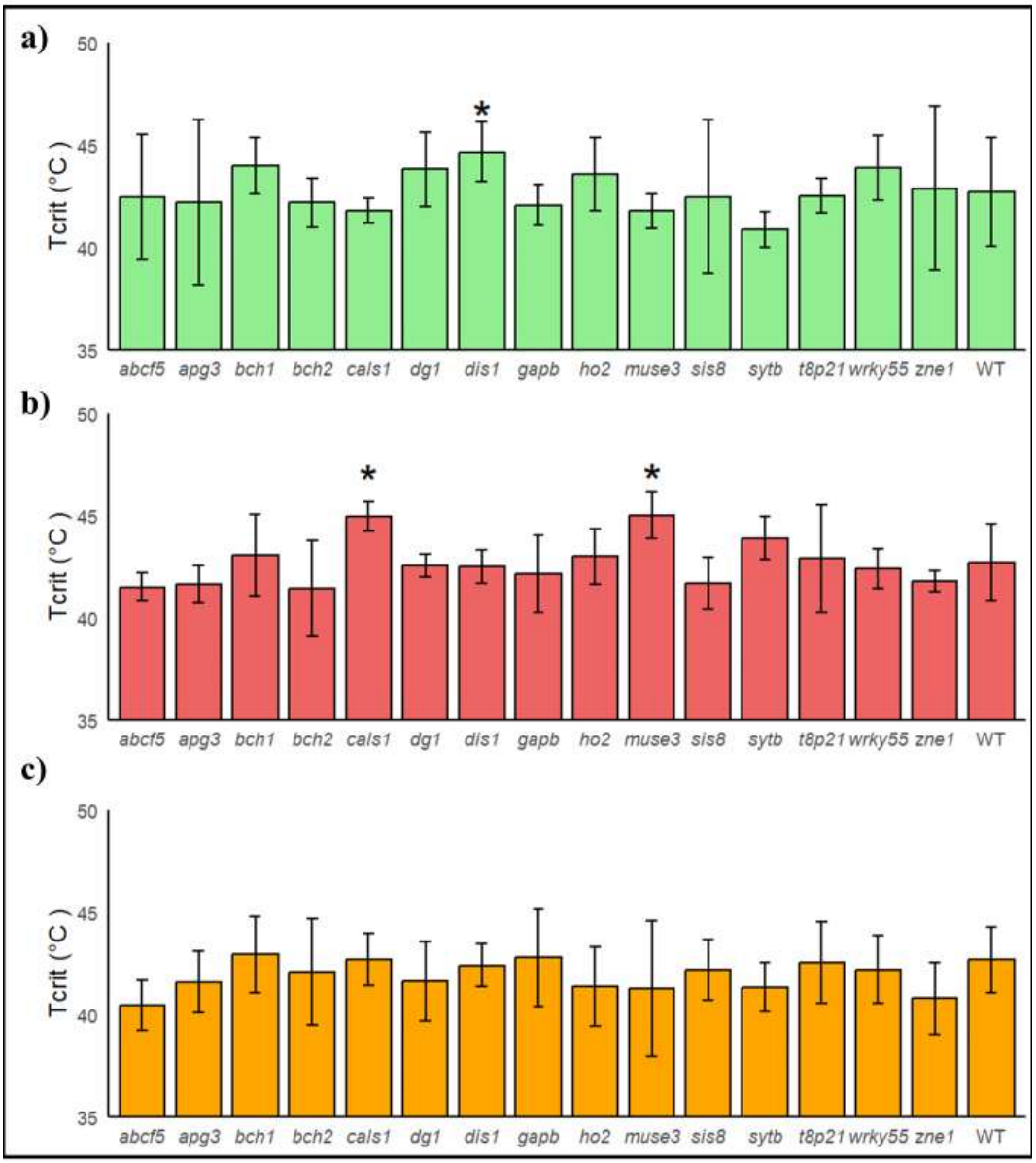

*Figure 4.3: Critical temperature (Tcrit) of T-DNA insertion mutants and WT (Col-0) of same treatment groups. T-DNA insertion mutants of A. thaliana genotypes and Col-0 (WT) a) in control conditions b) after prior exposure at 32°C for five days c) subsequent three days recovery. * denotes significant difference (P<0.05) to the WT of the same treatment. Error bars indicate SEM.*

Overall, in control conditions, none of the mutants showed differences in T_{crit} to the WT (**Figure 4.3**). Compared to WT, *Cals1* (+1°C), *muse3* (+2.2°C) and *Sytb* (+1°C) showed higher T_{crit} after prior heat exposure (**Figure 5.4**). Heat treatment of five days caused a significant increase in T_{crit} in *Cals1* by 3.14°C and *Muse3* by 3.25°C, which returned to levels seen in control conditions after three days of recovery (**Figure 4.3)**.

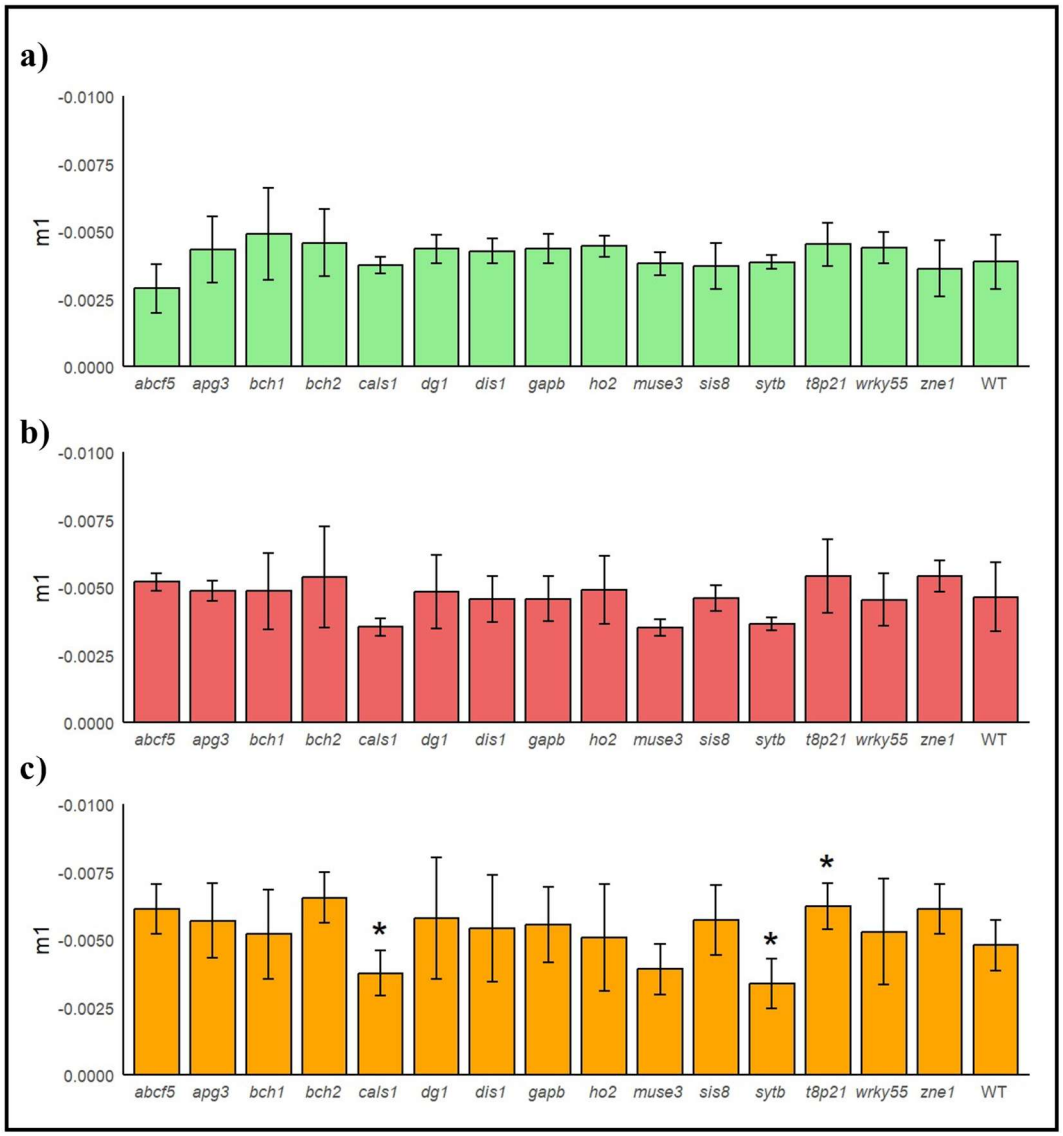

*Figure 4.4: Initial rate of response to heat (m_1) of T-DNA insertion mutants and WT (Col-0) of same treatment groups. T-DNA insertion mutants of A. thaliana genotypes and Col-0 (WT) a) in control conditions b) after prior exposure at 32°C for five days c) subsequent three days recovery. * denotes significant difference (P<0.05) to the WT of the same treatment. Error bars indicate SEM.*

In WT, the initial rate of response to heat did not change after five days heat stress, yet initial rate of response (m_1) was significantly slower in plants after three days recovery from heat. In the majority of the mutants (with the exception of *Sis8* and *Zne1*), five days heat stress did not cause a significant change in m_1 (**Figure 4.4**). In comparison to the WT, mutants showed little differences in m_1 with only *Cals1* (-0.04), (**Figure 4.4)**, and *Sytb* (-0.02) (**Figure 4.4**) showing a significantly slower rate of decline in F_v/F_m after prior heat exposure and *T8p21* (+0.02) (**Figure 4.4**) showing a faster rate of decline in F_v/F_m.

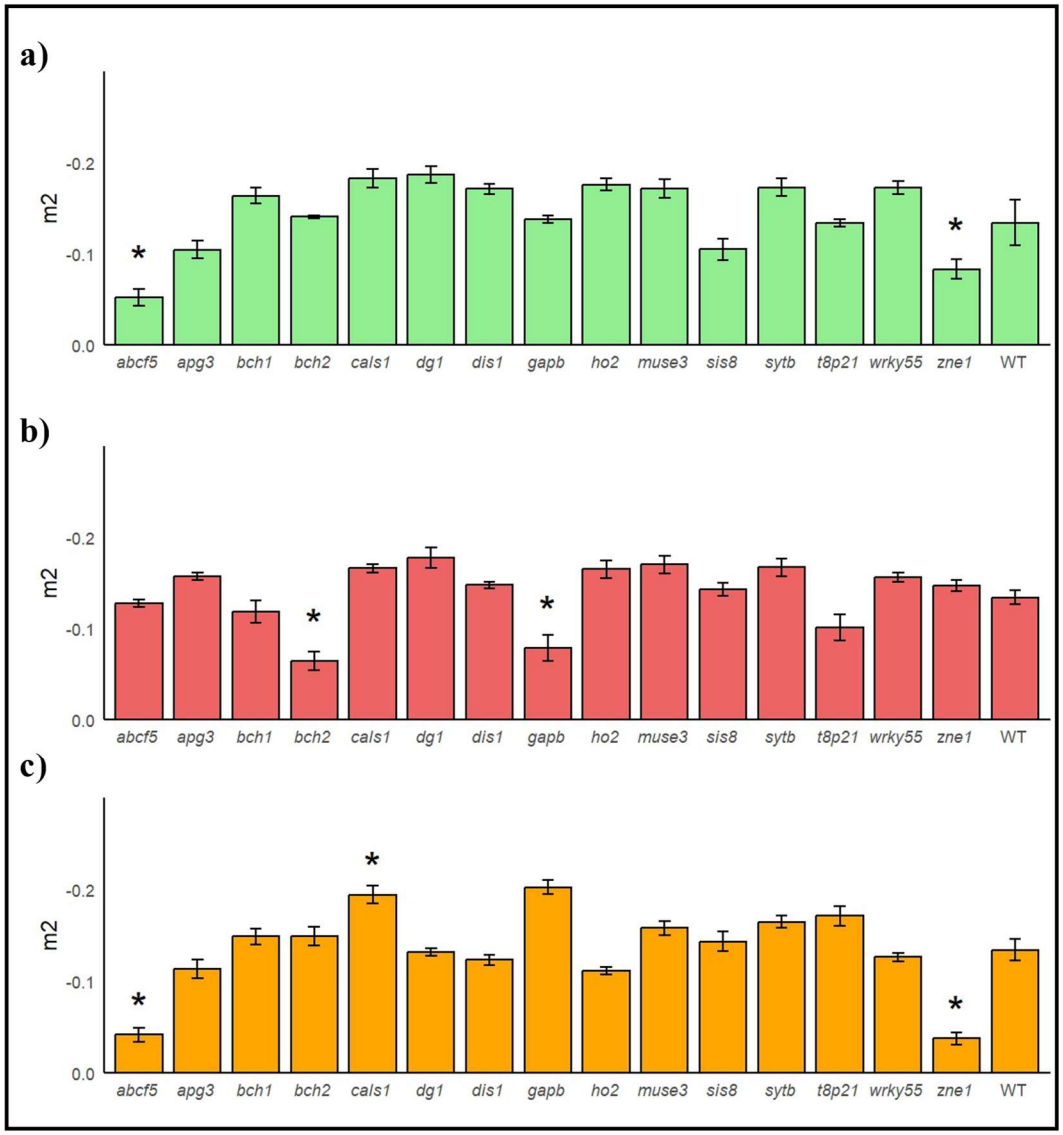

*Figure 4.5: Secondary rate of response to heat (M_2) of T-DNA insertion mutants and WT (Col-0) of same treatment groups. T-DNA insertion mutants of A. thaliana genotypes and Col-0 (WT) a) in control conditions b) after prior exposure at 32°C for five days c) subsequent three days recovery. * denotes significant difference (P<0.05) to the WT of the same treatment. Error bars indicate SEM.*

In control conditions, both *Abcf5* (+0.08) and *Zne1* (+0.05) had a significantly faster rate of secondary response to heat (m_2) than WT (**Figure 4.5**). When exposed to five days heat treatment, (*Bch2* (+0.08) and *Gapb* (+0.06)) showed significantly faster secondary response (m_2) to WT after five days of prior heat exposure (**Figure 4.5**). When comparing mutants to WT rates of m_2, *Abcf5* (+0.1) and *Zne1* (0.11) after 3-day recovery from heat stress, had a faster secondary response (m_2) (**Figure 4.5**)

4.3.2 Induction and relaxation of PSII after heat stress in selected mutants

The dynamic changes in PSII are important for maintaining photosynthetic productivity. This is measured by quantifying the rate of response of key fluorescence parameters to an increase and decrease in light intensity before and after heat stress.

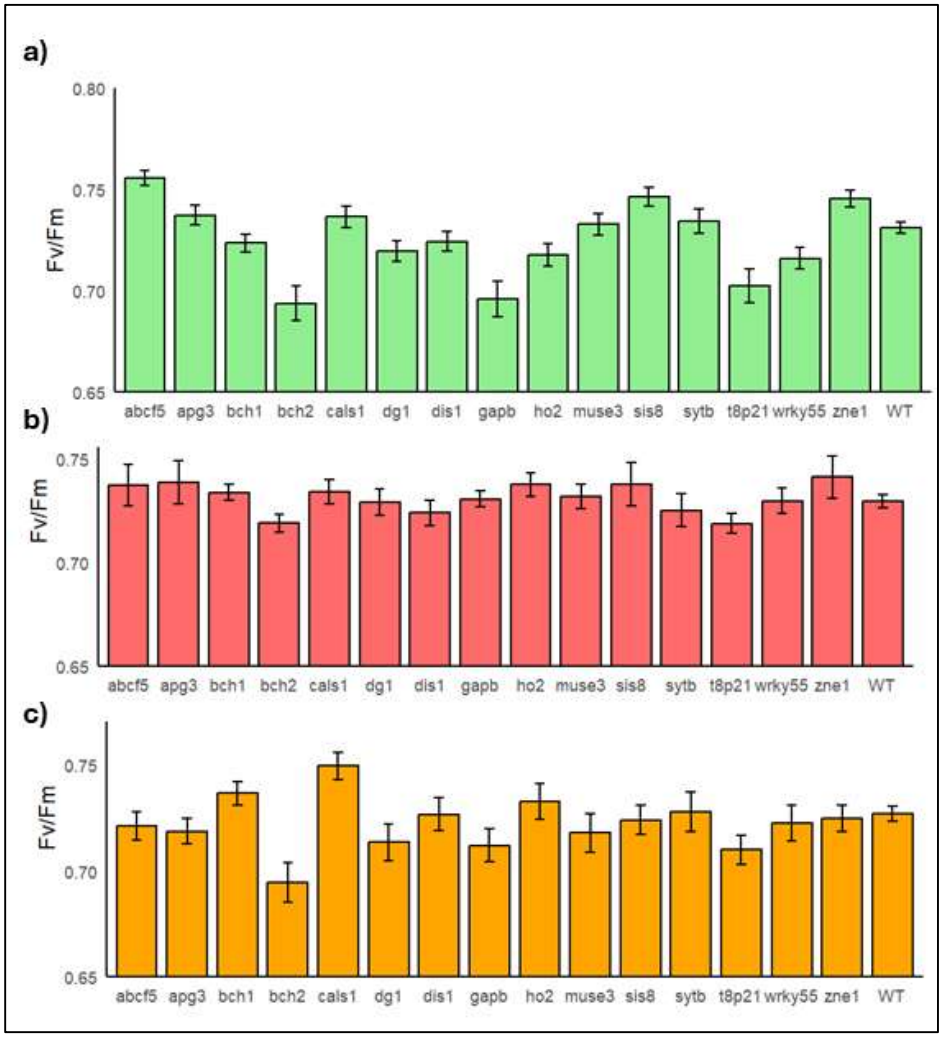

*Figure 4.6: F_v/F_m of T-DNA insertion mutants and WT (Col-0) of same treatment groups at stable light level L15. T-DNA insertion mutants of A. thaliana genotypes and Col-0 (WT) a) in control conditions b) after prior exposure at 32°C for five days c) subsequent three days recovery. * denotes significant difference (P<0.05) to the WT of the same treatment. Error bars indicate SEM.*

Figure 4.6 shows dark adapted F_v/F_m, lowered values of which are an indication of photoinhibitory damage or stress to PSII. While heat stress did result in a low F_v/F_m

in some lines, these were not significantly different from Col-0. and **Figure 4.6** confirms that there were no differences in F_v/F_m between mutants and WT.

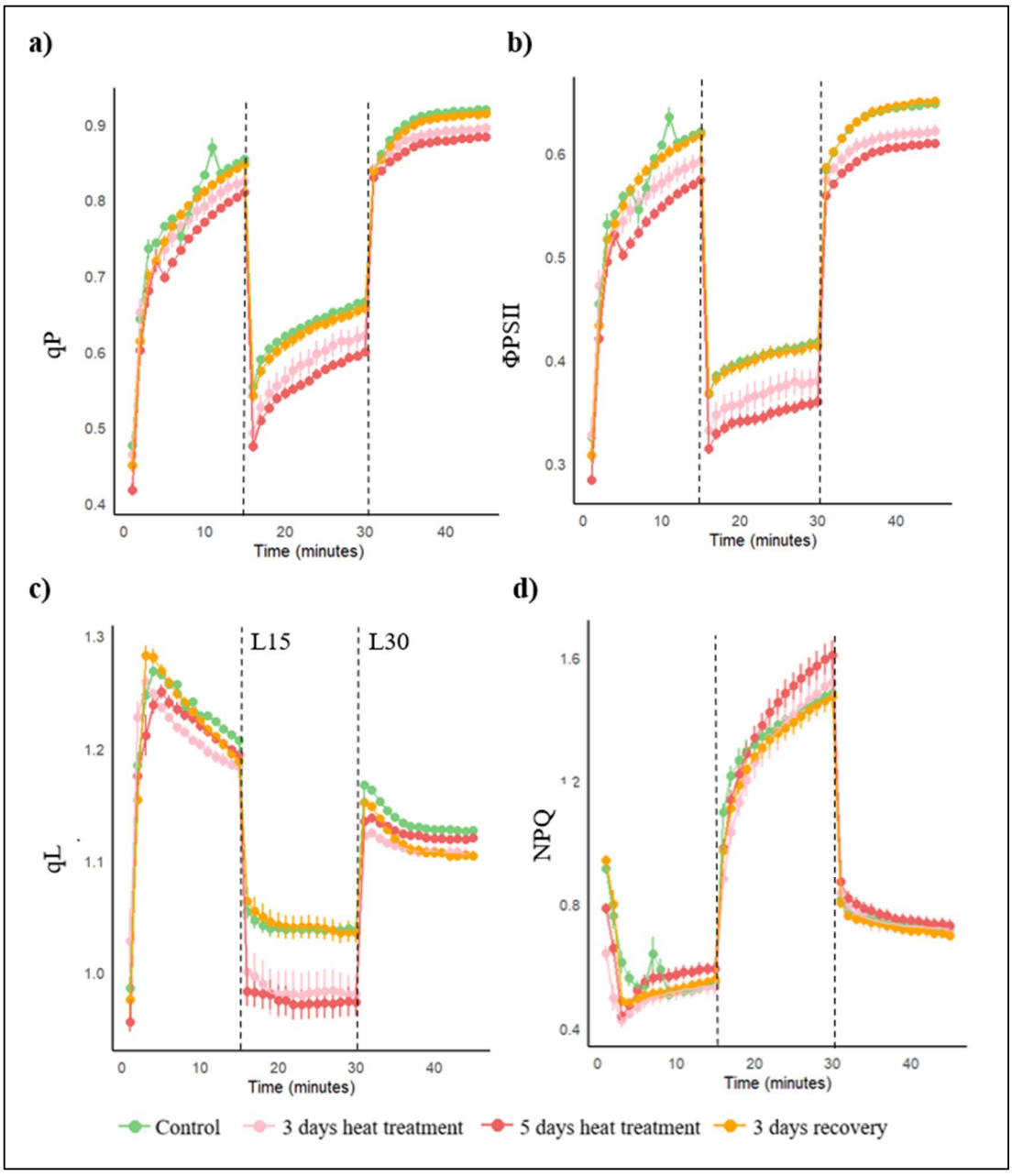

Figure 4.7: The response of chlorophyll fluorescence parameters (see Table 2 for full descriptions) to stepwise changes in photosynthetic photon flux density (--- PPFD) in A. thaliana Col-0 ecotype. After a dark adaptation period of 45mins, PPFD was increased to 500 µmol m^{-2} s^{-1} for 15 min. Subsequently, PPFD was decreased to 100 µmol m m^{-2} s^{-1} 1 for 15 min and then increased to 500 µmol m^{-2} s^{-1} for 15min. From measurements of maximal (Fm) and minimal (Fo) fluorescence the following parameters can be calculated: photochemical quenching (a—qP)PSII quantum yield of PSII (b— ΦPSII), fraction of open PSII reaction centres (c—qL), and maximum non-photochemical quenching (d—NPQ). Measurements were taken every minute and error bars indicate standard error.

Figure 4.7 shows important parameters measured in the light dynamic protocol in the WT. Trends in chlorophyll fluorescence were following patterns expected and as described in McAusland et al., (2019) i.e. a rise in NPQ in high light associated with a reduction in quantum efficiency. Generally, control values were similar to three days recovery indicating short term acclimation responses. For three and five days heat treatment, NPQ, ΦPSII, qL and qP were all lower than control or recovered plants (**Figure 4.7**).

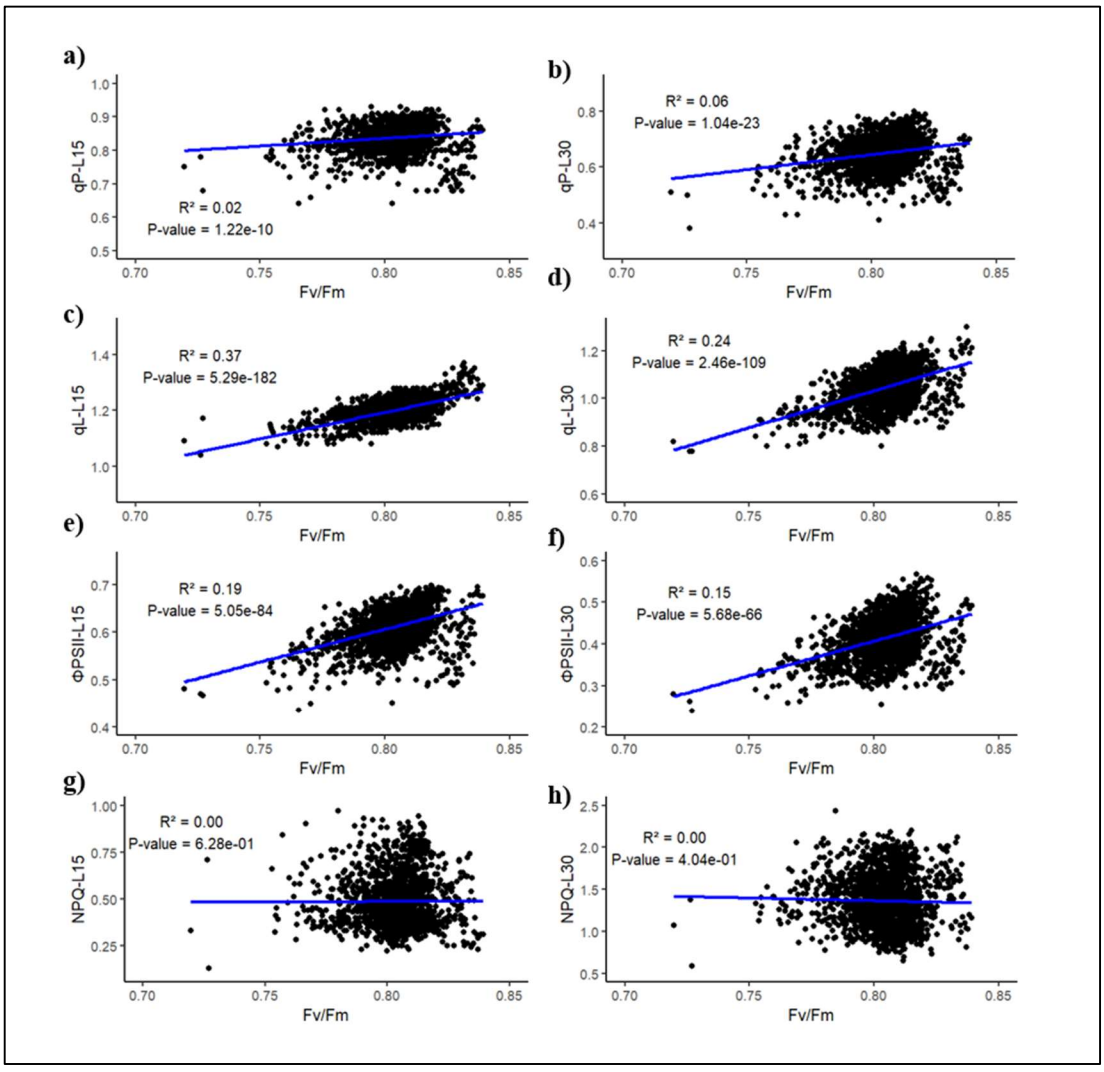

Figure 4.8: Correlation between F_v/F_m and other chlorophyll fluorescence parameters at steady state at L15 and L30. a/b) qP-photochemical quenching. c/d) qL-photochemical quenching. e/f) ΦPSII - fraction of open PSII reaction centres. g/h) NPQ

An F_v/F_m of lower than 0.83 indicates photosynthetic function below maximum levels. Due to the F_v/F_m being lower than 0.83, the potential influence of F_v/F_m on the measured parameters qP, qL, ΦPSII and NPQ was assessed- **Figure 4.8** shows results of a correlation analysis. All P values remained <0.05 except for NPQ at L15 and L30, suggesting that photoinhibited leaves resulted in lower quantum efficiency and fewer open reaction centres but did not influence values of NPQ. R^2 values among all correlations remained below 0.37 (**Figure 4.8**). The R^2 value for the correlation between qP and F_v/F_m in both stable light conditions (L15 and L30) were 0.03 and 0.06 respectively (**Figure 4.8**). Looking at qL values, there was a slightly higher positive correlation between F_v/F_m and qL, however the R^2 values still remained low at L15 and L30 (0.37 and 0.25 respectively) (**Figure 4.8**). The R^2 value for the correlation between qP and F_v/F_m in both stable light conditions (L15 and L30) were 0.2 and 0.16 respectively (**Figure 4.8**). With the correlation between both L15 and L30 NPQ had R^2 values were 0.00 at both L15 and L30 (**Figure 4.8**).

ΦPSII -the quantum yield of PSII

ΦPSII was assessed at the two most stable points L15 and L30. In the WT, there were no differences in ΦPSII between control conditions and three days heat, nor a significant difference in ΦPSII between control conditions and after three days recovery treatment. Five days heat stress caused a significant decrease in ΦPSII in WT at both L15 and L30.

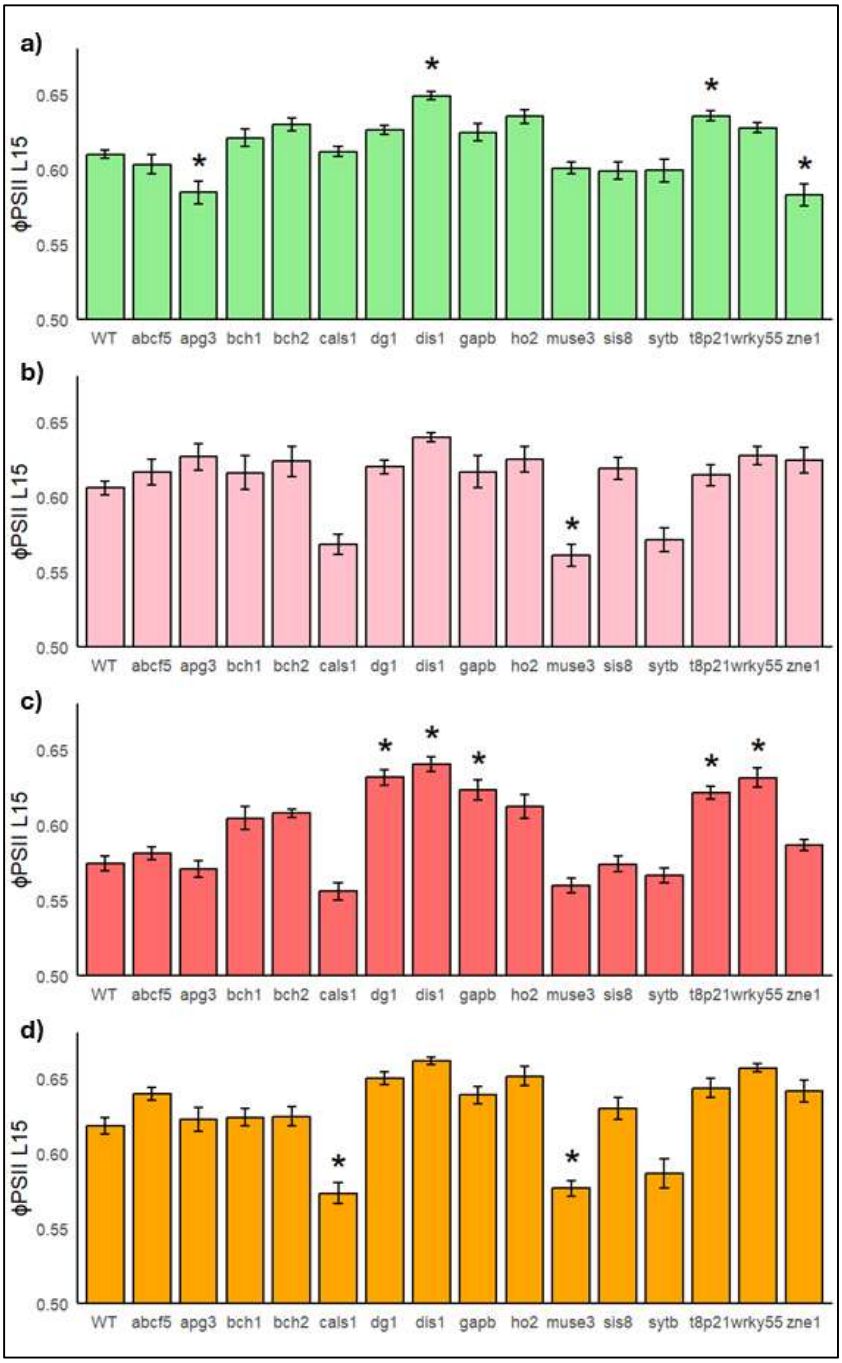

*Figure 4.9: ΦPSII of T-DNA insertion mutants and WT (Col-0) of same treatment groups at stable light level L15. T-DNA insertion mutants of A. thaliana genotypes and Col-0 (WT) a) in control conditions b) after prior exposure at 32°C for three days c) after prior exposure at 32°C for five days and d) subsequent three days recovery. * denotes significant difference (P<0.05) to the WT of the same treatment. Error bars indicate SEM.*

Figure 4.9 shows the ΦPSII of Mutants at L15, where in control conditions, *Apg3* (-0.025) and *Zne1* (-0.027) had a significantly lower ΦPSII, whereas *Bch2* (+0.020), *Dis1* (+0.039), *Ho2* (+0.25) and *T8p21* (+0.025) had a significantly higher ΦPSII.

After three days heat treatment two mutants had a significantly reduced ΦPSII compared to WT: *Cals1* (-0.038) and *Muse3* (-0.45), whereas after five days heat, five mutants showed a significantly higher ΦPSII than WT: *Dg1* (+0.056), *Dis1* (+0.065), *Gapb* (+0.048), *T8p21* (+0.046) and *Wrky55* (+0.056) (**Figure 4.9**). After three days recovery there were two mutants that had a significantly reduced ΦPSII: *Cals1* (-0.045) and *Muse3* (-0.042) (**Figure 4.9**).

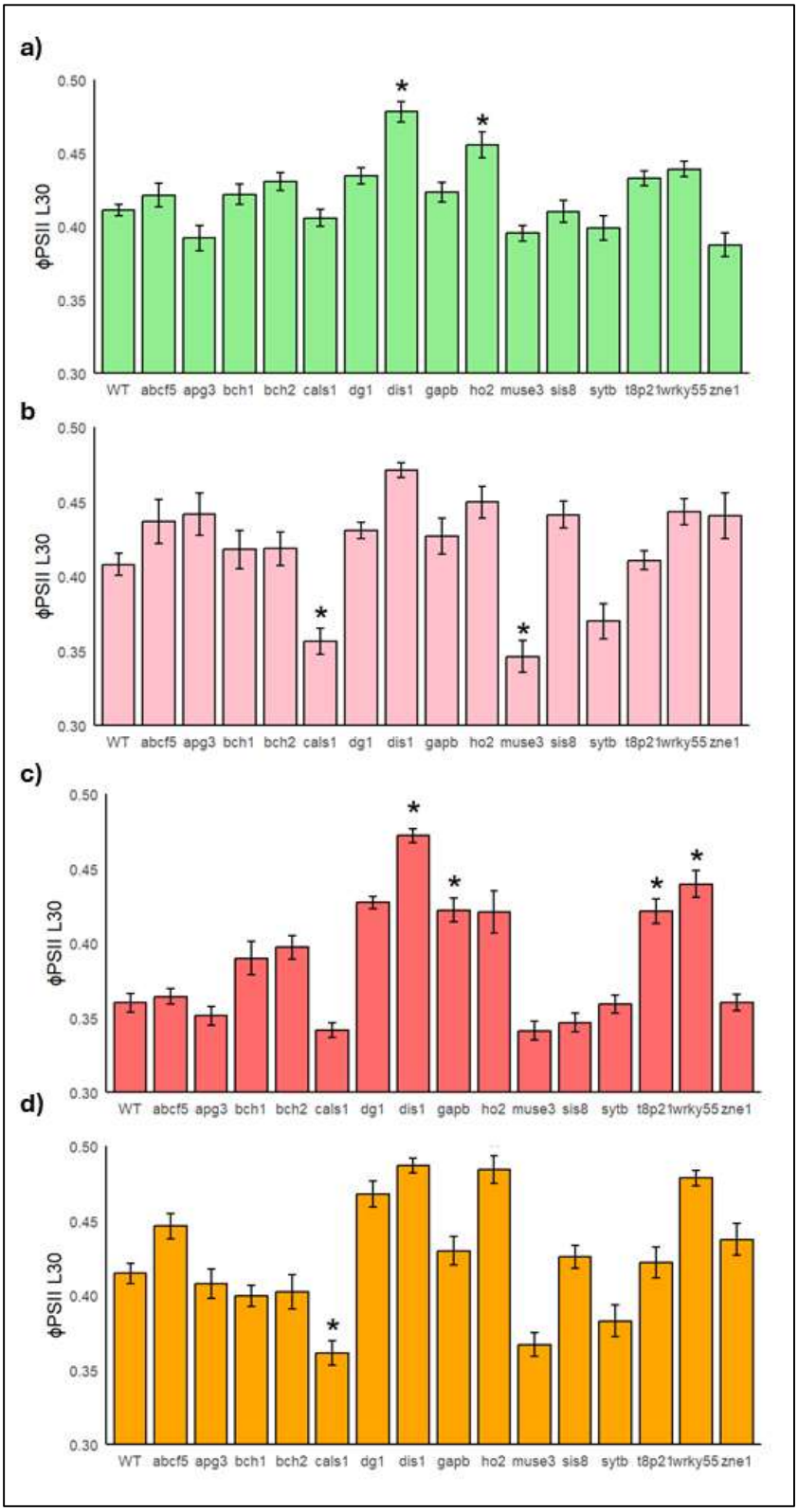

*Figure 4.10: F_q'/F_m' (ϕPSII) of T-DNA insertion mutants and WT (Col-0) of same treatment groups at stable light level L30. T-DNA insertion mutants of A. thaliana genotypes and Col-0 (WT) a) in control conditions b) after prior exposure at 32°C for three days c) after prior exposure at 32°C for five days and d) subsequent three days recovery. * denotes significant difference ($P<0.05$) to the WT of the same treatment. Error bars indicate SEM.*

Figure 4.10 shows the ϕPSII of Mutants at L30, where in control conditions only *Dis1* (+0.067) and *Ho2* (+0.044) had a significantly higher ΦPSII than the WT. *Dis1* (+0.063) was the only mutant to show a significantly higher ΦPSII than WT after three days heat stress, however *Cals1* (0.051) and *Muse3* (-0.062) showed a significantly lower ΦPSII than WT (**Figure 4.10**). After five days heat stress, six of the mutants showed a significantly higher ΦPSII than the WT: *Dg1* (+0.067), *Dis1* (+0.111), *Gapb* (0.062), *Ho2* (+0.061), *T8p21* (+0.061) and *Wrky55* (+0.079) (**Figure 4.10)**. After three days subsequent recovery, compared to the WT, *Dis1* (+0.174), *Ho2* (+0.069) and *Wrky55* (+0.064) had a significantly higher ΦPSII, whereas *Cals1* (-0.053) and *Muse3* (-0.048) had significantly lower ΦPSII (**Figure 4.10**).

qL

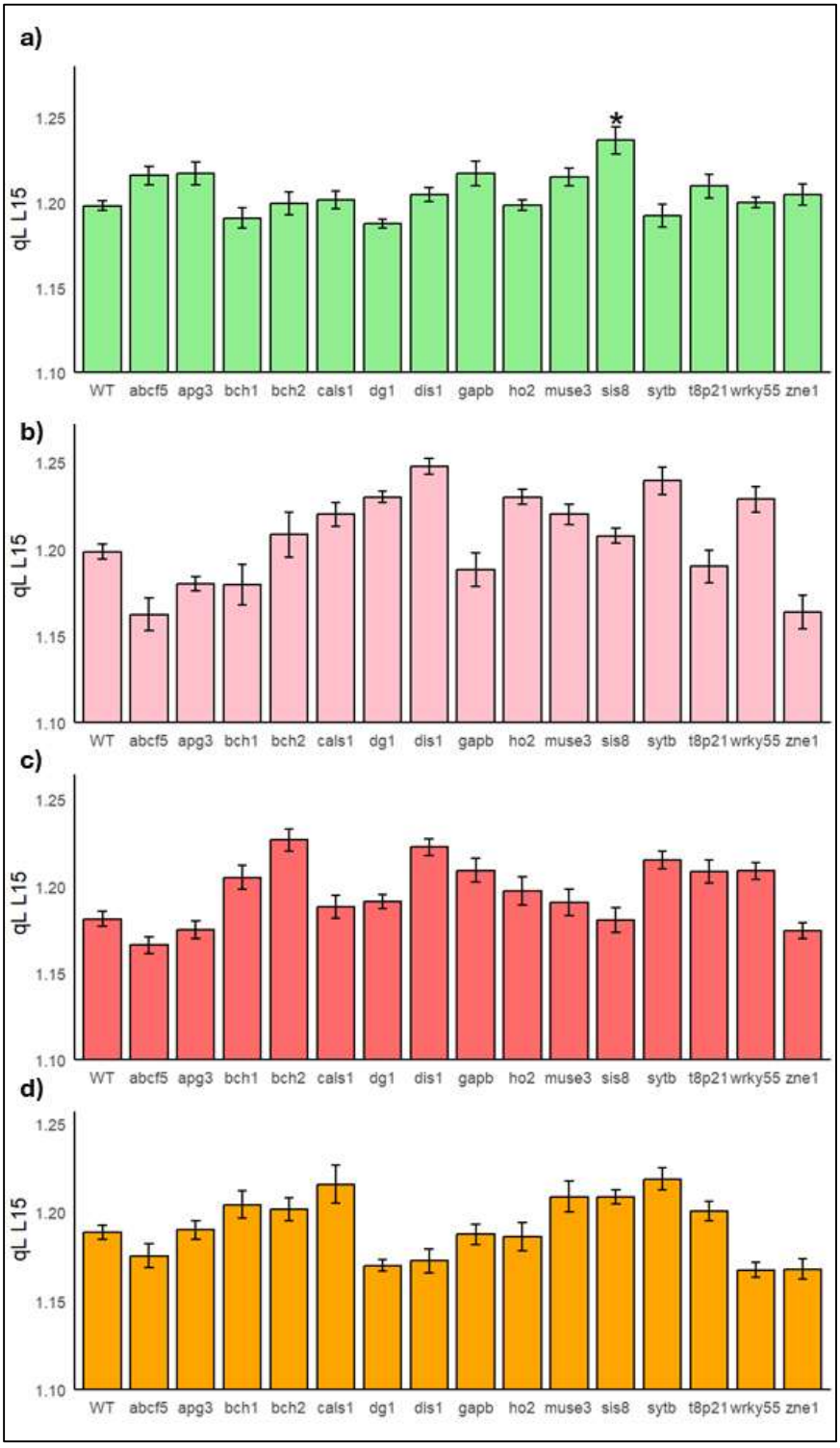

*Figure 4.11: qL of T-DNA insertion mutants and WT (Col-0) of same treatment groups at stable light level L15. T-DNA insertion mutants of A. thaliana genotypes and Col-0 (WT) a) in control conditions b) after prior exposure at 32°C for three days c) after prior exposure at 32°C for five days and d) subsequent three days recovery. * denotes significant difference (P<0.05) to the WT of the same treatment. Error bars indicate SEM.*

Figure 4.11 shows the qL of T-DNA insertion mutations at L15. The WT showed no significant changes in qL with heat treatment and subsequent recovery (**Figure 4.11**). In control conditions, *Dg1* was significantly ($P<0.05$)lower than the WT by -0.011 and *Ho2* was significantly higher by +0.0004. After three days and five days of heat stress, only *Abcf5* showed a significantly lower qL than the WT by -0.036 after three days heat and -0.013 after five days heat (**Figure 4.11**). After subsequent three days recovery, none of the mutants showed a significantly different qL to the WT.

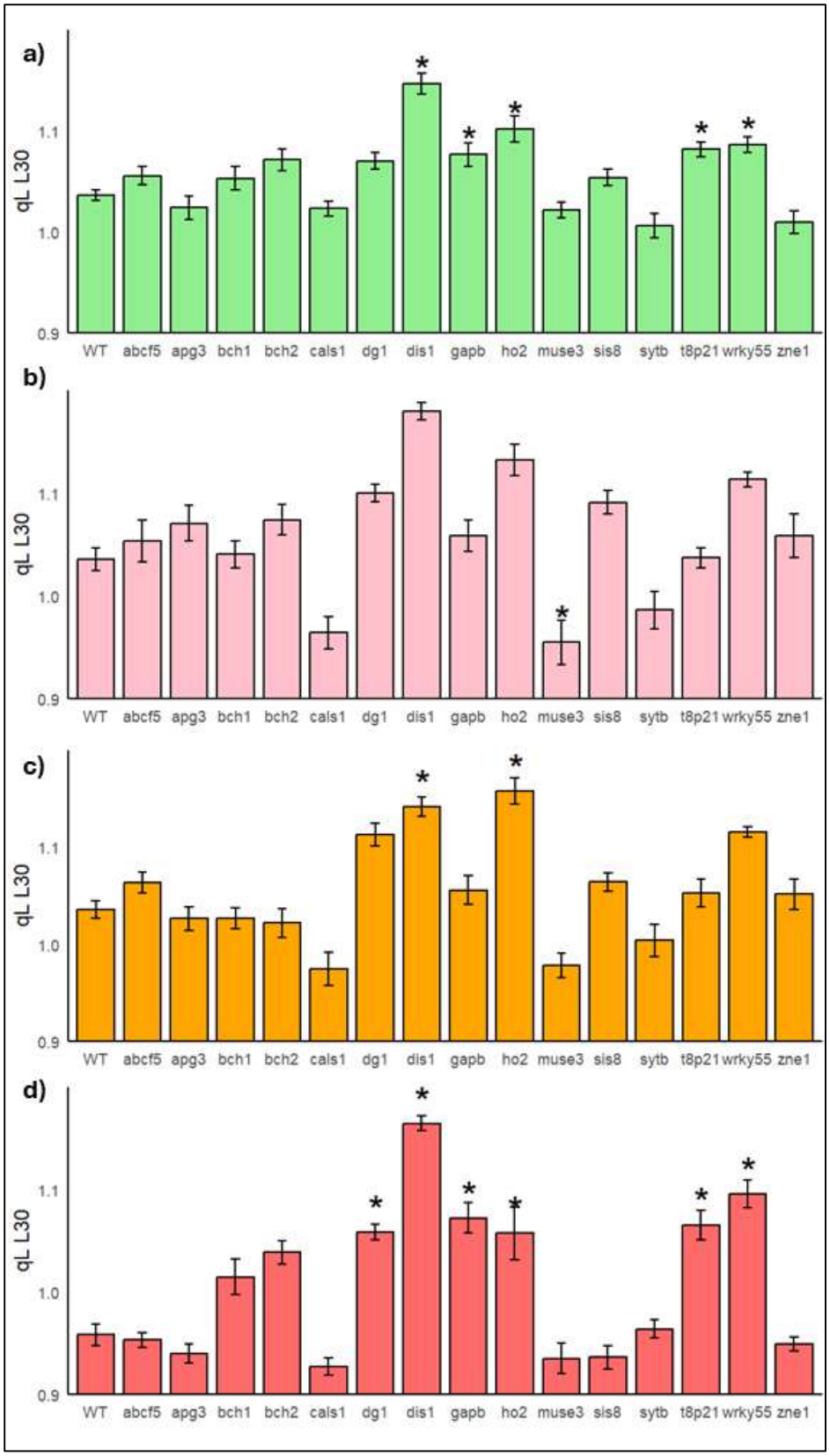

*Figure 4.12: qL of T-DNA insertion mutants and WT (Col-0) of same treatment groups at stable light level L30. T-DNA insertion mutants of A. thaliana genotypes and Col-0 (WT) a) in control conditions b) after prior exposure at 32°C for three days c) after prior exposure at 32°C for five days and d) subsequent three days recovery. * denotes significant difference (P<0.05) to the WT of the same treatment. Error bars indicate SEM.*

Figure 4.12 shows the qL of the T-DNA insertion mutants and Col-0 plants at L30. In control conditions, *Cals1* had a lower qL than the WT by 0.013 (**Figure 4.12**). None of the mutants showed a significant difference to the WT after heat stress of three and five days nor in subsequent recovery of three days (**Figure 4.12**).

qP

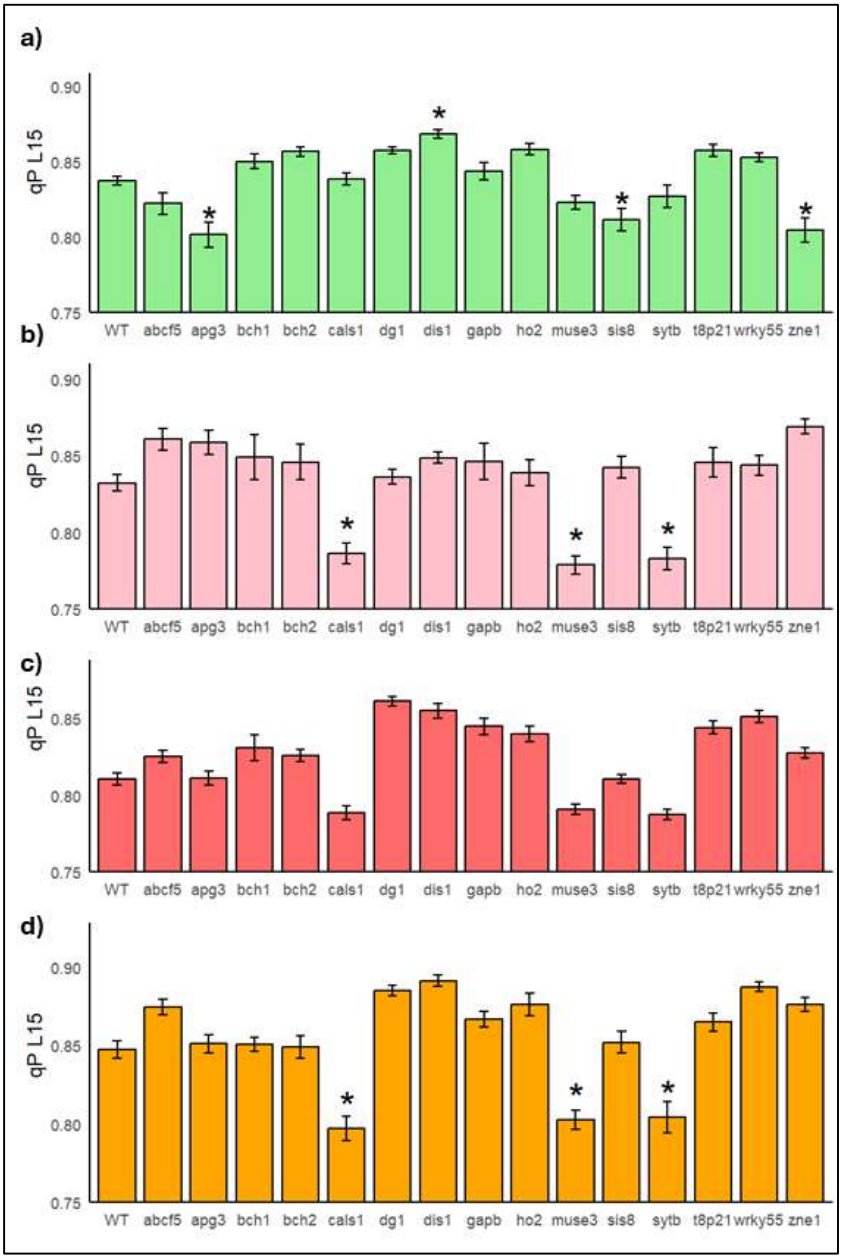

*Figure 4.13: qP of T-DNA insertion mutants and WT (Col-0) of same treatment groups at stable light level L15. T-DNA insertion mutants of A. thaliana genotypes and Col-0 (WT) a) in control conditions b) after prior exposure at 32°C for three days c) after prior exposure at 32°C for five days and d) subsequent three days recovery. * denotes significant difference (P<0.05) to the WT of the same treatment. Error bars indicate SEM.*

Figure 4.13 shows the qP of the T-DNA insertion mutations and WT Col-0 at L15. Heat had no significant effect on qP on the WT after three days heat stress or after three days recovery from stress, however a significant decrease was seen after five days heat stress (**Figure 4.13**). In control conditions, compared to WT, *Apg3* (-0.036), *Sis8* (-0.026) and *Zne1* (-0.033) all showed a significantly lower qP, whereas *Bch2*

(+0.019), *Dis1* (+0.031) and *T8p21* (+0.020) had a significantly higher qP than the WT (**Figure 4.13**). After three days heat stress *Cals1* (-0.046), *Muse3* (-0.053) and *Sytb* (-0.049) all showed a significantly lower qP than the WT (**Figure 4.13**). After five days heat stress, *Dg1* showed a significantly higher qP than the WT by 0.05. After three days recovery from heat, three mutants had a significantly lower qP than the WT: *Cals1* (-0.05), *Muse3* (-0.045) and *Sytb* (-0.043) (**Figure 4.13**).

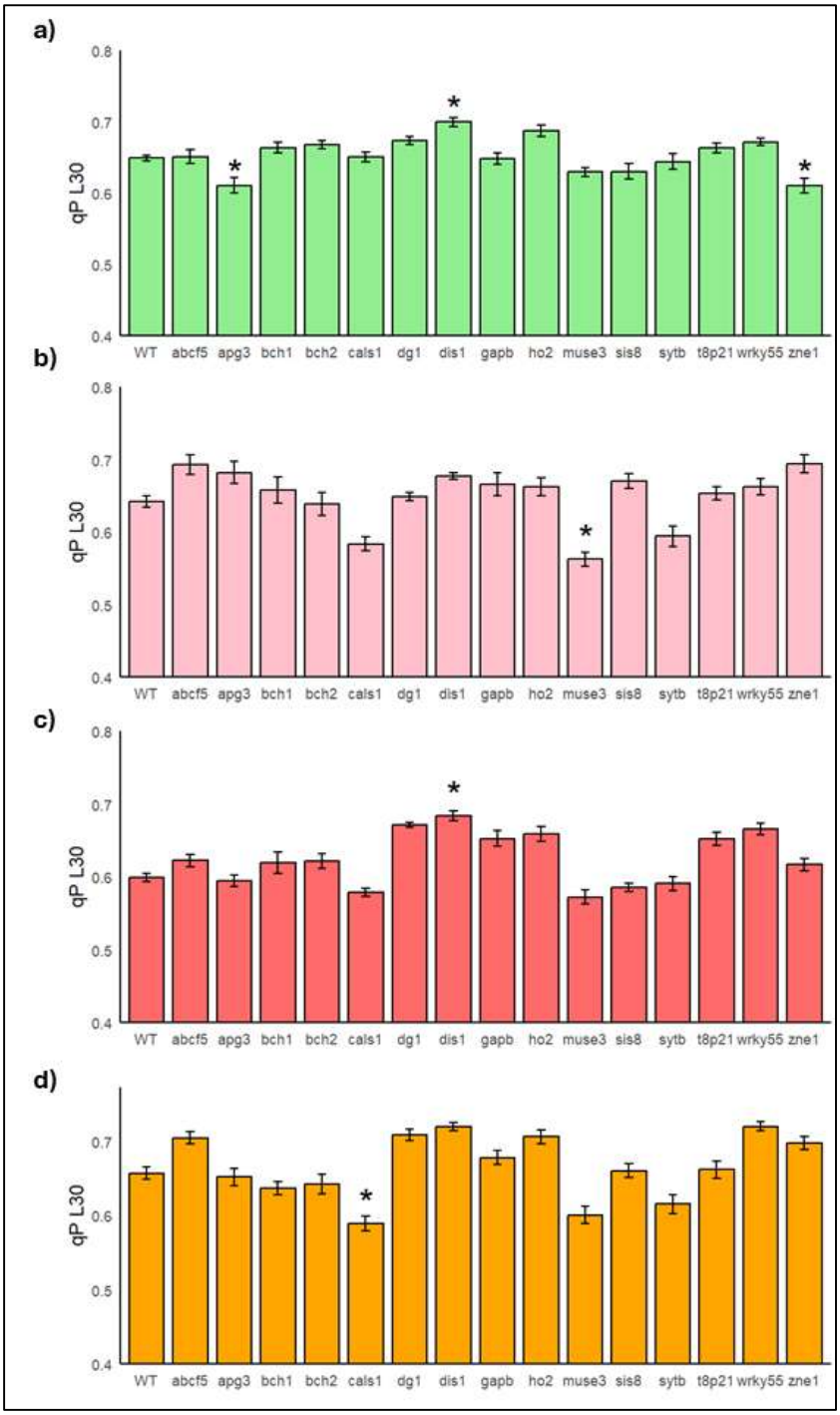

*Figure 4.14: qP of T-DNA insertion mutants and WT (Col-0) of same treatment groups at stable light level L30. T-DNA insertion mutants of A. thaliana genotypes and Col-0 (WT) a) in control conditions b) after prior exposure at 32°C for three days c) after prior exposure at 32°C for five days and d) subsequent three days recovery. * denotes significant difference (P<0.05) to the WT of the same treatment. Error bars indicate SEM.*

Figure 4.14 shows the qP of the T-DNA insertion mutations at L30. Heat had no significant effect on qP on the WT after three days heat stress or after three days recovery from stress, however a significant decrease was seen after five days heat

stress (**Figure 4.14**). In control conditions, compared to the WT, *Apg3* (-0.039) and *Zne1* (-0.039) were significantly lower while *Dis1* (0.051) and *Ho2* (+0.038) were significantly higher (**Figure 4.14**). After three days of heat stress, two of the mutants showed a significantly lower qP than the WT: *Cals1* (-0.059) and *Muse3* (-0.08) (**Figure 4.14**). Only the mutant *Dis1* showed a significantly higher qP than the WT by 0.084 (**Figure 4.14**). After three days recovery*Cals1* (0.068) and *Muse3* (0.057) all showed a significantly lower qP than the WT (**Figure 4.14**).

Non-photochemical quenching (NPQ)

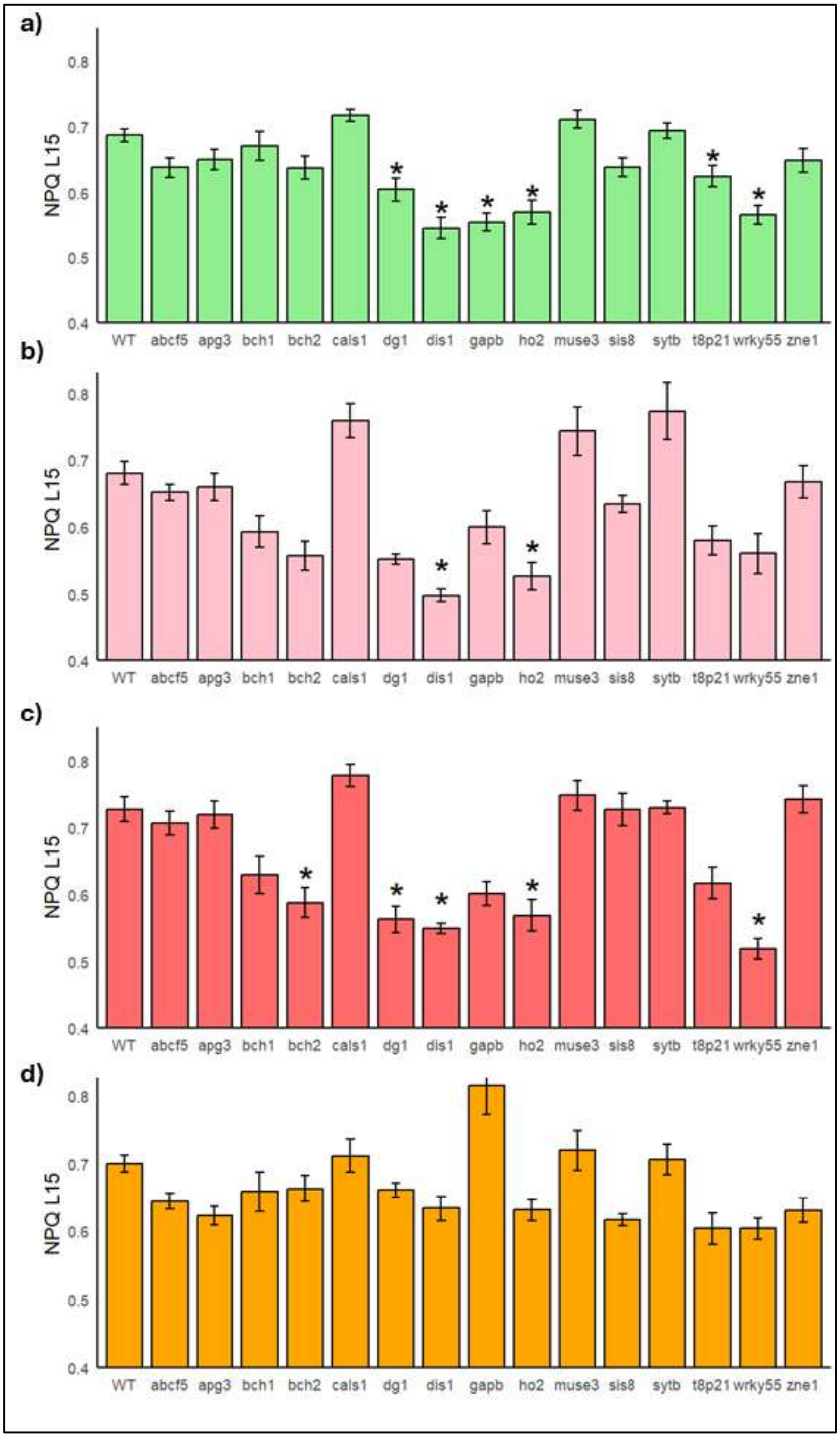

*Figure 4.15: NPQ of T-DNA insertion mutants and WT (Col-0) of same treatment groups at stable light level L15. T-DNA insertion mutants of A. thaliana genotypes and Col-0 (WT) a) in control conditions b) after prior exposure at 32°C for three days c) after prior exposure at 32°C for five days and d) subsequent three days recovery. * denotes significant difference (P<0.05) to the WT of the same treatment. Error bars indicate SEM.*

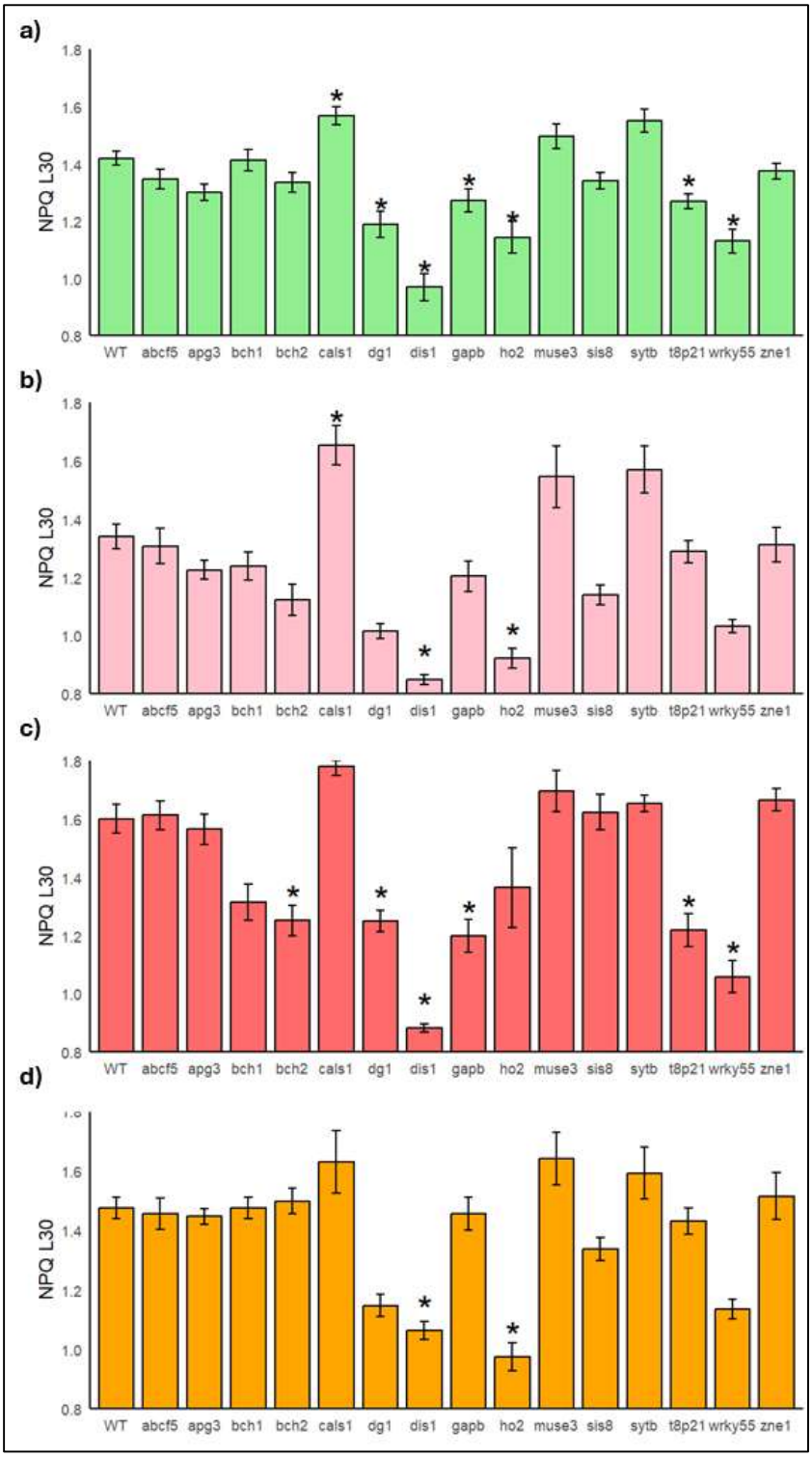

*Figure 4.16: NPQ of T-DNA insertion mutants and WT (Col-0) of same treatment groups at stable light level L15. T-DNA insertion mutants of A. thaliana genotypes and Col-0 (WT) a) in control conditions b) after prior exposure at 32°C for three days c) after prior exposure at 32°C for five days and d) subsequent three days recovery. * denotes significant difference (P<0.05) to the WT of the same treatment. Error bars indicate SEM.*

In WT ecotype heat stress of five days and subsequent three days recovery had no effect on the NPQ at L15 and L30 (**Figure 4.15, Figure 4.16**).

In control conditions, mutants *Dg1* (-0.08 L15 NPQ, -0.23 L30 NPQ), *Gapb* (-0.13 L15 NPQ, -0.15 L30 NPQ), *Ho2* (-0.12 L15 NPQ, -0.28 L30 NPQ), *T8p21* (-0.06 L15 NPQ, -0.15 Max NPQ), *Wrky55* (-0.12 L15 NPQ, -0.29 L30 NPQ) and *Dis1* (-0.14 L15 NPQ, -0.45 L30 NPQ) showed to have a significantly lower L15 NPQ (**Figure 4.15**) and L30 NPQ (**Figure 4.16**) than the WT under control conditions.

The mutants *Bch1* (-0.09 L15 NPQ, -0.1 L30 NPQ), *Dg1* (-0.13 L15 NPQ, -0.32 Max NPQ), *Ho2* (-0.15 L15 NPQ, -0.42 L30 NPQ), *T8p21* (-0.1 L15 NPQ, -0.05 Max NPQ), *Wrky55* (-0.12 L15 NPQ, -0.31 L30 NPQ) and *Dis1* (-0.18 L15 NPQ, -0.49 L30 NPQ) also showed a significantly lower L15 and L30 NPQ than the WT during three days in heat whereas *Cals1*(+0.08 L15 NPQ, +0.31 L30 NPQ) and *Sytb* (+0.09 L15 NPQ, +0.23 L30 NPQ) showed significantly higher L15 and L30 NPQ in comparison to the WT (**Figure 4.15, Figure 4.16**).

The mutants *Bch1* (-0.1 L15 NPQ, -0.29 Max NPQ), *Dg1* (-0.17 L15 NPQ, -0.35 Max NPQ), *Ho2* (-0.16 L15 NPQ, -0.24 Max NPQ), *T8p21* (-0.11 L15 NPQ, -0.38 Max NPQ), *Wrky55* (-0.121 L15 NPQ, -0.54 Max NPQ) and *Dis1* (-0.18 L15 NPQ, -0.72 Max NPQ) also showed significantly lower L15 and L30 NPQ during five days in heat compared to the WT. *Gapb* indicated a lower L15 NPQ (-0.13) after five days in heat however no significant difference to the WT in L30 NPQ (**Figure 4.15, Figure 4.16**).

After three days recovery from heat, *T8p21* (-0.1 L15 NPQ, -0.04, *Wrky55* (-0.1 L15 NPQ, -0.34 Max NPQ), and *Sis8* (-0.08 L15 NPQ, -0.14 Max NPQ) all had lower Maximum and L15 NPQs than the WT. *Gapb* was the only mutant to display an increased L15 NPQ (+0.12) to the WT after three days recovery (**Figure 4.15, Figure 4.16)**.

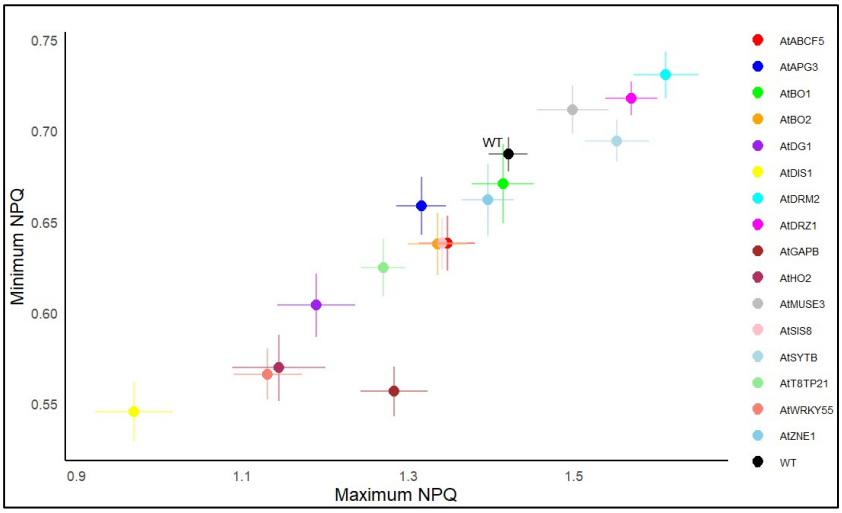

Figure 4.17: Shows maximum and L15 NPQ in 15 T-DNA insertion lines of A. thaliana and Col-0 (WT) in control conditions. Error bars denote SEM.

Figure 4.17 shows the relationship between maximum and L15 NPQ under control conditions, which shows a strong positive relationship. WT is seen to be 5th highest among the mutants in both average L15 and L30 NPQ. *Gapb* stands out among other mutants due to having one of the lowest L15 NPQs but having a slightly higher L30 NPQ in comparison to other genotypes (**Figure 4.17**)

Induction and relaxation of NPQ

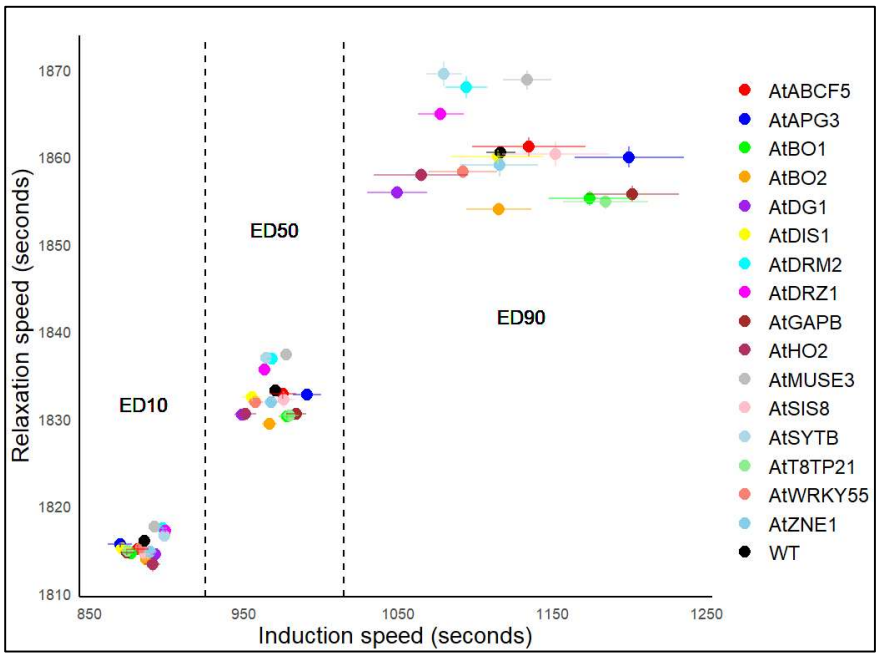

Figure 4.18: Time taken to reach Induction and time taken to reach Relaxation to 10% (ED10), 50% (ED50) and 90% (ED90) of NPQ L30 in 15 T-DNA insertion lines of A. thaliana and Col-0 (WT) in control conditions. Error bars denote SEM.

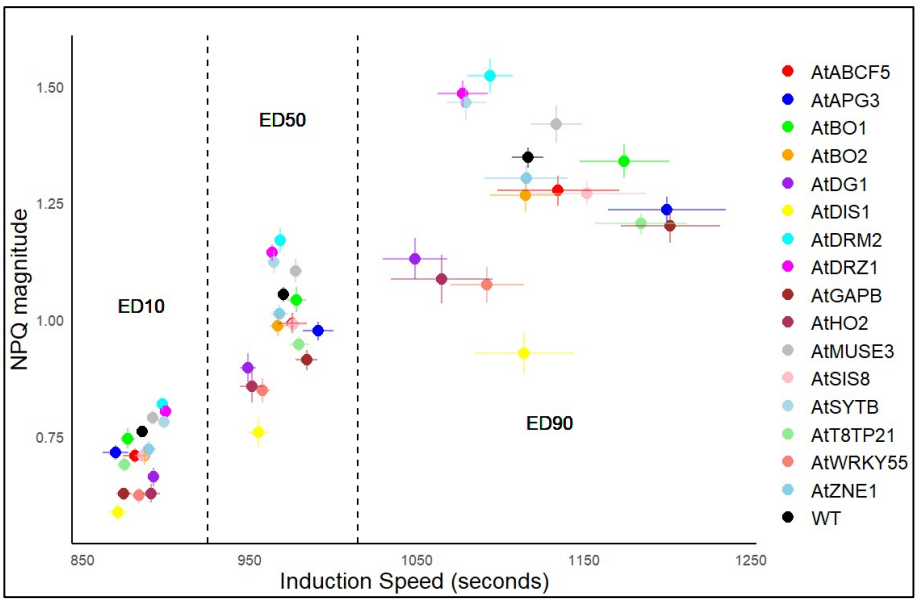

Figure 4.19: NPQ and time of Induction at 10% (ED10), 50% (ED50) and 90% (ED90) of NPQ L30 in 15 T-DNA insertion lines of A. thaliana and Col-0 (WT) in control conditions. Error bars denote SEM.

While the variation in time to reach ED10 and ED50 was similar between all tested genoytpes, there was a larger variation in time taken to reach ED90 (**Figure 4.19**). Variation in magnitude generally increased overtime, with some overlap between

mutants with high NPQ at ED10 and low NPQ at ED50, and mutants with high NPQ at ED50 and low NPQ at ED90.

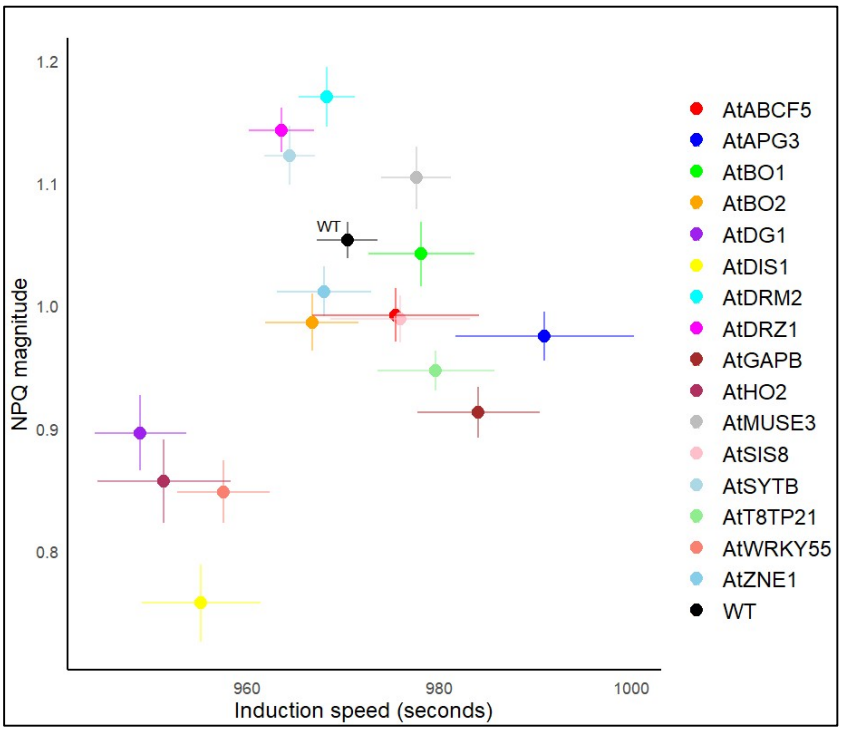

Figure 4.20: Magnitude of NPQ and time to reach Induction at 50% (ED50) of total NPQ in 15 T-DNA insertion lines of A. thaliana and Col-0 (WT). Error bars denote SEM.

Table 4.4: : Induction of NPQ to 50% of L30 NPQ

	Control			3 day heat treatment			5 day heat treatment			3 days recovery		
Genotype	Mean	SEM	Sig.	Mean	SEM	Sig.	Mean	SEM	Sig.	Mean	SEM	Sig.
WT	970.42 ±	3.12		991.67 ±	5.67		1016.8 ±	6.98		991.57 ±	5.74	
Zne1	968.02 ±	4.88		969.76 ±	11.1		1080.6 ±	12.4	*	968.21 ±	5.59	
Wrky55	957.54 ±	4.82		949.93 ±	7.29		959.47 ±	3.16		957.54 ±	5.39	
T8tp21	979.64 ±	6.09		963.11 ±	4.36		1004.3 ±	16.9		1013 ±	17	
Sytb	964.4 ±	2.66		1032.5 ±	5.81		1033.6 ±	8.41		994.16 ±	3.41	
Sis8	975.95 ±	7.29		988.87 ±	11.2		1076 ±	14.8	*	986.78 ±	7.66	
Muse3	977.6 ±	3.61		1040.4 ±	4.15	*	1041.4 ±	5.36		1001 ±	5.74	
Ho2	951.35 ±	6.96		932.46 ±	4.24		941.23 ±	1.04	*	940.24 ±	4.05	
Gapb	984.09 ±	6.36		963.09 ±	4.6		1042.7 ±	33.6		1006 ±	16.3	
Cals1	963.57 ±	3.43		1023.4 ±	6.03		1024.9 ±	4.87		1002.5 ±	6.12	
Dis1	955.22 ±	6.22		937.52 ±	3.04		965.28 ±	5.81		956.76 ±	1.92	
Dg1	948.88 ±	4.77		946.59 ±	4.38		952.81 ±	5.27	*	945.19 ±	3.16	
Bch2	966.74 ±	4.9		974.22 ±	4.52		1055.3 ±	38.5		1019.5 ±	17.1	
Bch1	978.14 ±	5.53		969.93 ±	7.03		1059.4 ±	31.8		1035.9 ±	19.6	
Apg3	990.98 ±	9.32		981.35 ±	12.3		1074.7 ±	14.7	*	986.05 ±	7.78	
Abcf5	975.45 ±	8.65		961.16 ±	8.2		1066.5 ±	13	*	966.87 ±	4.96	

*Table 4.4: Induction (seconds) of NPQ to 50% of L30 NPQ (ED50) in T-DNA insertion lines and WT (Col-0). *s indicate significant differences to WT (Col-0) in the same treatment group (P<0.05).*

No differences were seen in induction time taken to reach 50% (ED50) of L30 NPQ between mutants and WT in different treatment groups. After three days in heat treatment, *Muse3* showed a significantly slower induction rate than WT (+48.73 seconds), however no significant differences were seen after five days in heat treatment (**Table 4.4**). *Zne1* (+63.8 seconds), *Sis8* (+59.2 seconds), *Apg3* (+57.9 seconds), *Abcf5* (+49.7 seconds) took longer to reach ED50 after five days heat treatment than seen in WT, whereas *Ho2* (-75.4 seconds) and *Dg1* (-64.0 seconds) were quicker to reach ED50 (**Table 4.4**).

Table 4.5: magnitude of NPQ at 50% of L30 NPQ

Genotype	Control-ED50			3 days heat- ED50			5 days heat- ED50			3 days recovery		
	Mean	SEM	Sig.	Mean	SEM	Sig.	Mean	SEM	Sig.	Mean	SEM	Sig.
WT	1.054 ±	0.015		1.011 ±	0.028		1.165 ±	0.033		1.088 ±	0.023	
Zne1	1.012 ±	0.020		0.990 ±	0.038		1.204 ±	0.027		1.073 ±	0.046	
Wrky55	0.848 ±	0.026	*	0.796 ±	0.022		0.789 ±	0.022	*	0.869 ±	0.023	
T8p21	0.947 ±	0.016	*	0.934 ±	0.019		0.918 ±	0.036	*	1.018 ±	0.028	
Sytb	1.123 ±	0.024		1.172 ±	0.056		1.192 ±	0.017		1.149 ±	0.053	
Sis8	0.989 ±	0.019		0.887 ±	0.019		1.176 ±	0.041		0.977 ±	0.020	
Muse3	1.104 ±	0.026		1.144 ±	0.070		1.223 ±	0.045		1.181 ±	0.058	
Ho2	0.857 ±	0.034	*	0.724 ±	0.027	*	0.967 ±	0.063		0.803 ±	0.031	*
Gapb	0.913 ±	0.021	*	0.902 ±	0.033		0.900 ±	0.031	*	1.136 ±	0.039	
Cals1	1.143 ±	0.018		1.207 ±	0.046	*	1.280 ±	0.023		1.170 ±	0.064	
Dis1	0.758 ±	0.031	*	0.673 ±	0.013	*	0.716 ±	0.007	*	0.849 ±	0.022	
Dg1	0.896 ±	0.031	*	0.784 ±	0.015		0.906 ±	0.020		0.904 ±	0.022	
Bch2	0.987 ±	0.023		0.840 ±	0.033		0.920 ±	0.033	*	1.080 ±	0.025	
Bch1	1.042 ±	0.026		0.915 ±	0.035		0.972 ±	0.041		1.067 ±	0.028	
Apg3	0.975 ±	0.020		0.943 ±	0.020		1.143 ±	0.035		1.035 ±	0.010	
Abcf5	0.992 ±	0.022		0.980 ±	0.030		1.160 ±	0.031		1.050 ±	0.028	

*Table 4.5: Magnitude of NPQ (F_m–F_m')/F_m') at 50% of L30 NPQ (ED50) in T-DNA insertion lines and WT (Col-0). *s indicate significant differences to WT (Col-0) in the same treatment group (P<0.05).*

Table 4.5 shows NPQ values of T-DNA insertion mutants at ED50. In control conditions, at ED50, mutants *Wrky55* (-0.205), *T8p21* (-0.107), and *Dis1* (-0.296) exhibited significantly lower NPQ values than the WT. *Ho2* and *Gapb* had a much lower NPQ than the WT, with NPQ values of 0.857 and 0.913 lower respectively. Notably, *Dis1* exhibited a considerable decrease in NPQ, with a change of -0.296, indicating heightened sensitivity to heat stress. Additionally, several mutants did not show significant differences in magnitude of NPQ compared to WT.

After three days heat stress, the magnitude of NPQ in mutants at ED50 was significantly lower than the WT in *Ho2* (-0.287) and *Dis1* (-0.338), and significantly higher in the *Cals1* mutant by 0.196. After five days heat, *Wrky55* (-0.376), *T8p21* (-0.247), *Gapb* (-0.265), *Dis1* (-0.449), and *Bch2* (-0.245) showed a significantly lower magnitude of NPQ to the WT, however after three days subsequent recovery, *Ho2* was the only mutant to have a lower NPQ than the WT by -0.285.

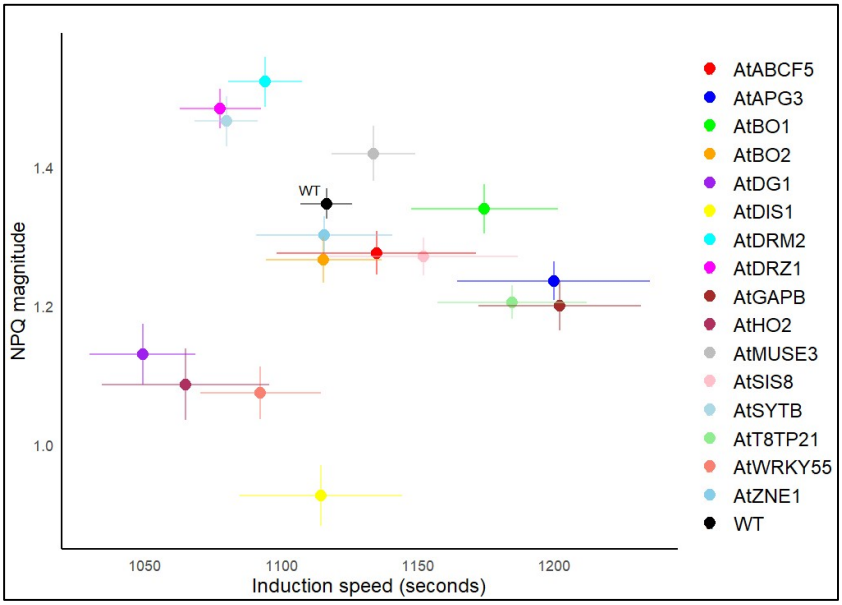

Figure 4.21: Showing Magnitude of NPQ (F_m–F_m')/F_m') and Speed of Induction at 90% (ED90) of total NPQ in 15 T-DNA insertion lines of A. thaliana and Col-0 (WT). Error bars denote SEM.

Figure 4.21 shows the spread of average magnitude of NPQ at ED90 and time to reach ED90 in the control group. Induction speed varied from 1049.2 to 1202 and magnitude of NPQ varied from 0.93 to 1.52.

Table 4.6: Induction of NPQ to 90% of L30 NPQ

	Control			3 day heat treatment			5 day heat treatment			3 days recovery		
Genotype	Mean	SEM	Sig.	Mean	SEM	Sig.	Mean	SEM	Sig.	Mean	SEM	Sig.
WT	1116.5 ±	9.43		1199.8 ±	22.1		1307.9 ±	27.9		1219.6 ±	25.1	
Zne1	1115.7 ±	24.9		1118.4 ±	47.1		1535.8 ±	49.4	*	1116.2 ±	26.3	
AtWRKY55	1092.3 ±	22.1		1053 ±	31		1101.7 ±	23.6		1097.2 ±	31.9	
AtT8P21	1184.5 ±	27.4		1079.5 ±	19		1293 ±	82		1297.7 ±	72.3	
Sytb	1079.8 ±	11.7		1343.4 ±	16.8		1361.5 ±	30.2		1217 ±	15.4	
Sis8	1152.2 ±	34.6		1190.9 ±	44.5		1528.7 ±	57.1	*	1192.3 ±	32.1	
Muse3	1133.7 ±	15.5		1387.6 ±	16		1414.6 ±	25		1245.7 ±	27.4	
Ho2	1064.9 ±	30.6		987.3 ±	13.2		991 ±	5.16	*	1041.2 ±	20	
Gapb	1202 ±	29.8		1074.1 ±	18.5		1410.3 ±	139		1266.9 ±	67.4	
Cals1	1077.6 ±	14.8		1304.2 ±	20		1335.6 ±	15.3		1250.2 ±	31.7	
Dis1	1114.6 ±	29.8		1004.8 ±	10		1176.4 ±	35.4		1106.6 ±	16.3	
Dg1	1049.2 ±	19.4		1025.2 ±	15.2		1045.5 ±	27		1020.6 ±	11.7	
Bch2	1115.4 ±	21.2		1137.4 ±	24.8		1487.7 ±	174		1332.3 ±	72.9	
Bch1	1174.4 ±	26.9		1118.3 ±	30.9		1488.9 ±	138		1418.9 ±	92	
Apg3	1199.7 ±	35.3		1166.6 ±	52.2		1553 ±	60.5	*	1197.8 ±	37.7	
Abcf5	1134.8 ±	36.5		1081.5 ±	35.3		1483 ±	51.3		1107.5 ±	22.9	

*Table 4.6: Induction (seconds) to 90% of L30 NPQ (ED90) in T-DNA insertion lines and WT (Col-0). *s indicate significant differences to WT (Col-0) in the same treatment group (P<0.05).*

No differences between mutants and WT in time of induction to ED90 were observed in control groups, three days in heat treatment or after three days recovery from heat **(Table 4.6)**. The only significant differences from the WT were seen in *Zne1* (+227.9 seconds), *Apg3* (+245.1 seconds) and *Sis8* (+220.8 seconds) which showed to have a significantly slower induction speed, and *Ho2* (-396.9 seconds) which had a significantly faster speed **(Table 4.6)**.

Table 4.7: Magnitude of NPQ at 90% of L30 NPQ

Genotype	Control – ED90			3 days heat -ED90			5 days heat -ED90			3 days recovery-ED90		
	Mean	SEM	Sig.	Mean	SEM	Sig.	Mean	SEM	Sig.	Mean	SEM	Sig.
WT	1.276 ±	0.031		1.242 ±	0.054		1.523 ±	0.045		1.374 ±	0.048	
Zne1	1.236 ±	0.027		1.169 ±	0.030		1.481 ±	0.049		1.364 ±	0.024	
Wrky55	1.339 ±	0.035		1.173 ±	0.045		1.246 ±	0.058		1.393 ±	0.035	
T8p21	1.266 ±	0.033		1.067 ±	0.049		1.185 ±	0.049	*	1.414 ±	0.039	
Sytb	1.130 ±	0.044	*	0.970 ±	0.023		1.181 ±	0.033		1.098 ±	0.034	
Sis8	0.927 ±	0.044	*	0.814 ±	0.017	*	0.849 ±	0.013	*	1.021 ±	0.028	
Muse3	1.522 ±	0.036	*	1.524 ±	0.080		1.597 ±	0.037		1.509 ±	0.091	
Ho2	1.484 ±	0.029		1.564 ±	0.063	*	1.681 ±	0.030		1.537 ±	0.097	
Gapb	1.200 ±	0.036	*	1.143 ±	0.048		1.139 ±	0.051	*	1.392 ±	0.051	
Cals1	1.087 ±	0.052	*	0.882 ±	0.033	*	1.285 ±	0.122		0.940 ±	0.044	*
Dis1	1.270 ±	0.027		1.089 ±	0.031		1.535 ±	0.056		1.264 ±	0.035	
Dg1	1.465 ±	0.036		1.491 ±	0.074		1.562 ±	0.027		1.504 ±	0.080	
Bch2	1.205 ±	0.024		1.218 ±	0.034		1.159 ±	0.053	*	1.349 ±	0.041	
Bch1	1.074 ±	0.038	*	0.985 ±	0.021		1.005 ±	0.049	*	1.082 ±	0.031	
Apg3	1.302 ±	0.026		1.247 ±	0.056		1.574 ±	0.036		1.426 ±	0.072	
Abcf5	1.347 ±	0.022		1.275 ±	0.039		1.514 ±	0.046		1.398 ±	0.034	

*Table 4.7: Magnitude of NPQ (F_m–F_m')/F_m') at 90% of L30 NPQ (ED90) in T-DNA insertion lines and WT (Col-0). *s indicate significant differences to WT (Col-0) in the same treatment group (P<0.05).*

Table 4.7 shows the magnitude of NPQ at ED90 as seen in **Figure 4.22**. In control conditions, mutants *Sytb* (-0.146), *Sis8* (-0.412), *Gapb* (-0.076), *Cals1* (-0.189) and *Bch1* (-0.202), all showed a lower magnitude of NPQ compared to the WT, whereas *Muse3* showed an increase in NPQ by 0.246. After three days of heat stress, only *Sis8* (-0.428) and *Cals1* (-0.338) had a significantly lower NPQ than the WT, and *Ho2* was seen to have a significantly higher NPQ by 0.322. After five days heat stress, five of the mutants showed a significantly lower magnitude of NPQ compared to the WT: *T8p21* (-0.337), *Sis8* (-0.674), *Gapb* (-0.383), *Bch2* (-0.364), and *Bch1* (-0.518), whereas after subsequent three days recovery, only *Cals1* (-0.435) had a significantly lower NPQ than WT.

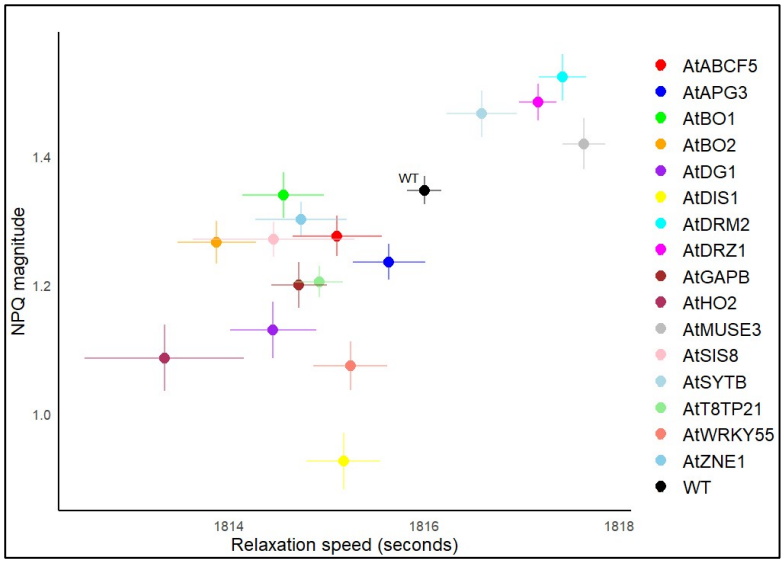

Figure 4.22: Showing NPQ and time to Induction at 10% (ED10) of total NPQ in 15 T-DNA insertion lines of A. thaliana and Col-0 (WT) in control conditions. Error bars denote SEM.

Figure 4.22 shows the spread of average magnitude of NPQ at ED10 and time to reach ED10 in the control group. Induction speed varied from 869.90 to 899.48 and magnitude of NPQ varied from 0.59 to 0.82.

Table 4.8: Induction of NPQ to 10% of L30 NPQ

	Control			3 day heat treatment			5 day heat treatment			3 days recovery		
Genotype	Mean	SEM	Sig.	Mean	SEM	Sig.	Mean	SEM	Sig.	Mean	SEM	Sig.
WT	885.75 ±	2.34		882.30 ±	2.55		870.65 ±	2.73		873.61 ±	2.70	
Zne1	889.48 ±	4.46		889.89 ±	7.37		866.72 ±	2.63		886.30 ±	4.81	
Wrky55	883.77 ±	4.48		891.01 ±	5.49		879.67 ±	8.24		879.71 ±	8.09	
T8p21	874.89 ±	4.17		896.59 ±	3.33		864.72 ±	10.15		875.56 ±	7.44	
Sytb	898.88 ±	2.65		873.48 ±	4.73		868.37 ±	3.87		874.54 ±	2.91	
Sis8	886.16 ±	4.86		883.00 ±	4.83		864.05 ±	1.86		877.25 ±	4.54	
Muse3	891.99 ±	2.53		866.51 ±	3.88		857.65 ±	4.13		872.46 ±	3.97	
Ho2	891.05 ±	5.09		899.38 ±	1.73		910.93 ±	3.63		882.13 ±	10.25	
Gapb	874.60 ±	4.57		899.53 ±	3.36		880.22 ±	9.03		877.70 ±	6.66	
Cals1	899.48 ±	2.46		877.45 ±	1.90		866.08 ±	1.51		873.36 ±	5.39	
Dis1	871.31 ±	5.77		897.19 ±	1.26		852.84 ±	8.73		872.61 ±	6.07	
Dg1	892.52 ±	3.23		900.00 ±	2.01		899.32 ±	6.28		900.31 ±	2.35	
Bch2	886.99 ±	3.03		884.16 ±	5.84		875.60 ±	9.65		866.61 ±	6.55	
Bch1	877.01 ±	4.29		888.20 ±	5.40		870.39 ±	7.44		859.18 ±	8.20	
Apg3	869.90 ±	7.74		884.97 ±	6.90		854.34 ±	3.91		874.51 ±	5.61	
Abcf5	881.26 ±	7.31		894.71 ±	6.03		867.55 ±	3.17		888.28 ±	4.34	

*Table 4.8: Induction (seconds) to 10% of L30 NPQ (ED10) in T-DNA insertion lines and WT (Col-0). *s indicate significant differences to WT (Col-0) in the same treatment group (P<0.05).*

When observing Induction times at ED10, no significant differences were observed between mutants and WT (**Table 4.8**)

Table 4.9: Magnitude of NPQ at 10% of L30 NPQ

Genotype	Control -ED10			3 days heat -ED10			5 days heat-ED10			3 days recovery-ED10		
	Mean	SEM	Sig.	Mean	SEM	Sig.	Mean	SEM	Sig.	Mean	SEM	Sig.
WT	0.760	± 0.010		0.747	± 0.019		0.815	± 0.021		0.778	± 0.014	
Zne1	0.721	± 0.018		0.732	± 0.026		0.834	± 0.021		0.719	± 0.022	
Wrky55	0.623	± 0.016	*	0.607	± 0.028		0.573	± 0.010	*	0.657	± 0.017	
T8p21	0.689	± 0.015	*	0.650	± 0.019		0.677	± 0.025		0.687	± 0.022	
Sytb	0.780	± 0.013		0.853	± 0.044		0.822	± 0.010		0.795	± 0.028	
Sis8	0.708	± 0.014		0.684	± 0.012		0.817	± 0.027		0.689	± 0.009	
Muse3	0.790	± 0.015		0.823	± 0.043		0.844	± 0.026		0.812	± 0.035	
Ho2	0.627	± 0.020	*	0.566	± 0.022	*	0.648	± 0.018		0.666	± 0.018	
Gapb	0.626	± 0.013	*	0.660	± 0.025		0.661	± 0.018	*	0.879	± 0.040	
Cals1	0.803	± 0.010		0.849	± 0.029		0.878	± 0.017		0.804	± 0.032	
Dis1	0.588	± 0.019	*	0.533	± 0.010	*	0.582	± 0.007	*	0.677	± 0.018	
Dg1	0.663	± 0.020	*	0.598	± 0.009		0.631	± 0.018	*	0.710	± 0.012	
Bch2	0.707	± 0.018		0.613	± 0.022		0.654	± 0.023	*	0.747	± 0.019	
Bch1	0.745	± 0.022		0.657	± 0.026		0.698	± 0.029		0.740	± 0.028	
Apg3	0.715	± 0.016		0.717	± 0.019		0.805	± 0.023		0.705	± 0.011	
Abcf5	0.709	± 0.016		0.717	± 0.012		0.798	± 0.020		0.726	± 0.013	

Table 4.9: Magnitude of NPQ (Fm–Fm')/Fm') at 10% of L30 NPQ (ED10) in T-DNA insertion lines and WT (Col-0). *s indicate significant differences to WT (Col-0) in the same treatment group (P<0.05).

Table 4.9 presents significant changes in NPQ magnitude at ED10 for various mutant genotypes compared to the WT control seen in **Figure 4.22** In control conditions, at ED10, *Wrky55* exhibited a lower NPQ of -0.138 from the WT, while *T8p21* showed a decrease of -0.071. Both *Ho2* and *Gapb* had lower NPQ of -0.133 and -0.134, respectively, compared to the WT (**Table 4.9, Figure 4.22** . *Dis1* had the most substantial decrease with -0.172, followed by *Dg1* with -0.098 (**Table 9, Figure 4.22**). However, *Sytb*, *Sis8*, *Muse3*, *Cals1*, *Bch2*, *Bch1*, *Apg3*, and *Abcf5* mutants showed no significant differences to the WT (**Table 4.9, Figure 4.22**).

After three days heat stress, only two mutants showed significant differences to the WT, where *Ho2* and *Dis1* showed a lower magnitude of NPQ changes of -0.022 and

0.010 respectively (**Table 4.9, Figure 4.22**). After five days of heat stress, five mutants showed a significantly lower NPQ magnitude to the WT: *Wrky55* (-0.242), *Gapb* (-0.155), *Dis1* (-0.233), *Dg1* (-0.184), and *Bch2* (-0.161) (**Table 4.9, Figure 4.22**). No mutants showed a significant difference in magnitude of NPQ compared to the WT after three days recovery from heat stress (**Table 4.9, Figure 4.22**).

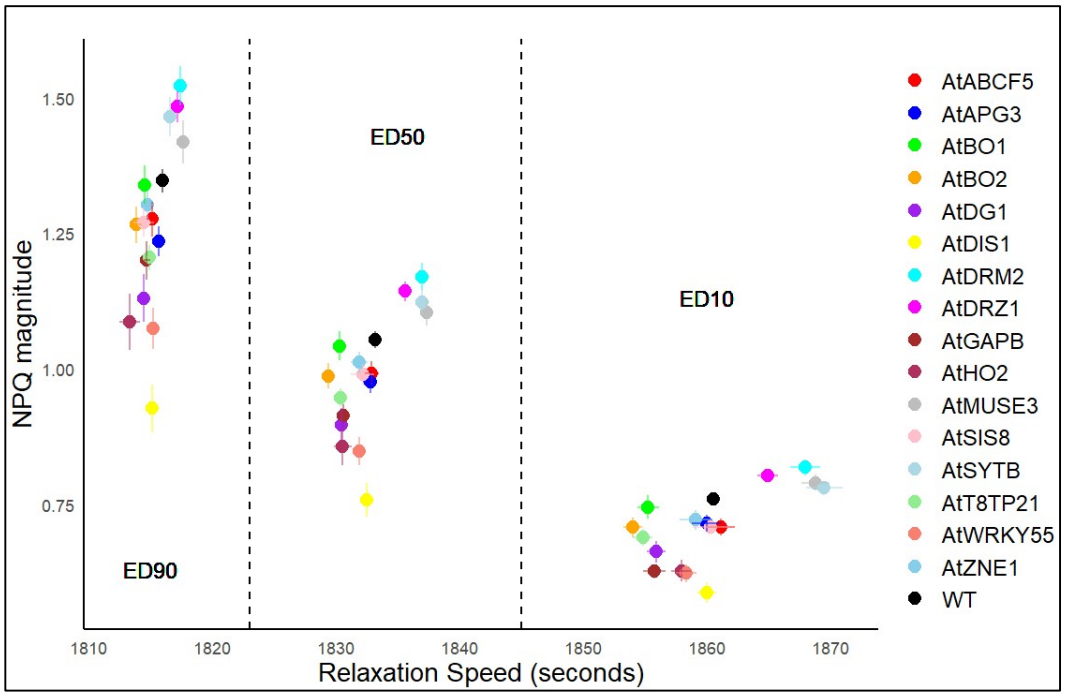

Figure 4.23: Showing Magnitude of NPQ (F_m–F_m')/F_m') and time to Relaxation at 10% (ED10), 50% (ED50) and 90% (ED90) of total NPQ in 15 T-DNA insertion lines of A. thaliana and Col-0 (WT) in control conditions. Error bars denote SEM.

Focussing on relaxation of NPQ, where time until 50% (ED50), 90% (ED90) and 10% (ED10) of L30 NPQ was measured, **Figure 4.23** depicts the spread of mean values. Variation in relaxation speed increased slightly from ED90 to ED50 and then saw a larger range of values from ED50 to ED10.

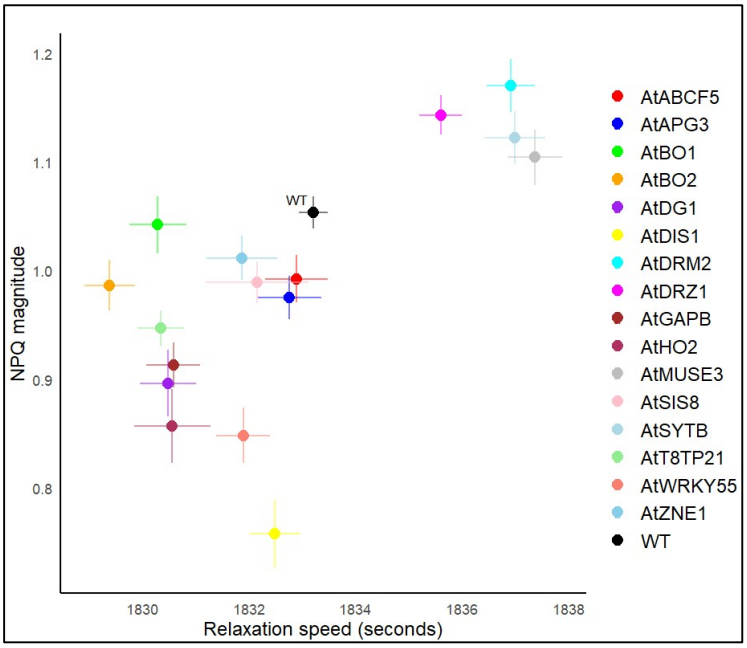

Figure 4.24: Showing magnitude of NPQ (F_m–F_m')/F_m') and time to Relaxation at 50% (ED50) of total NPQ in 15 T-DNA insertion lines of A. thaliana and Col-0 (WT) in control conditions. Error bars denote SEM.

Figure 4.24 shows the spread of average NPQ at ED50 and time to reach ED50 in the control group. Induction speed varied from 1829.4 to 1837.4 and magnitude of NPQ varied from 0.76 to 1.17.

Table 4.10: Relaxation of NPQ to 50% of L30 NPQ

	Control			3 day heat treatment			5 day heat treatment			3 day recovery		
Genotype	Mean	SEM	Sig.	Mean	SEM	Sig.	Mean	SEM	Sig.	Mean	SEM	Sig.
WT	1833.2 ±	0.27		1834.7 ±	0.5		1836.2 ±	0.7		1834.7 ±	0.46	
Zne1	1831.9 ±	0.66		1835.1 ±	0.94		1838.7 ±	1.13		1832 ±	0.79	
Wrky55	1831.9 ±	0.51		1831.5 ±	1.12		1831.8 ±	0.57		1831.9 ±	0.7	
T8p21	1830.3 ±	0.44	*	1833.2 ±	0.54		1830.7 ±	0.91	*	1831 ±	0.87	
Sytb	1837 ±	0.57	*	1839.6 ±	1.28	*	1842.9 ±	1.04	*	1837.4 ±	0.74	
Sis8	1832.2 ±	0.96		1835.5 ±	0.82		1839.2 ±	0.83		1833.7 ±	0.85	
Muse3	1837.4 ±	0.52	*	1838.2 ±	0.79		1844.8 ±	1.66	*	1836.3 ±	0.6	
Ho2	1830.6 ±	0.72		1828.6 ±	0.8	*	1828.3 ±	0.93	*	1828.3 ±	0.57	
Gapb	1830.6 ±	0.51	*	1833.3 ±	0.87		1833.7 ±	2.04		1833.7 ±	0.68	
Cals1	1835.6 ±	0.4	*	1839.1 ±	0.61	*	1841.4 ±	0.27	*	1836.4 ±	0.75	
Dis1	1832.5 ±	0.48		1830.9 ±	0.64		1831.6 ±	0.8		1829.2 ±	0.73	
Dg1	1830.5 ±	0.53		1828.9 ±	0.81	*	1830.6 ±	0.59	*	1829.1 ±	0.77	
Bch2	1829.4 ±	0.48	*	1831 ±	0.85		1831.8 ±	0.87		1832 ±	1.13	
Bch1	1830.3 ±	0.54	*	1833 ±	0.72		1833.6 ±	1.27		1832 ±	0.96	
Apg3	1832.8 ±	0.6		1833.4 ±	0.95		1837.5 ±	1.18		1833.5 ±	0.77	
Abcf5	1832.9 ±	0.59		1832.8 ±	0.95		1841.1 ±	0.72	*	1833.5 ±	0.61	

*Table 4.10: Relaxation (seconds) to 50% of L30 NPQ (ED50) in T-DNA insertion lines and WT (Col-0). *s indicate significant differences to WT (Col-0) in the same treatment group (P<0.05).*

Focusing on relaxation speed to reach ED50, there were many significant differences between mutants and WT. In control conditions, *T8p21* (-2.9 seconds), *Gapb* (-2.6 seconds), *Bch2* (-3.8 seconds) and *Bch1* (-2.9 seconds) all showed significantly faster rates of induction than the WT, whereas *Sytb* (+3.8 seconds), *Cals1*(+2.4 seconds) and *Muse3* (+4.2 seconds) all showed significantly slower relaxation of NPQ **(Table 4.10)**.After three days of heat treatment, *Sytb* (+4.9 seconds), *Cals1* (+4.4 seconds) compared to WT had significantly slower relaxation time to ED50, whereas *Ho2* (-6.1 seconds) and *Dg1* (-5.8 seconds) were significantly faster **(Table 4.10)**.

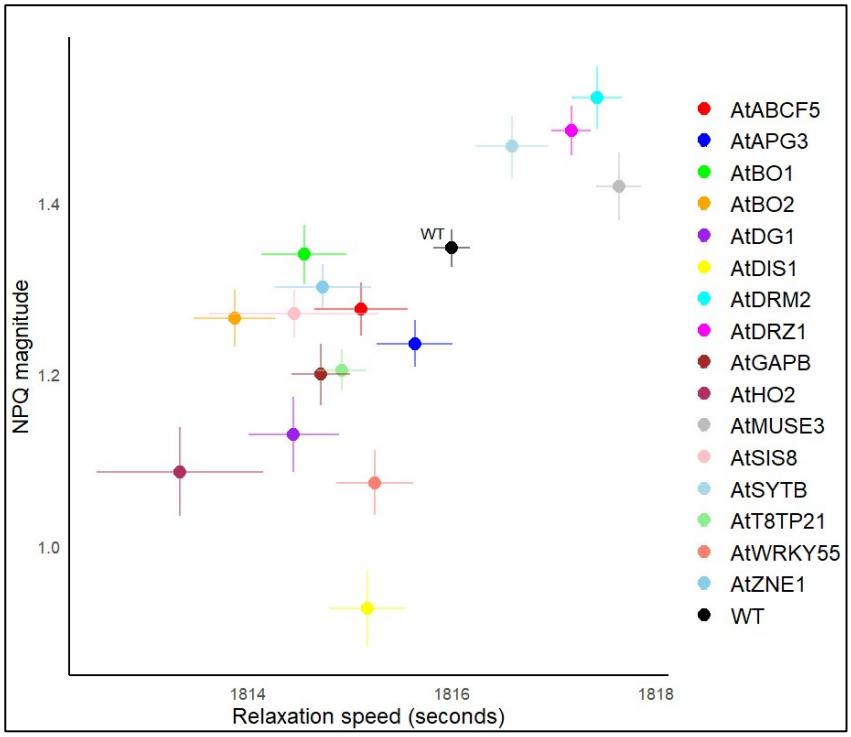

Figure 4.25: Showing magnitude of NPQ (Fm–Fm')/Fm') and time to Relaxation at 10% (ED10) of total NPQ in 15 T-DNA insertion lines of A. thaliana and Col-0 (WT) in control conditions. Error bars denote SEM.

Figure 4.25 shows the spread of average magnitude of NPQ at ED10 and time to reach ED10 in the control group. Induction speed varied from 1853.98 to 1869.49 and magnitude of NPQ varied from 0.59 to 0.82.

Table 4.11: Relaxation of NPQ to 10% of L30 NPQ

	Control			3 day heat treatment			5 day heat treatment			3 day recovery		
Genotype	Mean	SEM	Sig.	Mean	SEM	Sig.	Mean	SEM	Sig.	Mean	SEM	Sig.
WT	1860.53 ±	0.52		1863.07 ±	0.97		1865.84 ±	1.43		1862.45 ±	0.87	
Zne1	1859.09 ±	1.32		1864.78 ±	1.87		1870.48 ±	2.44		1858.07 ±	1.51	
Wrky55	1858.32 ±	0.83		1857.64 ±	2.03		1857.49 ±	1.13		1857.71 ±	1.25	
T8p21	1854.82 ±	0.80		1860.36 ±	1.14		1855.72 ±	1.51		1855.11 ±	1.49	
Sytb	1869.49 ±	1.44		1872.93 ±	3.12		1880.35 ±	2.51		1868.36 ±	1.36	
Sis8	1860.28 ±	1.45		1865.51 ±	1.32		1870.82 ±	1.81		1860.81 ±	1.56	
Muse3	1868.78 ±	1.11	*	1869.47 ±	1.66		1885.54 ±	4.55		1865.88 ±	1.33	
Ho2	1857.90 ±	0.77	*	1852.80 ±	1.29		1855.93 ±	0.94	*	1855.73 ±	2.58	
Gapb	1855.75 ±	0.93		1862.08 ±	1.55		1863.11 ±	2.87		1859.70 ±	1.14	
Cals1	1864.91 ±	0.80		1871.49 ±	1.34		1876.69 ±	0.88		1865.68 ±	1.53	
Dis1	1859.99 ±	0.78		1858.10 ±	1.14		1858.25 ±	1.28		1854.73 ±	1.41	
Dg1	1855.91 ±	0.77		1853.43 ±	1.24		1855.41 ±	0.93		1852.98 ±	1.29	
Bch2	1853.98 ±	0.75	*	1856.69 ±	1.48		1857.52 ±	1.51		1857.25 ±	2.06	
Bch1	1855.24 ±	0.85		1861.28 ±	1.25		1860.65 ±	1.93		1856.89 ±	1.70	
Apg3	1859.97 ±	1.18		1860.64 ±	1.85		1867.84 ±	2.40		1859.85 ±	1.66	
Abcf5	1861.16 ±	1.11		1863.07 ±	1.41		1875.42 ±	1.85		1861.08 ±	1.30	

*Table 4.11: Relaxation (seconds) to 10% of L30 NPQ (ED10) in T-DNA insertion lines and WT (Col-0). *s indicate significant differences to WT (Col-0) in the same treatment group (P<0.05).*

Time taken for NPQ to relax to ED10 was significantly slower in *Muse3* (+8.25) and significantly faster in *Ho2* (-2.63 seconds) and *Bch2* (-6.55 seconds) in comparison to WT **(Table 4.11).** After three days of heat stress, none of the mutants showed significant differences to the WT, but after five days heat stress *Ho2* (-9.91 seconds) had a significantly faster relaxation to ED10 **(Table 4.11).** None of the mutants showed significant differences to the WT after three days recovery from heat stress **(Table 4.11)**.

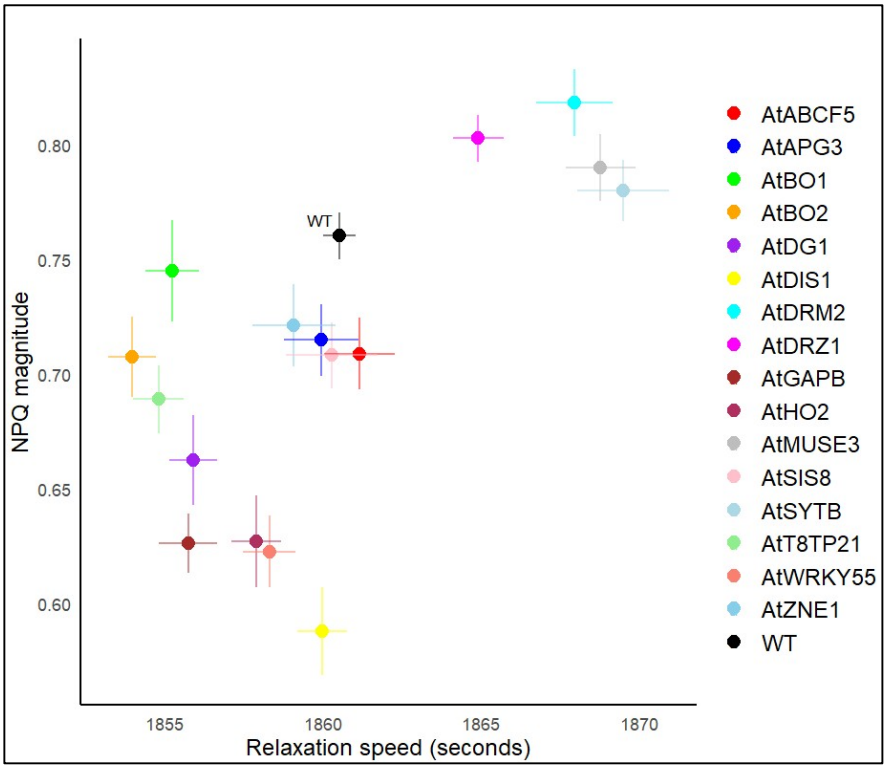

Figure 4.26: Showing magnitude of NPQ (F_m–F_m')/F_m') and time of Relaxation at 90% (ED90) of total NPQ in 15 T-DNA insertion lines of A. thaliana and Col-0 (WT) in control conditions. Error bars denote SEM.

Figure 4.26 shows the spread of average values of ED90 and time to reach ED90 in the control group. Induction speed varied from 1813.9 to 1817.6 and magnitude of NPQ varied from 0.93 to 1.52.

Table 4.12: Relaxation of NPQ to 90% of L30 NPQ

	Control			3 day heat treatment			5 day heat treatment			3 days recovery		
Genotype	Mean	SEM	Sig.	Mean	SEM	Sig.	Mean	SEM	Sig.	Mean	SEM	Sig.
WT	1816 ±	0.18		1816.9 ±	0.27		1817.6 ±	0.28		1817.2 ±	0.23	
Zne1	1814.7 ±	0.47		1816.4 ±	0.6		1818.8 ±	0.39		1815.6 ±	0.4	
Wrky55	1815.2 ±	0.38		1815 ±	0.66		1815.6 ±	0.42		1815.6 ±	0.46	
T8p21	1814.9 ±	0.24		1816.2 ±	0.27		1815 ±	0.62		1815.8 ±	0.51	
Sytb	1816.6 ±	0.36		1818.7 ±	0.65		1819.4 ±	0.21		1817.9 ±	0.4	
Sis8	1814.5 ±	0.83		1816.6 ±	0.55		1819.3 ±	0.32		1816.7 ±	0.46	
Muse3	1817.6 ±	0.22	*	1818.6 ±	0.29		1819.3 ±	0.24		1817.7 ±	0.19	
Ho2	1813.3 ±	0.82	*	1813.3 ±	0.61		1811 ±	1.2	*	1811.1 ±	1.08	
Gapb	1814.7 ±	0.28		1815.2 ±	0.6		1815.2 ±	1.62		1817.3 ±	0.43	
Cals1	1817.2 ±	0.19		1818.8 ±	0.24		1819.3 ±	0.18		1818 ±	0.3	
Dis1	1815.2 ±	0.38		1813.8 ±	0.54		1814.8 ±	0.57		1813.2 ±	0.72	
Dg1	1814.5 ±	0.44		1813.5 ±	0.57		1815 ±	0.47		1814 ±	0.56	
Bch2	1813.9 ±	0.4	*	1814.9 ±	0.55		1815.6 ±	0.52		1816 ±	0.67	
Bch1	1814.6 ±	0.42		1815.3 ±	0.78		1816.5 ±	0.97		1816.3 ±	0.53	
Apg3	1815.6 ±	0.37		1816.2 ±	0.45		1818.4 ±	0.46		1816.9 ±	0.28	
Abcf5	1815.1 ±	0.46		1813.8 ±	1.07	*	1819.5 ±	0.21		1816.1 ±	0.29	

*Table 4.12: Relaxation (seconds) to 90% of L30 NPQ (ED90) in T-DNA insertion lines and WT (Col-0). *s indicate significant differences to WT (Col-0) in the same treatment group (P<0.05).*

Time taken for NPQ to relax to ED90 was significantly slower in *Muse3* (+1.6 seconds) and significantly faster in *Ho2* (-2.7 seconds) and *Bch2* (-2.1 seconds) in comparison to WT **(Table 4.12).** After three days of heat stress, *Abcf5* (-3.1 seconds) had a faster relaxation speed, and after five days heat stress *Ho2* (-6.6 seconds) had a significantly faster relaxation to ED90 **(Table 4.12).** None of the mutants showed significant differences to the WT after three days recovery from heat stress **(Table 4.12)**.

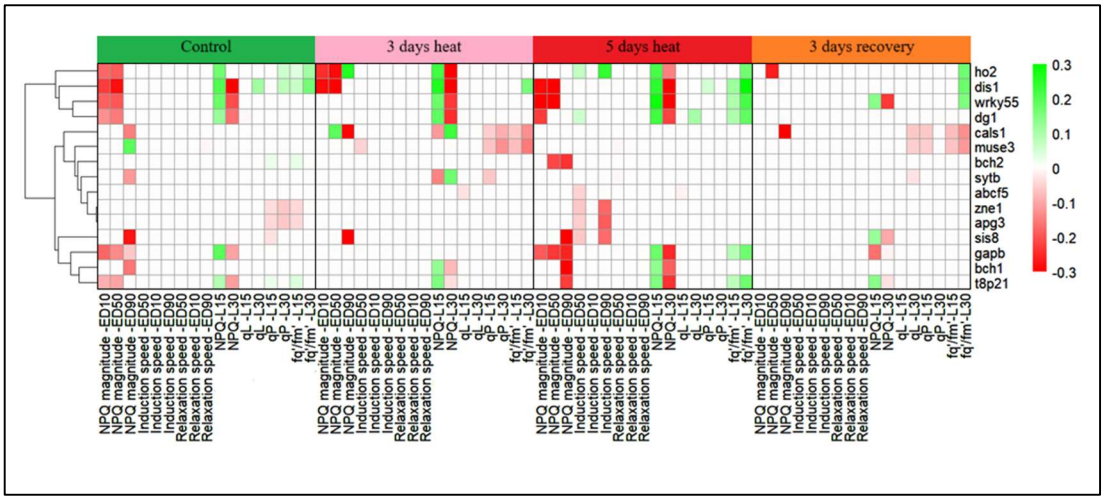

Figure 4.27. Heatmaps showing fold change in parameters between T-DNA insertion mutants and WT (Col-0) of same treatment groups. A. thaliana genotypes and Col-0 (WT) were exposed to 32°C for three days (3 days heat), five days (5 days heat) and then recovered in control conditions for three days (3 days recovery). Control represents control conditions at the same age as plants after five days heat treatment. White boxes indicate no significant differences (P<0.05). NPQ_L15 and speeds to induction and relaxation have been given inverse values so as to show beneficial phenotypic traits as positive values.

Overall, all of the mutants showed significant difference to the WT in photosynthetic parameters seen in **Figure 4.27**.

4.3.3 Changes in pigment content in selected mutants

Chlorophyll and carotenoid content of the 16 chosen T-DNA insertion lines in *A. thaliana* were assessed. Pigments were extracted from leaf samples of plants after three days and five days of 32°C heat treatment plus after three days of recovery from the five day heat stress.

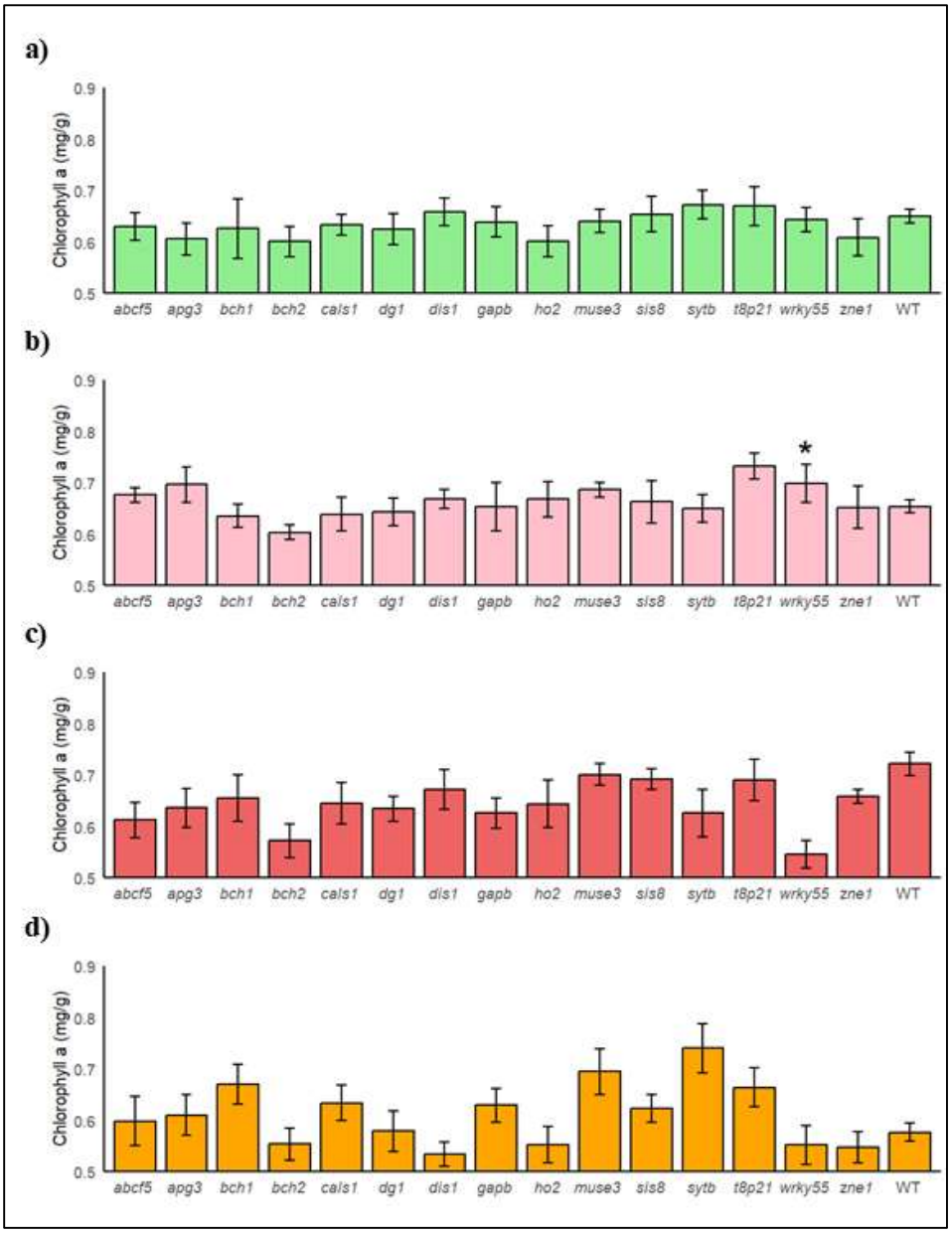

*Figure 4.28: Chlorophyll a content of T-DNA insertion mutants and WT (Col-0) of same treatment groups. T-DNA insertion mutants of A. thaliana genotypes and Col-0 (WT) a) in control conditions b) after prior exposure at 32°C for three days c) after prior exposure at 32°C for five days and d) subsequent three days recovery. * denotes significant difference (P<0.05) to the WT of the same treatment. Error bars indicate SEM.*

None of the mutants showed differences in Chlorophyll *a* content in control conditions (**Figure 4.28**). Of all the mutants, only *Wrky55* (+0.1mg/g) showed significant differences to the WT after five days heat stress (**Figure 4.28**), however no differences were seen after only three days in heat. No differences were seen between WT and the mutants after three days recovery from heat (**Figure 4.28**).

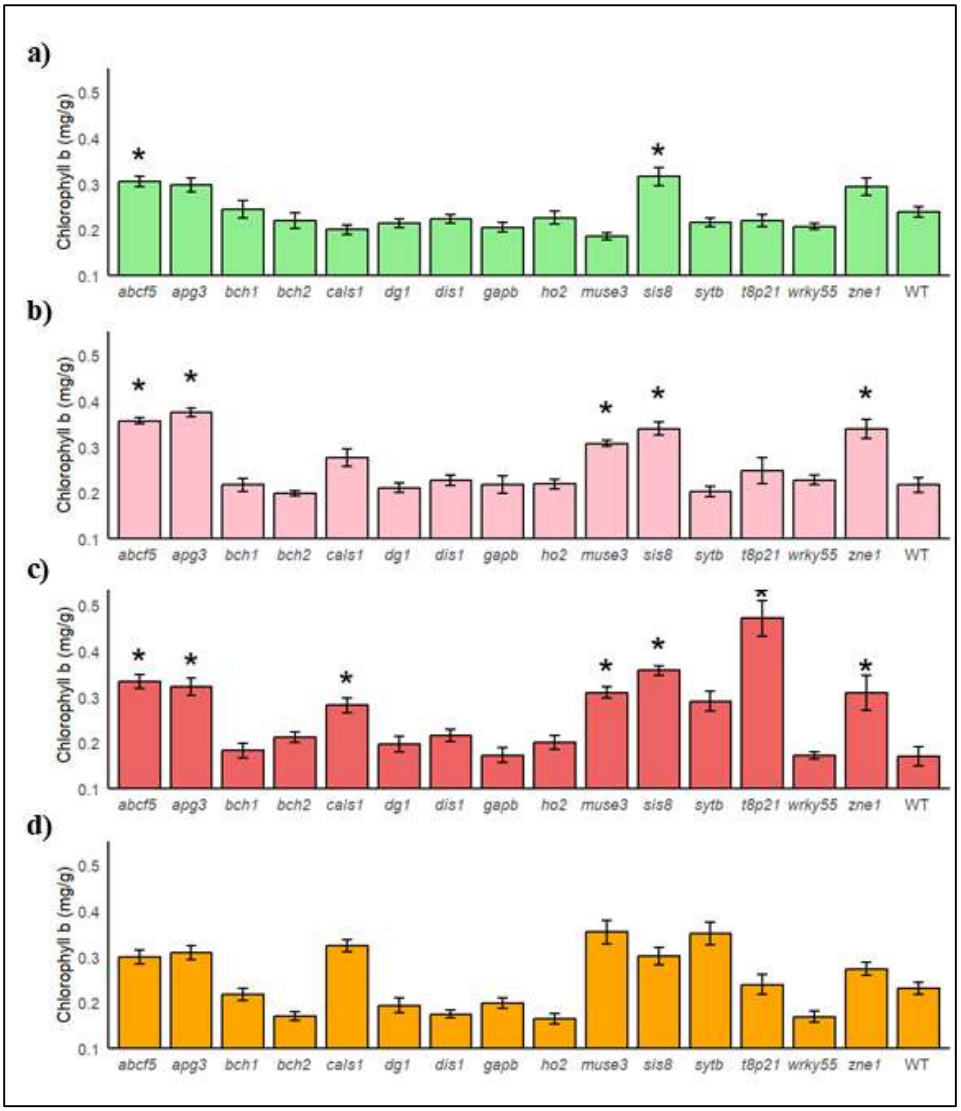

*Figure 4.29: Chlorophyll b content of T-DNA insertion mutants and WT (Col-0) of same treatment groups. T-DNA insertion mutants of A. thaliana genotypes and Col-0 (WT) a) in control conditions b) after prior exposure at 32°C for three days c) after prior exposure at 32°C for five days and d) subsequent three days recovery. * denotes significant difference (P<0.05) to the WT of the same treatment. Error bars indicate SEM.*

In control conditions, *Abcf5* and *Sis8* showed an increase in chlorophyll *b* content both by (+0.09mg/g) compared to WT respectively. After three days in heat, *Abcf5* (+0.14mg/g), *Apg3* (+0.17mg/g), *Zne1* (+0.13mg/g), *Muse3* (+0.09mg/g) and *Sis8* (+0.15mg/g) all showed a higher chlorophyll *b* content than WT (**Figure 4.29**). After five days in heat, compared to the WT the mutants *Cals1* (+0.11mg/g), *Muse3* (+0.14), *Sis8* (+0.19mg/g), *Zne1* (+0.14mg/g), *Apg3* (+0.17mg/g), *T8p21* (+0.3mg/g) and *Abcf5* (+0.16mg/g) all had significantly increased chlorophyll *b* content (**Figure 4.29**). None of the mutants showed significant differences to the WT after three days recovery from heat (**Figure 4.29**).

The mutants *T8p21*, *Cals1* and *Muse3* all showed to significantly increase in chlorophyll *b* content after exposed to five days heat stress whereas WT showed to decrease in chlorophyll *b* content after heat stress (**Figure 4.29**).

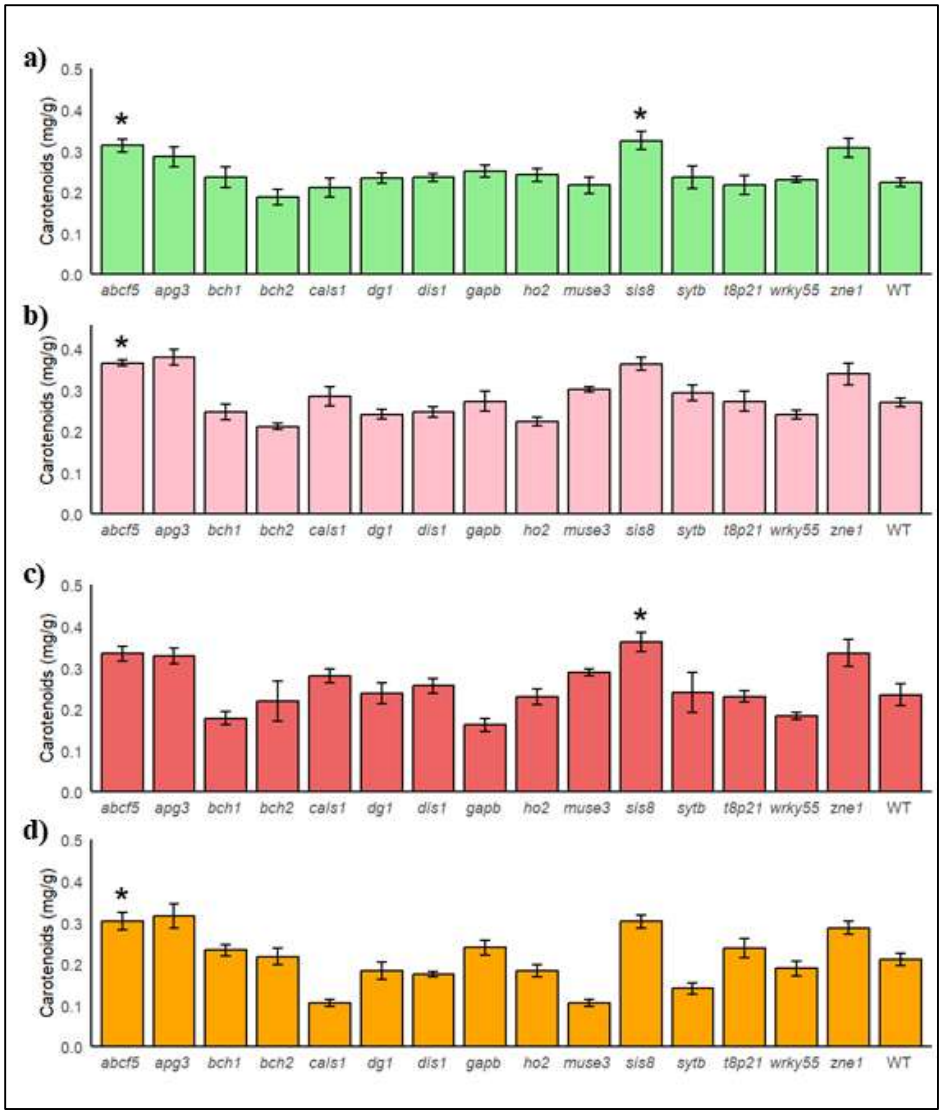

*Figure 4.30: Carotenoid content of T-DNA insertion mutants and WT (Col-0) of same treatment groups. T-DNA insertion mutants of A. thaliana genotypes and Col-0 (WT) a) in control conditions b) after prior exposure at 32°C for three days c) after prior exposure at 32°C for five days and d) subsequent three days recovery. * denotes significant difference (P<0.05) to the WT of the same treatment. Error bars indicate SEM.*

In control conditions only the mutants *Sis8* and *Abcf5* had increased carotenoid content compared to WT (**Figure 4.30**). *Abcf5* also showed higher carotenoid content than WT both after three days heat stress (+0.11mg/g) and three days recovery from five day heat stress (0.12mg/g). *Sis8* also had a 15mg/g higher carotenoid content than WT after five days heat (**Figure 4.30**).

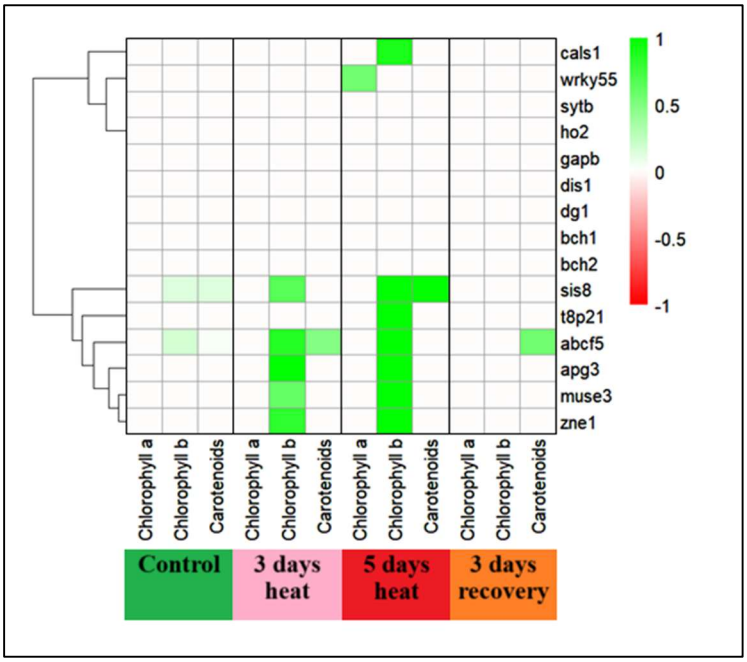

Figure 4.31. Heatmaps showing fold change in pigment content (mg/g) between T-DNA insertion mutants and WT (Col-0) of same treatment groups. A. thaliana genotypes and Col-0 (WT) were exposed to 32°C for three days (3 days heat), five days (5 days heat) and then recovered in control conditions for three days (3 days recovery). Control represents control conditions at the same age as plants after five days heat treatment. White boxes indicate no significant differences (P<0.05)

4.4 Discussion

In this chapter, T-DNA insertion lines previously highlighted in chapter 3 were phenotyped to assess them for tolerance to heat stress. By using chlorophyll fluorescence as a proxy, this chapter aimed to gather a picture of how these insertion lines perform in both control conditions and after heat stress as well as to identify genes important in heat stress tolerance.

4.4.1 Response of PSII to rapidly increasing temperatures

Few differences in Tcrit were seen between T-DNA insertion mutants and WT, with only three mutants showing any significant differences: *Dis1*, *Cals1* and *Muse3*. T_{crit} shows a critical value in which PSII mechanisms critically decline therefore leading to significantly reduced photosynthesis. While *Dis1* showed an increase in Tcrit in control conditions, it showed no differences to the WT in heat stress or subsequent recovery, indicating it may perform better with heat shock and perform averagely during prolonged heat stress. When heat stressed, *Cals1* and *Muse3* which has a

slightly lower average Tcrit than WT, increased in T_{crit} after five days heat stress, showing that several days heat may prime the plant for higher temperatures, giving a significantly higher T_{crit} than WT after five days heat stress.

Due to the way in which genes were selected as discussed in Chapter 3, it was expected that a larger proportion of the mutants would show an increased Tcrit under control conditions. T_{crit} may therefore not be a transferrable trait across species, especially given the large differences in ideal temperatures between rice and *A. thaliana*.

While in control conditions, none of the mutants showed significantly slower initial rate of response to heat (m_1), whereas after five days of heat treatment, *Sytb* and *Cals1* had faster initial response indicating that prior heat stress increases the sensitivity of PSII to heat stress under ~ 42°C (T_{crit}) in *A. thaliana*.

No mutants showed a significantly faster rate of secondary response to heat (m_2), and *Abcf5* and *Zne1* showed a significantly slower secondary response than WT both in control conditions and after prior heat exposure. *Gapb* and *Bch2* indicated they may show that prior heat exposure may slow the rate of secondary response to heat in these mutants after recovery.

4.4.2 Response of ΦPSII, qP and qL to heat stress

The F_v/F_m was assessed in order to test the mutants for photoinhibition. A lower F_v/F_m in any of the mutants would show the mutation may be causing photoinhibition in the plants and would therefore influence parameters tested such as ΦPSII, qL, qP and NPQ. The correlation between these parameters and F_v/F_m was calculated, and no correlations were found that would indicate F_v/F_m have a strong influence on ΦPSII, qL, qP or NPQ.

The findings here differ from that seen in Rice in the case of *bch1* and *bch2*, as the rice orthologue *dsm2* mutant shows a significant reduction in F_v/F_m and suggested a reduction in the xanthophyll cycle had an effect on the transfer efficiency of absorbed light energy to PSII reaction centres (Du et al., 2010)

qP

qP was assessed for, in order to see if the level of photochemical quenching differed in the T-DNA insertion mutants compared to the WT. In control conditions, compared to WT, *Apg3*, *Sis8* and *Zne1* all showed a significantly lower qP, indicating a baseline of a higher rate of operating efficiency in proportion to maximum efficiency whereas *Bch2*, *Dis1*, *Ho2* and *T8p21* had a significantly higher qP than the WT.

After heat stress, *Dg1*, *Cals1*, *Muse3* and *Sytb* all showed a significantly lower qP than the WT. After three days recovery from heat, three mutants had a significantly lower qP than the WT:, *Cals1*, *Muse3*, and *Sytb*.

qL

There were very few differences in qL seen between the mutants, with *Ho2* and *Dg1* showing a heightened qL in control conditions. This indicates a higher baseline proportion of open reaction centres. *Cals1* had a lower qL in control conditions indicating a lower proportion of open PSII reaction centres compared to the WT. *Abcf5* had a reduction in qL after heat stress, which could mirror trends in qL after high light intensities where reaction centres close, and are therefore cannot accept electrons. Overall very few differences were seen in qL, which shows many of these genes explored using T-DNA insertion mutants don't have an influence on qL, however those genes that have showed an increase in qL (particularly *Ho2* and *Dg1*) could also show other changes in photosynthetic traits because of the increase in baseline qL.

ΦPSII (F_q'/F_m')

The quantum yield of PSII (ΦPSII) - F_q'/F_m', was assessed before during and after heat stress. In control conditions four mutants showed significantly higher ΦPSII than the WT. Two mutants showed a significantly higher ΦPSII. *Muse3*, and *Cals1* showed a lower ΦPSII compared to the WT after both three days heat stress and three days recovery from heat. There were also trends in *Ho2*, *Wrky55* and *Dis1*, which had a higher ΦPSII than the WT after heat stress and recovery.

The reduction in ϕPSII seen in some of the T-DNA insertion mutations (*Muse3* and *Cals1*) show that there could be a reduction in utilisation of light for photochemistry, and the genes being knocked out may be components of PSII functionality. The results seen in *gapb* in control conditions confirms findings in Simkin et al., (2023) where there were also no significant differences in ΦPSII.

Heat reduces the electron transport efficiency in both PSII and PSI (Mathur et al., 2014) and in heat stress conditions, a decrease in ϕPSII has been reported in multiple species. The results seen in this study indicate some of the mutants that showed a higher ΦPSII after heat treatments are able to utilise a larger proportion of energy for photosynthesis during heat stress (Genty et al., 1989), important for retaining growth under heat stress. The higher ΦPSII after heat in these mutants can show increased PSII functionality and overall photosynthetic ability when analysed in tandem with other photosynthetic parameters.

4.4.3 Response of NPQ to heat stress.

Findings in the WT showed that heat stress after five days caused an expected increase in NPQ after five days, similar to reports in previous studies.

NPQ is a mechanism that is highly dependent on the amount of excess energy in PSII. In high light, a high NPQ is needed crucially to dissipate energy, and in limiting light conditions, a low NPQ is beneficial to allow more energy to go to photochemical reactions and drive plant growth and development. Therefore ideally, to maximise photosynthetic activity, plants would have a lower L15 NPQ and higher L30 NPQ, without altering speed of induction or relaxation. The majority of the mutants showed a decrease in NPQ magnitude when compared to WT in the same conditions. After five days heat stress, more mutants had a lower NPQ magnitude than the WT, than in control conditions. A large portion of the mutants showed a significant decrease in both maximum and L15 NPQ in control conditions and after three and five days of heat stress, with only one mutant showing a significantly higher L15 NPQ (*Gapb* after five days heat stress). The lower values of NPQ magnitude seen in some T-DNA insertion mutants shows the mutations could have beneficial effect on energy availability for photosynthesis in light limiting conditions.

Du et al., (2010) showed a significant reduction in NPQ in the rice orthologue mutant of *bch1* and *bch2*, whereas few differences were observed in *A. thaliana*, until ED90. The differences in NPQ may be larger in rice, due to its growth at higher temperatures, and therefore show larger differences to the WT, however there is still some overlap in species in terms of effect of orthologue genes on NPQ.

Field grown crops have to adapt to changes in light conditions, which can be rapid and frequent. Changes in these light conditions can even occur on cloudy days, due to leaf movement and shading from neighbouring plants and self-shading (Zhu et al., 2004; Burgess et al., 2017). In order to cope with excess light, NPQ induction needs to be quick, to reduce photodamage and ROS formation. In control conditions, none of the mutants showed any significant differences to the WT, therefore it is assumed that the genes selected for photosynthetic temperature traits, when grown in ideal temperatures, do not impact induction speeds of NPQ, even in differing magnitudes of NPQ.

High heat stress and high light stress can occur simultaneously, therefore the importance of the quick induction of NPQ even in heat stress conditions is paramount to avoid photodamage and ROS during heat stress. Induction speeds after heat after five days heat stress showed that four of the mutants had a significantly quicker induction speed than the WT, while two mutants showed a slower induction speed.

Once excess light is reduced, unnecessary levels of NPQ would reduce energy available for photosynthetic reactions. During the transition from saturated to limited light conditions, NPQ needs to relax quickly, otherwise competition with photochemistry would reduce ΦPSII and CO_2 fixation (Hubbart et al., 2012; Kromdijk et al., 2016). In control conditions, none of the mutants showed any significant differences in relaxation speeds to the WT, therefore it is assumed that the genes selected for photosynthetic temperature traits, when grown in ideal temperatures, do not alter relaxation speeds of NPQ. Similar to induction speeds, relaxation speeds after heat after five days heat stress showed that four of the mutants had a significantly quicker relaxation speed than the WT, while two mutants showed a slower relaxation speed.

4.4.4 T-DNA mutants show small differences in Chlorophyll *b*.

Very few significant differences between mutant and WT were seen in chlorophyll *a* content. The only difference seen was in *wrky55*, where after five days heat stress, chlorophyll *a* content was higher than that of the WT. Chlorophyll *b* content, in control conditions again showed few significant differences to the WT, one mutant (*Sis8*) having a higher content. Around half of the mutants showed significantly increased chlorophyll *b* content compared to the WT after five days of heat. The changes in chlorophyll *b* were seen more than chlorophyll *a*, which may be due to the use of microplate reader, when spectrophotometer method of measurement is more commonly used, as there may be more error or variation in the samples. If the sampling were to be repeated with more time available, a spectrophotometer could be used with all samples. Comparing overall chlorophyll content may also show further insight to differences between mutants and WT. Stunted growth caused by other biological factors may also contribute to differences seen in the study, with some mutants or the control showing reduced chlorophyll based on reduced growth or a change in health of the leaf.

Havaux and Tardy (1999) showed that a decrease in chlorophyll content may result in improved heat stress tolerance through decreasing leaf absorbance, reducing heating effect of solar radiation, however the decrease in chlorophyll *b* may just be due to the heat sensitivity of chlorophyll being higher, rather than the plant adapting to the heat stressed environment. Whilst there has been a clear relationship between chlorophyll and photosynthesis in previous studies (Emerson 1929), a reduction in chlorophyll does not always mean a reduction in photosynthetic rate (Gu et al., 2017), and a linear relationship between chlorophyll and photosynthesis is only linear below threshold light levels (Buttery and Buzzel 1977). Therefore, the reduction of chlorophyll *b* is not a cause for concern for the mutants when taken into account alongside the results of chlorophyll *a* content and carotenoid content, where only slight differences were seen between WT and mutants.

In Wang et al., (2020), *A. thaliana wrky55* T-DNA insertion mutants had a lower chlorophyll content than the WT after seven weeks post stratification, however no significant differences after four weeks, in both knockout and knockdown mutants. These results differed to results seen in the study, where *wrky55* had no significant

difference in chlorophyll levels in control conditions, indicating that the increase in chlorophyll levels may only be at specific growth stages. There were no significant differences in chlorophyll or carotenoid content in the *bch1* or *bch2* mutants, which is surprising considering the mutation is within the carotenoid biosynthesis pathway, and mutants in previous studies have been found to have reduced carotenoid content (Davison et al., 2002).

Carotenoid content of the mutants showed similar levels to that of the WT. Only two mutants (*Abcf5* and *Sis8*) showed an increase in carotenoid content after heat stress. Due to the importance of carotenoids role as protective pigments under stress (Maslova et al 2021), increase of carotenoids in heat stress can assist in rapid quenching of excited chlorophyll via energy transfer to short-lived excited carotenoid states (Skotnicova et al., 2021). Therefore, these two mutants show signs of increased photoprotection in heat stress. The increase in carotenoid content during heat could also be a factor when selecting target genes for fruit and vegetable breeding in areas of frequent heat stress, due to the economical and health benefits of higher carotenoid level.

4.5 Conclusions

Out of all the mutants, *Muse3* showed an increase in T_{crit} and during heat stress, maintained NPQ induction/relaxation speed, plus increased chlorophyll *b* content, and therefore may show most future potential. Larger scale experimentation could be done on these mutations to look at the same parameters at different ages of plants and in longer heat exposure. Another major step in taking any of these genes forward to select for breeding purposes would be to test these genes for yield in control and heat stress conditions in economically important crops such as cereals, especially rice as was the original selection process based on.

Tcrit was used as an important value to indicate photosynthetic heat tolerance in mutants (Ferguson et al., 2020). Due to T_{crit} being a parameter in which genes were selected for in orthologue rice genes (Chapter 3) It was surprising that none of the mutants showed a significantly lower Tcrit than that of the WT. However, only *Cals1*, *Muse3* and *Sytb h*ad a significant increase in Tcrit after heat treatment, which is

surprising given the selection process. The low number of mutants that showed to have an increase in T_{crit} in *A. thaliana* given the selection of Rice orthologues, may be due to PSII traits linked to T_{crit} are not conserved between rice and *A. thaliana*, or the differences in T_{crit} in *A. thaliana* are much smaller, or the genes may not be responsible for large differences in T_{crit} when not accompanied by other SNPs.

5 Identifying trends in high throughput screening of *A. thaliana* mutants for abiotic stress tolerance.

5.1 Introduction

5.1.1 High throughput screening: the big picture.

Plant phenotyping requires quantification of traits which can be used as measures of plant performance. Phenotyping can take substantial amounts of time and money, causing a bottle neck in production of crop improvement, therefore the importance of developing rapid and cost-effective measures to gather phenotypic data is important for future crop breeding (Araus and Cairns, 2014; Fahlgren et al., 2015; Mishra et al., 2016).

Chapter 4 discussed high throughput procedures to phenotype dynamic photosynthesis and photoprotection in both live whole plants and excised leaves. This extended to a rapid screen for pigment content in leaves, to gather a rounded picture of the effect of heat stress on T-DNA insertion mutants selected in Chapter 3. On top of screens done in Chapter 4, there are further screens that can be done to paint a bigger picture on the effect of these T-DNA insertion mutants.

With several high throughout screens, correlations between data can be used to see which of the parameters can give the best indication of heat stress tolerance. By analysing correlations between parameters, insight into any linkages between different screens can be gained with reference to heat stress tolerance.

This chapter will assess another two phenotypes: fertility and root architecture, due to their cost effective and rapid methods, while also looking for links between parameters discussed here and in Chapter 4. Therefore assumptions can be made about the most promising of these mutants, to see which genes may be most beneficial as targets for future crop breeding.

5.1.2 Heat stress affects fertility – an economically crucial factor in crop breeding.

Fertility is a key determinant in the yield of many crop species, including cereals, in which there is a direct association between floret fertility, grain number and yield (Fageria, 2007; Edmeades 2010). A genotype, in this study referring to T-DNA insertions, which causes a negative fertility phenotype such as sterility or reduced seed number, can many times be a factor that can halt considerations for crop breeding.

During heat stress, plant reproduction can be affected in a variety of tissues simultaneously, resulting in abnormal flower development, reduced size of flowers, and sterility of flowers. Other impacts include pollen grains being impaired and unable to germinate and disrupted gametogenesis resulting in abnormal formation of gametes. Increasing temperatures can also change timings of developmental phases such as vegetative to reproductive phase, which in turn alters flowering time.

Fertility can be rapidly assessed across a large dataset by a simple measure of silique length in *A. thaliana* due to the strong correlation between seed number and flower fertility due to self-pollination. Assessing fertility parameters in *A. thaliana* as a model species can be an early indicator of yield potential of crop species.

5.1.3 Root architecture and abiotic stress

Roots are essential for plant water and nutrient uptake from soils, therefore changes in root architecture including root depth, spread, root number and length of lateral roots can be key in adapting to changing environments. Root architecture improvement can also offer an important economic focus for root and tuber crops such as potato.

Optimisation of crop root systems for breeding has become a focus in terms of broader and deeper roots as well as looking at the microbiome and root hairs. Longer, deeper roots can take up more water from greater depths, while higher root length density increases the absorption of nutrients (Kawata et al., 1978, Nemoto et al., 1998). which is beneficial for plant growth and productivity (Potocka and Szymanowska-Pulka, 2018). In durum wheat, deeper roots have shown higher yields in the field (Li et al., 2019; Maccaferri et al., 2016), and the goal of improving wheat root architecture for

growth and productivity in other cultivars is achievable (Rizi and Mohammadi, 2023). Plant breeding for larger root systems has also been proposed as a method for increasing carbon storage by plants as a way of reducing atmospheric CO_2 (Kell 2011). Deeper and wider roots can also improve soil structure which can be a benefit in agricultural practices, as well as increasing uptake capacity of nutrients therefore mitigating nutrient leaching and runoff.

Root systems show great plasticity in response to abiotic stress in the environment, however environmental stress can have negative effects on root systems. Drought not only inhibits root growth and development (Comas et al., 2013) but inhibits nutrient uptake by the plant through affecting nutrient mobility and diffusion (Rouphael et al., 2012; Dijkstra et al., 2014). Salt alters water uptake by altering water potential in the soil, reducing water intake by roots, and inhibits nutrient uptake enzymes due to competition with salt ions (Van Zelm et al., 2020), therefore reducing growth and development. Salt ion accumulation also causes toxicity stress by negatively affecting cell cycles (West et al., 2004).

Heat stress is also seen to influence root systems, notably root length and lateral root density (McMicheal and Quisenberry, 1993; Seiler 1998; Nagel et al.,2009). Heat stress has also been shown to decrease nutrient and water uptake (Hendrick and Pregitzer, 1996; Luo et al., 2020), which in turn can lead to effects as previously described from drought stress. Another key aspect to analysis of abiotic stress response is the effect of heat stress on tolerance to other stresses (Heckathorn et al., 2013), as effects of abiotic stress such as heat and drought stress are additive.

Growing plants on agar plates to assess root architecture provides a non-destructive analysis of root growth under several abiotic treatments. Treatments such as drought and salinity stress can be easily imitated using added components of mannitol and NaCl to growth media. These methods allow for growth to be measured at several timepoints however 3D analysis of root structure and limitation of species on small plates can be a negative aspect of these methods. Variability among species should also be considered when using model species (as is commonly used in agar-based techniques) due to the large variation in responses to abiotic stress in roots (Fonseca de Lima et al., 2021). Abiotic stress treatments chosen for assessing changes in root architecture in this chapter were heat, drought and salt due to their causation of large

economic and food security losses and ease at which agar plates for *A. thaliana* growth can be adapted for these treatments.

5.1.4 Chapter Aims

In this chapter, T-DNA insertion mutants used in Chapter 3 and Chapter 4 were phenotyped further for traits useful in crop breeding and development. These mutants were not only assessed for fertility, but also for root architecture among other abiotic stressors, to gather initial indications as to whether genes of interest may confer other abiotic stress tolerance as well as heat (as explored in Chapter 4). These phenotypic assessments can also be combined in order to evaluate if any of the T-DNA insertion mutants have potential to be taken further in development in terms of designing future heat tolerant crops.

Due to the nature of quick high-throughput phenotyping and data collection, the traits seen in this chapter and Chapter 4 can be viewed as a whole, to look for links between unrelated traits. This may show which traits if any, have a positive or negative effect on other traits of interest, therefore providing focus for future

5.2 Methods

5.2.1 Fertility phenotyping

A. thaliana Columbia-0 (Col-0) ecotype along with the selected mutants were grown in Levington M3 compost with Biofungicide *Trichoderma asperellum* cepa T34 (T34) biological control in 10cm pots (two plants per pot). *A. thaliana* were grown until around day of bolting (+/- 1 day either side of bolting in order to limit number of plant groupings) in growth rooms at 22°C in 16hr days under fluorescent lighting with a 3:3:1 ratio of red:green:blue light with a Photosynthetic Photon Flux Density (PPFD) of 205(± 8.6 SD) µmol/m^2 /s. Hypoline™ (Bioline AgroSciences) was applied to soil surface of pots weekly for prevention of scarid fly larvae. Trays were rotated every week to minimise localised environmental effects. For heat treatment conditions, at point of bolting, eight plants (four pots) of each genotype were left in control conditions and eight plants were moved to a growth room of 32°C, at 16hr daylength and 28°C at night. Heat treatment growth rooms had same light intensity from that of

control conditions. Heat treatment of these plants lasted five days before being returned to the original growth conditions.

Fully developed siliques were measured from contact with the pedicel to tip of silique from the base of the stem to the furthest growing point on the largest main stem. Total number of siliques on this stem were also counted.

5.2.2 Root architecture phenotyping

A. thaliana seedlings were sterilized with 70% ethanol for 30s followed by 50% (v/v) bleach for five mins. The seeds were then rinsed in sterile water 5x before plating on ½ Murashige and Skoog (MS) media (2.2 g/L Murashige and Skoog media, Sigma) with 0.05% 2-(N-morpholino)ethanesulfonic acid (MES) (0.5g/L) and 1% Agar (10 g/L) at a pH of 5.8. Seeds were grown vertically on agar at 22°C and 16hr daylength for four days. After four days, seedlings were transferred to a new plate depending on treatments. For control and heat treatments, plates were made with ½ MS media (2.2 g/L Murashige and Skoog media, Sigma) with 0.05% MES (0.5g/L) and 1% Agar (10 g/L) at a pH of 5.8, for salinity treatments, 150mM NaCl was added to the media, and for Drought treatment, 200mM mannitol was added. Five seedlings of each genotype were placed on half of a plate, with Col-0 on the other half. Four plates were used per genotype and treatment. Plates were photographed laid flat and photographed to show the length of root growth adjacent to a scale. Control, salinity and drought treatments were placed again vertically in 22°C and 16hr daylength, whilst the heat treatment plates were placed at 32°C with the same daylength. After six days on the treatment plates, the plates were again photographed. Images of the plates were then analysed for root length at four days and ten days using software ImageJ.

5.2.3 Statistical analysis

Statistical analysis and visualisation of graphs were performed using R-studio (2023.12.1 Build 402) with R-4.3.1. Packages used included: ggpubr, sssci, ggplot2, plyr, multcompView, doBy, dyplyr, gghighlight, forcats, tidyverse, purr, sm, plotrix, Hmisc, corrplot, PerformanceAnalytics, fmsb, segmented, reshape2, DataCombine, stringer, broom, drc, and dplyr. Correlation matrices were also performed using R.

ANOVA was used throughout using R with Tukey HSD test used to assess significant differences between sample means. Analysis of covariance (ANCOVA) was used to assess root growth parameters with plate as covariate.

5.3 Results

5.3.1 Changes in root architecture after exposure to increased heat, salinity and simulated drought

When plotting a linear regression between root length at day four and day ten (not shown), R^2 value of the regression had a value of 0.04, which shows that root length at day four was not likely to be affecting root length at day ten.

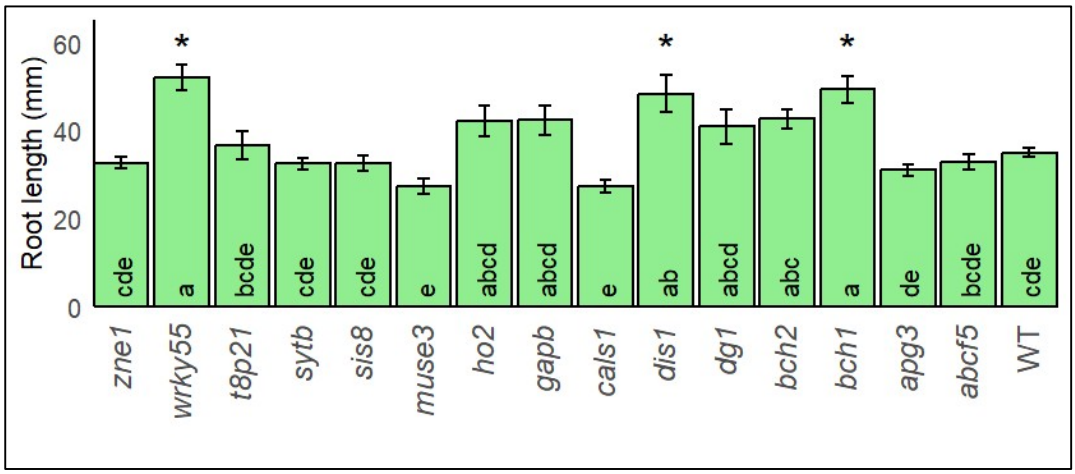

*Figure 5.1: Root lengths of 15 T-DNA insertion lines of A. thaliana compared to WT (Col-0). Seedlings were grown on ½ MS medium vertically on plates for ten days. *indicates significant difference (P<0.05) to the WT. Error bars indicate SEM.*

In control conditions, *Bch1* (+14.4mm), *Dis1* (+13.5mm) and *Wrky55* (+17.1mm) had significantly longer roots than WT **(Figure 5.1)**. No mutants were showno have significantly shorter roots than WT in control conditions **(Figure 5.1)**.

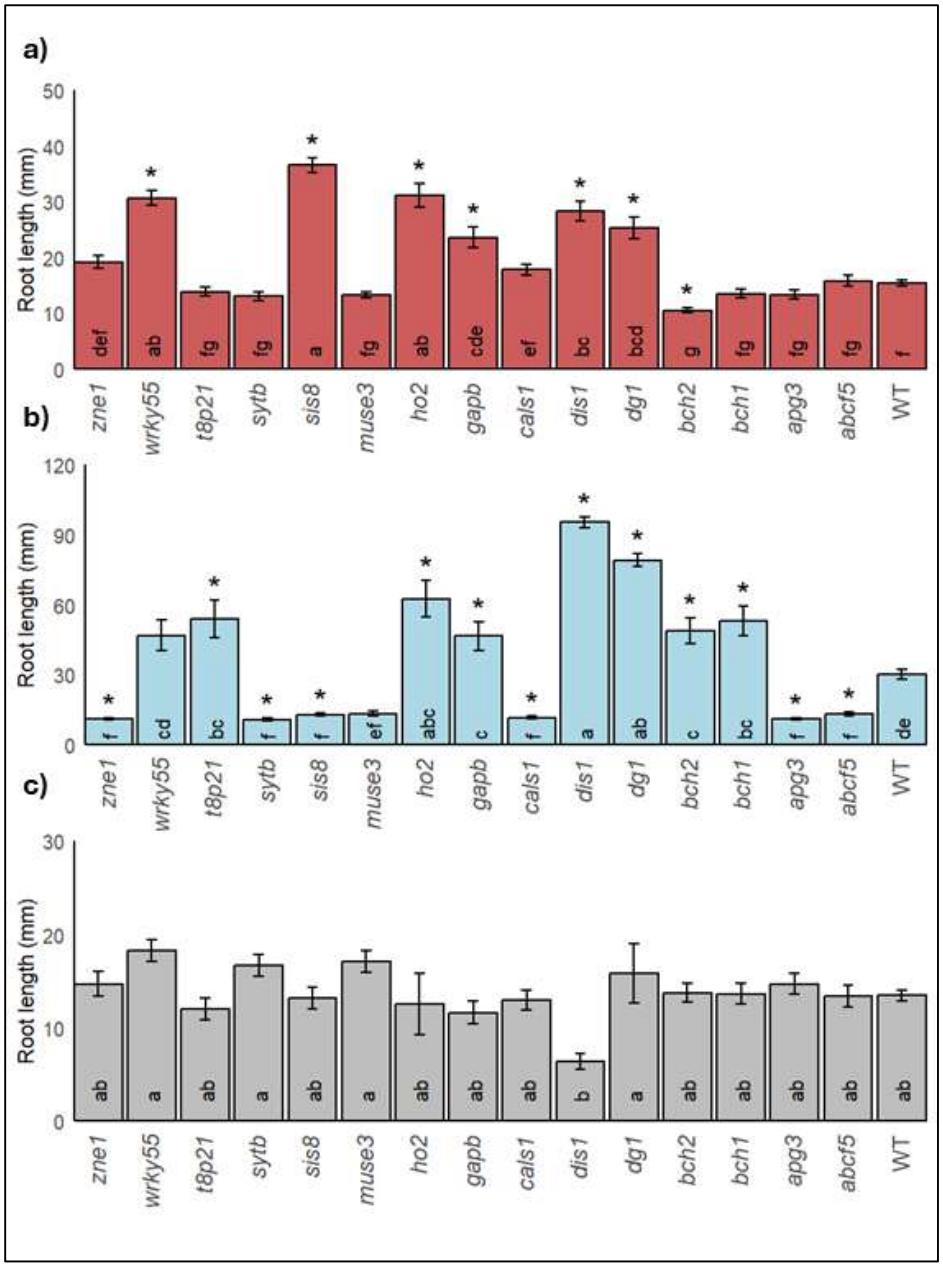

*Figure 5.2: Root lengths of 10 day old T-DNA insertion lines of A. thaliana compared to WT (Col-0) under grown at six days under stress treatment. a) Heat treatment b) drought treatment (mannitol) c) salinity treatment. Seedlings were grown on ½ MS medium vertically. Letters denote statistical significance and * denote significant difference (P<0.05) to the WT grown in the same treatment. Error bars indicate SEM.*

Bch1 (+22.8mm), *Bch2* (+18.6mm), *Dg1* (+49.05mm), *Gapb* (+16.44mm), *Dis1* (+65.3mm), *Ho2* (+32.4mm), *T8p21* (+23.8mm) and *Wrky55* (+16.6mm) showed increased root length under drought conditions compared to WT, while *Apg3* (-19.1mm), *Cals1* (-18.6mm), *Muse3* (-17mm), *Sis8* (-17mm), *Sytb* (-20.2mm), *Zne1* (-19.1mm) and *Abcf5* (-16.9mm) showed a significantly shorter root length **(Figure 5.2)**. Mutants showing significantly longer root lengths than WT in drought conditions had

a significantly increased root length than lengths seen in WT, except *Wrky55* and *Bch1*, where drought treatment showed similar root lengths to growth in control conditions **(Figure 5.2)**. All mutants that were shown to have a shorter root length than WT in drought conditions had a significantly shorter root length compared to when mutants were grown in control conditions **(Figure 5.2)**.

Heat treatment caused root lengths to decrease in all mutants (including WT) except *Ho2*, *Sis8*, *Cals1*, *Zne1*, *Abcf5*, *Gapb* and *Dg1*, where root lengths were similar to lengths seen under control conditions **(Figure 5.2)**. *Sis8* (+21.2mm) after heat treatment had significantly longer roots than those of WT and was the only mutant to show significant differences **(Figure 5.2)**.

In salinity treatment, no mutants showed any significant differences to that of the WT **(Figure 5.2)**. Mutants and WT showed salinity treatment to significantly decrease root length, except *Muse3* and *Sytb*, where root lengths were similar to lengths seen under control conditions **(Figure 5.2)**.

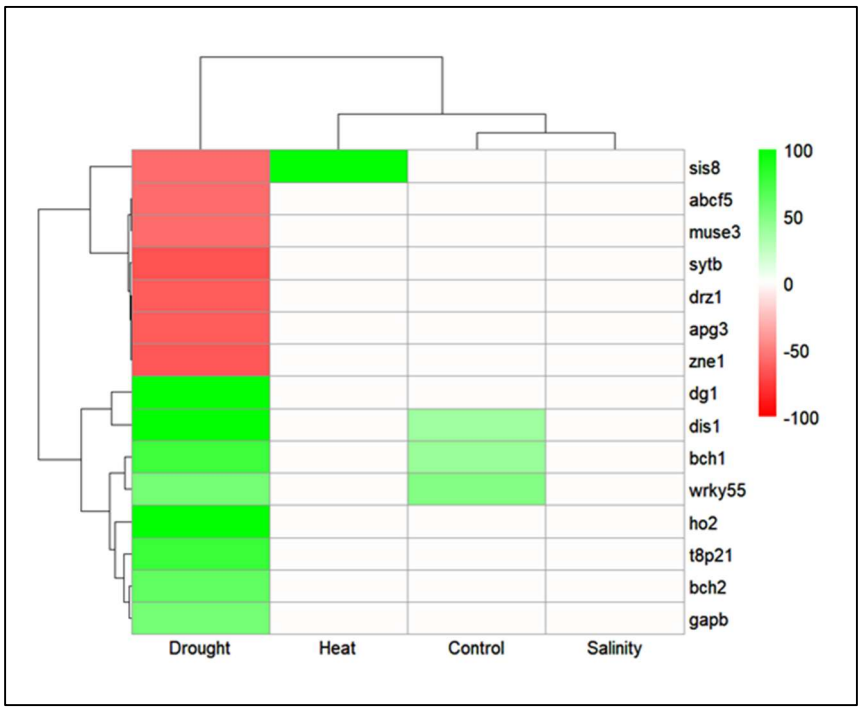

Figure 5.3: Heatmaps showing fold change in root length between T-DNA insertion mutants and WT (Col-0) of same treatment groups. A. thaliana seedlings were grown on ½ MS medium vertically on plates for ten days. White boxes indicate no significant differences (P<0.05).

Overall, there was a 50% split in mutants showing significantly longer or shorter roots than the WT when exposed to drought treatment (**Figure 5.3**). Only *Dg1*, *Dis1* and *Ho2* significantly increased in root length in drought treatment compared to the mutants in control conditions.

The majority of mutants showed significantly shorter roots when exposed to heat stress, however none of the mutants showed significantly shorter roots than the WT after heat treatment. A similar pattern was observed with salinity treatment.

5.3.2 Fertility of selected mutants under heat stress

Total siliques and silique length of 15 T-DNA insertion lines with and without five day heat treatments at time of bolting were assessed in order to assess fertility.

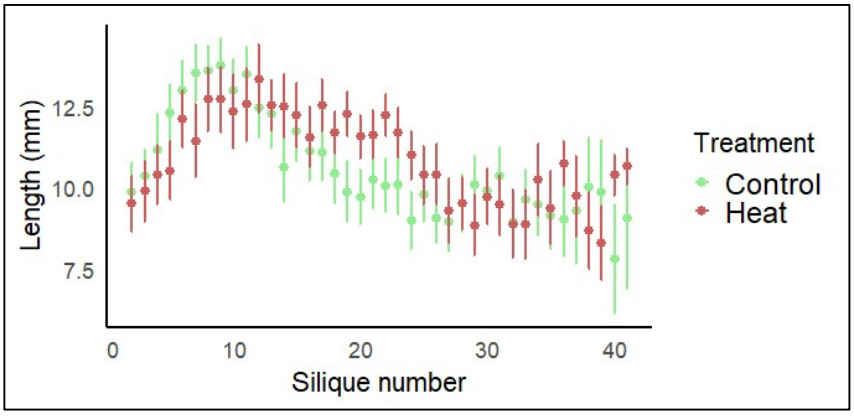

Figure 5.4: Characterisation of silique length at each position (silique number) along the main stem of Arabidopsis thaliana ecotype Col-0 (WT) after prior heat exposure at 32°C for five days (Heat) and under Control conditions. Silique number 0 represents the earliest silique to develop. Dots represent mean values at each position, and error bars signify SEM (n = 8).

Figure 5.4 shows characterisation of silique length in WT (Col-0), where heat treatment did not significantly alter lengths of silique. Between the earliest developed silique (0) and silique 10, there is a steady rise in length, before a slow shortening of length from silique ten to 28 where length begins to plateau (**Figure 5.4**)

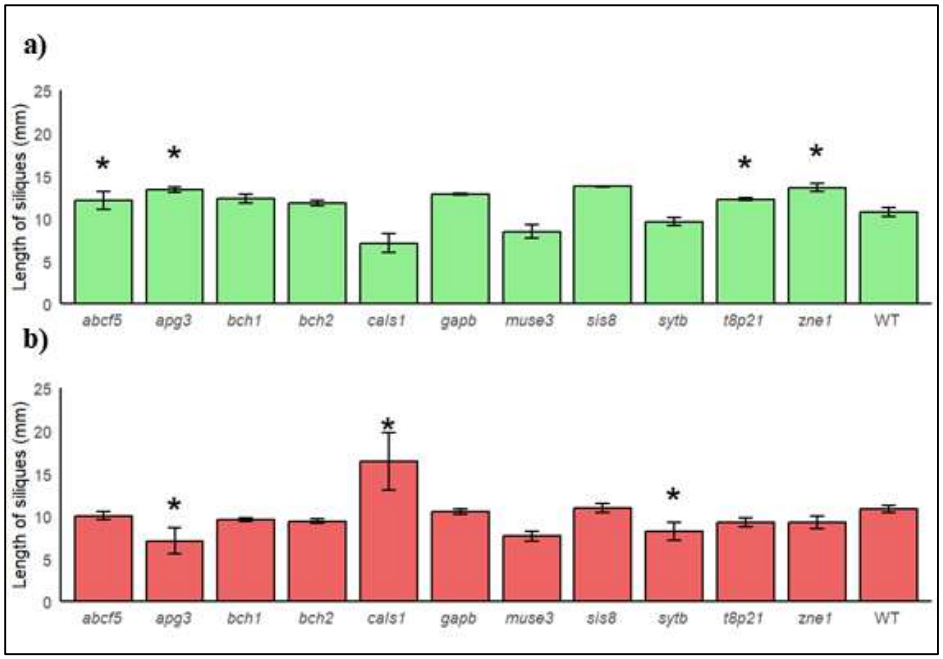

Figure 5.5: Silique length of T-DNA insertion mutants and WT (Col-0) of same treatment groups. T-DNA insertion mutants of A. thaliana genotypes and Col-0 (WT) a) in control conditions b) after prior exposure at 32°C for five days. denotes significant difference (P<0.05) to the WT of the same treatment. Error bars indicate SEM.*

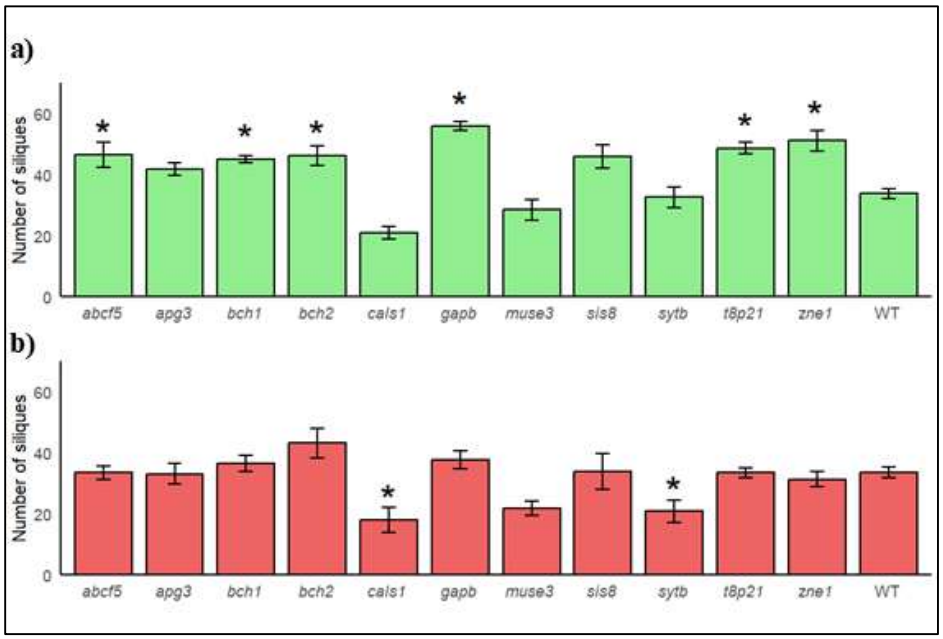

Figure 5.6: Silique length of T-DNA insertion mutants and WT (Col-0) of same treatment groups. T-DNA insertion mutants of A. thaliana genotypes and Col-0 (WT) a) in control conditions b) after prior exposure at 32°C for five days. denotes significant difference (P<0.05) to the WT of the same treatment. Error bars indicate SEM.*

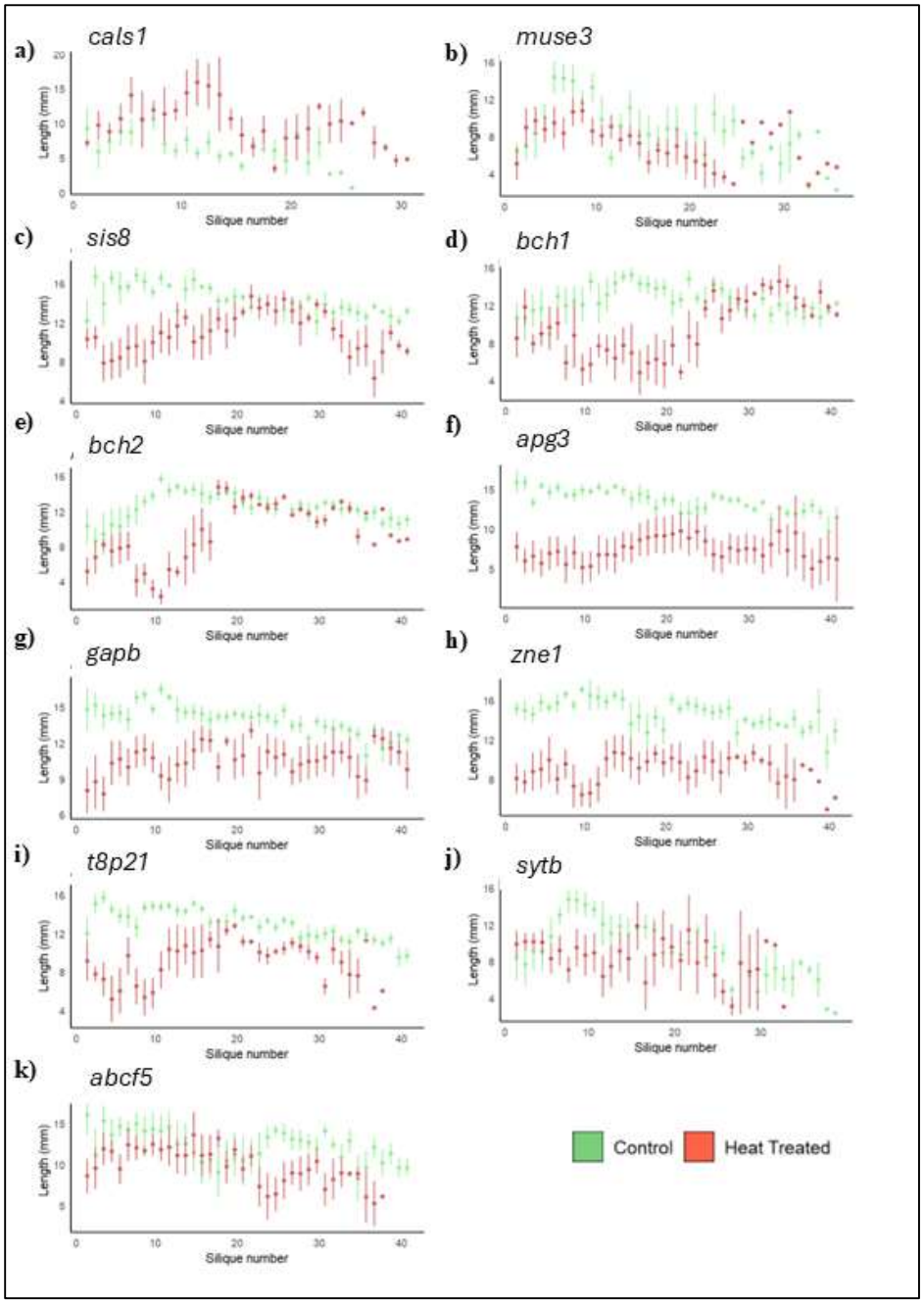

Figure 5.7: Silique lengths of T-DNA insertion mutants after prior exposure at 32°C for five days and under control conditions in: a) cals1, b) muse3, c) sis8, d) bch1, e) bch2, f) apg3, g) gapb, h) zne1, i) t8p21, j) sytb, k) abcf5. Error bars indicate SEM.

Zne1 (+17.4) showed to have a larger number of siliques and longer siliques throughout the stem than the WT when not exposed to heat, however after heat treatment, no differences between *Zne1* and WT were seen in silique number (**Figure 5.6**) and silique length (**Figure 5.5**). In **Figure 5.7**, lengths of siliques are seen to be shorter along the whole stem. While *Sytb* did not show any significant differences to the WT when in control conditions, after heat exposure, had fewer (-12.7) and shorter

siliques (-2.6mm) than the WT genotype (**Figure 5.5, Figure 5.6**). Heat treatment in *Sytb* did not cause a significant reduction in silique number or length compared to control conditions (**Figure 5.5, Figure 5.6**).

Bch1 (+11.4), *Bch2* (+12.6) and *Gapb* (+22.1) had significantly more siliques than the WT, yet after heat treatment showed similar results to the WT (**Figure 5.6**). Heat treatment caused a significant reduction in silique number in *Gapb* but still showed a similar number to that of WT after heat treatment (**Figure 5.6**). Only *Apg3* (+2.7mm) had longer siliques than WT in control conditions, yet after heat treatment had a significantly shorter silique length than the WT (**Figure 5.5**). In **Figure 5.7,** the significant reduction in silique length can be seen throughout the stem.

T8p21 (+15 total siliques, +1.5mm length) and *Abcf5* (+12.8 total siliques, +1.4mm length) had significantly more siliques and longer siliques than the WT in control conditions, yet after heat treatment showed similar results to the WT (**Figure 5.5, Figure 6.6**). In *T8p21*, heat treatment caused a significant reduction in number and silique length, yet this did not result in any significant differences to the WT (**Figure 5.5, Figure 5.6**). The reduction in length of silique can be seen more in the earlier development, particularly in siliques 1-15 (**Figure 5.7**).

After heat treatment, *Cals1* showed a significantly reduced silique number (-15.6) and significantly longer siliques (+5.6mm) than the WT, which was seen mostly in the longer siliques in position 9-16 (**Figure 5.5, Figure 5.6, Figure 5.7**).

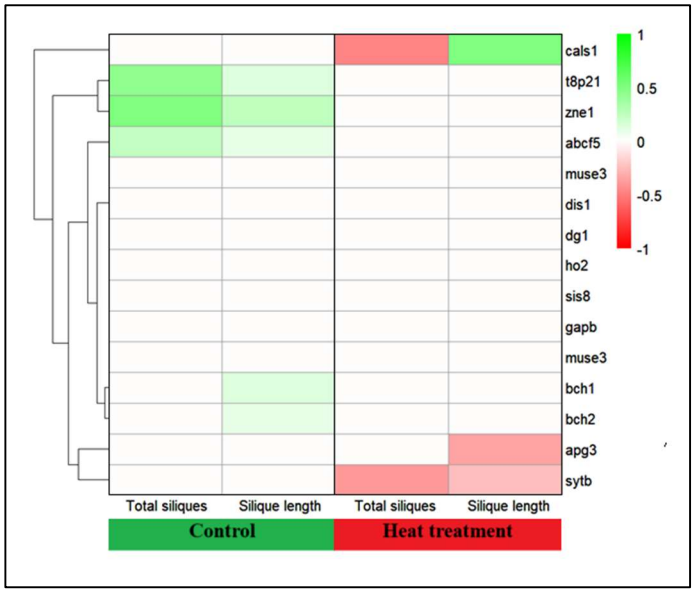

Figure 6.8. Heatmaps showing fold change in silique parameters between T-DNA insertion mutants and WT (Col-0) of same treatment groups. A. thaliana genotypes and Col-0 (WT) were exposed to 32°C for five days (Heat treated). White boxes indicate no significant differences (P<0.05)

Overall, heat treatment of five days negatively affected total number of siliques in *Gapb*, *T8p21* and *Zne1*, and negatively affected silique length in *Apg3*, *T8p21* and *Zne1*. *Cals1* was the only mutant to be positively affected by heat treatment, with an increase in silique length (**Figure 5.8, Figure 5.6**).

Compared to WT, in control conditions, *Abcf5*, *T8p21*, and *Zne1* had significantly longer and more siliques, and *Gapb*, *Bch1* and *Bch2* showed significantly longer siliques on average than WT (**Figure 5.5, Figure 5.6, Figure 5.8**). After heat treatment of 32°C for five days, *Apg3* and *Sytb* had significantly shorter siliques than WT, whereas *Cals1* was the only mutant to have longer siliques than the WT after heat treatment (**Figure 5.5, Figure 5.8**). *Cals1* and *Sytb* were both shown to have fewer siliques than the WT after heat treatment. Where there were significant differences in the silique lengths of the mutants, the lengths were affected from the first silique up to at least silique 20 (**Figure 5.7**).

5.3.3 Overall performance of T-DNA insertion mutations

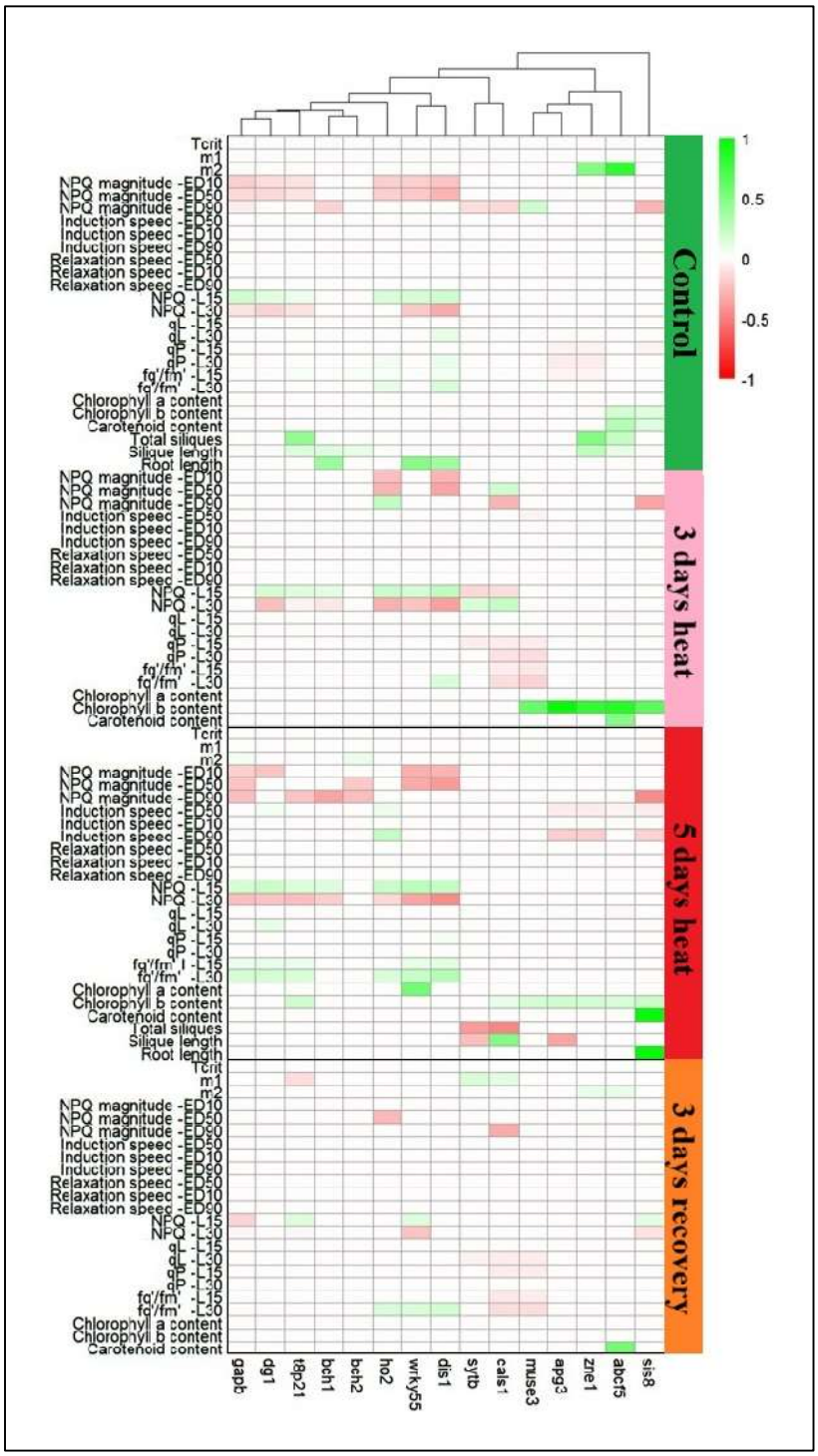

Figure 5.9 Heatmaps showing fold change in parameters between T-DNA insertion mutants and WT (Col-0) of same treatment groups. A. thaliana genotypes and Col-0 (WT) were exposed to 32°C for three days (3 days heat), five days (5 days heat) and then recovered in control conditions for three days (3 days recovery). Control represents control conditions at the same age as plants after five days heat treatment. White boxes indicate no significant differences (P<0.05). NPQ_L15, m_1, m_2 and speeds to induction and relaxation have been given inverse values so as to show beneficial phenotypic traits as positive values.

Looking overall at the performance of T-DNA insertion mutants, no mutants stood out as having performed outstandingly better than the WT, nor performed outstandingly badly compared to the WT.

Photosynthetic properties of T-DNA insertion mutants, where after heat stress, a large proportion of mutants showed an increase in ΦPSII compared to the WT. Several mutants showed significant differences in L15 and L30 NPQ, where compared to WT, many had a lower L15 NPQ and lower L30 NPQ both before and after heat stress.

While several of the mutants had differences in chlorophyll *b* content, especially after five days heat stress, out of the mutants relating to pigments (*bch1, bch2, apg3, gapb and dg1*), only *apg3* showed any significant difference to the WT.

5.3.4 Correlations between experimental parameters

Using a correlation matrix, parameters used (with the exception of root architecture, due to the large differences in growing media and plant age) were assessed for positive and negative correlations to each other.

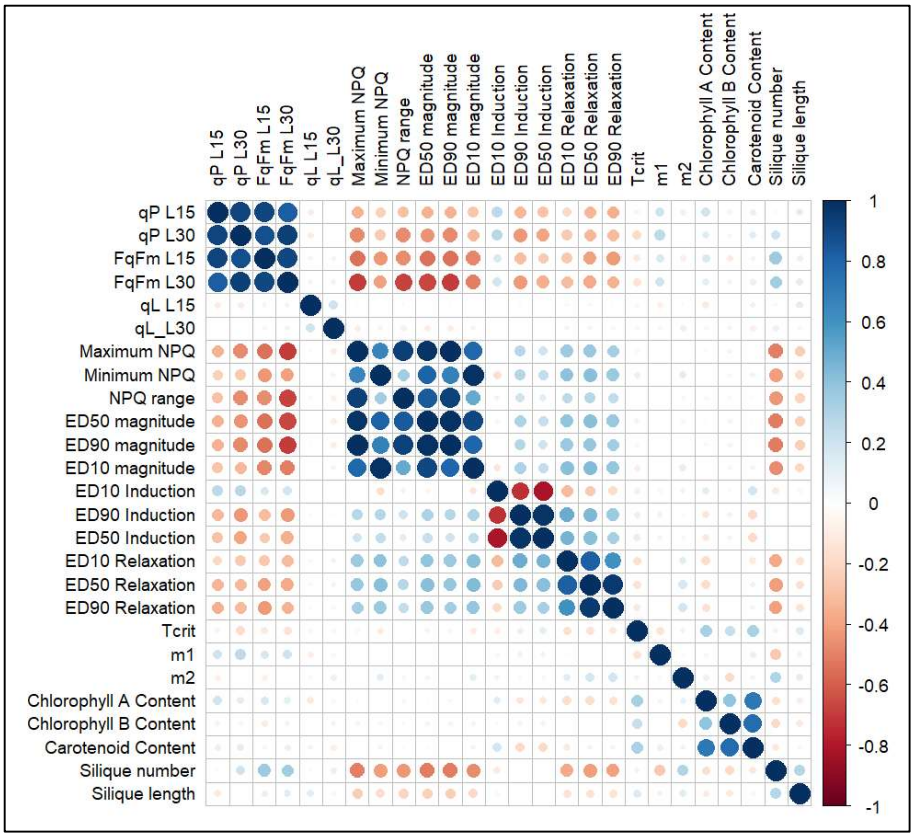

Figure 5.10. Correlation matrix among parameters used in Chapter 4 and 5 of plants of all genotypes measured five days after bolting in control conditions.

In **Figure 5.10**, many parameters that are related have strong correlations with each other, for example traits linked with NPQ or PSII efficiency, where clear groups can be seen. Pigment contents and qL had very little correlation with other parameters. qP and ΦPSII have reasonably strong positive and negative correlations with many of the other parameters, especially NPQ parameters.

Looking specifically at photosynthetic parameters, magnitude of NPQ had stronger correlations with other measured parameters than speed of induction or relaxation. Speed of relaxation had slightly stronger correlations with other traits than induction speed. Magnitude of NPQ had an inverse relationship with silique number. The parameters of T_{crit}, m1 and m2 had only weak correlations with other traits compared to other photosynthetic parameters tested, apart from qP and ΦPSII, where moderately strong correlations were observed

Looking specifically at unrelated parameters, pigment contents only had weak correlations with other traits. Looking just at pigment contents, chlorophyll *a* had a

stronger correlation with unrelated traits than chlorophyll *b* or carotenoids did. Silique number showed strong correlations with NPQ magnitudes plus speed of induction and relaxation of NPQ, and also was moderately linked with qP and F_q'/F_m' (ϕPSII).

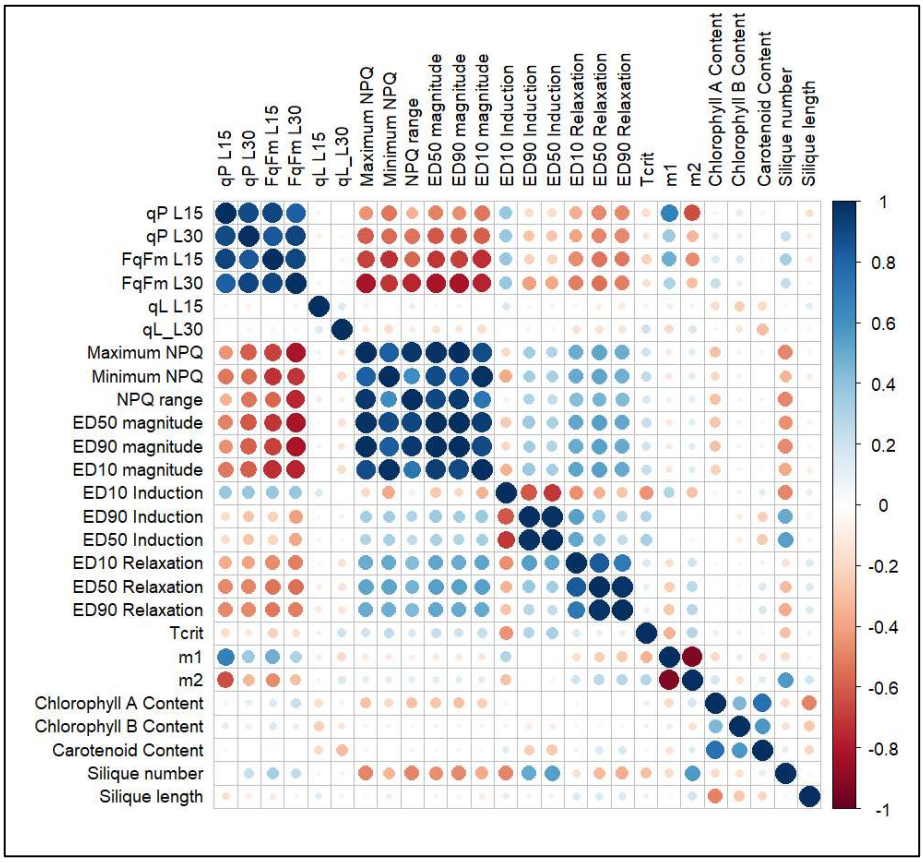

Figure 5.11. Correlation matrix showing correlations between different parameters used in Chapter 4 and 5 from only plants of all genotypes exposed to 32°C for five days measured five days after bolting.

Overall, the correlations seen in **Figure 5.10** are weaker than looking at correlations between parameters in just plants after heat stress in **Figure 5.11**. Magnitude of NPQ had a stronger negative correlation to qP and ΦPSII in plants after heat stress than correlation strength seen among all data. T_{crit}, m_1 and m_2 had stronger correlations with other traits after heat stress, including a stronger correlation between Tcrit and NPQ parameters. Looking at correlations between unrelated parameters in **Figure 6.10**, after heat stress , induction speed of NPQ had stronger correlation with silique length than seen in **Figure 5.11.**

5.4 Discussion

T-DNA insertion mutants in *A. thaliana* were assessed for fertility and root architecture traits in abiotic stress conditions. The results were then combined with results seen in Chapter 4, in order to assess which of the mutants may be best candidate gene mutations for future heat tolerant crop breeding. Traits across Chapter 4 and this chapter were used to assess whether unrelated traits may have links, which would aid future phenotyping experimental design.

5.4.1 T-DNA insertions do not have a detrimental effect on roots during heat stress

Root lengths were measured under multiple abiotic stress treatments to quickly gather quantitative analysis of root architecture phenotypes. This screen can also be useful to estimate whether these mutants have roles in other abiotic stresses that are commonly associated with heat, which can be used to effectively design future studies.

In control conditions, heat stress and salinity stress, mutations in the selected genes did not appear to have any detrimental effects on root lengths, as no mutants were shown to have significantly shorter root lengths than that of the WT. This can indicate that in these stresses, the mutants still have relatively the same root growth rates to that of the WT, however this analysis on root systems was done at an early stage of maturity, and on agar, therefore can only give early indications on the effect these mutations have on root architecture. Avoiding mutants with inhibited root growth will be essential for crop breeding, due to length and density of roots being linked to water and nutrient uptake and therefore resources needed for growth and development. Further analysis of root branching and root hair architecture could also quantify the spread and scope of root systems under mutations of the selected genes.

Findings in this study can be compared with that of Reboulet et al., (2010), where in *AtDIS1*, no differences in root growth were seen in control conditions over 24hrs, whereas findings showed an increase in root length. This suggests that it may take several days to clearly show significant differences in root traits. The findings by Reboulet et al., (2010) also showed that in dark grown seedlings, mutations in *AtDIS1*

had a decrease in root growth, which suggests that alongside results (done in light conditions), *AtDIS1* has a larger role in root growth in dark conditions than in light.

During drought, while half the roots had longer roots than the WT, half of the mutants showed a significantly shorter root, which could be caused by a greater inhibition of growth in drought conditions. In drought conditions it is important for the plant to use resources to increase root depth, in order to reach water deeper in the soil, therefore mutants showing inhibited growth during drought would not be good candidates for drought related stress tolerance. With the other half of the mutants showing significantly longer root lengths than the WT in drought, this shows mutations in selected genes may overcome the inhibition of root growth and development seen in droughted root system. It also may indicate that mechanisms involved in heat stress could be beneficial in drought stress.

Zeng et al., (2016) saw that At*GAPB* in drought conditions were intermittently up and downregulated, which could account for the significant differences in root length. In heat stress, At*GAPB* is only upregulated in shoots, which may be the reason for no differences in root length compared to WT after heat stress.

5.4.2 Mutants show no loss of silique size or number in control conditions.

Looking at fertility of the mutants provides insight as to whether they would be good candidates for future research into environmental stress tolerance, specifically heat, as fertility has a strong relationship with yield of crop species.

In control conditions, no mutant showed significant loss in fertility in comparison to the WT indicating that during normal growth, the T-DNA mutants are not directly involved with or have a large effect on fertility. The fertility screen also showed some genes that have better fertility phenotypes than the WT, with *Abcf5*, *T8p21*, *Zne1* showing in control conditions to have greater number of siliques and longer siliques than the WT, which indicates a possibility that mutations in these genes may produce higher yield in crop species.

During heat stress, whilst many of the mutants retained fertility phenotypes similar to that of the WT, some showed an increased susceptibility to heat in terms of silique

length and number. When heat was applied to *Sytb*, there were significantly fewer siliques and shorter siliques than the WT, implying a lower seed count. After five days heat stress, *Cals1* showed fewer siliques than the WT and *Apg3* showed to have shorter siliques, which also implies a lower seed count. The negative impacts these mutants have on plant fertility show that knockout mutants in genes may not be good candidates for crop breeding for heat stress tolerance due to possible negative impact on yield, however further tests could be done on overexpression mutants in these genes. Seed count could be examined in these mutants to confirm this. Although *Apg3*, *T8P21*, *Zne1* and *Gapb* showed a reduction in silique length or number when exposed to heat stress, the changes were not substantial enough that they showed significant differences to the WT when exposed to heat therefore further studies particularly in seed number should be done before determining if this shows a significant detrimental effect on fertility and therefore yield. Plant reproduction can be affected by heat in a number of ways and in a variety of tissues, in order to determine how genes play a role in fertility, mutants with affected phenotypes during heats stress can be assessed for male and female reproductive traits such as pollen sterility.

Those mutants with a decreased silique length after heat stress showed a reduction in length across the stem, not only in the siliques developing during or just after heat stress. This indicates that the mutations do not allow for recovery of silique length after heat stress has subsided.

By assessing fertility phenotypes, mutants that show negative traits can be easily ruled out from considerations for heat tolerant breeding, as even for mutants that show positive traits in other aspects of plant physiology, fertility indicates the most economically viable phenotypic trait. To see which genes show potential for increasing crop yield, parameters related to grain number, such as seed count can also be assessed.

5.4.3 T-DNA insertion mutants have few detrimental effects on traits assessed

Looking at the overall performance of T-DNA insertion mutants, no mutants stood out as having performed outstandingly better than the WT in control conditions or during heat stress. However, there were subtle beneficial differences among some parameters.

What is more important, at this stage in crop breeding, is the mutations did not cause any overwhelmingly negative traits, even though again some negative differences were seen, which indicates that mutations in the chosen genes do not severely impact plant function. The subtle differences seen in mutants and WT after heat stress are fewer than expected due to the method in which these mutants were chosen. Tcrit may show species specific mechanisms of heat stress tolerance, which may not be transferable across species, or from monocots to dicots.

In around half of the mutants, especially after heat stress, a lower L15 NPQ and lower L30 NPQ was seen, which highlights the potential scenario of the mutants faring better in low light conditions where NPQ isn't required but would be more detrimental in saturated light conditions when more NPQ is needed. The fact that this lower L15 and lower L30 NPQ is seen in tandem, means the negatives of having a lower L30 NPQ may not be as important as other negatives seen when weighing up performance of the mutants.

When weighing up mutants of interest for future crop breeding and potential, the mutants *Sytb*, *Cals1*, *Apg3* showed negative fertility phenotypes, so would not be regarded as potential candidates. *Sis8* showed a positive fertility phenotype, and few detrimental traits, however showed few positive traits after heat stress, performing similarly to that of the WT.

Bch1, *Bch2, T8tp2, Abcf5* and *Zne1* showed beneficial fertility traits in control, which shows better yield potential. Out of these, *T8p21* showed beneficial photosynthetic traits after heat stress, and *Abcf5* and *Zne1* showed increase in chlorophyll *b* after heat stress. Out of all the mutants, none showed a large number of negative traits after heat stress or in control conditions, but from performance, *Abcf5*, *Zne1* and *T8p21* performed best overall.

5.4.4 Correlations between parameters can link physiological processes

Correlations between traits assessed in both Chapter 4 and this chapter were calculated. As expected, related parameters had strong correlations, however correlations between unrelated parameters give us more information about traits linked

to other physiological processes happening within the plant. Correlations between unrelated parameters can give an indication of physiological links between processes within the plant, plus an indication of which parameters are most important when plant phenotyping.

The measures of qL at two stable points in the experimentation seen in chapter 4 had very little correlation with other parameters, therefore may not provide a relevant assessment of plant performance as a whole.

What stands out most from this study is the relationship between several photosynthetic parameters, in particular NPQ magnitude, and silique length. These correlations were stronger after heat stress. This emphasizes physiological links between silique length and NPQ and therefore can link NPQ traits with fertility.

This was also seen with correlations between silique length and Tcrit, m_1 and m_2 after prior heat stress. In particular, a strong negative correlation between m_2 and silique length was seen. This is of interest as m_2 is the rapid decline of F_v/F_m after the critical temperature, which is relatively unstudied, and suggests m_2 may be a more valuable parameter when looking at plant performance than initially thought.

5.5 Conclusions

While the yield potential of *Cals1*, *Sytb* and *Apg3* seem to be uncertain due to negative fertility traits, the rest of the mutants did not have major negative traits when it came to other parameters. *Abcf5*, *Zne1*, *Bch1*, *Bch2* and *T8p21*, were identified as the parameters with the most potential for future breeding for heat tolerance. The next steps would be to assess further growth and development parameters such as biomass and growth rate in heat stress exposure. This could be then used to design targeted mutagenesis in crop species.

As stated in chapter 3 and 4, the T-DNA insertion lines were selected for T_{crit} in Rice, however mutations in the *A. thaliana* orthologue genes showed little differences. The findings in this chapter showing that T_{crit} showed only weak correlations to other parameters, yet m_1 and m_2 show strong correlations with qP and ΦPSII. This could mean that while differences in T_{crit} are not seen across species, however m_1 and m_2 may be more transferable.

The high throughput screens done within this chapter and chapter 4, show that some of the parameters used can be good screens for crop breeding. Magnitude of NPQ, Speed of NPQ induction and relaxation, qP and ΦPSII can all be done in one screen over 45-minute measures and have all provided insight into unrelated traits. Of particular interest this chapter highlighted the links between the silique length and therefore fertility traits.

6 General Discussion

The process of developing abiotic stress resilient crops goes through clear steps from the experimental design to testing crops with targeted mutagenesis in the field. These steps can include:

1. Identification of genes of interest for mutagenesis
2. Developing mutant lines in model species
3. Initial phenotyping of mutants in model species
4. Developing mutant lines in crop species
5. Glasshouse/growth room studies of mutant lines in crop species
6. Phenotyping of mutant lines in crop species in the field
7. Abiotic stress field trials of mutant lines in crop species
8. Commercialisation of viable abiotic stress tolerant lines in crop species

In this study, chapters focussed on three of these key steps, identifying genes of interest, initial phenotyping of mutants, and bringing previously developed and characterised mutants from studies in the glasshouse and growth rooms into field conditions.

6.1 Candidate genes for targeted mutagenesis for abiotic stress tolerance

In this study mutants in the genes *Prt6*, *Abi5* and *Ntaq* in Barley (*Hordeum vulgare*) were examined as candidates for targeted mutagenesis in crops in the field, and 15 different mutants in *A. thaliana* for candidates for initial phenotyping for abiotic stress tolerance.

Table 6.1:Summary of findings

Gene	Previous publications	This study's findings
PRT6	**Mendiondo et al., 2016, Holdsworth et al., 2020** Mutants show tolerance to waterlogging in both Barley and A. thaliana and constitutive expression of anaerobic metabolism genes. Pathway linked to stress tolerance	• Alleles *prt6.k* and *prt6.i* showed promising results in both cultivars tested. • In backcrossed lines, (*prt6.e, prt6.k, prt6.i, prt6.h*) no major negative traits were found • Some alleles showed increased spike length, biomass partitioning, estimated weight at anthesis, grain number per spike and fruiting efficiency. • Some lines showed reduced biomass
NTAQ	**Holdsworth et al., 2020** Pathway linked to stress tolerance	• Few differences were seen between WT and mutants • *ntaq.i* showed a reduction in spike length as its only significant difference to the WT. • *ntaq.f* showed improved biomass partitioning and number of grains per spike
ABI5	**Kanai et al., 2010; Collin et al., 2020** Phosphorylation causes promotion of stress response genes	• Mutants showed a mix of positive and negative traits. • None of the mutants showed to have no negative traits, however this could be due to the lines not being backcrossed. • Fertility was seen to be reduced in 3/5 mutants (*abi5.d, abi5.e and abi5.w*)
DG1	**Chi et al., 2008; Yan et al., 2020** Disruption of chloroplast development in heat stress and control conditions. Reduction of F_v/F_m during heat stress	• During heat stress and in control conditions, there was also a lower L15 and L30 NPQ and magnitude of NPQ. • During heat mutants also had an increased ΦPSII and faster induction/ relaxation rate of NPQ
ZNE1	**Wang et al., 2021** Regulator of homeostasis as a Zn^{2+} transporter	• Mutants had a slower m_2, lower qP, plus a higher number of siliques, which were also found to be longer • During heat stress, NPQ had a slower induction rate and higher chlorophyll b concentration
T8P21	**Sharma et al., 2021** Showed more than a two-fold change response to heat in IR64 Annapurna seedlings	• In both heat and control treatments, mutants had a lower magnitude of NPQ as well as lower L15 and L30 NPQ and faster relaxation of NPQ • In control conditions mutants also had an increase in qP and ΦPSII, longer siliques and a higher number of siliques. • During heat stress, there was an increase in chlorophyll b content and a faster rate of m_1
MUSE3	**Adler et al., 2017** Differentially induced following heat stress	• In control treatments, mutants had a higher magnitude of NPQ and slower relaxation rates • After heat stress, mutants had a slower relaxation rate, lower qP, lower ϕPSII, increased chlorophyll a content and higher T_{crit}

		• Recovered plants showed a lower qP, qL and ϕPSII
SYTB	**Schapire et al., 2008; Yamazaki et al., 2008; Perez Sancho et al., 2015.** Mutations in *SYTB* have been found to have abiotic stress tolerance including heat resistance	• In control conditions, mutants showed a lower magnitude of NPQ and slower rates of NPQ relaxation • During heat treatments, mutants showed a lower L15 and L30 NPQ, slower rates of relaxation, lower qP, shorter siliques and fewer siliques • After recovery from heat mutants showed a slower m_1 and lower qP
SIS8	**Gao and Xiang 2008; Sharma et al., 2021** Possible on/off switch for stress response. In rice, expression showed more than a two-fold decrease in response to heat	• Mutants in control conditions had a lower magnitude of NPQ, lower qP, higher chlorophyll b content and higher carotenoid content • During heat stress, mutants had a higher magnitude of NPQ, faster rate of NPQ induction, higher carotenoid content, longer root length, and higher concentration of chlorophyll b • During recovery from heat, mutants showed a lower L15 and L30 NPQ
WRKY55	**Baxter et al., 2014; Rivas-San Vicente and Plasencia, 2011** Shown to be a positive regulator of ROS and SA in *A. thaliana*	• In control conditions, magnitude of NPQ was lower, induction of NPQ was faster, L15 and L30 NPQ was lower, and roots were longer. • During heat stress, mutants also showed a lower L15 and L30 NPQ and a lower NPQ magnitude, as well as higher ϕPSII and chlorophyll a content • After recovery from heat, NPQ induction was faster
CALS1	**Lui et al., 2022; Luan et al., 2023** Species specific regulation during heat stress. Linked to callose deposition in the phloem during heat stress	• Mutants have a lower magnitude of NPQ, slower rate of relaxation in both control conditions and after heat treatment • After heat treatment there was also a lower L15 and L30 NPQ, lower qP, lower ϕPSII, higher T_{crit}, slower rate of NPQ induction, higher chlorophyll b content, less siliques and longer siliques • In recovery, there was a faster rate of m_1, lower magnitude of NPQ, lower qL and lower ϕPSII
BCH1	**Tian et al., 2003; Du et al., 2010; Kim et al., 2009** *A. thaliana* mutants show reduction in F_v/F_m and reduction in pigment content. Both rice and *A. thaliana* mutants show NPQ induction/magnitude	• Mutants show a lower magnitude of NPQ, faster rate of relaxation, longer siliques, and longer roots. • During heat, there was a lower L15 and L30 NPQ and higher NPQ magnitude
BCH2	**Tian et al., 2003; Du et al., 2010; Kim et al., 2009** *A. thaliana* mutants show reduction in F_v/F_m and reduction in pigment content. Both rice and *A. thaliana* mutants show NPQ induction/magnitude	• Mutants showed a faster rate of NPQ relaxation, higher qP, higher ϕPSII and longer siliques • After heat treatment, mutants showed a faster rate of m_2 and lower magnitude of NPQ

GAPB	**Liu et al., 2020** Overexpression in rice has been shown to increase CO_2 assimilation rate and chlorophyll content. T-DNA mutants in *A. thaliana* shown to have a decrease in photosynthetic carbon fixation rates, and a lower rate of photosynthetic electron transport (J_{max})	• In control treatment, mutants showed a lower magnitude of NPQ and a lower L15 and L30 NPQ • In heat treatment, mutants showed a faster rate of m_2, a lower magnitude of NPQ, a higher L15 and L30 NPQ and higher ϕPSII
ABCF5	**Jangam et al., 2016; Rensink et al., 2005;** **Liu et al., 2011** Role in regulation of stress response, induced by abiotic stress	• In control conditions, mutants showed a slower rate of m_1, higher chlorophyll b content, higher carotenoid content, higher number of siliques, and longer siliques • After heat treatment, mutants showed a lower qL, higher chlorophyll b content, higher carotenoid content, slower induction of NPQ and a faster rate of m_2
APG3	**Motohashi et al., 2007** Mutants have reduction in content of chlorophyll-a, chlorophyll-b, and β-carotene	• In control conditions, mutants had a lower qP, lower ϕPSII • In eat treatment, mutants had around double the chlorophyll b content compared to WT and a slower rate of NPQ induction
HO2	**Li et al., 2014;** **Emborg et al., 2006** Rice mutants show reduction in chlorophyll accumulation, smaller reductions in chlorophyll are seen in *A. thaliana*	• In control conditions, mutants had a lower magnitude of NPQ, slower rate of NPQ relaxation, lower L15 NPQ, higher qL, higher qP and higher ϕPSII • After heat treatment, mutants showed to have a lower L15 and L30 NPQ, faster rate of NPQ induction and relaxation, and a higher ϕPSII
DIS1	**Jiang et al., 2012;** **Zhao et al., 2013;** **Sun et al., 2019;** **Qi et al., 2017** Mutants show reduced stomatal regulation and increased water loss	• In control conditions, mutants had a higher T_{crit}, lower magnitude of NPQ, higher qL, higher qP, and higher ϕPSII • In heat treatment, mutants had a higher magnitude of NPQ.

Table 6.1: Summary mutants studied: published findings and findings in this study.

One of the first steps to developing new genetic resources for crop development against abiotic stress is the identification of genes that may have a role in abiotic stress tolerance. Positive and negative effects on photosynthetic parameters such as NPQ and efficiency of PSII as well as other parameters such as pigment content, root length and fertility were seen among many of the T-DNA insertion mutations studied. Out of the 15 genes selected in *A. thaliana*, *Abcf5, Zne1,* and *T8p21,* were selected as the insertion mutations showing most promise, however there were only few significant differences in tested parameters. More information may have been gathered if biomass and growth was studied in the mutants, to give a larger idea of the effect they have on important traits alongside photosynthetic heat stress tolerance. These three mutants were

narrowed down from a large pool of genes, enabling for future wider studies to focus on these genes of interest.

Some of the mutants (*Gapb, sytb, cals1* and *Apg3*) were highlighted as having detrimental phenotypes in terms of photosynthesis (during and before heat), as well as reduced fertility. T-DNA insertion mutants performing badly indicates these genes downregulated may cause sensitivity, therefore they are of interest in further studies however methods in which the gene is overexpressed would be beneficial. Therefore, the identification of genes in this study isn't limited to mutants performing well.

This study tested mutagens of genes previously reported to increase abiotic stress resistance. While growth room and glasshouse trials provide initial data on plant characteristics and potential performance, field trials are needed for validating these findings in real-world agricultural conditions. By testing plants in field, they ensure that new plant varieties are not only scientifically sound but also practically viable and beneficial for farmers and ecosystems. Growth rooms and glasshouses provide controlled environments with stable temperature, humidity, and light conditions, whereas field trials expose plants to natural conditions, including variations in weather, soil types, and biotic factors (e.g., pests and diseases).

TILLING mutants in *prt6* in previous studies in a range of species have shown to have positive effects on the tolerance to abiotic stresses (Mendiondo et al., 2016; Riber et al., 2015, Weits et al., 2014; Gibbs et al 2011), but little is published about the performance in the field. Seeing results in Chapter 3, there were no concerning decreases in fitness among the *prt6* mutants, indicating that *prt6* mutants are suitable for further field trials including trials in abiotic stress conditions. This is similar to results by Mendiondo et al (2016), which showed differences in biomass and yield between RNAi lines and WT in waterlogged stress conditions, but not in non-stressed conditions. In this study, differences in timing of development was seen in the *prt6* mutants which may aid farming practices to avoid abiotic stress during key developmental steps of the crop such as flowering or GS31. Of note, there were key differences in lines due to location of mutations within the gene, with beneficial traits being seen more in mutants within the conserved UBR-box domain, even though the mutant targeting that domain had not been backcrossed, which usually would put any TILLING line at a disadvantage when comparing to WT. This indicates there may be

a benefit to concentrating on further development in mutants within the UBR-box domain, including *ubr.c* within Barley after backcrossing.

TILLING mutants in the *NTAQ* gene proved to be ideal candidates for further research, as a gene that may be of use in future stress resistance in crops, as mutations in two different locations in the gene provided very little negative effects on plant fitness. With the links between knockout of Arg/N-degron pathways and abiotic stress tolerance, this is new prospect for new genetic resources in crop plants for increasing stress tolerance.

Abi5 mutants were tested in the field, however at this stage in experimentation, due to the negative traits seen, without repeating testing after backcrossing out unwanted mutations, *abi5* mutants do not show a positive outlook in further breeding.

In summary, from these results, the *ubr.c* mutant, or other mutants in the UBR domain of the *PRT6* gene has been shown to be a good candidate for taking forward to further field trials, including those in abiotic stress conditions alongside mutations in *NTAQ* (with emphasis on mutations in the splice junction in exon 2). *ABCF5, ZNE1,* and *T8P21* have also been identified as potential candidates for heat stress tolerance enhancement, as well as *Gapb, sytb, Cals1* and *Apg3* as possible candidates for studies overexpressing genes for enhanced heat stress tolerance.

6.2 Chlorophyll fluorescence and GWAS as important tools for forward genetics.

Forward genetics is a molecular genetic approach to identify genes behind plant phenotypes. Due to the large number of genes within different plant species, with different mechanisms, pathways and biological roles, large screens such as GWAS and chlorophyll fluorescence screens are key tools in forward genetics. GWAS can uncover novel genes and biological pathways involved in trait development. This fundamental knowledge can lead to new targets for genetic modification or traditional breeding, potentially leading to breakthroughs in crop improvement.

Genes of interest were identified through a GWAS previously done by Robson et al., (2023), based on genes underlying loci associated with photosynthetic heat tolerance,

before testing T-DNA insertion mutants in orthologue *A. thaliana* genes for photosynthetic heat tolerance. Chlorophyll fluorescence screens for broader photosynthetic function in the plant can be a fast and efficient way to validate results of a GWAS screening for a single trait, which in this case was T_{crit}. Working with GWAS outputs and the high throughput screens enabled by chlorophyll fluorescence enables the testing of a large number of genes at once to accelerate the identification of candidate genes, as well as functional validation of heat stress tolerance. One of the genes targeted in T-DNA insertion mutations, T8p21 was previously relatively uncharacterised, and performed well under heat stress, which shows the effectiveness of using GWAS and chlorophyll fluorescence screens to identify novel genes linked to abiotic stress tolerance

One major finding that came out of this study, was not in the mutants but in the findings in correlations between parameters tested, with many chlorophyll fluorescence parameters, showing that photosynthetic parameters such as magnitude of NPQ and relaxation rate of NPQ and ΦPSII have strong correlations with silique number and weak correlations with silique length. There is very little prior knowledge about the links with yield parameters such as silique length. Araus et al., (1998) used chlorophyll fluorescence as a selection criterion for grain yield in wheat, where they found a correlation ($P < 0.001$) between grain yield and Fo. In wheat, Moffatt et al., (1990) descried a negative correlation between F_v and grain yield in controlled environments, but positively and not significantly correlated in the field conditions. As fertility in this study was not the prime focus of experimentation, only basic quantifications of fertility were observed (silique length and number), and given findings, further in depth parameters such as seed number may have given a clearer picture of correlations between photosynthetic parameters and yield. If a link was to be found in seed number, chlorophyll fluorescence parameters such as magnitude of NPQ and relaxation rate of NPQ and ΦPSII could provide a quick and efficient high throughput method of testing large numbers of lines for indications of increased yield.

6.3 Reflections on Methodology

A significant aspect of the experimental design in this study focused on testing mutants in the field using barley. As previously discussed, field trials are typically conducted following extensive studies in controlled glasshouse conditions to establish links to desirable traits, such as abiotic stress tolerance. While *PRT6* has been widely studied under these conditions in several publications, *ABI5* and *NTAQ* have been investigated to a lesser extent. Therefore, prior to field trials, additional experiments in glasshouse and growth room settings could have been conducted on these mutants to ensure a stronger foundation for field testing. Additionally, lines not yet backcrossed could have undergone further breeding to eliminate unwanted mutations, allowing for a clearer confirmation that observed phenotypes were indeed caused by mutations in the targeted genes.

Furthermore, T-DNA insertion mutants were tested for photosynthetic heat stress tolerance, fertility, and root architecture. Chlorophyll and carotenoid content were assessed using absorbance measurements taken with a plate reader. However, this method resulted in high data variance. Ideally, if time constraints had not been a factor, pigment contents would have been measured using a spectrophotometer with cuvettes, a method more commonly used in practice for greater accuracy. The study also observed differences in fertility, specifically in the length and number of siliques in *A. thaliana.* To further investigate these significant differences, additional analyses could have been performed, such as documenting aborted siliques or conducting pollen staining.

6.4 Future perspectives

As described, the mutants associated with genes assessed in this work at very different stages of using targeted mutagenesis for crop improvement for abiotic stress tolerance

The next steps for the work with identifying candidate genes for increased heat stress tolerance discussed in Chapter 4, Chapter 5 and Chapter 6, is to test a smaller group of those mutants: ones showing positive traits as well as ones showing sensitivity to heat, using different intensities of heat, and heat stress at different growth stages of the plant. It would be beneficial to expand on the findings in Chapter 5 and Chapter 6 by

including more parameters around growth and development, to compare with parameters used in this study, and get a better understanding of how mutations may perform in crop species. Targeted mutations in orthologues of the genes of interest could then be tested in crop species.

All mutants tested in the field (*Prt6, Abi5,* and *Ntaq*) need to be retested in another growing season in order to confirm findings, with an emphasis on reducing disease and pests. Trials can then take place in abiotic stress conditions. It is important to backcross those mutants that are yet to be backcrossed as unwanted mutations in the plants may be causing unwanted phenotypes. More growth room and glasshouse work would also be beneficial in *Abi5* and *Ntaq* mutants, including characterisation of mutants in these genes in *A. thaliana*. This would expand understanding of how these genes are involved in abiotic stress tolerance.

References

Abdallah, N.A., Elsharawy, H., Abulela, H.A., Thilmony, R., Abdelhadi, A.A. and Elarabi, N.I., 2022. Multiplex CRISPR/Cas9-mediated genome editing to address drought tolerance in wheat. *GM Crops & Food*, pp.1-17.

Adeyemi, O., Grove, I., Peets, S. and Norton, T., 2017. Advanced monitoring and management systems for improving sustainability in precision irrigation. *Sustainability*, *9*(3), p.353.

Ahn, Y.J., Claussen, K. and Zimmerman, J.L., 2004. Genotypic differences in the heat-shock response and thermotolerance in four potato cultivars. *Plant Science*, *166*(4), pp.901-911.

Ahsan, N., Lee, D.G., Lee, S.H., Lee, K.W., Bahk, J.D. and Lee, B.H., 2007. A proteomic screen and identification of waterlogging-regulated proteins in tomato roots. *Plant and Soil*, *295*, pp.37-51.

Akhtar, I. and Nazir, N., 2013. Effect of waterlogging and drought stress in plants. *International Journal of Water Resources and Environmental Sciences*, *2*(2), pp.34-40.

Alabdallah, N.M., Hasan, M.M., Hammami, I., Alghamdi, A.I., Alshehri, D. and Alatawi, H.A., 2021. Green synthesized metal oxide nanoparticles mediate growth regulation and physiology of crop plants under drought stress. *Plants*, *10*(8), p.1730.

Allakhverdiev, S.I., Kreslavski, V.D., Klimov, V.V., Los, D.A., Carpentier, R. and Mohanty, P., 2008. Heat stress: an overview of molecular responses in photosynthesis. *Photosynthesis Research*, 98, pp.541-550.

Alonso, J.M. and Stepanova, A.N., 2003. T-DNA mutagenesis in *A. thaliana*. *Plant Functional Genomics*, pp.177-187.

Alqurashi, M., 2019. *Investigating the role Of RAP2. 12 and GAPDH in photosynthetic CO_2 fixation to improve drought tolerance* (Doctoral dissertation, University of Essex).

Anderson, J.M., Chow, W.S. and Park, Y.I., 1995. The grand design of photosynthesis: acclimation of the photosynthetic apparatus to environmental cues. *Photosynthesis Research*, 46, pp.129-139.

Anderson, R., Bayer, P.E. and Edwards, D., 2020. Climate change and the need for agricultural adaptation. *Current Opinion In Plant Biology*, *56*, pp.197-202.

Araus, J.L. and Cairns, J.E., 2014. Field high-throughput phenotyping: the new crop breeding frontier. *Trends In Plant Science*, 19(1), pp.52-61.

Aro, E.M., Suorsa, M., Rokka, A., Allahverdiyeva, Y., Paakkarinen, V., Saleem, A., Battchikova, N. and Rintamäki, E., 2005. Dynamics of photosystem II: a proteomic approach to thylakoid protein complexes. *Journal Of Experimental Botany*, 56(411), pp.347-356.

Aslam, M.M., Rashid, M.A.R., Siddiqui, M.A., Khan, M.T., Farhat, F., Yasmeen, S., Khan, I.A., Raja, S., Rasool, F., Sial, M.A. and Yan, Z., 2022. Recent insights into signalling responses to cope drought stress in rice. *Rice Science*, *29*(2), pp.105-117.

Athar, H.U.R., Zafar, Z.U. and Ashraf, M., 2015. Glycinebetaine improved photosynthesis in canola under salt stress: evaluation of chlorophyll fluorescence parameters as potential indicators. *Journal Of Agronomy And Crop* Science, *201*(6), pp.428-442.

Baalmann, E., Scheibe, R., Cerff, R. and Martin, W., 1996. Functional studies of chloroplast glyceraldehyde-3-phosphate dehydrogenase subunits A and B expressed in Escherichia coli: formation of highly active A 4 and B 4 homotetramers and evidence that aggregation of the B 4 complex is mediated by the B subunit carboxy terminus. *Plant Molecular Biology*, *32*, pp.505-513.

Backhausen, J.E., Vetter, S., Baalmann, E., Kitzmann, C. and Scheibe, R., 1998. NAD-dependent malate dehydrogenase and glyceraldehyde 3-phosphate dehydrogenase isoenzymes play an important role in dark metabolism of various plastid types. *Planta*, *205*, pp.359-366.

Badhan, S., Ball, A.S. and Mantri, N., 2021. First report of CRISPR/Cas9 mediated DNA-free editing of 4CL and RVE7 genes in chickpea protoplasts. *International Journal Of Molecular Sciences*, *22*(1), p.396.

Bahrami, F., Arzani, A. and Rahimmalek, M., 2019. Photosynthetic and yield performance of wild barley (*Hordeum vulgare* ssp. spontaneum) under terminal heat stress. *Photosynthetica*, 57(1).

Bailey-Serres, J., Parker, J.E., Ainsworth, E.A., Oldroyd, G.E. and Schroeder, J.I., 2019. Genetic strategies for improving crop yields. *Nature*, *575*(7781), pp.109-118.

Baker, N.R. and Rosenqvist, E., 2004. Applications of chlorophyll fluorescence can improve crop production strategies: an examination of future possibilities. *Journal Of Experimental Botany*, *55*(403), pp.1607-1621.

Baker, N.R., 2008. Chlorophyll fluorescence: a probe of photosynthesis in vivo. *Annual Review Of Plant Biology*, 59, pp.89-113.

Balfagón, D., Rambla, J.L., Granell, A., Arbona, V. and Gomez-Cadenas, A., 2022. Grafting improves tolerance to combined drought and heat stresses by modifying metabolism in citrus scion. *Environmental And Experimental Botany*, 195, p.104793.

Banerjee, A. and Roychoudhury, A., 2017. Abscisic-acid-dependent basic leucine zipper (bZIP) transcription factors in plant abiotic stress. *Protoplasma*, *254*, pp.3-16.

Behrens, F.H., Schenke, D., Hossain, R., Ye, W., Schemmel, M., Bergmann, T., Häder, C., Zhao, Y., Ladewig, L., Zhu, W. and Cai, D., 2019. Suppression of abscisic acid biosynthesis at the early infection stage of *Verticillium longisporum* in oilseed rape (*Brassica napus*). *Molecular Plant Pathology*, *20*(12), pp.1645-1661.

Berendzen, K., Searle, I., Ravenscroft, D., Koncz, C., Batschauer, A., Coupland, G., Somssich, I.E. and Ülker, B., 2005. A rapid and versatile combined DNA/RNA extraction protocol and its application to the analysis of a novel DNA marker set polymorphic between *A thaliana. thaliana* ecotypes Col-0 and Landsberg erecta. *Plant Methods*, 1, pp.1-15.

Berry, J. and Bjorkman, O., 1980. Photosynthetic response and adaptation to temperature in higher plants. *Annual Review of Plant Physiology*, 31(1), pp.491-543.

Bertier, L.D., Ron, M., Huo, H., Bradford, K.J., Britt, A.B. and Michelmore, R.W., 2018. High-resolution analysis of the efficiency, heritability, and editing outcomes of CRISPR/Cas9-induced modifications of NCED4 in lettuce (Lactuca sativa). *G3: Genes, Genomes, Genetics,* 8(5), pp.1513-1521.

Bhatt, R.M. and Rao, N.S., 2005. Influence of pod load on response of okra to water stress. *Indian Journal of Plant Physiology*, *10*(1), p.54.

Bista, D.R., Heckathorn, S.A., Jayawardena, D.M. and Boldt, J.K., 2020. Effect of drought and carbon dioxide on nutrient uptake and levels of nutrient-uptake proteins in roots of barley. *American Journal of Botany*, 107(10), pp.1401-1409.

Bouvier, F., Keller, Y., d'Harlingue, A. and Camara, B., 1998. Xanthophyll biosynthesis: molecular and functional characterisation of carotenoid hydroxylases

from pepper fruits (Capsicum annuum L.). *Biochimica Et Biophysica Acta (BBA)-Lipids and Lipid Metabolism*, *1391*(3), pp.320-328.

Brizmohun, R., 2019, August. Impact of climate change on food security of small islands: The case of Mauritius. In *Natural Resources Forum* (Vol. 43, No. 3, pp. 154-163). Oxford, UK: Blackwell Publishing Ltd.

Brocard, I.M., Lynch, T.J. and Finkelstein, R.R., 2002. Regulation and role of the *A. thaliana* abscisic acid-insensitive 5 gene in abscisic acid, sugar, and stress response. *Plant Physiology*, *129*(4), pp.1533-1543.

Brody, S.S., 1958. New excited state of chlorophyll. *Science*, *128*(3328), pp.838-839.

Burgess, A.J., Retkute, R., Herman, T. and Murchie, E.H., 2017. Exploring relationships between canopy architecture, light distribution, and photosynthesis in contrasting rice genotypes using 3D canopy reconstruction. *Frontiers In Plant Science*, 8, p.244391.

Buttery, B.R. and Buzzell, R.I., 1977. The relationship between chlorophyll content and rate of photosynthesis in soybeans. *Canadian Journal Of Plant Science*, 57(1), pp.1-5.

Bykowski, M., Mazur, R., Wójtowicz, J., Suski, S., Garstka, M., Mostowska, A. and Kowalewska, Ł., 2021. Too rigid to fold: Carotenoid-dependent decrease in thylakoid fluidity hampers the formation of chloroplast grana. *Plant Physiology*, 185(1), pp.210-227.

Cao, M., Liu, X., Zhang, Y., Xue, X., Zhou, X.E., Melcher, K., Gao, P., Wang, F., Zeng, L., Zhao, Y. and Deng, P., 2013. An ABA-mimicking ligand that reduces water loss and promotes drought resistance in plants. *Cell Research*, *23*(8), pp.1043-1054.

Capell, T. and Christou, P., 2004. Progress in plant metabolic engineering. *Current Opinion In Biotechnology*, *15*(2), pp.148-154.

Casal, J.J. and Balasubramanian, S., 2019. Thermomorphogenesis. *Annual review of plant biology*, *70*(1), pp.321-346.

Bhargavi, B., Kalpana, K. and Reddy, J.K., 2017. Influence of water stress on morphological and physiological changes in Andrographis paniculata. *Indian Journal of Pure & Applied Biosciences, 5*, pp.1550-1556.

Casaretto, J. and Ho, T.H.D., 2003. The transcription factors HvABI5 and HvVP1 are required for the abscisic acid induction of gene expression in barley aleurone cells. *The Plant Cell*, *15*(1), pp.271-284.

Chang, L., Guo, A., Jin, X., Yang, Q., Wang, D., Sun, Y., Huang, Q., Wang, L., Peng, C. and Wang, X., 2015. The beta subunit of glyceraldehyde 3-phosphate dehydrogenase is an important factor for maintaining photosynthesis and plant development under salt stress—Based on an integrative analysis of the structural, physiological and proteomic changes in chloroplasts in *Thellungiella halophila*. *Plant Science*, *236*, pp.223-238.

Chawade, A., Sikora, P., Bräutigam, M., Larsson, M., Vivekanand, V., Nakash, M.A., Chen, T. and Olsson, O., 2010. Development and characterization of an oat TILLING-population and identification of mutations in lignin and β-glucan biosynthesis genes. *BMC Plant Biology*, *10*, pp.1-13.

Chen, C. and Chen, Z., 2000. Isolation and characterization of two pathogen-and salicylic acid-induced genes encoding WRKY DNA-binding proteins from tobacco. *Plant Molecular Biology*, *42*, pp.387-396.

Chen, L., Hao, L., Parry, M.A., Phillips, A.L. and Hu, Y.G., 2014. Progress in TILLING as a tool for functional genomics and improvement of crops. *Journal Of Integrative Plant Biology*, *56*(5), pp.425-443.

Chen, S., Zhang, N., Zhou, G., Hussain, S., Ahmed, S., Tian, H. and Wang, S., 2021. Knockout of the entire family of AITR genes in *A. thaliana* leads to enhanced drought and salinity tolerance without fitness costs. *BMC Plant Biology*, *21*, pp.1-15.

Chi, W., Ma, J., Zhang, D., Guo, J., Chen, F., Lu, C. and Zhang, L., 2008. The pentratricopeptide repeat protein DELAYED GREENING1 is involved in the regulation of early chloroplast development and chloroplast gene expression in *A. thaliana*. *Plant Physiology*, *147*(2), pp.573-584.

Chi, W., Mao, J., Li, Q., Ji, D., Zou, M., Lu, C. and Zhang, L., 2010. Interaction of the pentatricopeptide-repeat protein DELAYED GREENING 1 with sigma factor SIG6 in the regulation of chloroplast gene expression in *A. thaliana* cotyledons. *The Plant Journal*, *64*(1), pp.14-25.

Choi, H.I., Hong, J.H., Ha, J.O., Kang, J.Y. and Kim, S.Y., 2000. ABFs, a family of ABA-responsive element binding factors. *Journal Of Biological Chemistry*, *275*(3), pp.1723-1730.

Choudhary, J.R., Bhavyasree, R.K., Sheoran, S., Choudhary, M., Chandra, S., Kaswan, V. and Wani, S.H., 2023. Forward and Reverse Genetics in Crop Breeding. *Advanced Crop Improvement, Volume 1: Theory and Practice* (pp. 257-275).

Chovancek, E., Zivcak, M., Botyanszka, L., Hauptvogel, P., Yang, X., Misheva, S., Hussain, S. and Brestic, M., 2019. Transient heat waves may affect the photosynthetic capacity of susceptible wheat genotypes due to insufficient photosystem I photoprotection. *Plants*, 8(8), p.282.

Clark, K.A. and Krysan, P.J., 2010. Chromosomal translocations are a common phenomenon in Arabidopsis thaliana T-DNA insertion lines. *The Plant Journal*, *64*(6), pp.990-1001.

Cline, W.R., 2007. *Global warming and agriculture: Impact estimates by country*. Peterson Institute.

Clough, S.J. and Bent, A.F., 1998. Floral dip: a simplified method for Agrobacterium-mediated transformation of *A* thaliana*. thaliana*. *The Plant Jjournal*, *16*(6), pp.735-743.

Cohen, I., Zandalinas, S.I., Fritschi, F.B., Sengupta, S., Fichman, Y., Azad, R.K. and Mittler, R., 2021. The impact of water deficit and heat stress combination on the molecular response, physiology, and seed production of soybean. *Physiologia Plantarum*, *172*(1), pp.41-52.

Collin, A., Daszkowska-Golec, A., Kurowska, M. and Szarejko, I., 2020. Barley ABI5 (Abscisic Acid INSENSITIVE 5) is involved in abscisic acid-dependent drought response. *Frontiers In Plant Science*, *11*, p.1138.

Comas, L.H., Becker, S.R., Cruz, V.M.V., Byrne, P.F. and Dierig, D.A., 2013. Root traits contributing to plant productivity under drought. *Frontiers In Plant Science*, 4, p.442.

Cormack, R.S., Eulgem, T., Rushton, P.J., Köchner, P., Hahlbrock, K. and Somssich, I.E., 2002. Leucine zipper-containing WRKY proteins widen the spectrum of immediate early elicitor-induced WRKY transcription factors in parsley. *Biochimica et Biophysica Acta (BBA)-Gene Structure And Expression*, *1576*(1-2), pp.92-100.

Cui, D., Zhao, J., Jing, Y., Fan, M., Liu, J., Wang, Z., Xin, W. and Hu, Y., 2013. The *A. thaliana* IDD14, IDD15, and IDD16 cooperatively regulate lateral organ morphogenesis and gravitropism by promoting auxin biosynthesis and transport. *PLoS Genetics*, *9*(9), p.e1003759.

Cutler, S.R., Rodriguez, P.L., Finkelstein, R.R. and Abrams, S.R., 2010. Abscisic acid: emergence of a core signalling network. *Annual Review Of Plant Biology*, *61*, pp.651-679.

Dai Vu, L., Gevaert, K. and De Smet, I., 2019. Feeling the heat: searching for plant thermosensors. *Trends in Plant Science*, *24*(3), pp.210-219.

Dai, C., Lee, Y., Lee, I.C., Nam, H.G. and Kwak, J.M., 2018. Calmodulin 1 regulates senescence and ABA response in *A. thaliana*. *Frontiers In Plant Science*, *9*, p.803.

Dai, X., Xu, X., Lu, W. and Kuang, T., 2003. Photoinhibition characteristics of a low chlorophyll *b* mutant of high yield rice. *Photosynthetica*, 41, pp.57-60.

Dalle Carbonare, L., White, M.D., Shukla, V., Francini, A., Perata, P., Flashman, E., Sebastiani, L. and Licausi, F., 2019. Zinc excess induces a hypoxia-like response by inhibiting cysteine oxidases in poplar roots. *Plant physiology*, *180*(3), pp.1614-1628.

Davis, S.J., Bhoo, S.H., Durski, A.M., Walker, J.M. and Vierstra, R.D., 2001. The heme-oxygenase family required for phytochrome chromophore biosynthesis is necessary for proper photomorphogenesis in higher plants. *Plant Physiology*, *126*(2), pp.656-669.

Davison, P.A., Hunter, C.N. and Horton, P., 2002. Overexpression of β-carotene hydroxylase enhances stress tolerance in *A. thaliana*. *Nature*, 418(6894), pp.203-206.

De Marchi, R., Sorel, M., Mooney, B., Fudal, I., Goslin, K., Kwaśniewska, K., Ryan, P.T., Pfalz, M., Kroymann, J., Pollmann, S. and Feechan, A., 2016. The N-end rule pathway regulates pathogen responses in plants. *Scientific Reports*, *6*(1), pp.1-15.

De Souza, A.P., Burgess, S.J., Doran, L., Hansen, J., Manukyan, L., Maryn, N., Gotarkar, D., Leonelli, L., Niyogi, K.K. and Long, S.P., 2022. Soybean photosynthesis and crop yield are improved by accelerating recovery from photoprotection. *Science*, *377*(6608), pp.851-854.

Dejonghe, W., Okamoto, M. and Cutler, S.R., 2018. Small molecule probes of ABA biosynthesis and signalling. *Plant and Cell Physiology*, *59*(8), pp.1490-1499.

Dekker, J.P. and Boekema, E.J., 2005. Supramolecular organisation of thylakoid membrane proteins in green plants. *Biochimica Et Biophysica Acta (BBA) - Bioenergetics*, 1706(1-2), pp.12-39.

Desikan, R., Cheung, M.K., Bright, J., Henson, D., Hancock, J.T. and Neill, S.J., 2004. ABA, hydrogen peroxide and nitric oxide signalling in stomatal guard cells. *Journal Of Experimental Botany*, *55*(395), pp.205-212.

Desikan, R., Cheung, M.K., Bright, J., Henson, D., Hancock, J.T. and Neill, S.J., 2004. ABA, hydrogen peroxide and nitric oxide signalling in stomatal guard cells. *Journal Of Eexperimental Botany*, *55*(395), pp.205-212.

Dhankher, O.P. and Foyer, C.H., 2018. Climate resilient crops for improving global food security and safety. *Plant, Cell & Environment*, *41*(5), pp.877-884.

Dickin, E. and Wright, D., 2008. The effects of winter waterlogging and summer drought on the growth and yield of winter wheat (Triticum aestivum L.). *European Journal of Agronomy*, *28*(3), pp.234-244.

Dikjstra, F.D., He, M., Johansen, M.P., Harrison, J.J. and Keitel, C., 2014, August. Plant-microbe competition for nitrogen and phosphorous affected by drought. In 9th International IsoEcol Conference, Applications of Stable Isotope Techniques to Ecological Studies, 3rd-8th August. The University of Western Australia.

Ding, Y., Zhou, M., Wang, K., Qu, A., Hu, S., Jiang, Q., Yi, K., Wang, F., Cai, C., Zhu, C. and Chen, Z., 2023. Rice DST transcription factor negatively regulates heat tolerance through ROS-mediated stomatal movement and heat-responsive gene expression. *Frontiers In Plant Science*, *14*, p.1068296.

Dinneny, J.R., 2019. Developmental responses to water and salinity in root systems. *Annual Review of Cell and Developmental Biology*, *35*(1), pp.239-257.

Diretto, G., Welsch, R., Tavazza, R., Mourgues, F., Pizzichini, D., Beyer, P. and Giuliano, G., 2007. Silencing of beta-carotene hydroxylase increases total carotenoid and beta-carotene levels in potato tubers. *BMC Plant Biology*, *7*, pp.1-8.

Driever, S.M., Simkin, A.J., Alotaibi, S., Fisk, S.J., Madgwick, P.J., Sparks, C.A., Jones, H.D., Lawson, T., Parry, M.A. and Raines, C.A., 2017. Increased SBPase activity improves photosynthesis and grain yield in wheat grown in greenhouse conditions. *Philosophical Transactions Of The Royal Society B: Biological Sciences*, *372*(1730), p.20160384.

Du, H., Wang, N., Cui, F., Li, X., Xiao, J. and Xiong, L., 2010. Characterization of the β-carotene hydroxylase gene *DSM2* conferring drought and oxidative stress resistance by increasing xanthophylls and abscisic acid synthesis in rice. *Plant physiology*, *154*(3), pp.1304-1318.

Du, H., Wang, N., Cui, F., Li, X., Xiao, J. and Xiong, L., 2010. Characterisation of the β-carotene hydroxylase gene DSM2 conferring drought and oxidative stress resistance by increasing xanthophylls and abscisic acid synthesis in rice. *Plant Physiology*, *154*(3), pp.1304-1318.

Dwivedi, S.L., Ceccarelli, S., Blair, M.W., Upadhyaya, H.D., Are, A.K. and Ortiz, R., 2016. Landrace germplasm for improving yield and abiotic stress adaptation. *Trends in Plant Science*, *21*(1), pp.31-42.

Emborg, T.J., Walker, J.M., Noh, B. and Vierstra, R.D., 2006. Multiple heme oxygenase family members contribute to the biosynthesis of the phytochrome chromophore in *A. thaliana*. *Plant Physiology*, *140*(3), pp.856-868.

Emerson, R. and Lewis, C.M., 1942. The photosynthetic efficiency of phycocyanin in Chroococcus, and the problem of carotenoid participation in photosynthesis. *The Journal Of General* Physiology, *25*(4), pp.579-595.

Emerson, R., 1929. The relation between maximum rate of photosynthesis and concentration of chlorophyll. *The Journal Of General Physiology*, 12(5), pp.609-622.

Enders, T.A., Oh, S., Yang, Z., Montgomery, B.L. and Strader, L.C., 2015. Genome sequencing of Arabidopsis abp1-5 reveals second-site mutations that may affect phenotypes. *The Plant Cell*, *27*(7), pp.1820-1826.

Enns, L.C., Kanaoka, M.M., Torii, K.U., Comai, L., Okada, K. and Cleland, R.E., 2005. Two callose synthases, GSL1 and GSL5, play an essential and redundant role in plant and pollen development and in fertility. *Plant Molecular Biology*, 58, pp.333-349.

Fahlgren, N., Gehan, M.A. and Baxter, I., 2015. Lights, camera, action: high-throughput plant phenotyping is ready for a close-up. *Current Opinion In Plant Biology*, 24, pp.93-99.

Faus, I., Niñoles, R., Kesari, V. and Gadea, J., 2021. The ABCF3 gene of *A. thaliana* is functionally linked with GCN1 but not with GCN2 during stress and development. *Plant Molecular Biology Reporter*, 39(4), pp.663-672.

Ferguson, J.N., McAusland, L., Smith, K.E., Price, A.H., Wilson, Z.A. and Murchie, E.H., 2020. Rapid temperature responses of photosystem II efficiency forecast genotypic variation in rice vegetative heat tolerance. *The Plant Journal*, *104*(3), pp.839-855.

Ferreira, K.N., Iverson, T.M., Maghlaoui, K., Barber, J. and Iwata, S., 2004. Architecture of the photosynthetic oxygen-evolving center. *Science*, 303(5665), pp.1831-1838.

Finkelstein, R., Reeves, W., Ariizumi, T. and Steber, C., 2008. Molecular aspects of seed dormancy. *Annu. Rev. Plant Biol.*, *59*, pp.387-415.

Finkelstein, R.R. and Lynch, T.J., 2000. The *A. thaliana* abscisic acid response gene ABI5 encodes a basic leucine zipper transcription factor. *The Plant cell*, *12*(4), pp.599-609.

Fonseca de Lima, C.F., Kleine-Vehn, J., De Smet, I. and Feraru, E., 2021. Getting to the root of belowground high temperature responses in plants. *Journal Of Experimental Botany*, 72(21), pp.7404-7413.

Frank, H.A. and Cogdell, R.J., 1996. Carotenoids in photosynthesis. *Photochemistry And Photobiology*, 63(3), pp.257-264.

Furbank, R.T., von Caemmerer, S., Sheehy, J. and Edwards, G., 2009. C4 rice: a challenge for plant phenomics. *Functional Plant Biology*, *36*(11), pp.845-856.

Gao, L. and Xiang, C.B., 2008. The genetic locus At1g73660 encodes a putative MAPKKK and negatively regulates salt tolerance in *A. thaliana*. *Plant Molecular Biology*, *67*, pp.125-134.

Garzon, M. , Eifler, K. , Faust, A. , Scheel, H. , Hofmann, K. , Koncz, C. and Bachmair, A. (2007) PRT6/At5 g02310 encodes an *A. thaliana* ubiquitin ligase of the N-end rule pathway with arginine specificity and is not the CER3 locus. *FEBS Lett.* 581, 3189–3196.

Genty, B., Briantais, J.M. and Baker, N.R., 1989. The relationship between the quantum yield of photosynthetic electron transport and quenching of chlorophyll fluorescence. *Biochimica Et Biophysica Acta (BBA) - General Subjects*, 990(1), pp.87-92.

Gheidary, S., Akhzari, D. and Pessarakli, M., 2017. Effects of salinity, drought, and priming treatments on seed germination and growth parameters of Lathyrus sativus L. *Journal of Plant Nutrition*, *40*(10), pp.1507-1514.

Gibbs, D.J. , Bacardit, J. , Bachmair, A. and Holdsworth, M.J. (2014a) The eukaryotic N-end rule pathway: conserved mechanisms and diverse functions. *Trends Cell Biol.* 24, 603–611.

Gibbs, D.J. , Isa, N.M. , Movahedi, M. , Lozano-Juste, J. , Mendiondo, G.M. , Berckhan, S. and Holdsworth, M.J. (2014b) Nitric Oxide sensing in plants is mediated by proteolytic control of group VII ERF transcription factors. *Mol. Cell*, 53, 369–379

Gibbs, D.J. , Lee, S.C. , Isa, N.M. , Gramuglia, S. , Fukao, T. , Bassel, G.W. and Holdsworth, M.J. (2011) Homeostatic response to hypoxia is regulated by the N-end rule pathway in plants. *Nature*, 479, 415–418.

Gibbs, D.J. and Holdsworth, M.J., 2020. Every breath you take: New insights into plant and animal oxygen sensing. *Cell*, *180*(1), pp.22-24.

Gibbs, J. and Greenway, H., 2003. Mechanisms of anoxia tolerance in plants. I. Growth, survival and anaerobic catabolism. *Functional Plant Biology*, *30*(1), pp.1-47.

Gisk, B., Yasui, Y., Kohchi, T. and Frankenberg-Dinkel, N., 2010. Characterisation of the haem oxygenase protein family in *A thaliana. thaliana* reveals a diversity of functions. *Biochemical Journal*, 425(2), pp.425-434.

Gleick, P.H., 2000. *The world's water 2000-2001: the biennial report on freshwater resources*. Island Press.

Godfray, H.C.J., Crute, I.R., Haddad, L., Lawrence, D., Muir, J.F., Nisbett, N., Pretty, J., Robinson, S., Toulmin, C. and Whiteley, R., 2010. The future of the global food system. *Philosophical Transactions Of he Royal Society B: Biological Sciences*, *365*(1554), pp.2769-2777.

Gong, X., Su, Q., Lin, D., Jiang, Q., Xu, J., Zhang, J., Teng, S. and Dong, Y., 2014. The rice OsV4 encoding a novel pentatricopeptide repeat protein is required for chloroplast development during the early leaf stage under cold stress. *Journal Of Integrative Plant Biology*, *56*(4), pp.400-410.

Graciet, E. , Walter, F. , O'Maoileidigh, D. , Pollmann, S. , Meyerowitz, E.M. , Varshavsky, A. and Wellmer, F. (2009) The N-end rule pathway controls multiple functions during *A. thaliana* shoot and leaf development. *Proc. Natl. Acad. Sci. USA*, 106, 13618–13623.

Green, B. and Parson, W.W. eds., 2003. *Light-harvesting antennas in photosynthesis* (Vol. 13). Springer Science & Business Media.

Green, B.R., 2019. What happened to the phycobilisome? *Biomolecules*, 9(11), p.748.

Griffiths, A., Wessler, S., Lewontin, R., Gelbart, W., Suzuki, D., & Miller, J. (2004) 'Dissection of Gene Function', in Freeman, W.H. (ed.) *An Introduction to Genetic Analysis*. 8th edn. New York, NY: Freeman.

Gu, J., Zhou, Z., Li, Z., Chen, Y., Wang, Z. and Zhang, H., 2017. Rice (*Oryza sativa L.*) with reduced chlorophyll content exhibit higher photosynthetic rate and efficiency, improved canopy light distribution, and greater yields than normally pigmented plants. *Field Crops Research*, 200, pp.58-70.

Guidi, L., Landi, M., Penella, C. and Calatayud, A., 2016. Application of modulated chlorophyll fluorescence and modulated chlorophyll fluorescence imaging to study the environmental stress effect. *Annali Di Botanica*, 6, pp.39-56.

Guo, M., Rupe, M.A., Wei, J., Winkler, C., Goncalves-Butruille, M., Weers, B.P., Cerwick, S.F., Dieter, J.A., Duncan, K.E., Howard, R.J. and Hou, Z., 2014. Maize ARGOS1 (ZAR1) transgenic alleles increase hybrid maize yield. *Journal Of Experimental Botany*, *65*(1), pp.249-260.

Gururani, M.A., Venkatesh, J. and Tran, L.S.P., 2015. Regulation of photosynthesis during abiotic stress-induced photoinhibition. *Molecular Plant*, *8*(9), pp.1304-1320.

Harris, J.M., 2015. Abscisic acid: hidden architect of root system structure. *Plants*, *4*(3), pp.548-572.

Hartman, S., Liu, Z., Van Veen, H., Vicente, J., Reinen, E., Martopawiro, S., Zhang, H., Van Dongen, N., Bosman, F., Bassel, G.W. and Visser, E.J., 2019. Ethylene-mediated nitric oxide depletion pre-adapts plants to hypoxia stress. *Nature Communications*, *10*(1), p.4020.

Hashimoto, H., Uragami, C. and Cogdell, R.J., 2016. Carotenoids and photosynthesis. *Carotenoids in Nature: Biosynthesis, Regulation And Function*, pp.111-139.

Hauser, F., Waadt, R. and Schroeder, J.I., 2011. Evolution of abscisic acid synthesis and signalling mechanisms. *Current Biology*, *21*(9), pp.R346-R355.

Havaux, M. and Gruszecki, W.I., 1993. Heat-and light-induced chlorophyll *a* fluorescence changes in potato leaves containing high or low levels of the carotenoid zeaxanthin: Indications of a regulatory effect of zeaxanthin on thylakoid membrane fluidity. *Photochemistry And Photobiology*, 58(4), pp.607-614.

Havaux, M. and Tardy, F., 1999. Loss of chlorophyll with limited reduction of photosynthesis as an adaptive response of Syrian barley landraces to high-light and heat stress. *Functional Plant Biology*, 26(6), pp.569-578.

Havaux, M., 1993. Characterisation of thermal damage to the photosynthetic electron transport system in potato leaves. *Plant Science*, 94(1-2), pp.19-33.

Havaux, M., 1998. Carotenoids as membrane stabilizers in chloroplasts. *Trends in Plant Science*, 3(4), pp.147-151.

Haxo, F.T. and Blinks, L.R., 1950. Photosynthetic action spectra of marine algae. *The Journal Of general Physiology*, *33*(4), pp.389-422.

He, X., Luo, X., Wang, T., Liu, S., Zhang, X. and Zhu, L., 2020. GhHB12 negatively regulates abiotic stress tolerance in *A. thaliana* and cotton. *Environmental And Experimental Botany*, *176*, p.104087.

Heckathorn, S.A., Giri, A., Mishra, S. and Bista, D., 2013. Heat stress and roots. *Climate Change And Plant Abiotic Stress Tolerance*, pp.109-136.

Hendrick, R.L. and Pregitzer, K.S., 1996. Temporal and depth-related patterns of fine root dynamics in northern hardwood forests. *Journal Of Ecology*, pp.167-176.

Herzog, M., Striker, G.G., Colmer, T.D. and Pedersen, O., 2016. Mechanisms of waterlogging tolerance in wheat–a review of root and shoot physiology. *Plant, Cell & Environment*, *39*(5), pp.1068-1086.

Hikosaka, K., Ishikawa, K., Borjigidai, A., Muller, O. and Onoda, Y., 2006. Temperature acclimation of photosynthesis: mechanisms involved in the changes in temperature dependence of photosynthetic rate. *Journal of Experimental Botany*, *57*(2), pp.291-302.

Hinderhofer, K. and Zentgraf, U., 2001. Identification of a transcription factor specifically expressed at the onset of leaf senescence. *Planta: An International Journal Of Plant Biology*, *213*(3).

Hobo, T., Kowyama, Y. and Hattori, T., 1999. A bZIP factor, TRAB1, interacts with VP1 and mediates abscisic acid-induced transcription. *Proceedings Of The National Academy Of* Science*s*, *96*(26), pp.15348-15353.

Hogewoning, S.W., Wientjes, E., Douwstra, P., Trouwborst, G., Van Ieperen, W., Croce, R. and Harbinson, J., 2012. Photosynthetic quantum yield dynamics: from photosystems to leaves. *The Plant Cell*, 24(5), pp.1921-1935.

Holdsworth, M.J., Vicente, J., Sharma, G., Abbas, M. and Zubrycka, A., 2020. The plant N-degron pathways of ubiquitin-mediated proteolysis. *Journal Of Integrative Plant Biology*, *62*(1), pp.70-89.

Hong, B., Barg, R. and Ho, T.H.D., 1992. Developmental and organ-specific expression of an ABA-and stress-induced protein in barley. *Plant Molecular Biology*, *18*, pp.663-674.

Hsu, P.K., Dubeaux, G., Takahashi, Y. and Schroeder, J.I., 2021. Signalling mechanisms in abscisic acid-mediated stomatal closure. *The Plant Journal*, *105*(2), pp.307-321.

Huang, B. and Johnson, J.W., 1995. Root respiration and carbohydrate status of two wheat genotypes in response to hypoxia. *Annals of Botany*, *75*(4), pp.427-432.

Huang, Y., Li, C.Y., Qi, Y., Park, S. and Gibson, S.I., 2014. SIS 8, a putative mitogen-activated protein kinase kinase kinase, regulates sugar-resistant seedling development in *A. thaliana*. *The Plant Journal*, *77*(4), pp.577-588.

Hubbart, S., Ajigboye, O.O., Horton, P. and Murchie, E.H., 2012. The photoprotective protein PsbS exerts control over CO_2 assimilation rate in fluctuating light in rice. *The Plant Journal*, 71(3), pp.402-412.

Hülskamp, M., Miséra, S. and Jürgens, G., 1994. Genetic dissection of trichome cell development in *A. thaliana*. *Cell*, *76*(3), pp.555-566.

Ichimura, K., Shinozaki, K., Tena, G., Sheen, J., Henry, Y., Champion, A., Kreis, M., Zhang, S., Hirt, H., Wilson, C. and Heberle-Bors, E., 2002. Mitogen-activated protein kinase cascades in plants: a new nomenclature. *Trends In Plant* Science, *7*(7), pp.301-308.

Illouz-Eliaz, N., Nissan, I., Nir, I., Ramon, U., Shohat, H. and Weiss, D., 2020. Mutations in the tomato gibberellin receptors suppress xylem proliferation and reduce water loss under water-deficit conditions. *Journal of Experimental Botany*, 71(12), pp.3603-3612

IPCC, 2023, *Climate Change 2023: Synthesis Report. Contribution of Working Groups I, II and III to the Sixth Assessment Report of the Intergovernmental Panel on*

Climate Change, Core Writing Team, H. Lee and J. Romero (eds.), IPCC, Geneva, Switzerland. Available at: https://doi.org/10.59327/IPCC/AR6-9789291691647

Jagadish, S.K., Pal, M., Sukumaran, S., Parani, M. and Siddique, K.H., 2020. Heat stress resilient crops for future hotter environments. *Plant Physiology Reports*, *25*, pp.529-532.

Jahns, P. and Holzwarth, A.R., 2012. The role of the xanthophyll cycle and of lutein in photoprotection of photosystem II. *Biochimica Et Biophysica Acta (BBA) - Bioenergetics*, 1817(1), pp.182-193.

Janka, E., Körner, O., Rosenqvist, E. and Ottosen, C.O., 2015. Using the quantum yields of photosystem II and the rate of net photosynthesis to monitor high irradiance and temperature stress in chrysanthemum (Dendranthema grandiflora). *Plant Physiology And Biochemistry*, 90, pp.14-22.

Jedmowski, C., Ashoub, A., Momtaz, O. and Brüggemann, W., 2015. Impact of drought, heat, and their combination on chlorophyll fluorescence and yield of wild barley (*Hordeum spontaneum*). *Journal Of Botany*, 2015, pp.1-9.

Jiang, L., Lin, Y., Wang, L., Peng, Y., Yang, M., Jiang, Y., Hou, G., Liu, X., Li, M., Zhang, Y. and Zhang, Y., 2023. Genome-wide identification and expression profiling reveal the regulatory role of U-box E3 ubiquitin ligase genes in strawberry fruit ripening and abiotic stresses resistance. *Frontiers In Plant Science*, *14*, p.1171056.

Johnson, C.S., Kolevski, B. and Smyth, D.R., 2002. TRANSPARENT TESTA GLABRA2, a trichome and seed coat development gene of *A. thaliana*, encodes a WRKY transcription factor. *The Plant Cell*, *14*(6), pp.1359-1375.

Jung, J. , Won, S.Y. , Suh, S.C. , Kim, H. , Wing, R. , Jeong, Y. and Kim, M. (2007) The barley ERF-type transcription factor HvRAF confers enhanced pathogen resistance and salt tolerance in *A. thaliana*. *Planta*, 225, 575–588.

Jung, J., Won, S.Y., Suh, S.C., Kim, H., Wing, R., Jeong, Y., Hwang, I. and Kim, M., 2007. The barley ERF-type transcription factor HvRAF confers enhanced pathogen resistance and salt tolerance in *A. thaliana*. *Planta*, *225*, pp.575-588.

Kanai, M., Nishimura, M. and Hayashi, M., 2010. A peroxisomal ABC transporter promotes seed germination by inducing pectin degradation under the control of ABI5. *The Plant Journal*, *62*(6), pp.936-947.

Karki, T.B. and Gyawaly, P., 2021. Conservation agriculture mitigates the effects of climate change. *Journal Of Nepal Agricultural Research Council*, *7*, pp.122-132.

Karl, T.R. and Trenberth, K.E., 2003. Modern global climate change. *Science*, *302*(5651), pp.1719-1723.

Kawata, S.I., Harada, J. and Yamazaki, K., 1978. On the number and the diameter of crown root primordia in rice plants. *Japanese Journal Of Crop Science*, 47(4), pp.644-654.

Kedisso, E.G., Maredia, K., Guenthner, J. and Koch, M., 2022. Commercialization of genetically modified crops in Africa: opportunities and challenges. *African Journal of Biotechnology*, *21*(5), pp.188-197.

Kell, D.B., 2011. Breeding crop plants with deep roots: their role in sustainable carbon, nutrient and water sequestration. *Annals Of Botany*, 108(3), pp.407-418.

Khanal, S., Fulton, J. and Shearer, S., 2017. An overview of current and potential applications of thermal remote sensing in precision agriculture. *Computers and Electronics in Agriculture*, *139*, pp.22-32.

Kim, D., Alptekin, B. and Budak, H., 2018. CRISPR/Cas9 genome editing in wheat. *Functional & Integrative Genomics*, *18*, pp.31-41.

Kim, J. and DellaPenna, D., 2006. Defining the primary route for lutein synthesis in plants: the role of *A. thaliana* carotenoid β-ring hydroxylase CYP97A3. *Proceedings Of the National Academy Of Sciences*, *103*(9), pp.3474-3479.

Kim, J., Smith, J.J., Tian, L. and DellaPenna, D., 2009. The evolution and function of carotenoid hydroxylases in *A. thaliana*. *Plant and Cell Physiology*, *50*(3), pp.463-479.

Kim, J.M., Seok, O.H., Ju, S., Heo, J.E., Yeom, J., Kim, D.S., Yoo, J.Y., Varshavsky, A., Lee, C. and Hwang, C.S., 2018. Formyl-methionine as an N-degron of a eukaryotic N-end rule pathway. *Science*, *362*(6418),pp 0174.

Kipp, E. and Boyle, M., 2013. The effects of heat stress on reactive oxygen species production and chlorophyll concentration in *A thaliana. thaliana*. *Res Plant Sci*, 1(2), pp.20-3.

Kirda, C., 2002. Deficit irrigation scheduling based on plant growth stages showing water stress tolerance. *Food and Agricultural Organization of the United Nations, Deficit Irrigation Practices, Water Reports*, *22*(102), pp.3-10.

Kong, Y., Chen, S., Yang, Y. and An, C., 2013. ABA-insensitive (ABI) 4 and ABI5 synergistically regulate DGAT1 expression in *A. thaliana* seedlings under stress. *FEBS Lletters*, *587*(18), pp.3076-3082.

Kooyers, N.J., 2015. The evolution of drought escape and avoidance in natural herbaceous populations. *Plant Science*, *234*, pp.155-162.

Kramer, D.M., Johnson, G., Kiirats, O. and Edwards, G.E., 2004. New fluorescence parameters for the determination of QA redox state and excitation energy fluxes. *Photosynthesis Research*, 79, pp.209-218.

Krause, G.H. and Santarius, K.A., 1975. Relative thermostability of the chloroplast envelope. *Planta*, 127, pp.285-299.

Krinsky, N.I., 1993. Actions of carotenoids in biological systems. *Annual Review Of Nutrition*, 13(1), pp.561-587.

Kromdijk, J., Głowacka, K., Leonelli, L., Gabilly, S.T., Iwai, M., Niyogi, K.K. and Long, S.P., 2016. Improving photosynthesis and crop productivity by accelerating recovery from photoprotection. *Science*, 354(6314), pp.857-861.

Kumar, A.P., McKeown, P.C., Boualem, A., Ryder, P., Brychkova, G., Bendahmane, A., Sarkar, A., Chatterjee, M. and Spillane, C., 2017. TILLING by Sequencing (TbyS) for targeted genome mutagenesis in crops. *Molecular Breeding*, *37*, pp.1-12.

Kuromori, T., Seo, M. and Shinozaki, K., 2018. ABA transport and plant water stress responses. *Trends in Plant Science*, *23*(6), pp.513-522.

Lake, I.R., Hooper, L., Abdelhamid, A., Bentham, G., Boxall, A.B., Draper, A., Fairweather-Tait, S., Hulme, M., Hunter, P.R., Nichols, G. and Waldron, K.W., 2012. Climate change and food security: health impacts in developed countries. *Environmental Health perspectives*, *120*(11), pp.1520-1526.

Lamers, J., Van Der Meer, T. and Testerink, C., 2020. How plants sense and respond to stressful environments. *Plant Physiology*, *182*(4), pp.1624-1635.

Lavkush, A.K., Singh, S.S., NP, V., D Tiwari, R.K., Yadav, S.R. and Mishra, S.P., 2022. Evaluation of biochemical changes in wheat varieties as influenced by terminal heat stress under varying environments. *Journal Of Cereal Research* 14 (3): 291-298. *http://doi. org/10.25174/2582-2675/2022*, *131256*, p.291.

Lee, J.H., Hübel, A. and Schöffl, F., 1995. Derepression of the activity of genetically engineered heat shock factor causes constitutive synthesis of heat shock proteins and increased thermotolerance in transgenic *A. thaliana*. *The Plant Journal*, *8*(4), pp.603-612.

Lehmann, J. and Rillig, M., 2014. Distinguishing variability from uncertainty. *Nature Climate Change*, *4*(3), pp.153-153.

Leng, G. and Hall, J., 2019. Crop yield sensitivity of global major agricultural countries to droughts and the projected changes in the future. *Science Of The Total Environment*, *654*, pp.811-821.

Leng, P., Yuan, B. and Guo, Y., 2013. The role of abscisic acid in fruit ripening and responses to abiotic stress. *Journal Of Experimental Botany*, *65*(16), pp.4577-4588.

Leyshon, A.J. and Sheard, R.W., 1974. Influence of short-term flooding on the growth and plant nutrient composition of barley. *Canadian Journal of Soil Science*, *54*(4), pp.463-473.

Li, N., Euring, D., Cha, J.Y., Lin, Z., Lu, M., Huang, L.J. and Kim, W.Y., 2021. Plant hormone-mediated regulation of heat tolerance in response to global climate change. *Frontiers In Plant Science*, *11*, p.627969.

Li, Q., Zhu, F.Y., Gao, X., Sun, Y., Li, S., Tao, Y., Lo, C. and Liu, H., 2014. Young Leaf Chlorosis 2 encodes the stroma-localized heme oxygenase 2 which is required for normal tetrapyrrole biosynthesis in rice. *Planta*, *240*, pp.701-712.

Li, X., Ingvordsen, C.H., Weiss, M., Rebetzke, G.J., Condon, A.G., James, R.A. and Richards, R.A., 2019. Deeper roots associated with cooler canopies, higher normalized difference vegetation index, and greater yield in three wheat populations grown on stored soil water. *Journal Of Experimental Botany*, 70(18), pp.4963-4974.

Li, Y. and Chen, M., 2015. Novel chlorophylls and new directions in photosynthesis research. *Functional Plant Biology*, *42*(6), pp.493-501.

Liao, S., Qin, X., Luo, L., Han, Y., Wang, X., Usman, B., Nawaz, G., Zhao, N., Liu, Y. and Li, R., 2019. CRISPR/Cas9-induced mutagenesis of semi-rolled leaf1, 2 confers curled leaf phenotype and drought tolerance by influencing protein expression patterns and ROS scavenging in rice (*Oryza sativa L.*). *Agronomy*, *9*(11), p.728.

Licausi, F. , Kosmacz, M. , Weits, D.A. , Giuntoli, B. , Giorgi, F.M. , Voesenek, L.A.C.J. and van Dongen, J.T. (2011) Oxygen sensing in plants is mediated by an N-end rule pathway for protein destabilisation. *Nature*, 479, 419–422

Liu, J., Liu, Y., Wang, S., Cui, Y. and Yan, D., 2022. Heat stress reduces root meristem size via induction of plasmodesmal callose accumulation inhibiting phloem unloading in *A. thaliana*. *International Journal Of Molecular Sciences*, *23*(4), p.2063.

Liu, S., Wang, H. and Qin, F., 2023. Genetic dissection of drought resistance for trait improvement in crops. *The Crop Journal*, *11*(4), pp.975-985.

Liu, X., Tian, D., Li, C., Tang, B., Wang, Z., Zhang, R., Pan, Y., Wang, Y., Zou, D., Zhang, Z. and Song, S., 2023. GWAS Atlas: an updated knowledgebase integrating more curated associations in plants and animals. *Nucleic Acids Research*, *51*(D1), pp.D969-D976.

Liu, Y., Pan, T., Tang, Y., Zhuang, Y., Liu, Z., Li, P., Li, H., Huang, W., Tu, S., Ren, G. and Wang, T., 2020. Proteomic analysis of rice subjected to low light stress and overexpression of *OsGAPB* increases the stress tolerance. *Rice*, *13*, pp.1-10.

Liu, Z., Yan, H., Wang, K., Kuang, T., Zhang, J., Gui, L., An, X. and Chang, W., 2004. Crystal structure of spinach major light-harvesting complex at 2.72 Å resolution. *Nature*, 428(6980), pp.287-292.

Lloyd, A., Plaisier, C.L., Carroll, D. and Drews, G.N., 2005. Targeted mutagenesis using zinc-finger nucleases in *A. thaliana*. *Proceedings Of the National Academy Of Sciences*, *102*(6), pp.2232-2237.

Lou, D., Wang, H., Liang, G. and Yu, D., 2017. OsSAPK2 confers abscisic acid sensitivity and tolerance to drought stress in rice. *Frontiers In Plant Science*, *8*, p.993.

Luan, R., Liu, J., Tao, L., Fu, G. and Zhang, C., 2023. Comparative Transcriptome Analysis Reveals OsBGs and OsGSLs Influence Sugar Transport through Callose Metabolism under Heat Stress in Rice. *International Journal Of Molecular Sciences*, *24*(4), p.3175.

Luo, M., Dennis, E.S., Berger, F., Peacock, W.J. and Chaudhury, A., 2005. MINISEED3 (MINI3), a WRKY family gene, and HAIKU2 (IKU2), a leucine-rich repeat (LRR) KINASE gene, are regulators of seed size in *A. thaliana*. *Proceedings Of the National Academy Of Sciences*, *102*(48), pp.17531-17536.

Luo, X., Chen, Z., Gao, J. and Gong, Z., 2014. Abscisic acid inhibits root growth in *A. thaliana* through ethylene biosynthesis. *The Plant Journal*, *79*(1), pp.44-55.

Luo, Y., El-Madany, T., Ma, X., Nair, R., Jung, M., Weber, U., Filippa, G., Bucher, S.F., Moreno, G., Cremonese, E. and Carrara, A., 2020. Nutrients and water availability constrain the seasonality of vegetation activity in a Mediterranean ecosystem. *Global Change Biology*, 26(8), pp.4379-4400.

Lv, W.T., Lin, B., Zhang, M. and Hua, X.J., 2011. Proline accumulation is inhibitory to *A. thaliana* seedlings during heat stress. *Plant Physiology*, 156(4), pp.1921-1933.

Ma, Y., Freitas, H. and Dias, M.C., 2022. Strategies and prospects for biostimulants to alleviate abiotic stress in plants. *Frontiers In Plant Science*, *13*, p.1024243.

Maccaferri, M., El-Feki, W., Nazemi, G., Salvi, S., Canè, M.A., Colalongo, M.C., Stefanelli, S. and Tuberosa, R., 2016. Prioritizing quantitative trait loci for root system architecture in tetraploid wheat. *Journal Of Experimental Botany*, 67(4), pp.1161-1178.

Make Sun, J., Tian, Y., Lian, Q. and Liu, J.X., 2020. Mutation of *DELAYED GREENING1* impairs chloroplast RNA editing at elevated ambient temperature in *A. thaliana*. *Journal Of Genetics And Genomics*, *47*(4), pp.201-212.

Malik, A.I., Colmer, T.D., Lambers, H. and Schortemeyer, M., 2001. Changes in physiological and morphological traits of roots and shoots of wheat in response to different depths of waterlogging. *Functional Plant Biology*, *28*(11), pp.1121-1131.

Masipa, T., 2017. The impact of climate change on food security in South Africa: Current realities and challenges ahead. *Jàmbá: Journal Of Disaster Risk Studies*, *9*(1), pp.1-7.

Maslova, T.G., Markovskaya, E.F. and Slemnev, N.N., 2021. Functions of carotenoids in leaves of higher plants. *Biology Bulletin Reviews*, 11, pp.476-487.

Masson-Delmotte, V., Zhai, P., Pirani, A., Connors, S.L., Péan, C., Berger, S., Caud, N., Chen, Y., Goldfarb, L., Gomis, M.I. and Huang, M., 2021. Climate change 2021: the physical science basis. *Contribution of working group I to the sixth assessment report of the intergovernmental panel on climate change*, *2*(1), p.2391.

Mathur, S., Agrawal, D. and Jajoo, A., 2014. Photosynthesis: response to high temperature stress. *Journal Of Photochemistry and Photobiology B: Biology*, 137, pp.116-126.

Mathur, S., Jajoo, A., Mehta, P. and Bharti, S., 2011. Analysis of elevated temperature-induced inhibition of photosystem II using chlorophyll *a* fluorescence induction kinetics in wheat leaves (*Triticum aestivum*). *Plant Biology*, 13(1), pp.1-6.

Mazdiyasni, O. and AghaKouchak, A., 2015. Substantial increase in concurrent droughts and heatwaves in the United States. *Proceedings of the National Academy of Sciences*, *112*(37), pp.11484-11489.

McCallum, C.M., Comai, L., Greene, E.A. and Henikoff, S., 2000a. Targeting Induced Local Lesions IN Genomes (TILLING) for plant functional genomics. *Plant Physiology*, *123*(2), pp.439-442.

McCallum, C.M., Comai, L., Greene, E.A. and Henikoff, S., 2000b. Targeted screening for induced mutations. *Nature Biotechnology*, *18*(4), pp.455-457.

McMichael, B.L. and Quisenberry, J.E., 1993. The impact of the soil environment on the growth of root systems. *Environmental and Experimental Botany*, 33(1), pp.53-61.

Mendiondo, G.M., Gibbs, D.J., Szurman-Zubrzycka, M., Korn, A., Marquez, J., Szarejko, I., Maluszynski, M., King, J., Axcell, B., Smart, K. and Corbineau, F., 2016. Enhanced waterlogging tolerance in barley by manipulation of expression of the N-end rule pathway E3 ligase PROTEOLYSIS 6. *Plant Biotechnology Journal*, *14*(1), pp.40-50.

Meyer-Gauen, G., Schnarrenberger, C., Cerff, R. and Martin, W., 1994. Molecular characterization of a novel, nuclear-encoded, NAD+-dependent glyceraldehyde-3-phosphate dehydrogenase in plastids of the gymnosperm *Pinus sylvestris L*. *Plant Molecular Biology*, *26*, pp.1155-1166.

Michelot, A., Derivery, E., Paterski-Boujemaa, R., Guérin, C., Huang, S., Parcy, F., Staiger, C.J. and Blanchoin, L., 2006. A novel mechanism for the formation of actin-filament bundles by a nonprocessive formin. *Current Biology*, *16*(19), pp.1924-1930.

Miedes, E., Vanholme, R., Boerjan, W. and Molina, A., 2014. The role of the secondary cell wall in plant resistance to pathogens. *Frontiers In Plant Science*, 5, p.358.

Minhas, P.S., Rane, J. and Pasala, R.K., 2017. Abiotic stresses in agriculture: An overview. *Abiotic Stress Management For Resilient Agriculture*, pp.3-8.

Miri, H.R., 2009. Grain yield and morpho-physiological changes from 60 years of genetic improvement of wheat in Iran. *Experimental Agriculture*, 45(2), pp.149-163.

Mishra, K.B., Mishra, A., Klem, K. and Govindjee, 2016. Plant phenotyping: a perspective. *Indian Journal Of Plant Physiology*, 21, pp.514-527.

Motohashi, R., Yamazaki, T., Myouga, F., Ito, T., Ito, K., Satou, M., Kobayashi, M., Nagata, N., Yoshida, S., Nagashima, A. and Tanaka, K., 2007. Chloroplast ribosome release factor 1 (AtcpRF1) is essential for chloroplast development. *Plant Molecular Biology*, *64*, pp.481-497.

Muhammad, I., Shalmani, A., Ali, M., Yang, Q.H., Ahmad, H. and Li, F.B., 2021. Mechanisms regulating the dynamics of photosynthesis under abiotic stresses. *Frontiers In Plant Science*, *11*, p.615942.

Murakami, Y., Tsuyama, M., Kobayashi, Y., Kodama, H. and Iba, K., 2000. Trienoic fatty acids and plant tolerance of high temperature. *Science*, *287*(5452), pp.476-479.

Murata, N. ed., 1992. *Research in Photosynthesis: Proceedings Of the IXth International Congress on Photosynthesis, Nagoya, Japan, August 30-September 4, 1992* (Vol. 2). Springer Science & Business Media.

Murchie, E.H. and Burgess, A.J., 2022. Casting light on the architecture of crop yield. *Crop and environment*, *1*(1), pp.74-85.

Murniati, K., 2020. The impact of climate change on the household food security of upland rice farmers in Sidomulyo, Lampung Province, Indonesia. *Biodiversitas Journal Of Biological Diversity*, *21*(8).

Mustroph, A. , Zanetti, M.E. , Jang, C.J.H. , Holtan, H.E. , Repetti, P.P. , Galbraith, D.W. and Bailey-Serres, J. (2009) Profiling translatomes of discrete cell populations resolves altered cellular priorities during hypoxia in *A. thaliana*. *Proc. Natl. Acad. Sci. USA*, 106, 18843–18848.

Muth, J., Hartje, S., Twyman, R.M., Hofferbert, H.R., Tacke, E. and Prüfer, D., 2008. Precision breeding for novel starch variants in potato. *Plant Biotechnology Journal*, *6*(6), pp.576-584.

Nadarajah, K.K., 2020. ROS homeostasis in abiotic stress tolerance in plants. *International Jjournal Of Molecular* Science*s*, *21*(15), p.5208.

Nagel, K.A., Kastenholz, B., Jahnke, S., Van Dusschoten, D., Aach, T., Mühlich, M., Truhn, D., Scharr, H., Terjung, S., Walter, A. and Schurr, U., 2009. Temperature responses of roots: impact on growth, root system architecture and implications for phenotyping. *Functional Plant Biology*, 36(11), pp.947-959.

Nash, D., Miyao, M. and Murata, N., 1985. Heat inactivation of oxygen evolution in photosystem II particles and its acceleration by chloride depletion and exogenous manganese. *Biochimica Et Biophysica Acta (BBA)-Bioenergetics*, 807(2), pp.127-133.

Nath, K., Jajoo, A., Poudyal, R.S., Timilsina, R., Park, Y.S., Aro, E.M., Nam, H.G. and Lee, C.H., 2013. Towards a critical understanding of the photosystem II repair mechanism and its regulation during stress conditions. *FEBS Letters*, *587*(21), pp.3372-3381.

Nelson, N. and Junge, W., 2015. Structure and energy transfer in photosystems of oxygenic photosynthesis. *Annual Review Of Biochemistry*, 84, pp.659-683.

Nelson, N. and Yocum, C.F., 2006. Structure and function of photosystems I and II. *Annu. Rev. Plant Biol.*, 57, pp.521-565.

Nemoto, H., Suga, R., Ishihara, M. and Okutsu, Y., 1998. Deep rooted rice varieties detected through the observation of root characteristics using the trench method. *Japanese Journal Of Breeding*, 48(3), pp.321-324.

Ng, L.M., Melcher, K., Teh, B.T. and Xu, H.E., 2014. Abscisic acid perception and signalling: structural mechanisms and applications. *Acta Pharmacologica Sinica*, *35*(5), pp.567-584.

Nguyen, K.T., Mun, S.H., Lee, C.S. and Hwang, C.S., 2018. Control of protein degradation by N-terminal acetylation and the N-end rule pathway. *Experimental & Molecular Medicine*, *50*(7), pp.1-8.

Niyogi, K.K., Grossman, A.R. and Björkman, O., 1998. *A. thaliana* mutants define a central role for the xanthophyll cycle in the regulation of photosynthetic energy conversion. *The Plant Cell*, *10*(7), pp.1121-1134.

Nouri, M.Z., Moumeni, A. and Komatsu, S., 2015. Abiotic stresses: insight into gene regulation and protein expression in photosynthetic pathways of plants. *International Jjournal Of Molecular* Science*s*, *16*(9), pp.20392-20416.

Numan, M., Serba, D.D. and Ligaba-Osena, A., 2021. Alternative strategies for multi-stress tolerance and yield improvement in millets. *Genes*, *12*(5), p.739.

O'Malley, R.C., Barragan, C.C. and Ecker, J.R., 2015. A user's guide to the *A. thaliana* T-DNA insertion mutant collections. *Plant Functional Genomics: Methods and Protocols*, pp.323-342.

O'Malley, R.C., Barragan, C.C. and Ecker, J.R., 2015. A user's guide to the Arabidopsis T-DNA insertion mutant collections. *Plant Functional Genomics: Methods and Protocols*, pp.323-342.

Ogata, T., Ishizaki, T., Fujita, M. and Fujita, Y., 2020. CRISPR/Cas9-targeted mutagenesis of OsERA1 confers enhanced responses to abscisic acid and drought stress and increased primary root growth under nonstressed conditions in rice. *PloS One*, *15*(12), p.e0243376.

Osanai, T., Kanesaki, Y., Nakano, T., Takahashi, H., Asayama, M., Shirai, M., Kanehisa, M., Suzuki, I., Murata, N. and Tanaka, K., 2005. Positive regulation of sugar catabolic pathways in the cyanobacterium Synechocystis sp. PCC 6803 by the group 2 σ factor SigE. *Journal Of Biological Chemistry*, *280*(35), pp.30653-30659.

Osnato, M. , Stile, M.R. , Wang, Y.M. , Meynard, D. , Curiale, S. , Guiderdoni, E. and Rossini, L. (2010) Cross Talk between the KNOX and ethylene pathways is mediated by intron-binding transcription factors in barley. *Plant Physiol.* 154, 1616–1632

Pan, J., Sharif, R., Xu, X. and Chen, X., 2021. Mechanisms of waterlogging tolerance in plants: Research progress and prospects. *Frontiers In Plant Science*, *11*, p.627331.

Pan, X., Li, Y. and Stein, L., 2005. Site preferences of insertional mutagenesis agents in *A. thaliana*. *Plant Physiology*, *137*(1), pp.168-175.

Parry, M.A., Andralojc, P.J., Scales, J.C., Salvucci, M.E., Carmo-Silva, A.E., Alonso, H. and Whitney, S.M., 2013. Rubisco activity and regulation as targets for crop improvement. *Journal Of Experimental Botany*, *64*(3), pp.717-730.

Patanè, C., Saita, A. and Sortino, O., 2013. Comparative effects of salt and water stress on seed germination and early embryo growth in two cultivars of sweet sorghum. *Journal of Agronomy and Crop Science*, *199*(1), pp.30-37.

Pérez-Sancho, J., Vanneste, S., Lee, E., McFarlane, H.E., Esteban del Valle, A., Valpuesta, V., Friml, J., Botella, M.A. and Rosado, A., 2015. The *A. thaliana* synaptotagmin1 is enriched in endoplasmic reticulum-plasma membrane contact sites and confers cellular resistance to mechanical stresses. *Plant Physiology*, *168*(1), pp.132-143.

Pfündel, E., 1998. Estimating the contribution of photosystem I to total leaf chlorophyll fluorescence. *Photosynthesis Research*, 56, pp.185-195.

Pollard, T.D., 2007. Regulation of actin filament assembly by Arp2/3 complex and formins. *Annu. Rev. Biophys. Biomol. Struct.*, *36*(1), pp.451-477.

Ponnamperuma, F.N. and Kozlowski, T.T., 1984. Flooding and plant growth. *Ed. TT Kozłowski, Orlando, Florida: Academic Press, 1984.*, p.9.

Poorter, H., Fiorani, F., Pieruschka, R., Wojciechowski, T., van der Putten, W.H., Kleyer, M., Schurr, U. and Postma, J., 2016. Pampered inside, pestered outside? Differences and similarities between plants growing in controlled conditions and in the field. *New Phytologist*, *212*(4), pp.838-855.

Postiglione, A.E. and Muday, G.K., 2020. The role of ROS homeostasis in ABA-induced guard cell signalling. *Frontiers In Plant Science*, *11*, p.968.

Potocka, I. and Szymanowska-Pułka, J., 2018. Morphological responses of plant roots to mechanical stress. *Annals Of Botany*, 122(5), pp.711-723.

Potuschak, T., Stary, S., Schlögelhofer, P., Becker, F., Nejinskaia, V. and Bachmair, A., 1998. PRT1 of *A* thaliana*. thaliana* encodes a component of the plant N-end rule pathway. *Proceedings Of the National Academy Of Sciences*, *95*(14), pp.7904-7908.

Prokisch, J., Ferroudj, A., Labidi, S., El-Ramady, H. and Brevik, E.C., 2024. Biological Nano-Agrochemicals for Crop Production as an Emerging Way to Address Heat and Associated Stresses. *Nanomaterials*, 14(15), p.1253.

Pucker, B., Kleinbölting, N. and Weisshaar, B., 2021. Large scale genomic rearrangements in selected *A* thaliana*. thaliana* T-DNA lines are caused by T-DNA insertion mutagenesis. *BMC genomics*, *22*, pp.1-21.

Qayyum, A., Razzaq, A., Ahmad, M. and Jenks, M.A., 2011. Water stress causes differential effects on germination indices, total soluble sugar and proline content in wheat (Triticum aestivum L.) genotypes. *African Journal of Biotechnology*, *10*(64), pp.14038-14045.

Qi, T., Wang, J., Sun, Q., Day, B., Guo, J. and Ma, Q., 2017. TaARPC3, contributes to wheat resistance against the stripe rust fungus. *Frontiers In Plant Science*, *8*, p.1245.

Qi, X., Li, Q., Ma, X., Qian, C., Wang, H., Ren, N., Shen, C., Huang, S., Xu, X., Xu, Q. and Chen, X., 2019. Waterlogging-induced adventitious root formation in cucumber is regulated by ethylene and auxin through reactive oxygen species signalling. *Plant, Cell & Environment*, *42*(5), pp.1458-1470.

Qiu, Z., Kang, S., He, L., Zhao, J., Zhang, S., Hu, J., Zeng, D., Zhang, G., Dong, G., Gao, Z. and Ren, D., 2018. The newly identified heat-stress sensitive albino 1 gene affects chloroplast development in rice. *Plant Science*, *267*, pp.168-179.

Queiroz, M.S., Oliveira, C.E., Steiner, F., Zuffo, A.M., Zoz, T., Vendruscolo, E.P., Silva, M.V., Mello, B.F., Cabral, R.C. and Menis, F.T., 2019. Drought stresses on seed germination and early growth of maize and sorghum. *Journal of Agricultural Science*, *11*(2), p.310.

Quintarelli, V., Radicetti, E., Allevato, E., Stazi, S.R., Haider, G., Abideen, Z., Bibi, S., Jamal, A. and Mancinelli, R., 2022. Cover crops for sustainable cropping systems: a review. *Agriculture*, *12*(12), p.2076.

Raczynska, K.D., Le Ret, M., Rurek, M., Bonnard, G., Augustyniak, H. and Gualberto, J.M., 2006. Plant mitochondrial genes can be expressed from mRNAs lacking stop codons. *FEBS Letters*, *580*(24), pp.5641-5646.

Radford, J.E., Vesk, M. and Overall, R.L., 1998. Callose deposition at plasmodesmata. *Protoplasma*, 201, pp.30-37.

Rangappa, K., Das, A., Layek, J., Basavaraj, S., Debnath, S., Bhupenchandra, I., Devi, A.G., Mohapatra, K.P., Choudhury, B.U. and Mishra, V.K., 2024. Conservation tillage and residue management practices in rice improves stress tolerance of succeeding vegetable pea by regulating physiological traits in Eastern Himalayas. *Scientia Horticulturae*, *327*, p.112842.

Rani, P. and Reddy, R.G., 2023. Climate change and its impact on food security. *International Journal Of Environment And Climate Change*, *13*(3), pp.104-108.

Ray, D.K., Mueller, N.D., West, P.C. and Foley, J.A., 2013. Yield trends are insufficient to double global crop production by 2050. *PloS one*, *8*(6), p.e66428.

Raybould, A. and Poppy, G.M., 2012. Commercializing genetically modified crops under EU regulations: objectives and barriers. *GM Crops & Food*, *3*(1), pp.9-20.

Razmjoo, K., Heydarizadeh, P. and Sabzalian, M.R., 2008. Effect of salinity and drought stresses on growth parameters and essential oil content of Matricaria chamomile. *Int. J. Agric. Biol*, *10*(4), pp.451-454.

RDevelopmentCoreTeam (2012) *R: A Language and Environment for Statistical Computing*. Vienna, Austria: R Foundation for Statistical Computing.

Reboulet, J.C., Kumar, P. and Kiss, J.Z., 2010. DIS1 and DIS2 play a role in tropisms in *A* thaliana*. thaliana*. *Environmental And Eexperimental Botany*, *67*(3), pp.474-478.

Ren, R., Gao, J., Yin, D., Li, K., Lu, C., Ahmad, S., Wei, Y., Jin, J., Zhu, G. and Yang, F., 2021. Highly efficient leaf base protoplast isolation and transient expression systems for orchids and other important monocot crops. *Frontiers In Plant Science*, *12*, p.626015.

Ribeiro, C., Stitt, M. and Hotta, C.T., 2022. How stress affects your budget—Stress impacts on starch metabolism. *Frontiers In Plant Science*, *13*, p.774060.

Riber, W., Müller, J.T., Visser, E.J., Sasidharan, R., Voesenek, L.A. and Mustroph, A., 2015. The greening after extended darkness1 is an N-end rule pathway mutant with high tolerance to submergence and starvation. *Plant Physiology*, *167*(4), pp.1616-1629.

Ristic, Z., Bukovnik, U. and Prasad, P.V., 2007. Correlation between heat stability of thylakoid membranes and loss of chlorophyll in winter wheat under heat stress. *Crop Science*, 47(5), pp.2067-2073.

Rizi, M.S. and Mohammadi, M., 2023. Breeding crops for enhanced roots to mitigate against climate change without compromising yield. *Rhizosphere*, 26, p.100702.

Robbins, N.E. and Dinneny, J.R., 2018. Growth is required for perception of water availability to pattern root branches in plants. *Proceedings of the National Academy of Sciences*, *115*(4), pp.E822-E831.

Robson, J.K., Ferguson, J.N., McAusland, L., Atkinson, J.A., Tranchant-Dubreuil, C., Cubry, P., Sabot, F., Wells, D.M., Price, A.H., Wilson, Z.A. and Murchie, E.H., 2023. Chlorophyll fluorescence-based high-throughput phenotyping facilitates the genetic dissection of photosynthetic heat tolerance in African (*Oryza glaberrima*) and Asian (*Oryza sativa*) rice. *Journal Of Experimental Botany*, *74*(17), pp.5181-5197.

Rodrigues, J., Inzé, D., Nelissen, H. and Saibo, N.J., 2019. Source–sink regulation in crops under water deficit. *Trends in Plant Science*, *24*(7), pp.652-663.

Rodríguez-Peña, J.M., García, R., Nombela, C. and Arroyo, J., 2010. The high-osmolarity glycerol (HOG) and cell wall integrity (CWI) signalling pathways interplay: a yeast dialogue between MAPK routes. *Yeast*, *27*(8), pp.495-502.

Ross, C.A., Liu, Y. and Shen, Q.J., 2007. The *WRKY* gene family in rice (*Oryza sativa*). *Journal Of Integrative Plant Biology*, *49*(6), pp.827-842.

Rosso, M.G., Li, Y., Strizhov, N., Reiss, B., Dekker, K. and Weisshaar, B., 2003. An *A* thaliana*. thaliana* T-DNA mutagenized population (GABI-Kat) for flanking sequence tag-based reverse genetics. *Plant Molecular Biology*, *53*, pp.247-259.

Roth, M.S., Gallaher, S.D., Westcott, D.J., Iwai, M., Louie, K.B., Mueller, M., Walter, A., Foflonker, F., Bowen, B.P., Ataii, N.N. and Song, J., 2019. Regulation of oxygenic photosynthesis during trophic transitions in the green alga *Chromochloris zofingiensis*. *The Plant Cell*, *31*(3), pp.579-601

Rouphael, Y., Cardarelli, M., Schwarz, D., Franken, P. and Colla, G., 2012. Effects of drought on nutrient uptake and assimilation in vegetable crops. *Plant Responses to Drought Stress: From Morphological To Molecular Features*, pp.171-195.

RStudio (2012) *RStudio: Integrated Development Environment for R (Version 0.95.262)*. Boston, MA: R Studio.

Ruban, A.V. and Belgio, E., 2014. The relationship between maximum tolerated light intensity and photoprotective energy dissipation in the photosynthetic antenna: chloroplast gains and losses. *Philosophical Transactions Of The Royal Society B: Biological Sciences*, 369(1640), p.20130222.

Ruban, A.V. and Murchie, E.H., 2012. Assessing the photoprotective effectiveness of non-photochemical chlorophyll fluorescence quenching: a new approach. *Biochimica Et Biophysica Acta (BBA)-Bioenergetics*, 1817(7), pp.977-982.

Rushton, D.L., Tripathi, P., Rabara, R.C., Lin, J., Ringler, P., Boken, A.K., Langum, T.J., Smidt, L., Boomsma, D.D., Emme, N.J. and Chen, X., 2012. WRKY transcription factors: key components in abscisic acid signalling. *Plant Biotechnology Journal*, *10*(1), pp.2-11.

Rushton, P.J., Somssich, I.E., Ringler, P. and Shen, Q.J., 2010. WRKY transcription factors. *Trends In Plant* Science, *15*(5), pp.247-258.

Rushton, P.J., Torres, J.T., Parniske, M., Wernert, P., Hahlbrock, K. and Somssich, I.E., 1996. Interaction of elicitor-induced DNA-binding proteins with elicitor response elements in the promoters of parsley PR1 genes. *The EMBO Journal*, *15*(20), pp.5690-5700.

Sabetta, W., Alba, V., Blanco, A. and Montemurro, C., 2011. sunTILL: a TILLING resource for gene function analysis in sunflower. *Plant Methods*, *7*, pp.1-13.

Saeed, B., Das, M. and Khurana, P., 2015. Overexpression of β-carotene hydroxylase1 (BCH1) in Indian mulberry, Morus indica cv. K2, confers tolerance against UV, high temperature and high irradiance stress induced oxidative damage. *Plant Cell, Tissue And Organ Culture (PCTOC)*, *120*, pp.1003-1014.

Saeed, F., Chaudhry, U.K., Raza, A., Charagh, S., Bakhsh, A., Bohra, A., Ali, S., Chitikineni, A., Saeed, Y., Visser, R.G. and Siddique, K.H., 2023. Developing future heat-resilient vegetable crops. *Functional & Integrative Genomics*, *23*(1), p.47.

Saibo, N.J., Lourenço, T. and Oliveira, M.M., 2009. Transcription factors and regulation of photosynthetic and related metabolism under environmental stresses. *Annals Of Botany*, *103*(4), pp.609-623.

Sakuma, Y., Maruyama, K., Qin, F., Osakabe, Y., Shinozaki, K. and Yamaguchi-Shinozaki, K., 2006. Dual function of an *A. thaliana* transcription factor DREB2A in water-stress-responsive and heat-stress-responsive gene expression. *Proceedings Of the National Academy Of Sciences*, *103*(49), pp.18822-18827.

Sala, O.E., Stuart Chapin, F.I.I.I., Armesto, J.J., Berlow, E., Bloomfield, J., Dirzo, R., Huber-Sanwald, E., Huenneke, L.F., Jackson, R.B., Kinzig, A. and Leemans, R., 2000. Global biodiversity scenarios for the year 2100. *Science*, *287*(5459), pp.1770-1774.

Sales, C.R., Molero, G., Evans, J.R., Taylor, S.H., Joynson, R., Furbank, R.T., Hall, A. and Carmo-Silva, E., 2022. Phenotypic variation in photosynthetic traits in wheat grown under field versus glasshouse conditions. *Journal Of Experimental Botany*, *73*(10), pp.3221-3237.

Sathi, K.S., Masud, A.A.C., Anee, T.I., Rahman, K., Ahmed, N. and Hasanuzzaman, M., 2022. Soybean plants under waterlogging stress: Responses and adaptation mechanisms. In *Managing Plant production under changing environment* (pp. 103-134). Singapore: Springer Nature Singapore.

Schapire, A.L., Voigt, B., Jasik, J., Rosado, A., Lopez-Cobollo, R., Menzel, D., Salinas, J., Mancuso, S., Valpuesta, V., Baluska, F. and Botella, M.A., 2008. *A. thaliana* synaptotagmin 1 is required for the maintenance of plasma membrane integrity and cell viability. *The Plant Cell*, *20*(12), pp.3374-3388.

Schnitter, R. and Berry, P., 2019. The climate change, food security and human health nexus in Canada: A framework to protect population health. *International Jjournal Of Environmental Research And Public Health*, *16*(14), p.2531.

Schwartz, S.H., Qin, X. and Zeevaart, J.A., 2003. Elucidation of the indirect pathway of abscisic acid biosynthesis by mutants, genes, and enzymes. *Plant Physiology*, *131*(4), pp.1591-1601.

Seiler, C., Harshavardhan, V.T., Rajesh, K., Reddy, P.S., Strickert, M., Rolletschek, H., Scholz, U., Wobus, U. and Sreenivasulu, N., 2011. ABA biosynthesis and degradation contributing to ABA homeostasis during barley seed development under control and terminal drought-stress conditions. *Journal Of Experimental Botany*, *62*(8), pp.2615-2632.

Seiler, G.J., 1998. Influence of temperature on primary and lateral root growth of sunflower seedlings. *Environmental And Experimental Botany*, 40(2), pp.135-146.

Seki, M., Kamei, A., Yamaguchi-Shinozaki, K. and Shinozaki, K., 2003. Molecular responses to drought, salinity and frost: common and different paths for plant protection. *Current Opinion In Biotechnology*, *14*(2), pp.194-199.

Sessions, A., Burke, E., Presting, G., Aux, G., McElver, J., Patton, D., Dietrich, B., Ho, P., Bacwaden, J., Ko, C. and Clarke, J.D., 2002. A high-throughput *A. thaliana* reverse genetics system. *The Plant Cell*, *14*(12), pp.2985-2994.

Setter, T.L. and Waters, I., 2003. Review of prospects for germplasm improvement for waterlogging tolerance in wheat, barley and oats. *Plant And Soil*, *253*, pp.1-34.

Shahwar, D., Ahn, N., Kim, D., Ahn, W. and Park, Y., 2023. Mutagenesis-based plant breeding approaches and genome engineering: a review focused on tomato. *Mutation Research/Reviews in Mutation Research*, p.108473.

Shanmugam, S., Boyett, V.A. and Khodakovskaya, M., 2021. Enhancement of drought tolerance in rice by silencing of the OsSYT-5 gene. *PloS One*, *16*(10), p.e0258171.

Sharkey, T.D., 1989. Evaluating the role of Rubisco regulation in photosynthesis of C3 plants. *Philosophical Transactions Of The Royal Society Of London. B, Biological Sciences*, *323*(1216), pp.435-448.

Sharkey, T.D., 2005. Effects of moderate heat stress on photosynthesis: importance of thylakoid reactions, rubisco deactivation, reactive oxygen species, and thermotolerance provided by isoprene. *Plant, Cell & Environment*, 28(3), pp.269-277.

Sharma, D., Kaur, H., Kapoor, H.K., Sharma, R., Kaur, H. and Kyum, M., 2022. Genome Editing: A Review of the Challenges and Approaches. *Genome Editing: Current Technology Advances And Applications For Crop Improvement*, pp.71-101.

Sharma, E., Borah, P., Kaur, A., Bhatnagar, A., Mohapatra, T., Kapoor, S. and Khurana, J.P., 2021. A comprehensive transcriptome analysis of contrasting rice cultivars highlights the role of auxin and ABA responsive genes in heat stress response. *Genomics*, *113*(3), pp.1247-1261.

Shen, J.R., Henmi, T. and Kamiya, N., 2008. Structure and function of photosystem II. *Photosynthetic Protein Complexes: A Structural Approach*, pp.83-106.

Sher, A., Arfat, M.Y., Ul-Allah, S., Sattar, A., Ijaz, M., Manaf, A., Qayyum, A., Zuan, A.T.K., Nasif, O. and Gasparovic, K., 2021. Conservation tillage improves productivity of sunflower (Helianthus annuus L.) under reduced irrigation on sandy loam soil. *Plos One*, *16*(12), p.e0260673.

Shin, J., Mahmud, M.S., Rehman, T.U., Ravichandran, P., Heung, B. and Chang, Y.K., 2022. Trends and prospect of machine vision technology for stresses and diseases detection in precision agriculture. *AgriEngineering*, *5*(1), pp.20-39.

Shinozaki, K. and Yamaguchi-Shinozaki, K., 2007. Gene networks involved in drought stress response and tolerance. *Journal Of Experimental Botany*, *58*(2), pp.221-227.

Signora, L., De Smet, I., Foyer, C.H. and Zhang, H., 2001. ABA plays a central role in mediating the regulatory effects of nitrate on root branching in *A. thaliana*. *The Plant Journal*, *28*(6), pp.655-662.

Simkin, A.J., Alqurashi, M., Lopez-Calcagno, P.E., Headland, L.R. and Raines, C.A., 2023. Glyceraldehyde-3-phosphate dehydrogenase subunits A and B are essential to maintain photosynthetic efficiency. *Plant Physiology*, *192*(4), pp.2989-3000.

Sirko, A., Wawrzyńska, A., Brzywczy, J. and Sieńko, M., 2021. Control of ABA signalling and crosstalk with other hormones by the selective degradation of pathway components. *International Journal Of Molecular Sciences*, *22*(9), p.4638.

Skirycz, A. and Inzé, D., 2010. More from less: plant growth under limited water. *Current Opinion in Biotechnology*, *21*(2), pp.197-203.

Skotnicová, P., Staleva-Musto, H., Kuznetsova, V., Bína, D., Konert, M.M., Lu, S., Polívka, T. and Sobotka, R., 2021. Plant LHC-like proteins show robust folding and static non-photochemical quenching. *Nature Communications*, 12(1), p.6890.

Slade, A.J., McGuire, C., Loeffler, D., Mullenberg, J., Skinner, W., Fazio, G., Holm, A., Brandt, K.M., Steine, M.N., Goodstal, J.F. and Knauf, V.C., 2012. Development of high amylose wheat through TILLING. *BMC plant biology*, *12*, pp.1-17.

Song, Q., Wang, Y., Qu, M., Ort, D.R. and Zhu, X.G., 2017. The impact of modifying photosystem antenna size on canopy photosynthetic efficiency—Development of a new canopy photosynthesis model scaling from metabolism to canopy level processes. *Plant, Cell & Environment*, 40(12), pp.2946-2957.

Song, Q., Zhang, G. and Zhu, X.G., 2013. Optimal crop canopy architecture to maximise canopy photosynthetic CO_2 uptake under elevated CO_2–a theoretical study using a mechanistic model of canopy photosynthesis. *Functional Plant Biology*, *40*(2), pp.108-124.

Song, Y., Xiang, F., Zhang, G., Miao, Y., Miao, C. and Song, C.P., 2016. Abscisic acid as an internal integrator of multiple physiological processes modulates leaf senescence onset in *A. thaliana*. *Frontiers In Plant Science*, *7*, p.181.

Soni, M.L., Subbulakshmi, V., Sheetal, K.R., Yadava, N.D. and Dagar, J.C., 2017. Agroforestry for increasing farm productivity in water-stressed ecologies. *Agroforestry: Anecdotal to Modern Science*, pp.369-411.

Sun, G., Feng, C., Guo, J., Zhang, A., Xu, Y., Wang, Y., Day, B. and Ma, Q., 2019. The tomato Arp2/3 complex is required for resistance to the powdery mildew fungus Oidium neolycopersici. *Plant, Cell & Environment*, *42*(9), pp.2664-2680.

Sun, J., Qiu, C., Ding, Y., Wang, Y., Sun, L., Fan, K., Gai, Z., Dong, G., Wang, J., Li, X. and Song, L., 2020. Fulvic acid ameliorates drought stress-induced damage in tea plants by regulating the ascorbate metabolism and flavonoids biosynthesis. *BMC Genomics*, *21*, pp.1-13.

Sun, Q., Zhou, X., Yang, L., Xu, H. and Zhou, X., 2023. Integration of phosphoproteomics and transcriptome studies reveals ABA signalling pathways regulate UV-B tolerance in *rhododendron chrysanthum* leaves. *Genes*, *14*(6), p.1153.

Sun, Z., Gantt, E. and Cunningham, F.X., 1996. Cloning and functional analysis of the β-carotene hydroxylase of *A* thaliana*. thaliana*. *Journal Of Biological Chemistry*, *271*(40), pp.24349-24352.

Suzuki, N., Rivero, R.M., Shulaev, V., Blumwald, E. and Mittler, R., 2014. Abiotic and biotic stress combinations. *New Phytologist*, *203*(1), pp.32-43.

Suzuki, T., Eiguchi, M., Kumamaru, T., Satoh, H., Matsusaka, H., Moriguchi, K., Nagato, Y. and Kurata, N., 2008. MNU-induced mutant pools and high performance TILLING enable finding of any gene mutation in rice. *Molecular Genetics and Genomics*, *279*, pp.213-223.

Suzuki, Y., Ishiyama, K., Sugawara, M., Suzuki, Y., Kondo, E., Takegahara-Tamakawa, Y., Yoon, D.K., Suganami, M., Wada, S., Miyake, C. and Makino, A., 2021. Overproduction of chloroplast glyceraldehyde-3-phosphate dehydrogenase improves photosynthesis slightly under elevated [CO_2] conditions in rice. *Plant and Cell Physiology*, *62*(1), pp.156-165.

Suzuki, Y., Ohkubo, M., Hatakeyama, H., Ohashi, K., Yoshizawa, R., Kojima, S., Hayakawa, T., Yamaya, T., Mae, T. and Makino, A., 2007. Increased Rubisco content in transgenic rice transformed with the 'sense'rbcS gene. *Plant and Cell Physiology*, *48*(4), pp. 626–637.

Takenaka, M., Zehrmann, A., Verbitskiy, D., Kugelmann, M., Härtel, B. and Brennicke, A., 2012. Multiple organellar RNA editing factor (MORF) family proteins are required for RNA editing in mitochondria and plastids of plants. *Proceedings Of The National Academy Of Sciences*, *109*(13), pp.5104-5109.

Tan, X., Xu, H., Khan, S., Equiza, M.A., Lee, S.H., Vaziriyeganeh, M. and Zwiazek, J.J., 2018. Plant water transport and aquaporins in oxygen-deprived environments. *Journal of Plant Physiology*, *227*, pp.20-30.

Tardieu, F. and Tuberosa, R., 2010. Dissection and modelling of abiotic stress tolerance in plants. *Current Opinion in Plant Biology*, *13*(2), pp.206-212.

Tardieu, F., Simonneau, T. and Muller, B., 2018. The physiological basis of drought tolerance in crop plants: a scenario-dependent probabilistic approach. *Annual Review of Plant Biology*, *69*(1), pp.733-759.

Tardieu, F., Simonneau, T. and Muller, B., 2018. The physiological basis of drought tolerance in crop plants: a scenario-dependent probabilistic approach. *Annual Review of Plant Biology*, *69*(1), pp.733-759.

Teoh, E.Y., Teo, C.H., Baharum, N.A., Pua, T.L. and Tan, B.C., 2022. Waterlogging stress induces antioxidant defence responses, aerenchyma formation and alters metabolisms of banana plants. *Plants*, *11*(15), p.2052.

Tian, L. and DellaPenna, D., 2001. Characterisation of a second carotenoid β-hydroxylase gene from *A. thaliana* and its relationship to the LUT1 locus. *Plant Molecular Biology*, *47*, pp.379-388.

Tian, L., 2003. *Cloning and characterization Of carotenoid hydroxylases in A thaliana. thaliana*. Michigan State University.

Tian, L.X., Zhang, Y.C., Chen, P.L., Zhang, F.F., Li, J., Yan, F., Dong, Y. and Feng, B.L., 2021. How does the waterlogging regime affect crop yield? A global meta-analysis. *Frontiers In Plant Science*, *12*, p.634898.

Timms, R.T. and Koren, I., 2020. Tying up loose ends: the N-degron and C-degron pathways of protein degradation. *Biochemical Society Transactions*, *48*(4), pp.1557-1567.

Trought, M.C.T. and Drew, M.C., 1980. The development of waterlogging damage in wheat seedlings (Triticum aestivum L.) I. Shoot and root growth in relation to changes in the concentrations of dissolved gases and solutes in the soil solution. *Plant and Soil*, *54*, pp.77-94.

Uauy, C., Paraiso, F., Colasuonno, P., Tran, R.K., Tsai, H., Berardi, S., Comai, L. and Dubcovsky, J., 2009. A modified TILLING approach to detect induced mutations in tetraploid and hexaploid wheat. *BMC Plant Biology*, *9*, pp.1-14.

Ülker, B. and Somssich, I.E., 2004. WRKY transcription factors: from DNA binding towards biological function. *Current Opinion In in Plant Biology*, *7*(5), pp.491-498.

United Nations (2024) *What is climate change?* Available at: https://www.un.org/en/climatechange/what-is-climate-change (Accessed: 20 December 2024).

Uno, Y., Furihata, T., Abe, H., Yoshida, R., Shinozaki, K. and Yamaguchi-Shinozaki, K., 2000. *A. thaliana* basic leucine zipper transcription factors involved in an abscisic acid-dependent signal transduction pathway under drought and high-salinity conditions. *Proceedings Of the National Academy Of Sciences*, *97*(21), pp.11632-11637.

Van Zelm, E., Zhang, Y. and Testerink, C., 2020. Salt tolerance mechanisms of plants. *Annual Review Of Plant Biology*, 71, pp.403-433.

Varshavsky, A., 2019. N-degron and C-degron pathways of protein degradation. *Proceedings Of the National Academy Of Sciences*, *116*(2), pp.358-366.

Vogel, E., Donat, M.G., Alexander, L.V., Meinshausen, M., Ray, D.K., Karoly, D., Meinshausen, N. and Frieler, K., 2019. The effects of climate extremes on global agricultural yields. *Environmental Research Letters*, *14*(5), p.054010.

Wang X, Yesbergenova-Cuny Z, Biniek C, Bailly C, El-Maarouf-Bouteau H, Corbineau F (2018) Revisiting the role of ethylene and N-end rule pathway on chilling-induced dormancy release in *A. thaliana* seeds. *Int J Mol Sci* 19: 3577

Wang, H., Han, S., Siao, W., Song, C., Xiang, Y., Wu, X., Cheng, P., Li, H., Jásik, J., Mičieta, K. and Turňa, J., 2015. *A. thaliana* synaptotagmin 2 participates in pollen germination and tube growth and is delivered to plasma membrane via conventional secretion. *Molecular Plant*, *8*(12), pp.1737-1750.

Wang, H., Wang, H., Shao, H. and Tang, X., 2016. Recent advances in utilizing transcription factors to improve plant abiotic stress tolerance by transgenic technology. *Frontiers In* in *Plant Science*, *7*, p.67.

Wang, J., Lewis, M.E., Whallon, J.H. and Sink, K.C., 1995. Chromosomal mapping of T-DNA inserts in transgenic Petunia by in situ hybridisation. *Transgenic Research*, *4*, pp.241-246.

Wang, S., Li, Y. and Ma, C., 2016. Synaptotagmin-1 C2B domain interacts simultaneously with SNAREs and membranes to promote membrane fusion. *Elife*, *5*, p.e14211.

Wang, X., Guo, C., Peng, J., Li, C., Wan, F., Zhang, S., Zhou, Y., Yan, Y., Qi, L., Sun, K. and Yang, S., 2019. ABRE-BINDING FACTORS play a role in the feedback regulation of ABA signalling by mediating rapid ABA induction of ABA co-receptor genes. *New Phytologist*, *221*(1), pp.341-355.

Wang, X., He, Y., Zhang, C., Tian, Y.A., Lei, X., Li, D., Bai, S., Deng, X. and Lin, H., 2021. Physiological and transcriptional responses of *Phalaris arundinacea* under waterlogging conditions. *Journal Of Plant Physiology*, *261*, p.153428.

Wang, Y., Cui, X., Yang, B., Xu, S., Wei, X., Zhao, P., Niu, F., Sun, M., Wang, C., Cheng, H. and Jiang, Y.Q., 2020. WRKY55 transcription factor positively regulates leaf senescence and the defence response by modulating the transcription of genes implicated in the biosynthesis of reactive oxygen species and salicylic acid in *A. thaliana*. *Development*, 147(16), p.dev189647.

Wang, Y., Yang, J., Miao, R., Kang, Y. and Qi, Z., 2021. A novel zinc transporter essential for *A. thaliana* zinc and iron-dependent growth. *Journal Of Plant Physiology*, *256*, p.153296.

Waters, B.M. and Grusak, M.A., 2008. Quantitative trait locus mapping for seed mineral concentrations in two *A* thaliana. *thaliana* recombinant inbred populations. *New Phytologist*, *179*(4), pp.1033-1047.

Weits, D.A., Giuntoli, B., Kosmacz, M., Parlanti, S., Hubberten, H.M., Riegler, H., Hoefgen, R., Perata, P., Van Dongen, J.T. and Licausi, F., 2014. Plant cysteine oxidases control the oxygen-dependent branch of the N-end-rule pathway. *Nature Communications*, *5*(1), p.3425.

West, G., Inzé, D. and Beemster, G.T., 2004. Cell cycle modulation in the response of the primary root of *A. thaliana* to salt stress. *Plant Physiology*, 135(2), pp.1050-1058.

Woody, S.T., Austin-Phillips, S., Amasino, R.M. and Krysan, P.J., 2007. The WiscDsLox T-DNA collection: an *A. thaliana* community resource generated by using an improved high-throughput T-DNA sequencing pipeline. *Journal Of Plant Research*, *120*, pp.157-165.

Wu, H., Tito, N. and Giraldo, J.P., 2017. Anionic cerium oxide nanoparticles protect plant photosynthesis from abiotic stress by scavenging reactive oxygen species. *ACS Nano*, *11*(11), pp.11283-11297.

Wu, J., Cho, E., Willett, W.C., Sastry, S.M. and Schaumberg, D.A., 2015. Intakes of lutein, zeaxanthin, and other carotenoids and age-related macular degeneration during 2 decades of prospective follow-up. *JAMA Ophthalmology*, 133(12), pp.1415-1424.

Wu, J., Yan, G., Duan, Z., Wang, Z., Kang, C., Guo, L., Liu, K., Tu, J., Shen, J., Yi, B. and Fu, T., 2020. Roles of the Brassica napus DELLA protein BnaA6. RGA, in modulating drought tolerance by interacting with the ABA signalling component BnaA10. ABF2. *Frontiers In in Plant Science*, *11*, p.577.

Wu, M., Tu, A., Feng, H., Guo, Y., Xu, G., Shi, J., Chen, J., Yang, J. and Zhong, K., 2023. Genome-Wide Identification and Analysis of the ABCF Gene Family in Triticum aestivum. *International Journal Of Molecular Sciences*, 24(22), p.16478.

Xiong, L. and Zhu, J.K., 2003. Regulation of abscisic acid biosynthesis. *Plant Physiology*, *133*(1), pp.29-36.

Yadav, R.K., Tripathi, M.K., Tiwari, S., Tripathi, N., Asati, R., Chauhan, S., Tiwari, P.N. and Payasi, D.K., 2023. Genome editing and improvement of abiotic stress tolerance in crop plants. *Life*, *13*(7), p.1456.

Yamaguchi-Shinozaki, K. and Shinozaki, K., 2006. Transcriptional regulatory networks in cellular responses and tolerance to dehydration and cold stresses. *Annu. Rev. Plant Biol.*, *57*, pp.781-803.

Yamamoto, Y., 2016. Quality control of photosystem II: the mechanisms for avoidance and tolerance of light and heat stresses are closely linked to membrane fluidity of the thylakoids. *Frontiers In in Plant Science*, 7, p.208231.

Yamazaki, T., Kawamura, Y., Minami, A. and Uemura, M., 2008. Calcium-dependent freezing tolerance in *A. thaliana* involves membrane resealing via synaptotagmin SYT1. *The Plant Cell*, *20*(12), pp.3389-3404.

Yigit, N., Sevik, H., Cetin, M. and Kaya, N., 2016. Determination of the effect of drought stress on the seed germination in some plant species. *Water Stress in Plants*, 43, p.62.

Yin, Y., Qin, K., Song, X., Zhang, Q., Zhou, Y., Xia, X. and Yu, J., 2018. BZR1 transcription factor regulates heat stress tolerance through FERONIA receptor-like kinase-mediated reactive oxygen species signalling in tomato. *Plant and Cell Physiology*, *59*(11), pp.2239-2254.

Yoshida, S., Ito, M., Callis, J., Nishida, I. and Watanabe, A., 2002. A delayed leaf senescence mutant is defective in arginyl-tRNA: protein arginyltransferase, a component of the N-end rule pathway in *A. thaliana*. *The Plant Journal*, *32*(1), pp.129-137.

Yoshioka-Nishimura, M., 2016. Close relationships between the PSII repair cycle and thylakoid membrane dynamics. *Plant And Cell Physiology*, 57(6), pp.1115-1122.

Zafar, S.A., Hameed, A., Ashraf, M., Khan, A.S., Li, X. and Siddique, K.H., 2020. Agronomic, physiological and molecular characterisation of rice mutants revealed the key role of reactive oxygen species and catalase in high-temperature stress tolerance. *Functional Plant Biology*, *47*(5), pp.440-453.

Zandalinas, S.I., Fritschi, F.B. and Mittler, R., 2021. Global warming, climate change, and environmental pollution: recipe for a multifactorial stress combination disaster. *Trends in Plant Science*, *26*(6), pp.588-599.

Zeng, D. and Luo, X., 2012. Physiological effects of chitosan coating on wheat growth and activities of protective enzyme with drought tolerance. *Open Journal of Soil Science*, *2*(03), p.282.

Zeng, L., Deng, R., Guo, Z., Yang, S. and Deng, X., 2016. Genome-wide identification and characterisation of Glyceraldehyde-3-phosphate dehydrogenase genes family in wheat (*Triticum aestivum*). *BMC Genomics*, *17*, pp.1-10.

Zhang, H., Liu, D., Yang, B., Liu, W.Z., Mu, B., Song, H., Chen, B., Li, Y., Ren, D., Deng, H. and Jiang, Y.Q., 2020. *A. thaliana* CPK6 positively regulates ABA signalling and drought tolerance through phosphorylating ABA-responsive element-binding factors. *Journal Of Experimental Botany*, *71*(1), pp.188-203.

Zhang, H., Zhang, J., Wei, P., Zhang, B., Gou, F., Feng, Z., Mao, Y., Yang, L., Zhang, H., Xu, N. and Zhu, J.K., 2014. The CRISPR/C as9 system produces specific and homozygous targeted gene editing in rice in one generation. *Plant Biotechnology Jjournal*, *12*(6), pp.797-807.

Zhang, H., Zhang, L., Gao, B., Fan, H., Jin, J., Botella, M.A., Jiang, L. and Lin, J., 2011. Golgi apparatus-localized synaptotagmin 2 is required for unconventional secretion in *A. thaliana*. *PLoS One*, *6*(11), p.e26477.

Zhang, K., Zhang, Y., Sun, J., Meng, J. and Tao, J., 2021. Deterioration of orthodox seeds during ageing: Influencing factors, physiological alterations and the role of reactive oxygen species. *Plant Physiology And Biochemistry*, *158*, pp.475-485.

Zhang, X., Han, Y., Han, X., Zhang, S., Xiong, L. and Chen, T., 2023. Peptide chain release factor DIG8 regulates plant growth by affecting ROS-mediated sugar transportation in *A. thaliana*. *Frontiers In Plant Science*, *14*, p.1172275.

Zhao, J., Ju, M., Qian, J., Zhang, M., Liu, T. and Zhang, K., 2021. A Tobacco Syringe Agroinfiltration-Based Method for a Phytohormone Transporter Activity Assay Using Endogenous Substrates. *Frontiers In Plant Science*, *12*, p.660966.

Zhao, Y., Pan, Z., Zhang, Y., Qu, X., Zhang, Y., Yang, Y., Jiang, X., Huang, S., Yuan, M., Schumaker, K.S. and Guo, Y., 2013. The actin-related Protein2/3 complex regulates mitochondrial-associated calcium signalling during salt stress in *A. thaliana*. *The Plant Cell*, *25*(11), pp.4544-4559.

Zhao, Z., Zhu, Y., Erhardt, M., Ruan, Y. and Shen, W.H., 2009. A non-canonical transferred DNA insertion at the BRI1 locus in *A. thaliana*. *Journal Of Integrative Plant Biology*, *51*(4), pp.367-373.

Zheng, C., Jiang, D., Liu, F., Dai, T., Jing, Q. and Cao, W., 2009. Effects of salt and waterlogging stresses and their combination on leaf photosynthesis, chloroplast ATP synthesis, and antioxidant capacity in wheat. *Plant Science*, *176*(4), pp.575-582.

Zheng, S., Su, M., Wang, L., Zhang, T., Wang, J., Xie, H., Wu, X., Haq, S.I.U. and Qiu, Q.S., 2021. Small signalling molecules in plant response to cold stress. *Journal Of Plant Physiology*, *266*, p.153534.

Zhou, Z., Majeed, Y., Naranjo, G.D. and Gambacorta, E.M., 2021. Assessment for crop water stress with infrared thermal imagery in precision agriculture: A review and future prospects for deep learning applications. *Computers and Electronics in Agriculture*, *182*, p.106019.

Zhu, X.G., Long, S.P. and Ort, D.R., 2010. Improving photosynthetic efficiency for greater yield. *Annual Review Of Plant Biology*, 61, pp.235-261.

Zhu, X.G., Ort, D.R., Whitmarsh, J. and Long, S.P., 2004. The slow reversibility of photosystem II thermal energy dissipation on transfer from high to low light may cause large losses in carbon gain by crop canopies: a theoretical analysis. *Journal Of Experimental Botany*, 55(400), pp.1167-1175.

Zou, J.J., Zheng, Z.Y., Xue, S., Li, H.H., Wang, Y.R. and Le, J., 2016. The role of *A. thaliana* Actin-Related Protein 3 in amyloplast sedimentation and polar auxin transport in root gravitropism. *Journal Of Experimental Botany*, *67*(18), pp.5325-5337.

Appendix I

NTAQ alignment

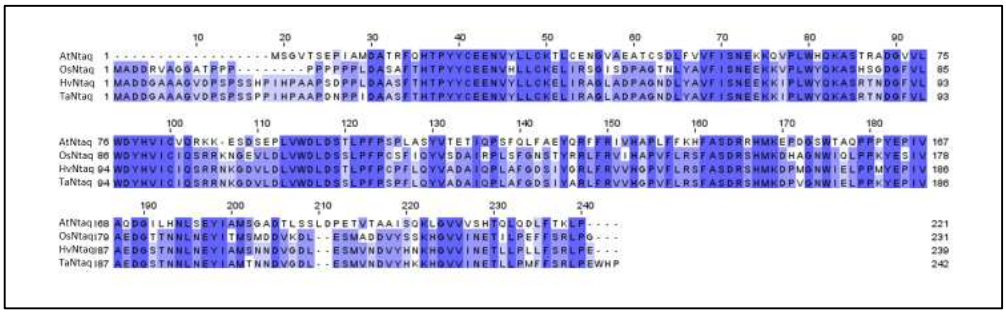

Figure I.2: A multiple sequence alignment of four species in the NTAQ gene showing conserved areas in blue.

ABI5 alignment

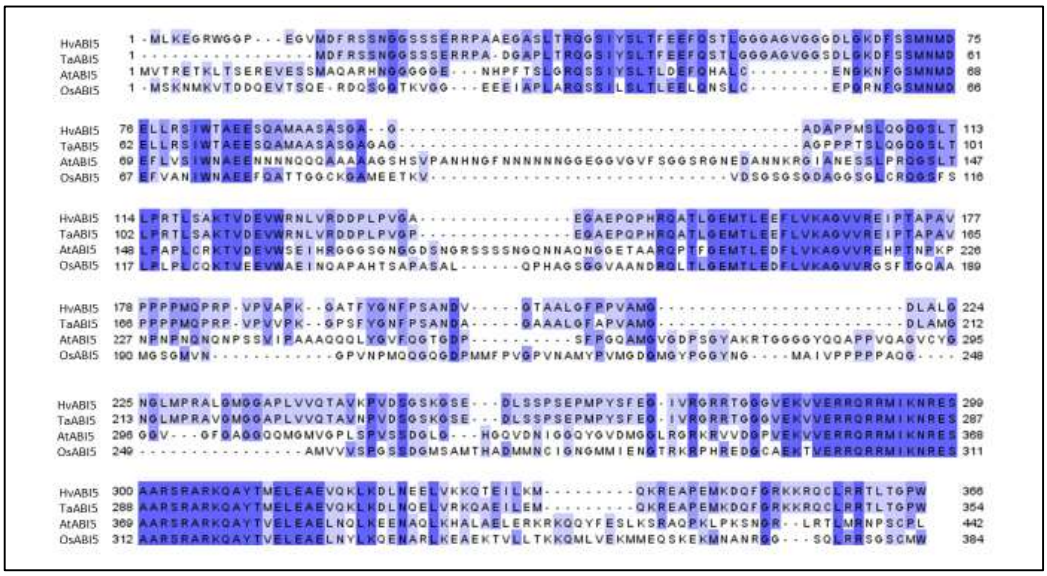

Figure I.2: A multiple sequence alignment of 4 species in the ABI5 gene showing conserved areas in blue.

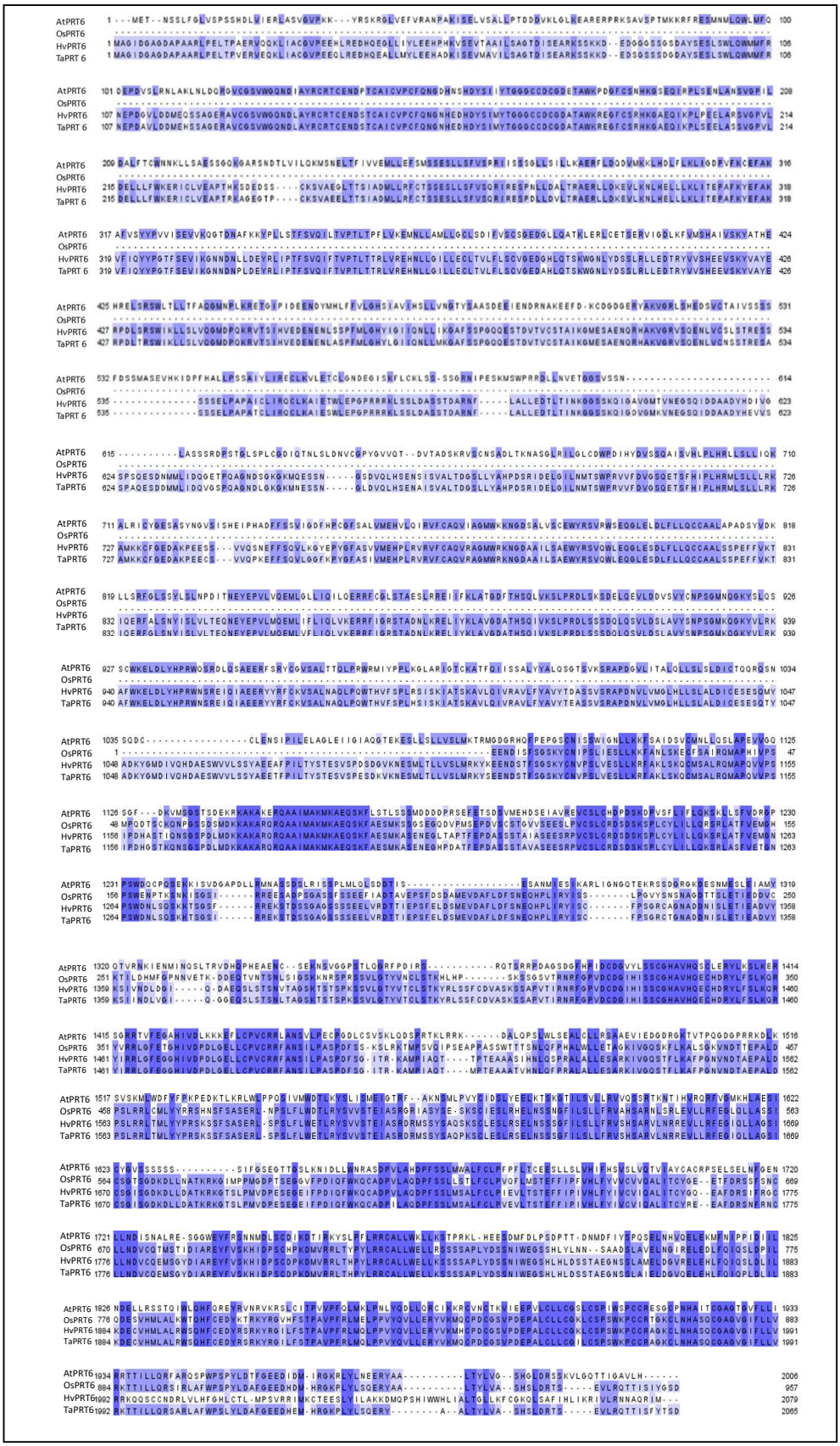

Figure I.3: A multiple sequence alignment of four species in the PRT6 gene showing conserved areas in blue.

Appendix II: Field growth conditions

N.B. All information in appendix II provided by University of Nottingham technicians Matthew Tovey and John Ferguson.

Previous crop:	Winter Oats
SNS N Index:	7.7 kg/ha, SNS Index 1
Soil Indices:	P:5, K:2+, Mg:4, pH:7.1
Sowing date:	28/05/2021
Seed rate (m-2):	360 seeds
Drill type:	Haldrup
Row width (m):	0.2
Plot length (m):	1.0
Plot width (m):	0.4

Cultivations:

Date	Details
11/09/2020	Subsoil
13/09/2020	Plough + Press
06/04/2021	Deep Tine Cultivate
15/05/2021	Power Harrow
28/05/2021	Roll after drilling

Chemical applications:

Type	Date	Details
Fertiliser	09/05/2021	174 kg/ha 34.5% Nitram (60kg/ha N) into seedbed
Fertiliser	30/06/2021	Opte Man @ 3l/ha
Fertiliser	10/08/2021	203 kg/ha 34.5% Nitram (70kg/ha N) into seedbed
Fertiliser	10/08/2021	Master Manganesium + Te @ 2kg/ha
Fertiliser	10/08/2021	Opte Man @ 3l/ha
Herbicide	27/02/2021	Touchdown Quattro @ 2.0 l/ha
Herbicide	28/05/2021	Liberator @ 0.3l/ha + Picona @ 2.5l/ha
Herbicide	23/06/2021	Zypar @ 1l/ha
Fungicide	30/06/2021	Mobius @ 0.5l/ha + Pheonix @ 1l/ha
Fungicide	15/07/2021	Kestrel @ 0.5l/ha + Ceratavo Plus @ 0.3l/ha
Fungicide	10/08/2021	Mobius @ 0.6 l/ha + Kestrel @ 0.6 l/ha

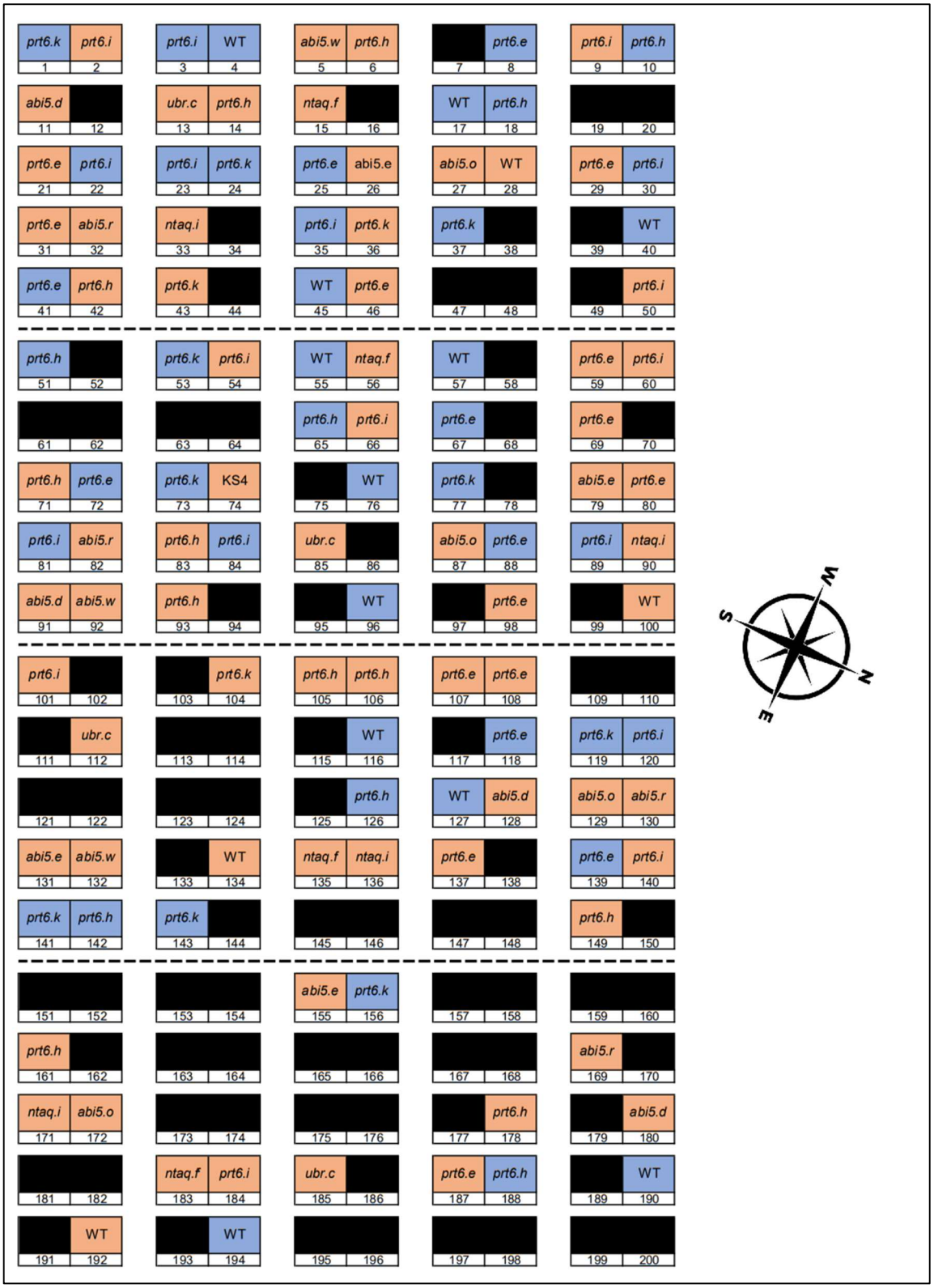

Figure II.1: Plot layout of the field containing Hordeum vulgare TILLING mutants used in this study and wild types (WT), with orange boxes signifying lines in the Sebastian cultivar background and blue boxes representing plants in the Voyager cultivar background. Black boxes represent Barley plants not used in the study grown to reduce edge effects. Boxes represent plots of 1m length by 0.2m width, each containing two rows.

Appendix III: Genotyping of TILLING lines within *Prt6*

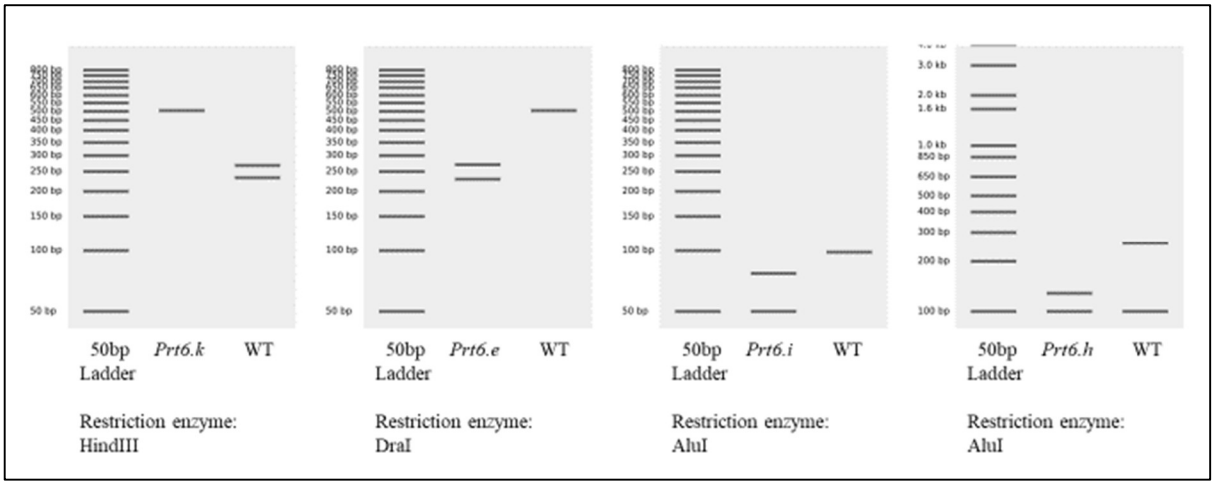

Figure III.1: Virtual restriction digests (Benchling.com) showing the expected bands seen when running a restriction digest with the corresponding restriction enzyme and primers seen in Table 3.2.

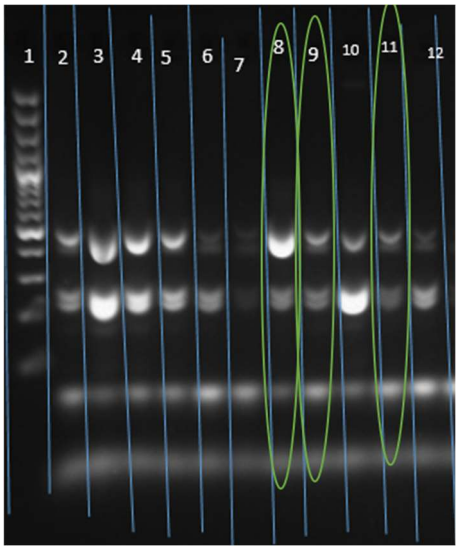

Figure III.2: Example of gel visualisation of PCR products in order to determine prt6k homozygous mutants. Note that homozygous lines show both WT and mutant bands (as confirmed through sequencing by Kate Rochenbach (AbInBev), however the larger PCR product is brighter than the smaller product. Green circles highlight homozygous mutants.

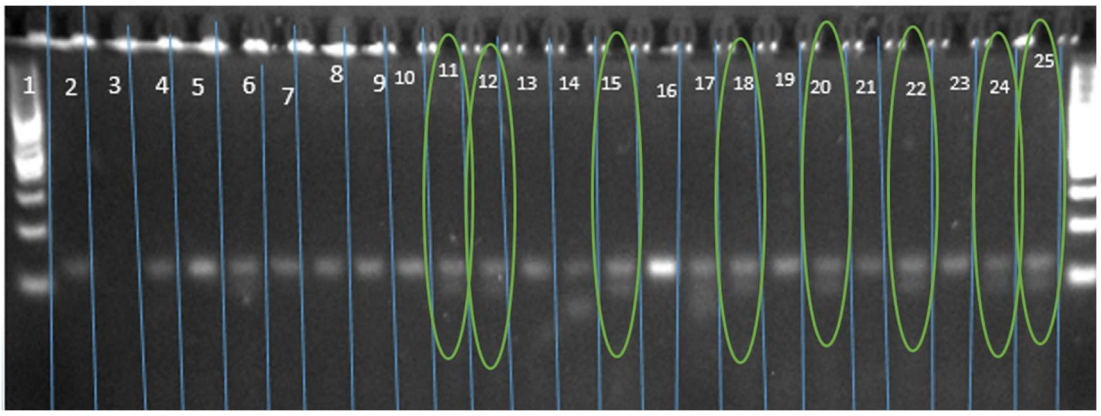

Figure III.3: Example of gel visualisation of PCR products in order to determine prt6.i homozygous mutants. Green circles highlight homozygous mutants.

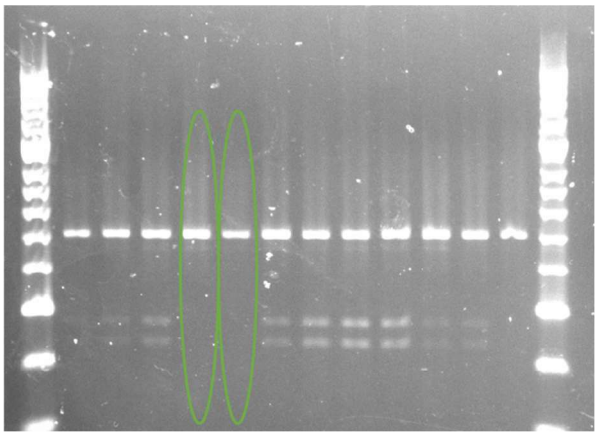

Figure III.3: Example of gel visualisation of PCR products in order to determine prt6.e homozygous mutants. Green circles highlight homozygous mutants.

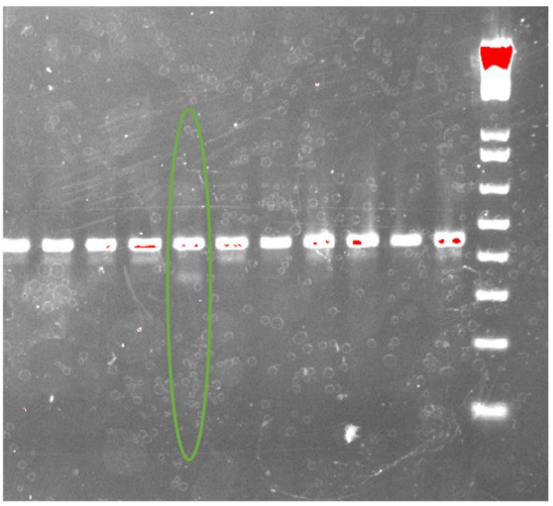

Figure III.3: Example of gel visualisation of PCR products in order to determine prt6.h homozygous mutants. Green circles highlight homozygous mutants.

Appendix IV: Pathlength equations

[1]

$$Pathlength\ of\ sample = \frac{(WaterA_{977} - WaterA_{900})}{0.18}$$

$$\text{Absorbance corrected to 1°C m} = \frac{Microplate\ absorbance\ reading - blank}{Pathlength}$$

[2]

$$\text{Chlorophyll a (mg/g)} = \frac{V\left(12.25(A_{663} - A_{750})\right) - \left(2.55(A_{646} - A_{750})\right)}{1000W}$$

$$\text{Chlorophyll b (mg/g)} = \frac{V\left(20.31(A_{646} - A_{750})\right) - \left(4.91(A_{663} - A_{750})\right)}{1000W}$$

$$\text{Chlorophyll a + b (mg/g)}\ \frac{V\left(17.768(A_{663} - A_{750})\right) + \left(7.34(A_{646} - A_{750})\right)}{1000W}$$

$$\text{Total carotenoids (mg/g)} = \frac{V(1000A_{470} - 3.27(Chl\ a) - 104(Chl\ b)}{1000W}$$

$$Where\ A = absorption\ value \qquad V = volume\ of\ extract(ml)$$

$$W = weight\ of\ leaves\ (mg)$$

Appendix V: Genotyping of T-DNA insertion mutations

These images show Example visualisations of T-DNA insertion mutations in *A. thaliana* as discussed in Chapters 4, 5 and 6.

Apg3

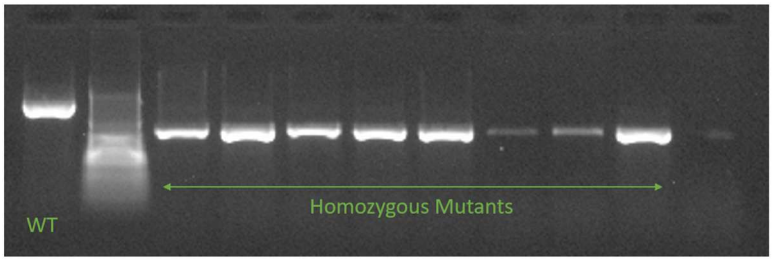

Figure V.1: Example of gel visualisation of PCR products in order to confirm Apg3 homozygous mutants. FP, RP and primer Lbbl.3 used

Ho2

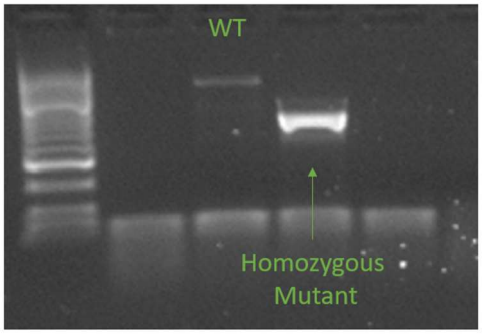

Figure V.2: Example of gel visualisation of PCR products in order to confirm Apg3 homozygous mutants. FP, RP and primer Lbbl.3 used.

Abcf5

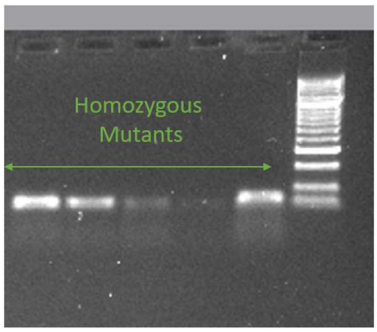

Figure V.3: Example of gel visualisation of PCR products in order to confirm Abcf5 homozygous mutants. FP, RP and primer Lbbl.3 used. WT not shown

T8p21

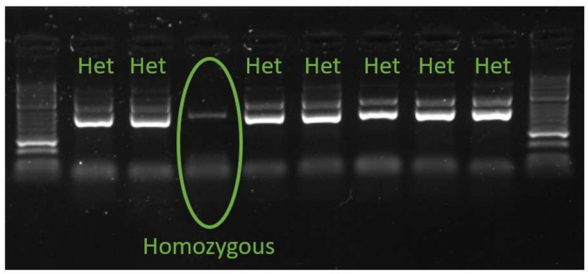

Figure III.4: Example of gel visualisation of PCR products in order to confirm T8p21 homozygous mutants. FP, RP and primer Lbbl.3 used. Circle shows homozygous mutant. WT not shown

Wrky55

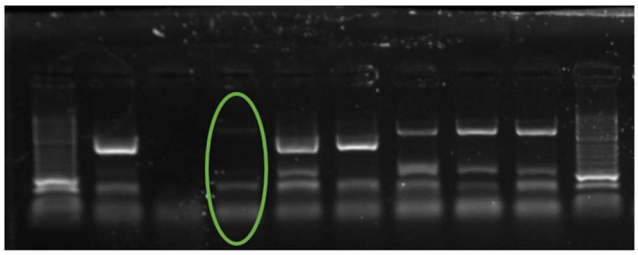

Figure V.5: Example of gel visualisation of PCR products in order to determine Wrky55 homozygous mutants. Green circle highlights homozygous mutant. WT not shown

Zne1

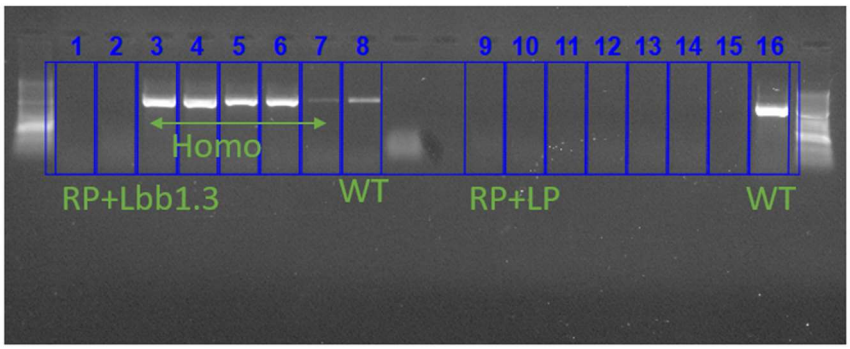

Figure V.6: Example of gel visualisation of PCR products in order to determine Zne1 homozygous mutants. Samples run in same order with separate sets of primers as shown.

Muse3

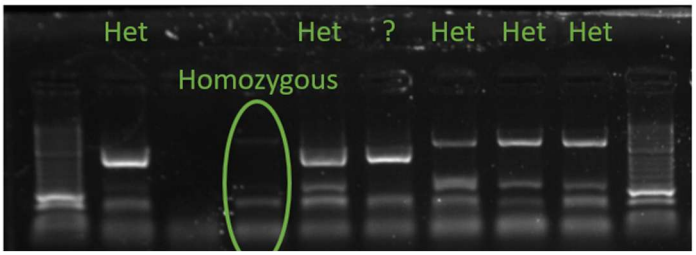

Figure V.7: Example of gel visualisation of PCR products in order to determine Muse3 homozygous mutants. Green circle highlights homozygous mutant. WT not shown

Sytb

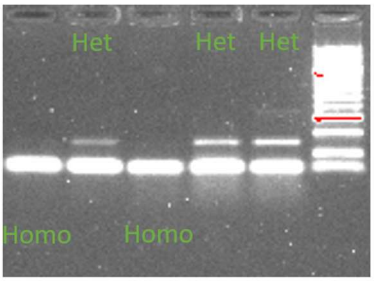

Figure V.8: Example of gel visualisation of PCR products in order to determine Sytb homozygous mutants. WT not shown

Sis8

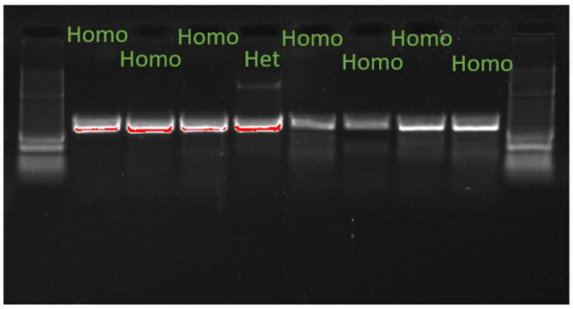

Figure V.9: Example of gel visualisation of PCR products in order to determine Sis8 homozygous mutants. WT not shown

Gapb

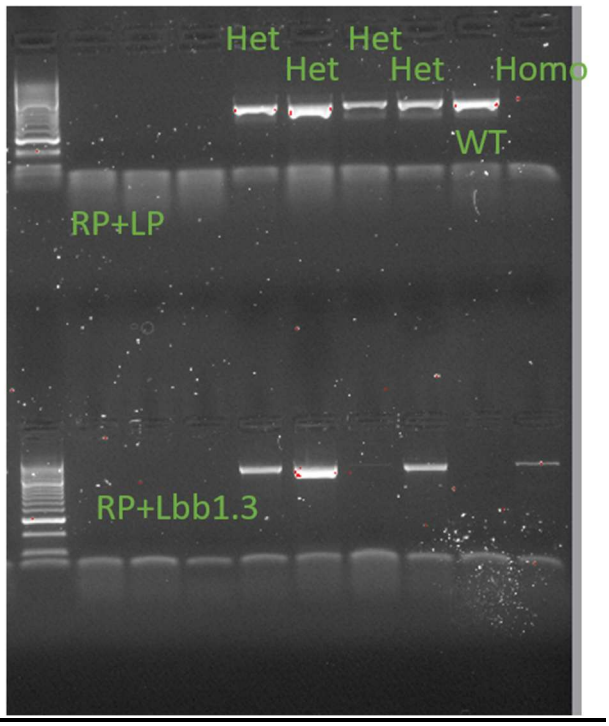

Figure V.10: Example of gel visualisation of PCR products in order to determine Muse3 homozygous mutants. Samples are positioned in the same position on each comb for different sets of primers.